Structural, Spectroscopic, and Kinetic Investigation of Cysteamine Dioxygenase

Ву

Rebeca L. Fernandez

A dissertation submitted in partial fulfillment of the requirements for the degree of

Doctor of Philosophy

(Chemistry)

at the

UNIVERSITY OF WISCONSIN-MADISON

2021

Date of final oral examination: 18 June 2021

The dissertation is approved by the following members of the Final Oral Committee:

Helen Blackwell, Professor, Chemical Biology Thomas C. Brunold, Professor, Inorganic Chemistry Andrew R. Buller, Professor, Chemical Biology Judith N. Burstyn, Professor, Chemical Biology Brian G. Fox, Professor, Biochemistry

Structural, Spectroscopic, and Kinetic Investigation of Cysteamine Dioxygenase Rebeca Fernandez

Under the supervision of Professor Thomas C. Brunold at the University of Wisconsin-Madison

Abstract

Thiol dioxygenases (TDOs) are mononuclear. non-heme Fe(II)-dependent metalloenzymes that catalyze the oxidation of thiol-containing substrates to their respective sulfinates. Cysteine dioxygenase (CDO), the best characterized TDO, contains a 3-histidine (3-His) coordination environment distinct from the well-characterized 2-His-1-carboxylate facial triad observed in most mononuclear non-heme Fe(II) enzymes. Four other classes of TDOs have been discovered with unique substrate specificity and reactivity: cysteamine dioxygenase (ADO), 3mercaptopropionate dioxygenase (MDO), mercaptosuccinate dioxygenase (MSDO), and plant cysteine dioxygenase (PCO). In this dissertation, the geometric and electronic structures of mouse ADO have been investigated using a combined crystallographic, spectroscopic, and computational approach. The spectroscopic techniques employed, including electronic absorption (Abs), magnetic circular dichroism (MCD), and electron paramagnetic resonance (EPR), are selective for the different metal ion oxidation sites and sensitive to changes in the coordination environment of the metal ion. Complementary information was obtained via kinetic exploration and quantum mechanics/molecular mechanics (QM/MM) calculations for substrate-bound Fe(II)ADO.

ADO catalyzes the oxidation of cysteamine (aminoethanethiol, 2-AET) and N-terminal cysteine (Nt-Cys) peptides. Our EPR and MCD studies have revealed that 2-AET binds monodentate to the Fe cofactor. Subsequently, the X-ray crystal structure of ADO has been determined to a 1.9 Å resolution. This structure shows that ADO possesses a 3-His active site and reveals a wide substrate access tunnel. An additional, smaller tunnel is observed that leads from the opposite face of the protein to the active site through which co-substrate oxygen may be delivered to the Fe cofactor. This tunnel is lined by two Cys residues that could serve as a redox

sensor to regulate O₂ delivery in response to changes in the intracellular redox potential. Finally, EPR spectroscopy has been used to obtain insight into the nature of the species that are formed upon incubation of Fe(III)ADO with substrate/substrate analogues and the superoxide surrogates azide and cyanide, which serve as models of putative reaction intermediates. A comparison of the EPR *g*-values obtained for cyanide/cysteamine-bound Fe(III)ADO and those reported for cyanide/Cys-bound Fe(III)CDO reveals that the interaction of the thiol substrate with outer-sphere residues is considerably weaker in ADO than in CDO.

Acknowledgments

I can't begin to articulate all of the feelings and gratitude that I have for the people that have helped me get to this point. I hope that by acknowledging you, you recognize just how important you are to me and how you have sustained me during graduate school.

To the Brunold group. Thank you for supporting each other from Day 1. We are a hodge-podge of students that function in very different ways and yet work extremely well together. Elizabeth and Josh, you've been there for most of my panic and all of my success and have supported me through it all. Becky, Laura, and Ryan I have absolutely loved watching you grow, and I cannot wait to see the amazing things you do. Zach and Nick, you are both joys to mentor. I genuinely expect incredible things from each of you. Steph, I would not be the scientist or person I am today without your mentorship. Thank you for taking the time to show me the science, the concert venues, and the biking scene in Madison. Most of all, Thomas, thank you for your unending support and praise during graduate school. You let me run with my project and develop an independence and drive that has been critical for my success. Your perspective on life, on departmental service, and on our science has been truly invaluable. I left every one of our meetings more relaxed and confident.

To the staff in the Department that I have had the pleasure to work with, you are truly what keeps this building functional. Kristi, I have missed our interactions during pandemic. Jeff, thank you for making me laugh and for keeping me sane. Heike, Bob, Cathy, and Lingchao, thank you for letting me stumble into your offices and add to your plate. You manage an incredible instrument center and a lot of needy students (like me). Desiree, I am so happy Steph made you teach me how to knit. I treasure our frank conversations. They fuel me and help keep me going.

To my mentoring committee, Judith, Brian, Helen, and Andrew. Each of you has shaped the scientist that I am today. Judith your unending passion for everything, whether service or science, is something that I admire. Brian, your feedback has been invaluable; you welcomed this naïve chemist into your lab and somehow, with the help of so many awesome people, taught me

to speak biochemistry. Helen, I cannot even begin to thank you for the incredible program that you run. The community that you created has shaped the way I approach problems. Thank you for always asking great research questions. Andrew, you are an excellent mentor that gives 100% to every single person that walks into your office. When I grow up, I want to be you.

To the Delta Program and the GSFLC, thank you for giving graduate school meaning. So often it is easy to get lost in research and I would not have made it without the eye-opening perspective of these two groups. Andjela, Tesia, and Adam, thank you for being more than chemists. I enjoyed the classes we took together and our reflections on their importance in Chemistry education. Andjela and Tesia, you two are incredible. You taught me how to manage people and be a leader. I can't think of any other way to put it than you two inspire me.

To my November Project community, I never thought I would find another group of people willing to work out before the sun rises, outside, year-round. You are part of what I will miss the most about Madison. Amrita, my dear, thank you for all of the hot goss, I'll see you in Warwick.

To my friends in Chemistry, thanks for being so weird. I love you all so much and the conversations we've had and the time we've spent together have made me a better person. Ways in which that is true: I shower less, listen more, bike (year-round!), question the world around me, laugh more, have learned what an α -helix is, love tequila, sew, listen to good music, camp, like beer, read better books, trail run, have a good bike seat, buy new clothes at the Dig-n-Save, and learned to cook.

I look like my mom, and I laugh like my dad. Everything I have been able to accomplish is because I have two encouraging, loving, supportive parents. Mami y Papi, gracias por todo. I am only as successful as I have been because you two professors raised me in an academic world. To my Fernandez family, I have loved getting to know you as people. Gabi and I know that you would do anything for us. Gabi, you are my bro-bro.

Zack, you're cool too.

Dedication

For Federico Torres Fernández and Aram Nersissian

Table of Contents

Abstract	i
Acknowledgments	iii
Dedication	V
Table of Contents	vi
Chapter 1: Cysteamine Dioxygenase's Place in a Thiol Dioxygenase Universe	2
1.1 Overview	2
1.2 Cysteine Dioxygenase (CDO)	4
1.3 3-mercaptopropionate dioxygenase (MDO)	8
1.4 Plant Cysteine Oxygenase (PCO)	10
1.5 Cysteamine dioxygenase (ADO)	13
1.6 Research Overview	17
1.7 References	18
Chapter 2: Spectroscopic Investigation of Cysteamine Dioxygenase	29
2.1 Introduction	29
2.2 Materials and Methods	32
2.3 Results	35
2.4 Discussion	42
2.5 References	46
Chapter 3: Spectroscopic Investigation of Iron(III) Cysteamine Dioxygenase in the F	resence of
Substrate (Analogues): Implications for the Nature of Substrate-Bound Reaction Int	ermediates
	52
3.1 Introduction	52
3.2 Materials and methods	55
3.3 Results	56
3.4 Discussion	63

3.5 Conclusion	66
3.6 References	67
Chapter 4: Crystal Structure of Cysteamine Dioxygenase Reveals the Origin of the	ne Large
Substrate Scope of this Vital Mammalian Enzyme	73
4.1 Introduction	73
4.2 Results	76
4.3 Discussion	84
4.4 Materials and Methods	88
4.5 References	91
Chapter 5. Production, purification, and kinetic characterization of recombinant mouse A	ADO 100
5.1 Introduction	100
5.2 Methods	102
5.3 Results	104
5.4 Discussion & Future Directions	109
5.5 Conclusions	110
5.6 References	110
Chapter 6: Bioinformatic analysis reveals the atypical structure/function relation	ıships in
cysteamine dioxygenase	118
6.1 Conspectus	118
6.2 Bioinformatic Analysis of ADOs and PCOs	120
6.3 Cysteine Dioxygenase (CDO)	122
6.4 3-mercaptopropionate dioxygenase (MDO)	126
6.5 Plant Cysteine Dioxygenase (PCO)	127
6.6 Cysteamine dioxygenase (ADO)	130
6.7 Conclusions	135
6.8 Methods	135

		٠	
١,	ı	ı	
v	ı	ı	
-	-	-	-

	6.9 References	136
Chapte	r 7: Conclusions and Future Directions	145
	7.1 Research Progress on Cysteamine Dioxygenase	145
	7.2 Additional Variant Studies	147
	7.3 Trapping of Catalytic Intermediates	149
	7.4 Structural and Computational Investigation of PCO and ADO	149
	7.5 Final Outlook	150
	7.6 References	150
Capítul	o 8: Una investigación sobre cisteamina dioxigenasa	153
	¿Que son las proteínas y cómo las como?	153
	¿Por qué nos importa el azufre?	155
	¿Cómo hago estas "investigaciones"?	155
	¿Qué uso para ver a ADO?	156
	¿Qué descubrí?	157
	¿Por qué importa?	159
	Looking at Cysteamine Dioxygenase	159
	What are proteins and how do I eat them?	160
	Why do we care about sulfur?	161
	How do I "do research"?	162
	What do I use to see ADO?	162
	Why does it matter?	165
Chapte	r 9: Student-Led Climate Assessment Promotes a Healthy Graduate School Environ	ment
		167
	9.1 Introduction	167
	9.2 Survey Process	169
	9.3 Representative Survey Findings	174

	9.4 Recommendations and	Initiatives	Implemented	Based	on	Climate	Survey	Results
								181
	9.5 Conclusions							183
	9.6 References							185
Appen	dix							189
	Chapter 2							189
	Chapter 3							191
	Chapter 4							194
	Chapter 9							200

CHAPTER 1

CYSTEAMINE DIOXYGENASE'S PLACE IN A THIOL DIOXYGENASE UNIVERSE

Chapter 1: Cysteamine Dioxygenase's Place in a Thiol Dioxygenase Universe

1.1 Overview

The cupin superfamily of proteins is highly represented among all domains with members spanning archaea, bacteria, and eukarya. 1,2 These proteins display remarkable functional diversity with members catalyzing reactions ranging from hydroxylation to dioxygenation to isomerization.^{3,4} Cupin proteins are primarily metalloenzymes that share a low overall degree of sequence identity while maintaining two short, highly conserved sequence motifs (cupin motif 1 and 2) that feature metal-binding residues. One large subcategory within this superfamily is comprised of mononuclear non-heme Fe(II)-dependent enzymes that use molecular oxygen to catalyze a wide range of reactions. These enzymes can be broadly separated into two groups based on the identity of the amino acid sidechains that serve as metal-binding ligands. The first subset of mononuclear non-heme Fe(II)-dependent enzymes within the cupin superfamily contain an Fe cofactor bound by two histidines and one carboxylate side chain (2-His-1-carboxylate), rendering a monoanionic binding motif.⁵⁻⁷ In the resting Fe(II) state, one to three labile solvent molecules typically occupy the remaining coordination sites. Enzymes such as TauD,8 iso penicillin N synthase, 9 and prolyl hydroxylase 10 exemplify this 2-His-1-carboxylate binding motif and have been well-characterized. The second category of cupin-type mononuclear non-heme Fe(II)-dependent metalloenzymes coordinate their metallocofactor via a neutral three histidine (3-His) binding motif. These enzymes have been significantly less well-studied.

The largest grouping of 3-His binding proteins comprises thiol dioxygenases (TDOs), whose primary functions are to convert a substrate with a sulfhydryl group to its sulfinic acid derivative via the addition of both oxygen atoms from molecular oxygen (**Scheme 1.1**). The first TDOs to be discovered, cysteine dioxygenase (CDO)¹¹ and cysteamine dioxygenase (ADO),¹² were originally purified from liver tissue in the 1960s and later biochemically characterized in 2006¹³ and 2007,¹⁴ respectively. In the past 15 years, three more TDOs have been discovered with distinct substrate specificity: 3-mercaptopropionate dioxygenase (MDO),^{15,16} plant cysteine

dioxygenase (PCO),¹⁷ and mercaptosuccinate dioxygenase (MSDO).¹⁸ Only a few other enzymes have been established via X-ray crystallography to feature a 3-His triad, including EgtB,¹⁹ SznF,²⁰ diketone-cleaving dioxygenase,²¹ and gentisate 1,2-dioxygenase.²²

Scheme 1.1. Oxidation of thiol-containing substrates catalyzed by TDOs

In recent years, considerable progress has been made toward understanding the geometric and electronic structures of TDOs and the contributions of their unique secondary sphere residues to their function. While an Fe cofactor bound by a 3-His triad has been implicated in all TDOs (Figure 1.1),²³ these cupin proteins differ in their key secondary sphere residues. To facilitate discussion of the relationship between ADO and its closest TDO homologs, Figure 1.2 features a multiple sequence alignment (MSA) to highlight residues that contribute to structure and function and align with divergences in enzyme substrate specificity (Figure 1.2). Interestingly, the active sites of PCO and ADO closely resemble each other, while the active sites of CDO and MDO share similarities. Key structural, spectroscopic, and biochemical properties of the different TDOs are summarized in the following sections.

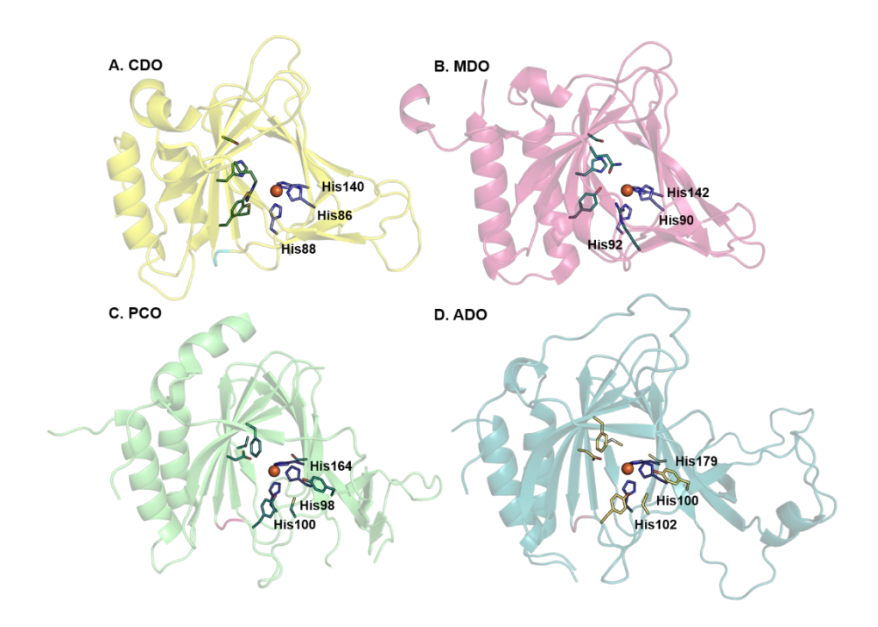


Figure 1.1. X-ray crystal structures of A. CDO (PDB: 4JTO), B. MDO (PDB: 2ATF), C. PCO (PDB: 6S7E), and D. ADO (PDB: 7LVZ) proteins. In each panel, the 3His triad (purple sticks) binds the Fe cofactor (orange sphere).

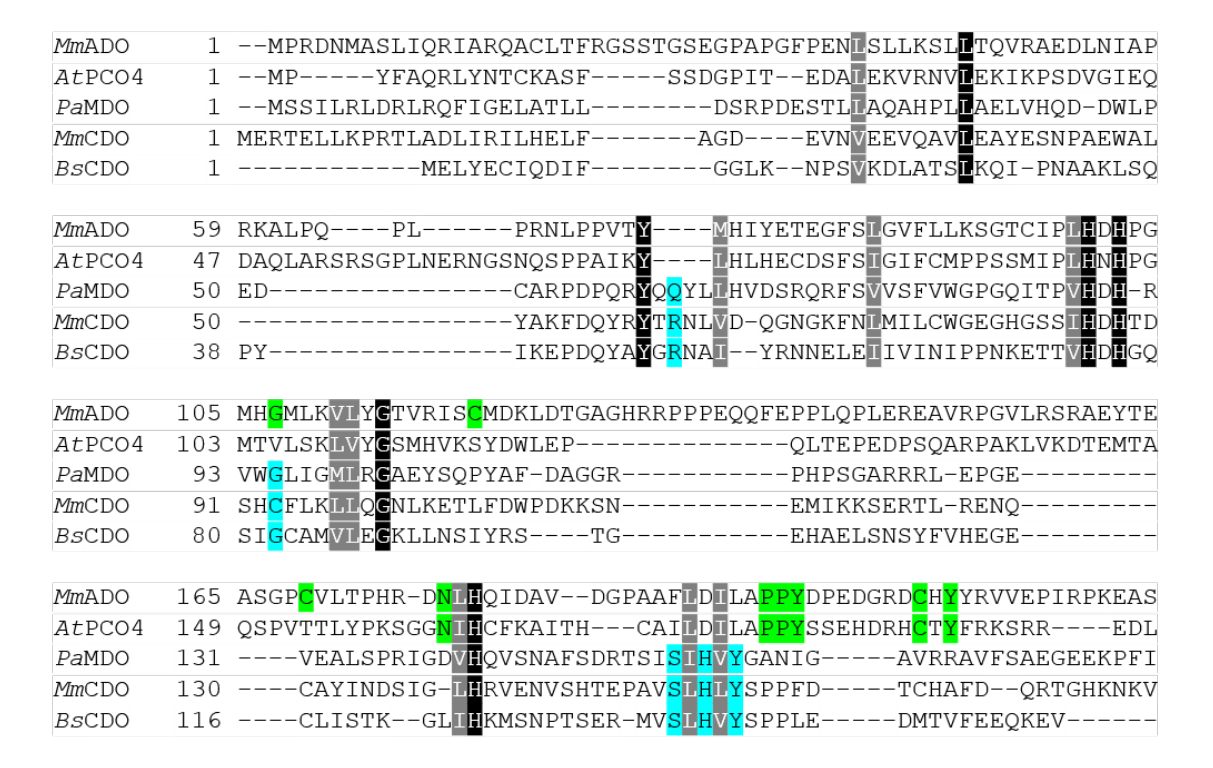


Figure 1.2. Multiple sequence alignment showing key residues within thiol dioxygenases. The PCO4 sequence from *Arabidopsis thaliana* (*At*PCO4), the MDO sequence from *Pseudomonas aeruginosa* (*Pa*MDO), and the CDO sequences from *Mus musculus* (*Mm*CDO) and *Bacillus subtilis* (*Bs*CDO) are compared to the *Mus musculus* ADO (*Mm*ADO) sequence.

1.2 Cysteine Dioxygenase (CDO)

The best-characterized TDO, CDO, was shown to oxidize cysteine (Cys) to cysteine sulfinic acid (CSA) by incorporating both oxygen atoms from co-substrate O₂ into Cys (**Scheme 1.2**).^{24–26} The regulation of Cys is vital to mammalian cellular function as a build-up of Cys, or its disulfide form cystine, can cause blockages²⁷ and organ failure.^{28,29} CSA can be further broken down into pyruvate and sulfite or decarboxylated into hypotaurine. A buildup of Cys can contribute to neurological malfunction and has been linked to Alzheimer's and Parkinson's diseases.^{30–32}

Because a lack of regulation of these sulfur-containing compounds has proven to be cytotoxic and neurotoxic to mammals, developing a fundamental understanding of the broad mechanism of thiol dioxygenase function is of considerable interest.

An X-ray crystal structure of Cys-bound CDO revealed that binding of the native substrate Cys occurs in a bidentate fashion, involving the coordination of the Fe cofactor by the sulfur and nitrogen atoms. CDO has been demonstrated to be extremely substrate specific, and only two alternative substrates have been identified; namely, D-Cys and cysteamine (2-aminoethanethiol, 2-AET).³³ However, neither of these alternative substrates are oxidized at a rate comparable to L-Cys, and the corresponding reactions are significantly more oxidatively decoupled than the native reaction.³³ Homocysteine³⁴ and selenocysteine (SeCys)³⁵ have both been shown to bind tightly to the Fe(II)CDO center, though neither is oxidized by this enzyme. A spectroscopic study using magnetic circular dichroism (MCD), resonance Raman (rR), electron paramagnetic resonance (EPR) techniques confirmed that the catalytically active species is Fe(II)CDO and revealed that although SeCys binds to the Fe center in a similar fashion as Cys, it does not act as a substrate for CDO.³⁵

Scheme 1.2. Oxidation of Cys to CSA as catalyzed by CDO.

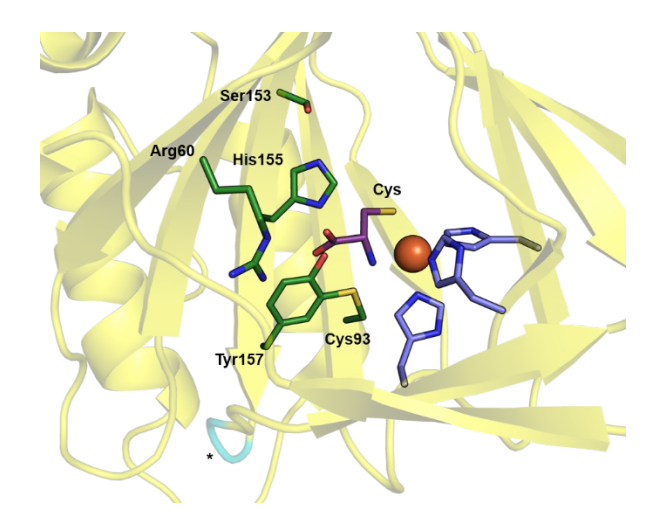


Figure 1.3. Active site region of Cys-bound *Rn*CDO. The Fe ion (orange sphere) is bound by His86, His88, and His140 (lavender) and Cys (purple). Other amino acids in the active site are highlighted in green and include Arg60, Cys93, Ser153, His155, and Tyr157. The * marks a *cis*-peptide bond.

The exceptional substrate specificity of mammalian CDO is determined by the unique secondary coordination sphere that includes residue Arg60, a Ser153-His155-Tyr157 catalytic triad, a *cis*-peptide bond between residues Ser158 and Pro159, and a thioether cross-link between Cys93 and Tyr157 (*Mm*CDO numbering, **Figure 1.3**). In substrate-bound CDO, the Cys carboxylate tail forms a salt bridge with the side chain of Arg60. Site directed substitution of Arg60 by Ala reduces the catalytic efficiency ~82-fold, demonstrating that this interaction directly affects protein function ($k_{cat}/K_M = 3200 \text{ M}^{-1}\text{s}^{-1}$ and 39 M⁻¹s⁻¹ for WT and Arg60Ala CDO, respectively).³⁶ Intriguingly, Cys93-Tyr157 cross-link formation (see below) in the Arg60Ala CDO variant can be induced by the addition of both Cys and 2-AET. Although cross-link formation is not a direct observation of turnover, Dominy et al. hypothesized that the Arg60Ala CDO variant would have relaxed substrate specificity.³⁶

The presence of a Ser-His-Tyr motif has been used successfully in screens of protein sequences to identify members of the cupin superfamily with CDO activity, which also led to the discovery of several bacterial homologs.³⁷ According to a Cys-bound CDO crystal structure,³⁸

these three residues engage in an extended hydrogen bonding network in the active site of the protein. In the active site of *Rn*CDO, Ser153 hydrogen bonds to His155,³⁹ which in turn hydrogen bonds to Tyr157. The His155Ala CDO variant³³ displays a ~100-fold decrease in activity relative to WT enzyme. The absence of the His-Tyr hydrogen bond and the His imidazole ring in the His155Ala CDO variant increases the conformational freedom of the Cys93-Tyr157 cross-link, allowing a water molecule to bind to the Cys-Fe(II)CDO adduct in the position typically occupied by oxygen.

Together the Ser153-His155-Tyr157 residues have been shown via X-ray crystallography to form a catalytic triad important for supporting the role of Tyr157 as a catalytic acid/base.³⁹ Intriguingly, the position of a Tyr157 is also controlled by the presence of a *cis*-peptide bond between Ser158 and Pro159. This *cis*-peptide bond, together with the Cys93-Tyr157 cross-link, lock the Tyr hydroxyl group into a favorable position for hydrogen bonding to substrate Cys and the superoxide moiety that is formed during O₂ activation Cys.^{16,40} The catalytic triad has a key role in controlling the coordination environment of the Fe center which distinguishes the incredible substrate specificity observed for CDO.

Also present near the primary coordination sphere is an unusual cross-link between Cys93 and Tyr157, whose role with regards to CDO function has been the subject of many studies. 33,39,41–44 Eukaryotic CDOs are distinguished by the post-translational formation of a thioether bond between residues Cys93 and Tyr157 (*Mm*CDO numbering). This cross-link is generated during turnover of the enzyme, and although not required for catalysis, its presence causes at least a 20-fold increase in protein activity. 45 A kinetic study of cross-linked and non-cross-linked CDO demonstrated that while both isoforms are active, the optimal pH decreases with the presence of the cross-link as the formation of the thioether bond decreases the pKa of Tyr157. 46 Equally important, the cross-link also ties up the Cys side chain to prevent any deleterious interactions involving the thiolate of Cys93. Interestingly, bacterial CDOs lack the Cys-Tyr cross-link, and

remain as active as eukaryotic CDOs.³⁷ In bacterial CDOs the key Cys residue is replaced by a smaller Gly residue.

Treatment of Cys-bound Fe(III)CDO with excess cyanide, a spectroscopic superoxide surrogate, causes the high-spin (S = 5/2) EPR signal to be replaced by a low-spin (S = 1/2) signal, demonstrating the direct coordination of cyanide to Cys-bound Fe(III)CDO to form a six-coordinate adduct. Interestingly, the cyano/Cys-Fe(III)CDO complex not only provides a model of a putative reaction intermediate, but also displays EPR parameters that are sensitive to the absence or presence of the Cys-Tyr cross-link.³³ QM/MM optimized structures of non-cross-linked and cross-linked cyano/Cys-bound Fe(III)CDO adducts demonstrate that the orientation of the cyanide ligand and carboxylic acid group of substrate Cys is sensitive to the presence of the cross-link; in the absence of the cross-link, the Fe-C-N unit is significantly more linear.³³ Fiedler and coworkers⁴⁷ were able to establish the structural basis for subtle differences in EPR *g* values between active site models of non-cross-linked and cross-linked cyanide/Cys-bound Fe(III)CDO, as well as synthetic mimics. The presence of the Cys-Tyr cross-link lengthens the Fe—S bond and induces a decrease in the Fe-C-N angle, causing an increased spread of *g* values. These cross-link induced perturbations exemplify the precise tuning of the secondary sphere residues designed to bind and turnover substrate.

1.3 3-mercaptopropionate dioxygenase (MDO)

The proteins now known as MDOs were originally identified as bacterial CDOs, ⁴⁸ and referred to as "Gln-type" enzymes. However, MDOs were soon distinguished from their TDO counterparts. Sequence alignment of known CDOs revealed a seemingly new category of proteins in which the key CDO residue Arg60 was substituted by a Gln (*Mm*CDO numbering). However, these "Gln-type" enzymes were found to display much higher rates for the conversion of 3-mercaptopropionate (3-MPA) to 3-sulfinopropanoate than for Cys oxidation (**Scheme 1.3**), and they were subsequently reclassified as MDOs. ^{15,16} Due to the unique secondary sphere residues found in the MDO active site, this enzyme displays enhanced substrate specificity for its native

substrate 3-MPA. Unlike other TDOs, different orthologs of MDO are able to oxidize substrate analogues in addition to 3-MPA; e.g., *Av*MDO additionally turns over L-Cys and 2-AET,¹⁵ and *Pa*MDO also turns over L-Cys.¹⁶

Scheme 1.3. Oxidation of 3-MPA to 3-sulfinopropionic acid as catalyzed by MDO.

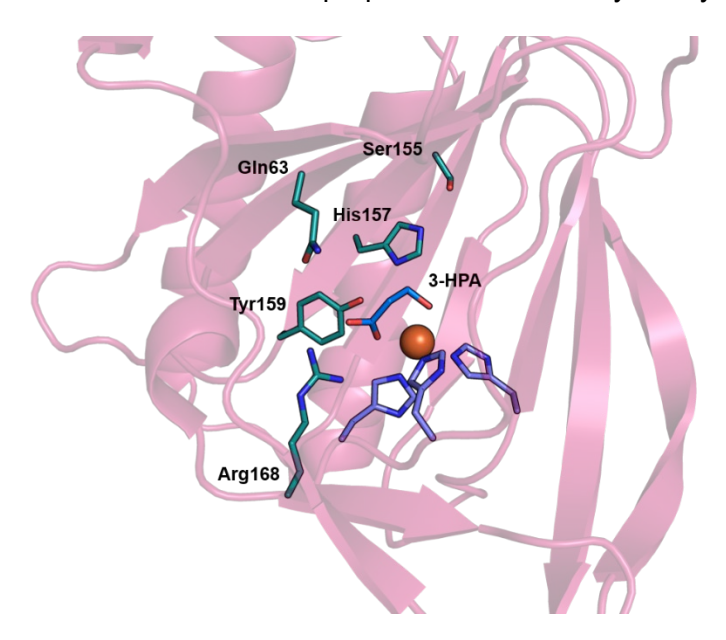


Figure 1.4. Active site region of 3-HPA-bound *Pa*MDO. The Fe ion (orange sphere) is bound by His90, His92, and His142 (lavender) and the substrate analogue 3-HPA (blue). Other amino acids in the active site are highlighted in teal and include Gln63, Ser155, His157, Tyr159, and Arg168.

The crystal structure of MDO revealed a number of similarities between the active sites of this enzyme and CDO. Most notable is the conservation of the 3-His binding motif typical of TDOs, as well as the Ser-His-Tyr catalytic triad first identified in CDO (**Figure 1.4**). Importantly, this enzyme lacks the *cis*-peptide bond featured in CDO. Similar to bacterial CDO, MDO is also unable to form the Cys-Tyr covalent cross-link, as a Gly is present at the position occupied by Cys93 in eukaryotic CDOs. Aloi et al.⁴⁰ predicted that the lack of a cis-peptide bond, in addition to the absence of the

thioether bond would, allow the formation of a stabilizing salt bridge between Arg168 and the carboxylate tail of 3-MPA when bound to the Fe cofactor.

The mode by which the native substrate 3-MPA binds to *Av*MDO and *Pa*MDO remains an active field of research. A Mössbauer study led to the proposal that both 3-MPA and Cys bind to *Pa*MDO in a monodentate fashion via their thiolate moieties. ¹⁶ Recently, however, an X-ray crystal structure was published of *Av*MDO complexed with the substrate analogue and competitive inhibitor 3-hydroxypropionic acid (3-HPA). ⁴⁹ The structure, corroborated by a computational analysis and spectroscopic evidence, demonstrates that 3-HPA and 3-MPA coordinate bidentate to the Fe cofactor. To stabilize the substrate analogue, and by extension the native substrate, the side chain of Arg168 participates in a hydrogen bonding interaction with the carboxylate tail.

1.4 Plant Cysteine Oxygenase (PCO)

The importance of regulating intracellular sulfur-containing compounds via oxidation is sufficiently high that TDOs have evolved across all forms of life. In plants, the molecular adaptation to high oxygen concentrations (hypoxia) is mediated by substrates that belong to the group VII ethylene response factors (ERF-VIIs) proteins. Five members of the ERF-VII family have been identified in *Arabidopsis thaliana* that feature the conserved N-terminal motif CGGA(I/V)ISD(F/Y). The concentrations of these five N-terminal cysteine peptides (Nt-Cys), RAP2.2, RAP2.3, RAP2.12, HRE1, and HRE2,^{50,51} are controlled by five plant cysteine oxidases (PCOs).⁵² These five PCOs oxidize Nt-Cys to their corresponding CSA, although their specificity and efficiency varies by ERF-VII substrate (**Scheme 1.4**). Oxidation of Nt-Cys marks the ERF-VII peptide for arginylation by arginyltransferases and subsequent ubiquitination and degradation.

Scheme 1.4. Oxidation of Nt-Cys peptides to the corresponding sulfinic acids as catalyzed by PCO.

In *Arabidopsis*, overproduction of an ERF-VII protein improved tolerance to submergence and up-regulation of genes associated with the hypoxic response.⁵¹ As such, the studies of PCOs have largely been motivated by a desire to optimize flood tolerance of plants. By controlling the plant hypoxic response mechanism within the N-degron pathway, which PCOs affect, researchers hope to engineer more flood resistant plants. Importantly, the X-ray crystal structures of PCO4 and PCO5 were recently published by White et al.¹⁷ This study suggested that site-specific substitution of key residues guided by structural knowledge could provide an effective route to improving stress tolerance in plants.

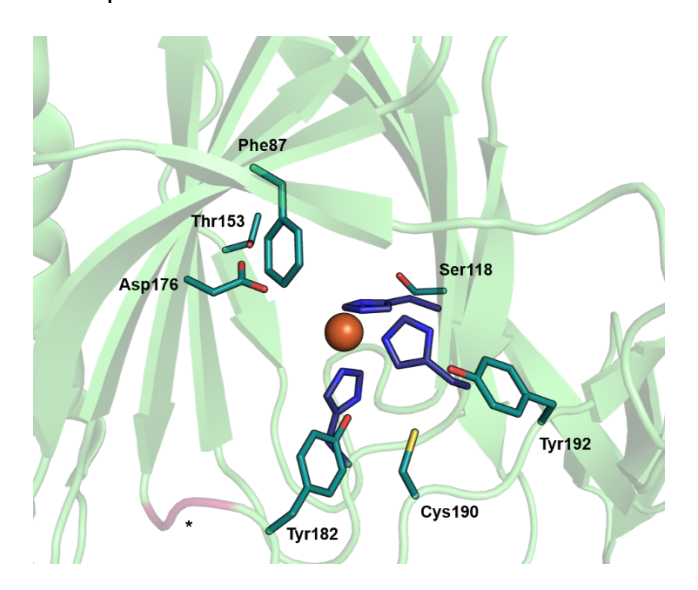


Figure 1.5. Active site region of *At*PCO4. The Fe ion (orange sphere) is bound by His98, His100, and His164 (purple). Other amino acids in the active site are highlighted in teal and include Phe87, Ser118, Thr153, Asp176, Tyr182, Cys190, and Tyr192. The * marks a *cis*-peptide bond.

Comparison of the first X-ray crystal structures of PCO enzymes to those of CDO and MDO highlight many dissimilarities. Although PCOs feature a 3-His triad that bind an Fe cofactor (**Figure 1.5**), few other residues are conserved in the active site of PCOs that have been well-characterized in CDOs. For example, the Ser-His-Tyr catalytic triad is absent in PCO. Instead, sequence alignment in conjunction with structural comparisons disclose that the catalytic triad is replaced by residues Asp176, Ile177, and Leu178. Substitution of Asp176 by an Asn proved to

almost abolish the specific activity of the enzyme. Additionally, the levels of Fe incorporation into this variant were extremely low. Inclusion of a reductant and iron supplementation during the activity assay restored some activity, although the specific activity of the Asp176Asn PCO variant remained ~7-fold lower than that of the WT enzyme.

As discussed above, the catalytic activity of mammalian CDOs is enhanced by the formation of a thioether cross-link between Cys93 and Tyr157. A distinct thioether cross-link motif has been proposed to exist in human ADO, between Cys220 and Tyr222 by Wang et al. (see below). For this reason, and because PCO and ADO share relevant sequence homology in this region (Figure 1.1), the possibility was evaluated that a cross-link could also be formed in PCO4 at residue Cys190, which is sandwiched between Tyr182 and Tyr192. However, no electron density for a cross-link was observed in the X-ray crystal structures of PCO4 and PCO5. In addition, tandem MS/MS analysis did not identify a cross-link, even after incubation of the enzyme with substrate. Finally, substitution of Cys190 by an Ala did not affect enzymatic activity. Alternatively, replacement of Tyr182 by a Phe was found to cause a ~7-fold decrease in specific activity, indicating that Tyr182 may play a role in substrate positioning.

As the only published crystal structures of PCO do not show bound substrate, much is left to speculation as to which specific interactions within the outer coordination sphere facilitate substrate recognition and binding. Inspection of the PCO4 protein surface reveals a prominent tunnel to the active site through which Nt-Cys substrate is likely to coordinate to the Fe. The PCO4 active site opening is marked by a hairpin loop (residues Tyr182 to Cys190) consisting almost exclusively of charged, polar residues. White et al. speculated that this hairpin loop, close to the active site, may play a role in substrate binding and recognition. The specific position of this loop is defined by a *cis*-peptide bond between residues Pro180 and Pro181. As described above, in CDO this *cis*-peptide bond has been observed to play a pivotal role in positioning the thioether cross-linking residue Tyr157 (*Mm*CDO numbering, **Figure 1.3**) within the active site.

1.5 Cysteamine dioxygenase (ADO)

The gene responsible for ADO production was identified when Dominy et al. noticed a discrepancy between the levels of taurine and CDO in various tissues. ¹⁴ This discovery suggested that the conversion of cysteamine (2-aminoethanethiol, 2-AET) to hypotaurine by ADO could be responsible for the majority of taurine production in some tissues, particularly the brain. Thus, ADO was believed to play a significant role in taurine biosynthesis. Ten years later, Masson et al. reported a new ADO substrate, regulators of G protein signaling 4 and 5 (RGS4 and RGS5), and demonstrated that ADO, like PCO,⁵⁴ oxidizes Nt-Cys polypeptides.⁵⁵ The Nt-Cys peptides that are oxidized by PCO have been shown to influence the hypoxic response to waterlogging in plant systems, known as the N-degron pathway.⁵² PCO produces an N-terminal CSA moiety that then undergoes arginylation by the arginyl transferase ATE1. Similar to PCO substrates, RGS4 and RGS5 function as substrates of the mammalian N-degron pathway.⁵⁶ Additionally, RGS4 and RGS5 have been shown in cardiomyocytes to inhibit G-protein-mediated signaling.⁵⁷

In 2007, Dominy et al. identified that ADO converted substrate 2-AET to hypotaurine with a K_M of 3.8 mM and k_{cat} of 1.6 s⁻¹ at pH 8.0 (**Scheme 1.5A**). Although the enzyme shares the 3-His active site first observed in CDO, ADO was shown to be unable to turn over the substrate analogue Cys. Additionally, Cys did not serve as an effective inhibitor; i.e., even when a 6-fold molar excess of Cys over 2-AET was used, only a 35% decrease in activity was observed. Intriguingly, Masson et al. discovered that, in fact, ADO oxidizes RGS5 more effectively than 2-AET, with a K_M of 71.5 μ M and a k_{cat} of 16.9 s⁻¹ (**Scheme 1.5B**). ⁵⁵

Scheme 1.5. Reactions catalyzed by ADO. A. Oxidation of 2-AET to hypotaurine. B. Oxidation of Nt-Cys peptides to their corresponding sulfinic acids.

The study conducted by Dominy et al. presented a sequence alignment of ADO and CDO that highlighted many dissimilarities between these two enzymes. ¹⁴ Although the 3-His triad was maintained, no other secondary sphere residues identified in CDO were conserved in the *Mm*ADO sequence. Notably, the ADO sequence lacks the residues necessary for the Cys-Tyr cross-link observed in mammalian CDOs. However, in 2019 Wang et al. posited the existence of a new cross-link motif in human ADO (*Hs*ADO). Genetic incorporation of an unnatural amino acid, 3, 5,-difluoro-tyrosine, in conjunction with mass spectrometry and NMR experiments identified a thioether bond between Cys220 and Tyr222 (*Hs*ADO numbering). ⁵³ Substitution of Tyr222 by an Ala was found to cause a modest (~3-fold) decrease in activity, seemingly supporting the existence of cross-link in the WT enzyme. However, in CDO, cross-link formation has a much larger effect on enzyme turnover, leading to an ~20-fold increases in activity. Thus, although the Tyr222 residue appears to moderately affect protein function, its exact catalytic role has yet to be determined.

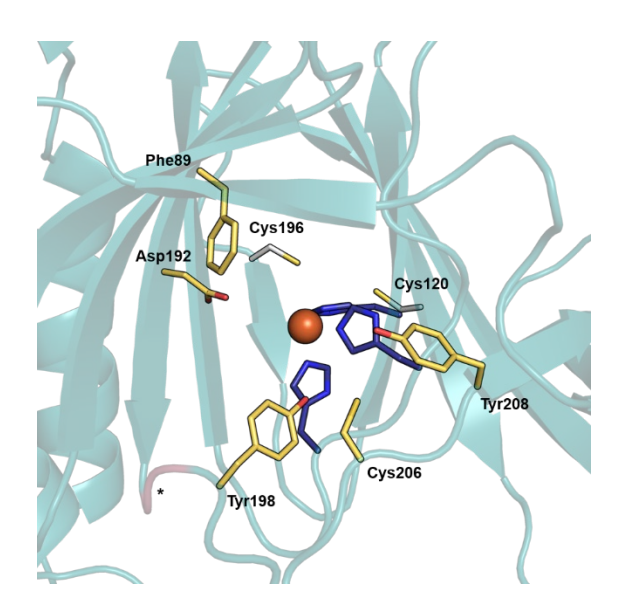


Figure 1.6. Active site region of *Mm*ADO. The Fe ion (orange sphere) is bound by His100, His102, and His179 (purple). Other amino acids in the active site are highlighted in yellow and include Phe89, Cys120, Asp192, Cys196, Tyr198, Cys206, and Tyr208. The * marks a *cis*-peptide bond.

The first X-ray crystal structure of ADO presented later in this thesis affords the structural basis for assessing the importance of residues proposed via MSA to be critical to ADO function. In the ADO active site (Figure 1.6) few residues are within 5 Å of the cofactor; the closest residues are Asp192 and Phe89 at a distance of 4.37 and 6.94 Å, respectively. Located 8.43 Å from the Fe is the purported cross-linking residue Tyr208. The X-ray crystal structure revealed a lack of electron density between Cys206 and Tyr208, indicating that MmADO does not form a thioether cross-link under the experimental conditions used to obtain the single crystals for X-ray crystallography. Intriquingly, equidistant from Cys206 is Tyr198, which sandwiches Cys206 between aromatic residues. In ADO, the positioning of Tyr198 is influenced by a cis-peptide bond between Pro196 and Pro197 (Figure 1.6, pink highlight). In CDO, a similar cis-peptide bond has been shown to be critical for the proper positioning of the cross-linking Tyr157 for maximum catalytic activity. 16 The Pro196-Pro197-Tyr198 motif identified in ADO is also maintained in the PCO4 sequence (Pro180-Pro181-Tyr182). As described above, replacement of Tyr182 with a Phe (equivalent to Tyr198 in MmADO) significantly decreased the activity of the PCO4 variant. Tyr182 in PCO4 and Tyr198 in MmADO are both similarly positioned near the end of the putative substrate access tunnel to the active site, and after a cis-Pro peptide bond. Thus, it is likely that in ADO, replacement of Tyr198 will influence enzymatic activity more than substitution of Tyr208.

The specificity of TDOs is governed by the secondary sphere residues and sequence motifs that promote substrate binding and recognition. Critical to the function of CDO and MDO are residues Ser153, His155, and Tyr157 (*Mm*CDO numbering), as they engage in an extended hydrogen-bonding network that supports advantageous substrate and co-substrate coordination.³⁶ These residues are not conserved in the sequence of *Mm*ADO but rather replaced by residues Asp192, Ile193, and Leu194, suggesting that the positioning of substrates 2-AET and

Nt-Cys occurs via distinct binding interactions. Intriguingly, in PCO4 the sequence and structural location of this Asp-Ile-Leu motif is preserved, underscoring the likely importance of these residues. Although an X-ray crystal structure of substrate-bound ADO is not yet available, 2-AET (analogue)-bound Fe(II)- and Fe(III)ADO species have previously been spectroscopically characterized. MCD and EPR^{23,58} spectroscopic studies provided evidence for monodentate coordination of the terminal thiolate residues for both 2-AET and Nt-Cys. A computational study of 2-AET and Nt-Cys-bound ADO, using molecular dynamics and quantum mechanics/molecular mechanics, demonstrates that the large substrate cavity lends 2-AET large conformational freedom. In contrast to 2-AET, the large size of the Nt-Cys peptide allows for interactions with more residues lining the active site cavity, *i.e.* Asp 192 and Tyr198.

The necessity of ordered binding of the Cys substrate prior to co-substrate oxygen coordination was demonstrated spectroscopically for CDO. By extension, it is likely that ordered binding of Nt-Cys, followed by O₂, also occurs in ADO. On the basis of structural and computational data, Nt-Cys peptide substrates are predicted to enter the active site and coordinate to the Fe(II) ion through a large substrate access tunnel. Inspection of the ADO surface uncovers an additional, smaller tunnel that leads from the protein surface to the active site, lined by residues Cys120 and Cys169. Although an intra-disulfide bond between these two residues is not observed in the ADO X-ray crystal structure, these two residues are ~4 Å apart and within bonding distance of each other. We hypothesize that upon Nt-Cys binding, the peptide would fill the large tunnel, precluding co-substrate oxygen from binding. Thus, the smaller access tunnel, gated by Cys120 and Cys169, could serve to transport O₂ to the active site. Delivery of oxygen via this pathway would cause a coupling of the turnover rate to the intracellular redox potential, instead of the intracellular substrate concentration.

1.6 Conclusions

Many intracellular thiol oxidation reactions are known to occur via enzymatic catalysis. Some of the TDOs that catalyze these reactions show a high degree of substrate specificity, which

allows them to precisely regulate the level of a particular thiol substrate. The importance of the secondary coordination sphere in tailoring substrate specificity and reactivity is apparent from the significant variation in key TDO residues and sequence motifs. Originally, CDO and MDO were both believed to catalyze Cys oxidation, and were first distinguished as either "Arg- or Gln-type" enzymes. Further kinetic characterization separated the two enzymes as they differed in their native substrate specificity. Recently, both PCO and ADO have been shown to oxidize Nt-Cys peptides. The X-ray crystal structures of these two TDOs display very similar active site structures and key sequence motifs in the outer coordination sphere. Importantly, in ADO a hypothesized co-substrate access tunnel is lined by Cys120 and Cys169, which may serve as a gating mechanism to prevent ADO from depleting the cell of all Nt-Cys containing molecules under conditions of high O_2 levels. The newly obtained X-ray crystal structure of ADO provides an excellent framework for answering this, and many additional questions about the structure/function relationships of ADO.

1.6 Research Overview

In this thesis, I have employed a combination of spectroscopic, crystallographic, and kinetic tools to investigate the geometric and electronic structures of ADO. The primary spectroscopic techniques employed include electronic absorption, magnetic circular dichroism (MCD), and electron paramagnetic resonance (EPR). The crystallization of ADO paired with a quantum mechanics/molecular mechanics computational approach was used to evaluate the structure of substrate-bound ADO and propose possible roles for newly identified outer-sphere residues.

 In Chapter 2, I present a spectroscopic study of substrate- and substrate analogue-bound ADO. Collectively, MCD and EPR results support monodentate, thiolate-only coordination of substrate 2-AET to the Fe cofactor.

- Chapter 3 describes electronic absorption and EPR studies of superoxide surrogates, azide and cyanide, that model potential intermediates in substrate- and substrateanalogue bound Fe(III)ADO.
- In Chapter 4 the very first X-ray crystal structure of ADO is presented. This structure
 highlights key residues and sequence motifs that define the unique substrate specificity of
 this previously poorly-characterized thiol dioxygenase.
- Chapter 5 outlines the development of a quantitative activity assay to perform kinetic characterization of TDOs. The accuracy of this assay was tested by replicating CDO kinetics after which the oxidation of cysteamine to hypotaurine by ADO was measured.
- Chapter 6 summarizes a project conducted in partnership with my undergraduate mentee
 Nicholas Juntunen during the Covid-19 pandemic. The sequence similarity network
 studies of thiol dioxygenases speculates carried out in this project highlight the
 structure/function relationships that exist between these 3-His mononuclear non-heme
 iron enzymes.
- Chapter 7 concludes my doctoral research by proposing promising experimental avenues for future investigations of ADO.
- The writing of Chapter 8 was supported by the Wisconsin Initiative for Science Literacy (WISL). This chapter reports the key findings of Chapter 2 in a manner approachable by non-scientists.
- In addition to research, I have sought to make the spaces around me better for the next generation of graduate students. Chapter 9 summarizes a graduate-student led effort to develop a climate survey to assess, advocate for, and improve the well-being and mental health of graduate students and postdocs.

1.7 References

(1) Dunwell, J. M.; Khuri, S.; Gane, P. J. Microbial Relatives of the Seed Storage Proteins of

- Higher Plants: Conservation of Structure and Diversification of Function during Evolution of the Cupin Superfamily. *Microbiol. Mol. Biol. Rev.* **2000**, *64* (1), 153–179. https://doi.org/10.1128/mmbr.64.1.153-179.2000.
- (2) Uberto, R.; Moomaw, E. W. Protein Similarity Networks Reveal Relationships among Sequence, Structure, and Function within the Cupin Superfamily. *PLoS One* 2013, 8 (9). https://doi.org/10.1371/journal.pone.0074477.
- (3) Dunwell, J. M.; Purvis, A.; Khuri, S. Cupins: The Most Functionally Diverse Protein Superfamily? *Phytochemistry* **2004**, *65* (1), 7–17. https://doi.org/10.1016/j.phytochem.2003.08.016.
- (4) Stipanuk, M. H.; Simmons, C. R.; Karplus, P. A.; Dominy, J. E. Thiol Dioxygenases: Unique Families of Cupin Proteins. *Amino Acids* 2011, 41 (1), 91–102. https://doi.org/10.1007/s00726-010-0518-2.
- (5) Straganz, G. D.; Nidetzky, B. Variations of the 2-His-1-Carboxylate Theme in Mononuclear Non-Heme Fe II Oxygenases. *ChemBioChem* 2006, 7 (10), 1536–1548. https://doi.org/10.1002/cbic.200600152.
- (6) Leitgeb, S.; Nidetzky, B. Structural and Functional Comparison of 2-His-1-Carboxylate and 3-His Metallocentres in Non-Haem Iron(II)-Dependent Enzymes. *Biochem. Soc. Trans.* 2008, 36 (6), 1180–1186. https://doi.org/10.1042/BST0361180.
- (7) Koehntop, K. D.; Emerson, J. P.; Que, L. The 2-His-1-Carboxylate Facial Triad: A Versatile Platform for Dioxygen Activation by Mononuclear Non-Heme Iron(II) Enzymes.
 J. Biol. Inorg. Chem. 2005, 10 (2), 87–93. https://doi.org/10.1007/s00775-005-0624-x.
- (8) Price, J. C.; Barr, E. W.; Tirupati, B.; Bollinger, J. M.; Krebs, C. The First Direct Characterization of a High-Valent Iron Intermediate in the Reaction of an α-Ketoglutarate-Dependent Dioxygenase: A High-Spin Fe(IV) Complex in Taurine/α-Ketoglutarate Dioxygenase (TauD) from Escherichia Coli. *Biochemistry* **2003**, *42* (24), 7497–7508. https://doi.org/10.1021/bi0330139.

- (9) Roach, P. L.; Clifton, I. J.; Charles, M. H.; Shibata, N.; Schofield, C. J.; Hajdu, J.; Baldwin, J. E. Structure of Isopenicillin N Synthase Complexed with Substrate and the Mechanism of Penicillin Formation. *Nature* 1997, 387 (1991), 827–830.
- (10) McDonough, M. A.; Li, V.; Flashman, E.; Chowdhury, R.; Mohr, C.; Liénard, B. M. R.; Zondlo, J.; Oldham, N. J.; Clifton, I. J.; Lewis, J.; McNeill, L. A.; Kurzeja, R. J. M.; Hewitson, K. S.; Yang, E.; Jordan, S.; Syed, R. S.; Schofield, C. J. Cellular Oxygen Sensing: Crystal Structure of Hypoxia-Inducible Factor Prolyl Hydroxylase (PHD2). *Proc. Natl. Acad. Sci. U. S. A.* 2006, *103* (26), 9814–9819. https://doi.org/10.1073/pnas.0601283103.
- (11) Yamaguchi, K.; Hosokawa, Y. Cysteine Dioxygenase. *Methods Enzymol.* **1987**, *143* (C), 395–403. https://doi.org/10.1016/0076-6879(87)43069-3.
- (12) Cavallini, D.; Scandurra, R.; De Marco, C. The Enzymatic Oxidation of Cysteamine to Hypotaurine in the Presence of Sulfide. *J. Biol. Chem.* **1963**, 238 (9), 2999–3005.
- McCoy, J. G.; Bailey, L. J.; Bitto, E.; Bingman, C. A.; Aceti, D. J.; Fox, B. G.; Phillips, G. N. Structure and Mechanism of Mouse Cysteine Dioxygenase. *Proc. Natl. Acad. Sci.*2006, 103 (9), 3084–3089. https://doi.org/10.1073/pnas.0509262103.
- (14) Dominy, J. E.; Simmons, C. R.; Hirschberger, L. L.; Hwang, J.; Coloso, R. M.; Stipanuk, M. H. Discovery and Characterization of a Second Mammalian Thiol Dioxygenase, Cysteamine Dioxygenase. *J. Biol. Chem.* 2007, 282 (35), 25189–25198. https://doi.org/10.1074/jbc.M703089200.
- (15) Pierce, B. S.; Subedi, B. P.; Sardar, S.; Crowell, J. K. The "Gln-Type" Thiol Dioxygenase from Azotobacter Vinelandii Is a 3-Mercaptopropionic Acid Dioxygenase. *Biochemistry* 2015, *54* (51), 7477–7490. https://doi.org/10.1021/acs.biochem.5b00636.
- (16) Tchesnokov, E. P.; Fellner, M.; Siakkou, E.; Kleffmann, T.; Martin, L. W.; Aloi, S.; Lamont,
 I. L.; Wilbanks, S. M.; Jameson, G. N. L. The Cysteine Dioxygenase Homologue from
 Pseudomonas Aeruginosa Is a 3-Mercaptopropionate Dioxygenase. *J. Biol. Chem.* 2015,

- 290 (40), 24424–24437. https://doi.org/10.1074/jbc.M114.635672.
- (17) White, M. D.; Carbonare, L. D.; Puerta, M. L.; Iacopino, S.; Edwards, M.; Dunne, K.; Pires, E.; Levy, C.; McDonough, M. A.; Licausi, F.; Flashman, E. Structures of Arabidopsis Thaliana Oxygen-Sensing Plant Cysteine Oxidases 4 and 5 Enable Targeted Manipulation of Their Activity. *Proc. Natl. Acad. Sci. U. S. A.* 2020, 117 (37), 23140– 23147. https://doi.org/10.1073/pnas.2000206117.
- (18) Brandt, U.; Schürmann, M.; Steinbüchel, A. Mercaptosuccinate Dioxygenase, a Cysteine Dioxygenase Homologue, from Variovorax Paradoxus Strain B4 Is the Key Enzyme of Mercaptosuccinate Degradation. *J. Biol. Chem.* 2014, 289 (44), 30800–30809. https://doi.org/10.1074/jbc.M114.579730.
- (19) Goncharenko, K. V.; Vit, A.; Blankenfeldt, W.; Seebeck, F. P. Structure of the Sulfoxide Synthase EgtB from the Ergothioneine Biosynthetic Pathway. *Angew. Chemie - Int. Ed.* 2015, 54 (9), 2821–2824. https://doi.org/10.1002/anie.201410045.
- (20) Ng, T. L.; Rohac, R.; Mitchell, A. J.; Boal, A. K.; Balskus, E. P. An N-Nitrosating Metalloenzyme Constructs the Pharmacophore of Streptozotocin. *Nature* 2019, 566 (7742), 94–99. https://doi.org/10.1038/s41586-019-0894-z.
- (21) Diebold, A. R.; Neidig, M. L.; Moran, G. R.; Straganz, G. D.; Solomon, E. I. The Three-His Triad in Dke1: Comparisons to the Classical Facial Triad. *Biochemistry* **2010**, *49* (32), 6945–6952. https://doi.org/10.1021/bi100892w.
- (22) Chen, J.; Li, W.; Wang, M.; Zhu, G.; Liu, D.; Sun, F.; Hao, N.; Li, X.; Rao, Z.; Zhang, X. C. Crystal Structure and Mutagenic Analysis of GDOsp, a Gentisate 1,2-Dioxygenase from Silicibacter Pomeroyi. *Protein Sci.* 2008, 17 (8), 1362–1373. https://doi.org/10.1110/ps.035881.108.
- (23) Fernandez, R. L.; Dillon, S. L.; Stipanuk, M. H.; Fox, B. G.; Brunold, T. C. Spectroscopic Investigation of Cysteamine Dioxygenase. *Biochemistry* 2020, 59 (26), 2450–2458. https://doi.org/10.1021/acs.biochem.0c00267.

- (24) Stipanuk, M. H.; Dominy, J. E.; Lee, J.-I.; Coloso, R. M. Mammalian Cysteine Metabolism: New Insights into Regulation of Cysteine Metabolism. *J. Nutr.* 2006, 136 (6 Suppl), 1652S-1659S.
- (25) Lombardini, J. B.; Singer, T. P.; Boyer, P. D. Cysteine Oxygenase. II. Studies on the Mechanism of the Reaction with 18oxygen. *J. Biol. Chem.* **1969**, *244* (5), 1172–1175. https://doi.org/10.1016/S0021-9258(18)91825-9.
- (26) Chai, S. C.; Jerkins, A. A.; Banik, J. J.; Shalev, I.; Pinkham, J. L.; Uden, P. C.; Maroney, M. J. Heterologous Expression, Purification, and Characterization of Recombinant Rat Cysteine Dioxygenase. *J. Biol. Chem.* 2005, 280 (11), 9865–9869.
 https://doi.org/10.1074/jbc.M413733200.
- (27) Schulz, J. B.; Lindenau, J.; Seyfriend, J.; Dichgans, J. Glutathione, Oxidative Stress and Neurodegeneration. *Eur. J. Biochem.* **2000**, *267*, 4904–4911.
- (28) Wilmer, M. J.; Emma, F.; Levtchenko, E. N. The Pathogenesis of Cystinosis: Mechanisms beyond Cystine Accumulation. *Am. J. Physiol. Ren. Physiol.* 2010, 299 (5). https://doi.org/10.1152/ajprenal.00318.2010.
- (29) Elmonem, M. A.; Veys, K. R.; Soliman, N. A.; Van Dyck, M.; Van Den Heuvel, L. P.; Levtchenko, E. Cystinosis: A Review. *Orphanet J. Rare Dis.* **2016**, *11* (1), 1–17. https://doi.org/10.1186/s13023-016-0426-y.
- (30) Simmons, C. R.; Hirschberger, L. L.; Machi, M. S.; Stipanuk, M. H. Expression, Purification, and Kinetic Characterization of Recombinant Rat Cysteine Dioxygenase, a Non-Heme Metalloenzyme Necessary for Regulation of Cellular Cysteine Levels. *Protein Expr. Purif.* 2006, 47 (1), 74–81. https://doi.org/10.1016/j.pep.2005.10.025.
- (31) Heafield, M. T.; Fearn, S.; Steventon, G. B.; Waring, R. H.; Williams, A. C.; Sturman, S. G. Plasma Cysteine and Sulphate Levels in Patients with Motor Neurone, Parkinson's and Alzheimer's Disease. *Neurosci. Lett.* 1990, 110 (1–2), 216–220. https://doi.org/10.1016/0304-3940(90)90814-P.

- (32) Slivka, A.; Cohen, G. Brain Ischemia Markedly Elevates Levels of the Neurotoxic Amino Acid, Cysteine. *Brain Res.* **1993**, *608* (1), 33–37. https://doi.org/10.1016/0006-8993(93)90770-N.
- (33) Li, W.; Blaesi, E. J.; Pecore, M. D.; Crowell, J. K.; Pierce, B. S. Second-Sphere Interactions between the C93-Y157 Cross-Link and the Substrate-Bound Fe Site Influence the O2 Coupling Efficiency in Mouse Cysteine Dioxygenase. *Biochemistry* 2013, 52 (51), 9104–9119. https://doi.org/10.1021/bi4010232.
- (34) Tchesnokov, E. P.; Wilbanks, S. M.; Jameson, G. N. L. A Strongly Bound High-Spin Iron(II) Coordinates Cysteine and Homocysteine in Cysteine Dioxygenase. *Biochemistry* 2012, *51* (1), 257–264. https://doi.org/10.1021/bi201597w.
- (35) Gardner, J. D.; Pierce, B. S.; Fox, B. G.; Brunold, T. C. Spectroscopic and Computational Characterization of Substrate-Bound Mouse Cysteine Dioxygenase: Nature of the Ferrous and Ferric Cysteine Adducts and Mechanistic Implications. *Biochemistry* **2010**, 49 (29), 6033–6041. https://doi.org/10.1021/bi100189h.
- (36) Dominy, J. E.; Hwang, J.; Guo, S.; Hirschberger, L. L.; Zhang, S.; Stipanuk, M. H. Synthesis of Amino Acid Cofactor in Cysteine Dioxygenase Is Regulated by Substrate and Represents a Novel Post-Translational Regulation of Activity. *J. Biol. Chem.* 2008, 283 (18), 12188–12201. https://doi.org/10.1074/jbc.M800044200.
- (37) Dominy, J. E.; Simmons, C. R.; Karplus, P. A.; Gehring, A. M.; Stipanuk, M. H. Identification and Characterization of Bacterial Cysteine Dioxygenases: A New Route of Cysteine Degradation for Eubacteria. *J. Bacteriol.* 2006, 188 (15), 5561–5569. https://doi.org/10.1128/JB.00291-06.
- (38) Driggers, C. M.; Cooley, R. B.; Sankaran, B.; Hirschberger, L. L.; Stipanuk, M. H.; Karplus, P. A. Cysteine Dioxygenase Structures from PH 4 to 9: Consistent Cys-Persulfenate Formation at Intermediate PH and a Cys-Bound Enzyme at Higher PH. *J. Mol. Biol.* **2013**, *425* (17), 3121–3136. https://doi.org/10.1016/j.jmb.2013.05.028.

- (39) Simmons, C. R.; Liu, Q.; Huang, Q.; Hao, Q.; Begley, T. P.; Karplus, P. A.; Stipanuk, M. H. Crystal Structure of Mammalian Cysteine Dioxygenase: A Novel Mononuclear Iron Center for Cysteine Thiol Oxidation. *J. Biol. Chem.* 2006, 281 (27), 18723–18733. https://doi.org/10.1074/jbc.M601555200.
- (40) Aloi, S.; Davies, C. G.; Karplus, P. A.; Wilbanks, S. M.; Jameson, G. N. L. Substrate Specificity in Thiol Dioxygenases. *Biochemistry* 2019, 2398–2407. https://doi.org/10.1021/acs.biochem.9b00079.
- (41) Li, J.; Koto, T.; Davis, I.; Liu, A. Probing the Cys-Tyr Cofactor Biogenesis in Cysteine Dioxygenase by the Genetic Incorporation of Fluorotyrosine. *Biochemistry* 2019, 58 (17), 2218–2227. https://doi.org/10.1021/acs.biochem.9b00006.
- (42) Driggers, C. M.; Kean, K. M.; Hirschberger, L. L.; Cooley, R. B.; Stipanuk, M. H.; Karplus, P. A. Structure-Based Insights into the Role of the Cys–Tyr Crosslink and Inhibitor Recognition by Mammalian Cysteine Dioxygenase. *J. Mol. Biol.* 2016, 428 (20), 3999–4012. https://doi.org/10.1016/j.jmb.2016.07.012.
- (43) Siakkou, E.; Rutledge, M. T.; Wilbanks, S. M.; Jameson, G. N. L. Correlating Crosslink Formation with Enzymatic Activity in Cysteine Dioxygenase. *Biochim. Biophys. Acta -Proteins Proteomics* 2011, 1814 (12), 2003–2009. https://doi.org/10.1016/j.bbapap.2011.07.019.
- (44) Njeri, C. W.; Ellis, H. R. Shifting Redox States of the Iron Center Partitions CDO between Crosslink Formation or Cysteine Oxidation. *Arch. Biochem. Biophys.* 2014, 558, 61–69. https://doi.org/10.1016/j.abb.2014.06.001.
- (45) Ye, S.; Wu, X.; Wei, L.; Tang, D.; Sun, P.; Bartlam, M.; Rao, Z. An Insight into the Mechanism of Human Cysteine Dioxygenase: Key Roles of the Thioether-Bonded Tyrosine-Cysteine Cofactor. *J. Biol. Chem.* 2007, 282 (5), 3391–3402. https://doi.org/10.1074/jbc.M609337200.
- (46) Davies, C. G.; Fellner, M.; Tchesnokov, E. P.; Wilbanks, S. M.; Jameson, G. N. L. The

- Cys-Tyr Cross-Link of Cysteine Dioxygenase Changes the Optimal Ph of the Reaction without a Structural Change. *Biochemistry* **2014**, *53* (50), 7961–7968. https://doi.org/10.1021/bi501277a.
- (47) Fischer, A. A.; Miller, J. R.; Jodts, R. J.; Ekanayake, D. M.; Lindeman, S. V; Brunold, T. C.; Fiedler, A. T. Spectroscopic and Computational Comparisons of Thiolate-Ligated Ferric Nonheme Complexes to Cysteine Dioxygenase: Second-Sphere Effects on Substrate (Analogue) Positioning. *Inorg. Chem.* 2019, 58 (24), 16487–16499. https://doi.org/10.1021/acs.inorgchem.9b02432.
- (48) Driggers, C. M.; Hartman, S. J.; Karplus, P. A. Structures of Arg- and Gln-Type Bacterial Cysteine Dioxygenase Homologs. *Protein Sci.* 2015, 24 (1), 154–161. https://doi.org/10.1002/pro.2587.
- (49) York, N. J.; Lockart, M. M.; Sardar, S.; Khadka, N.; Shi, W.; Stenkamp, R. E.; Zhang, J.; Kiser, P. D.; Pierce, B. S. Structure of 3-Mercaptopropionic Acid Dioxygenase with a Substrate Analog Reveals Bidentate Substrate Binding at the Iron Center. *J. Biol. Chem.* 2021, 296, 100492. https://doi.org/10.1016/j.jbc.2021.100492.
- (50) Licausi, F.; Van Dongen, J. T.; Giuntoli, B.; Novi, G.; Santaniello, A.; Geigenberger, P.; Perata, P. HRE1 and HRE2, Two Hypoxia-Inducible Ethylene Response Factors, Affect Anaerobic Responses in Arabidopsis Thaliana. *Plant J.* 2010, 62 (2), 302–315. https://doi.org/10.1111/j.1365-313X.2010.04149.x.
- (51) Licausi, F.; Kosmacz, M.; Weits, D. A.; Giuntoli, B.; Giorgi, F. M.; Voesenek, L. A. C. J.; Perata, P.; Van Dongen, J. T. Oxygen Sensing in Plants Is Mediated by an N-End Rule Pathway for Protein Destabilization. *Nature* 2011, 479 (7373), 419–422. https://doi.org/10.1038/nature10536.
- (52) Weits, D. A.; Giuntoli, B.; Kosmacz, M.; Parlanti, S.; Hubberten, H. M.; Riegler, H.; Hoefgen, R.; Perata, P.; Van Dongen, J. T.; Licausi, F. Plant Cysteine Oxidases Control the Oxygen-Dependent Branch of the N-End-Rule Pathway. *Nat. Commun.* 2014, 5.

- https://doi.org/10.1038/ncomms4425.
- (53) Wang, Y.; Griffith, W. P.; Li, J.; Koto, T.; Wherritt, D. J.; Fritz, E.; Liu, A. Cofactor Biogenesis in Cysteamine Dioxygenase: C-F Bond Cleavage with Genetically Incorporated Unnatural Tyrosine. *Angew. Chemie Int. Ed.* 2018, 57 (27), 8149–8153. https://doi.org/10.1002/anie.201803907.
- (54) White, M. D.; Kamps, J. J. A. G.; East, S.; Taylor Kearney, L. J.; Flashman, E. The Plant Cysteine Oxidases from Arabidopsis Thaliana Are Kinetically Tailored to Act as Oxygen Sensors. *J. Biol. Chem.* 2018, 293 (30), 11786–11795.
 https://doi.org/10.1074/jbc.RA118.003496.
- (55) Masson, N.; Keeley, T. P.; Giuntoli, B.; White, M. D.; Lavilla Puerta, M.; Perata, P.; Hopkinson, R. J.; Flashman, E.; Licausi, F.; Ratcliffe, P. J. Conserved N-Terminal Cysteine Dioxygenases Transduce Responses to Hypoxia in Animals and Plants. Science (80-.). 2019, 364 (6448), 65–69. https://doi.org/10.1126/science.aaw0112.
- (56) Lee, M. J.; Tasaki, T.; Moroi, K.; An, J. Y.; Kimura, S.; Davydov, I. V.; Kwon, Y. T. RGS4 and RGS5 Are in Vivo of the N-End Rule Pathway. *Proc. Natl. Acad. Sci. U. S. A.* 2005, 102 (42), 15030–15035. https://doi.org/10.1073/pnas.0507533102.
- (57) Tamirisa, P.; Blumer, K. J.; Muslin, A. J. RGS4 Inhibits G-Protein Signaling in Cardiomyocytes. *Circulation* 1999, 99 (3), 441–447. https://doi.org/10.1161/01.CIR.99.3.441.
- (58) Wang, Y.; Davis, I.; Chan, Y.; Naik, S. G.; Griffith, W. P.; Liu, A. Characterization of the Nonheme Iron Center of Cysteamine Dioxygenase and Its Interaction with Substrates. *J. Biol. Chem.* 2020, 295 (33), 11789–11802. https://doi.org/10.1074/jbc.ra120.013915.
- (59) Pierce, B. S.; Gardner, J. D.; Bailey, L. J.; Brunold, T. C.; Fox, B. G. Characterization of the Nitrosyl Adduct of Substrate-Bound Mouse Cysteine Dioxygenase by Electron Paramagnetic Resonance: Electronic Structure of the Active Site and Mechanistic Implications. *Biochemistry* 2007, 46 (29), 8569–8578. https://doi.org/10.1021/bi700662d.

- (60) Kumar, D.; Thiel, W.; De Visser, S. P. Theoretical Study on the Mechanism of the Oxygen Activation Process in Cysteine Dioxygenase Enzymes. *J. Am. Chem. Soc.* 2011, 133 (11), 3869–3882. https://doi.org/10.1021/ja107514f.
- (61) Krebs, C.; Bollinger, J. M. Non-Heme Fe (IV)— Oxo Intermediates. Acc. Chem. Res. 2007, 40 (7), 484–492.
- (62) Blaesi, E. J.; Gardner, J. D.; Fox, B. G.; Brunold, T. C. Spectroscopic and Computational Characterization of the NO Adduct of Substrate-Bound Fe(II) Cysteine Dioxygenase: Insights into the Mechanism of O2 Activation. *Biochemistry* 2013, 52 (35), 6040–6051. https://doi.org/10.1021/bi400825c.

CHAPTER 2

SPECTROSCOPIC INVESTIGATION OF CYSTEAMINE DIOXYGENASE

This chapter has been published under the following: Fernandez, R. L.; Dillon, S. L.; Stipanuk, M. H.; Fox, B. G.; Brunold, T. C. Spectroscopic Investigation of Cysteamine Dioxygenase. *Biochemistry* **2020**. *59*, 2450-2458. https://doi.org/10.1021/acs.biochem.0c00267.

Chapter 2: Spectroscopic Investigation of Cysteamine Dioxygenase

2.1 Introduction

Taurine plays many essential roles in mammalian metabolism.^{1–4} This sulfonic acid-containing metabolite helps to maintain homeostasis of important intracellular ions through osmotic regulation, preservation of cardiac and vascular functions, protection of neural cells from excitotoxicity, and stabilization of skeletal muscle membranes, among many functions.^{1–3} The best-studied pathway for taurine biosynthesis starts with the O₂-dependent conversion of cysteine (Cys) to cysteine sulfinic acid by cysteine dioxygenase (CDO). Cysteine sulfinic acid is then further broken down to hypotaurine and, finally, taurine.

Scheme 2.1. Simplified schematic of multiple pathways of Cys metabolism, where the number of steps required for the conversion of reactant to product is highlighted by the number of arrows. CDO catalyzes the first step in the conversion of Cys to cysteine sulfinic acid. ADO catalyzes the conversion of cysteamine to hypotaurine.^{4,5}

Hypotaurine is also produced by the oxidation of cysteamine (2-aminoethanethiol, 2-AET), catalyzed by cysteamine dioxygenase (ADO, **Scheme 2.1**).^{4,5} Cys serves as a building block for the formation of coenzyme A, which is in turn degraded by pantetheinase into pantetheine and 2-

AET. Although an enzyme responsible for the oxidation of 2-AET to hypotaurine has been postulated since the 1960's, 6-8 the investigation of ADO has been hindered by the reliance on isolating the enzyme from crude tissue. The gene responsible for ADO production was finally discovered in 2007 when Dominy *et al.* found a discrepancy between the levels of taurine biosynthesis and CDO expression in various tissues. This finding suggested that the generation of hypotaurine by ADO turnover may be responsible for the majority of taurine production in some tissues, particularly the brain. Thus, ADO appears to play a larger role in taurine biosynthesis and Cys catabolism than had originally been assumed. Interestingly, a recent report argued that the function of ADO has been misidentified and its primary function is instead to oxidize aminoterminal Cys residues of proteins in response to hypoxia. The protection is instead to oxidize aminoterminal Cys residues of proteins in response to hypoxia.

Recently, four known non-heme Fe^{II}-dependent thiol dioxygenases [collectively TDOs: CDO, ADO, 3-mercaptopropionate dioxygenase (MDO), and mercaptosuccinate dioxygenase (MSDO)], have been identified as members of the cupin superfamily with essential roles in mammalian Cys metabolism. Proteins in the cupin superfamily are typically metalloproteins that show low overall sequence identity but contain two short, highly conserved primary sequence motifs, Gx₅HxHx₃₋₆Ex₆G (cupin motif 1) and Gx₅₋₇PxGx₂Hx₃N (cupin motif 2), separated by an inter-motif region that varies both in length (~15-50 residues) and amino acid sequence. 11 X-ray crystallographic studies have shown that the CDO and MDO active sites feature an Fe^{II} center that is coordinated by a 3-Histidine (3-His) triad (Figure 2.1). 12,13 This binding motif is exceedingly rare in Fe^{II}-dependent oxygenases, which typically adopt a 2-His-1-carboxylate motif. 14,15 Only a small number of other proteins have been definitively established by crystallography to feature this Fe binding motif, including diketone-cleaving dioxygenase, ¹⁶ gentisate 1,2-dioxygenase, ¹⁷ and SznF.¹⁸ An unusual crosslink between Cys93 and Tyr157 present near the primary coordination sphere of CDO (Figure 2.1, left) plays a role in properly orienting substrate and suppressing water coordination to Cys-bound Fe^{II}CDO to preserve an open coordination site for O₂. ^{19,20} Cys-Tyr crosslinks have only been observed in two other enzymes; namely, galactose

oxidase, where it serves as a reversible one-electron source,²¹ and NirA, where its function is unknown.²²

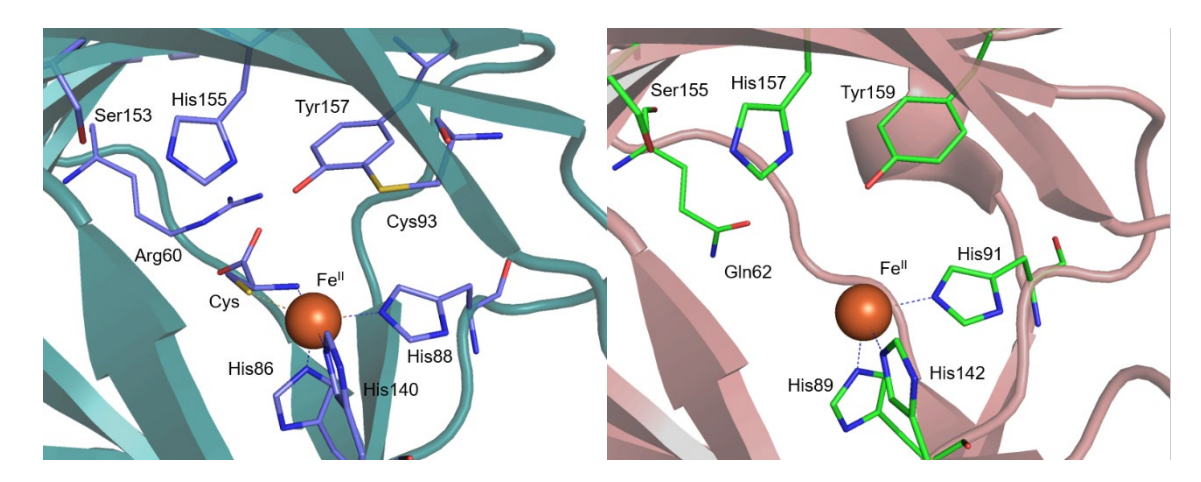


Figure 2.1. Left: Active site region of the crystal structure of Cys-bound *Mus musculus* CDO (PDB code: 4JTO).²³ Right: Active site region of the crystal structure of resting MDO from *Pseudomonas aeruginosa* (PDB code: 4TLF).¹³

While the three-dimensional structure of ADO is not yet known, a sequence alignment with *Mus musculus* CDO revealed that despite the low sequence identity (14%), strong similarities exist between these enzymes, including the two cupin motifs.¹¹ Importantly, both CDO and ADO lack the highly conserved glutamate residue found in cupin motif 1 that is typical of other metal-binding cupin proteins. This sequence alignment of CDO and ADO also predicts the conservation of the 3-His facial triad that binds Fe^{II} in CDO. The substitution of one of these histidine residues of ADO by an alanine completely abolished catalytic activity, further supporting the hypothesis that this enzyme contains a 3-His facial triad.²⁴

Interestingly, the total iron content in as-isolated ADO is much higher than in CDO, suggesting important differences in the active site pocket. Indeed, residues deemed to play a role in the catalytic cycle of CDO or in maintaining the structural integrity, including a Ser153-His155-Tyr157 "catalytic triad" and the Cys93 involved in the Cys-Tyr crosslink of mammalian CDOs (**Figure 2.1**), are not conserved in ADO. The substitution of Cys93 in CDO by a Gly in ADO suggests that the latter might be more similar to MDO or bacterial CDOs, which do not possess

this crosslink (**Figure 2.1**). ^{12,25} However, the existence of a Cys220-Tyr222 crosslink in ADO in a distinct location from the CDO crosslink was recently established via genetic incorporation of an unnatural amino acid, 3,5-difluoro-tyrosine into ADO and characterization of this species with mass spectrometry and NMR spectroscopy. ²⁶ Interestingly, Arg60 (mouse CDO numbering, **Figure 2.1, left**), which has been postulated to play a role in regulating substrate specificity in CDO, is also not conserved in ADO. MDOs have been shown by X-ray crystallography to feature a Gln at the position corresponding to Arg60 of CDO (**Figure 2.1, right**), ^{13,27} and are unable to efficiently produce cysteine sulfinic acid from Cys; instead, they have evolved to utilize 3-mercaptopropionic acid (3-MPA) as their native substrate. ²⁵ The absence of both of these residues in ADO (based on sequence alignment) reveals another important difference in the active sites between these paralogs and suggests that amino acid variations among the active sites may play an important role in modulating substrate specificity.

Although CDO is capable of converting 2-AET to hypotaurine, the specific activity is reduced more than 10-fold relative to Cys oxidation. Similarly, ADO displays high substrate specificity, and is unable to convert Cys to cysteine sulfinic acid despite the structural similarities between 2-AET and Cys.²⁴ To gain further understanding of the potential differences between the active sites of ADO and CDO, we have used magnetic circular dichroism (MCD) and electron paramagnetic resonance (EPR) spectroscopies to study complexes of ADO with its native substrate 2-AET, as well as the weakly competitive inhibitor Cys,²⁴ and another structurally similar substrate analogue, 3-MPA. Collectively, our data yield new insight into the geometric and electronic structures of the ADO active site and provide clues regarding the origin of the substrate specificity displayed by this enzyme.

2.2 Materials and Methods

Recombinant Gene Expression and Protein Purification. A codon-optimized ADO gBlock was ordered from Integrated DNA Technology and inserted into a pET small ubiquitin-related modifier (SUMO) expression vector via Gibson Assembly.²⁸ The sequence of the cloned gene was verified

at the University of Wisconsin-Madison Biotechnology Center. ADO was produced as previously described with minor changes. Escherichia coli Rosetta 2(DE3) cells were grown at 37 °C in 4 L of LB medium (containing 10 g tryptone, 10 g NaCl, 5 g of yeast extract per liter). All cultures were inoculated with 50 μ g/mL kanamycin and 34 μ g/mL chloramphenicol. The cells were grown to an OD600 of ~4 and gene overexpression was induced by the addition of isopropyl- β -D-thiogalactopyranoside to a final concentration of 0.2 mM and supplemented with ferrous ammonium sulfate to a final concentration of 100 μ M. Four hours post-induction, cells were harvested via centrifugation at 4,402×g for 20 min at 4 °C. The cell paste was flash frozen and stored at -80 °C overnight.

Frozen cell paste was thawed in 80 mL of 20 mM Tris buffer, pH 8.0, containing 250 mM NaCl, 5 mM imidazole, 1mM TCEP and four tablets of Roche Complete protease inhibitor (IMAC Buffer A). The cell suspension was lysed via pulsed sonication (15 s on, 30 s off for 10 min on ice). Soluble protein was separated from cellular debris by centrifugation for 30 min at 48,400×g at 4 °C. After filtering the supernatant with a 0.8 µm filter, the filtrate was applied to a 5-mL HisTrap-FF column. Protein was eluted in a linear gradient of IMAC Buffer A and 20 mM Tris, pH 8.0, containing 250 mM NaCl and 500 mM imidazole (IMAC Buffer B). As reported previously, two elution peaks were observed at ~5 mM imidazole ~75 mM imidazole (15% IMAC Buffer B).²⁴ Stain-free sodium dodecyl sulfate-polyacrylamide gel electrophoresis (SDS-PAGE) was used to verify the presence of target protein (~42 kDa total: 28 kDa target protein and 14kDa SUMO tag) in both peaks. Due to its higher purity, only protein associated with the second peak was kept for further purification. The fractions containing SUMO-tagged ADO were pooled, concentrated to 1 mL, and dialyzed overnight at 4 °C against a 20 mM Tris, pH 8.0, containing 250 mM NaCl to remove imidazole. The following morning the protein was concentrated to ~5 mg/mL, divided into two aliquots so as not to overload the column, and applied to a HiLoad 16/600 Superdex 200pg gel filtration column. The protein was separated into two elution peaks, with the second peak corresponding to 42 kDa expected for the folded, soluble fusion protein. Fractions containing the most pure and active ADO as judged by SDS-PAGE and a qualitative activity assay, were pooled and concentrated (**Figure A2.1**). Total protein yield was estimated using the absorbance at 280 nm and an extinction coefficient of 41.4 mM⁻¹cm⁻¹, calculated via ExPASy²⁹ from the SUMO-tag and ADO protein sequences. The Fe^{II} and total Fe contents of the protein were determined through a colorimetric assay using the iron chelator 2,4,6-tris(2-pyridyl)-s-triazine (TPTZ) and an ε₅₉₅ of 22.1 mM⁻¹cm⁻¹.^{30,31} The assay was performed in the presence and absence of a reductant (hydroxylamine) to determine the proportion of Fe^{II} versus Fe^{III} initially present. As the fraction of Fe-bound ADO active sites was ~70-80%, the concentration of protein (0.6 mM for MCD spectroscopy and 0.5 mM for EPR spectroscopy) cited herein refers to the Fe-bound fraction, not that of the total protein. Protein aliquots to be used for spectroscopic characterization were flash frozen and stored at -80 °C.

Enzyme activity assays. Enzymatic activity was determined qualitatively using thin layer chromatography (TLC), similar to methods established for CDO.³² Briefly, SUMO-tagged ADO was incubated aerobically with 20 mM 2-AET in Tris buffer, pH 8.0 at 37 °C for 30 min. Samples were heat denatured to stop the reaction and centrifuged for 5 min at 14,000 rpm in a table-top centrifuge to remove precipitated protein. The supernatant was spotted onto a silica TLC plate and placed in a beaker containing 20:20:60 (v/v) H₂O/acetic acid/1-butanol running solution. After one hour, the plate was removed and developed with a 1.5% ninhydrin solution (w/v) in 3% (v/v) acetic acid in ethanol. Heat activation of the stain allowed for the identification of bands associated with 2-AET and hypotaurine by comparison with a control standard (Figure A2.3). Two peaks arise from our 2-AET standard; while the origin of the lower feature is not conclusively known, we postulate that the second peak could be due to cystamine formation.

Sample preparation. Samples used for MCD spectroscopy were prepared anaerobically in a glovebox under a nitrogen atmosphere, while those used for EPR spectroscopy were prepared aerobically. Where applicable, 2-AET was added at 5-fold molar excess over Fe-bound ADO,

while the substrate analogues L-cysteine (Cys) and 3-mercaptopropionic acid (3-MPA) were added at a 10-fold molar excess. For MCD spectroscopic studies of Fe^{III}ADO, a sub-stoichiometric amount of dithionite relative to the total iron content was added to reduce the fraction of Fe^{III}-bound sites to the Fe^{III} state. Samples for low-temperature (LT) MCD studies also contained 55% (v/v) glycerol as a glassing agent.

Spectroscopy. LT MCD spectra were collected with a Jasco J-715 spectropolarimeter in conjunction with an Oxford Instruments SM4000-8T magnetocryostat. MCD spectra are presented as the difference between spectra obtained with the magnetic field aligned parallel and antiparallel to the light propagation axis to eliminate contributions from the CD background and glass strain. For Cys-bound ADO, variable temperature, variable field (VTVH) MCD data were collected by measuring the signal intensity as a function of magnetic field at a constant wavelength (477 nm = 20.964 cm⁻¹) for several fixed temperatures. The data were fitted with the S=1/2 Brillouin function³³

$$B_{1/2}(x) = \tanh(x)$$

where $x = \frac{u_J H}{k_B T}$, μ_j is the Bohr magneton, H is the field (in Tesla), k_B is the Boltzmann constant, and T is the temperature.

X-band EPR data were collected using a Bruker ELEXSYS E500 spectrometer. The sample temperature was maintained at 20 K by an Oxford ESR 900 continuous flow liquid He cryostat regulated by an Oxford ITC-503S temperature controller. All spectra were obtained using the following experimental parameters: frequency = 9.386 GHz; microwave power = 12.62 mW; modulation amplitude = 3 G; modulation frequency = 100 kHz. The program EasySpin (version 5.2.25) was used to fit the experimental EPR spectra.³⁴

2.3 Results

As-isolated ADO is a translucent pale yellow in color, likely reflecting the small, but significant, fraction of active sites containing Fe^{III}. ³⁵ Upon addition of 2-AET, the protein solution

turns faint blue in color, indicative of substrate coordinating to the Fe^{III}-bound active sites. Indeed, the pair of positively signed features at 14,400 and ~17,800 cm⁻¹ in the low-temperature (LT) MCD spectrum of the 2-AET adduct of as-isolated ADO (**Figure 2.2A**), which is absent in the MCD spectrum of as-isolated, resting ADO (data not shown), provides compelling evidence for the formation of an inner-sphere complex between Fe^{III}ADO and 2-AET. These features are highly characteristic of S→Fe^{III} charge transfer (CT) transitions of high-spin (S=5/2) Fe^{III}-thiolate complexes, which implies that 2-AET coordinates to Fe^{III}ADO via its thiol group.³⁶ The MCD spectrum of as-isolated ADO incubated with 2-AET also exhibits a large temperature dependent feature in the near UV-region, as well as the onset to a weaker temperature dependent feature in the near IR-region.

To more definitively establish the origin of the features at 14,400 and 17,800 cm⁻¹ in the LT MCD spectrum of as-isolated ADO in the presence of 2-AET, LT MCD spectra were also collected for dithionite-reduced Fe^{II}ADO incubated with 2-AET (**Figure 2.3**). The loss of these features in the reduced sample corroborates their assignment as S→Fe^{III} CT transitions arising from Fe^{III}ADO. In contrast, the positively signed features in the near-UV and the near-IR region are retained upon Fe^{III} reduction, indicating that they are associated with Fe^{III}ADO. The onset to the feature in the near-IR region at 10,000 cm⁻¹ is likely due to an Fe^{III} d→d transition, based on a comparison with MCD data reported for other Fe^{III} complexes.³⁷ However, further spectroscopic studies are needed to conclusively assign these features (note that the near UV feature is also present in the MCD spectrum of resting ADO).

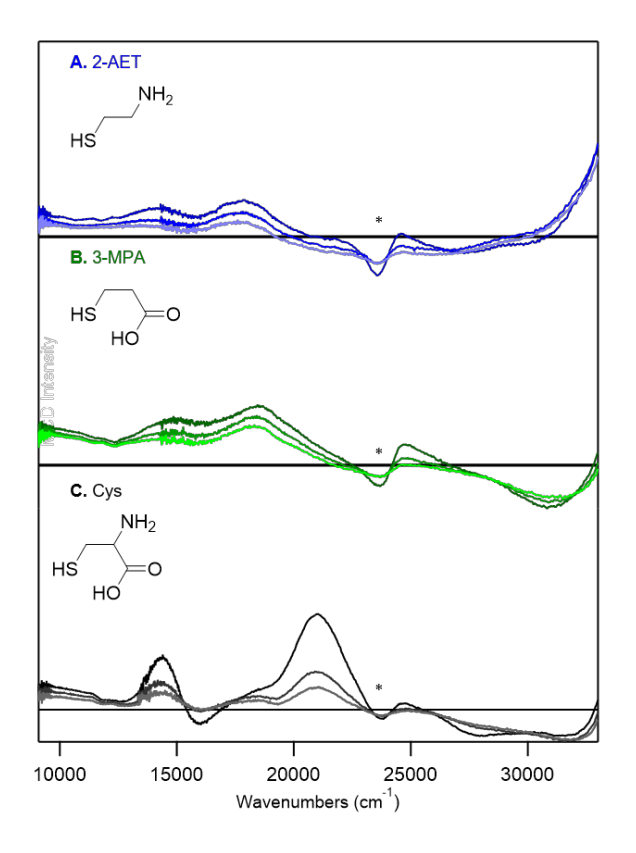


Figure 2.2. MCD spectra at 4, 15, and 25 K of as-isolated ADO incubated with various substrate (analogues): A) ADO incubated with a 5-fold excess of 2-AET; B) ADO incubated with a 10-fold excess of 3-MPA; C) ADO incubated with a 10-fold excess of Cys. The feature indicated by * arises from a minor heme impurity.

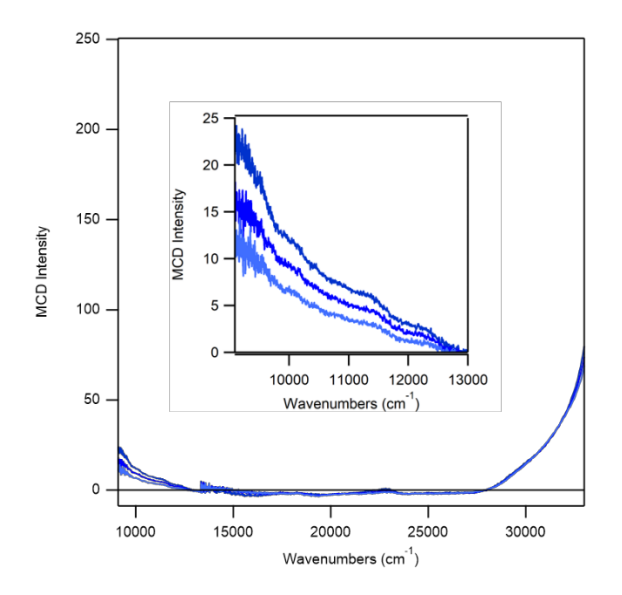


Figure 2.3. MCD spectra at 4, 15, and 25 K of FellADO incubated with a 5-fold excess of 2-AET.

Our research group and others gained important insights into the nature of substrate/active site interactions in the Fe^{II}-dependent thiol dioxygenases CDO and MDO by utilizing substrate analogues. ^{31,32,35,38,39} Here, we have employed the same strategy by incubating as-isolated ADO with Cys and 3-MPA. Previous work has revealed that Cys is not a substrate for ADO; however, it does act as a weak competitive inhibitor, suggesting that it is capable of binding to the active site. ²⁴ Moreover, while both 2-aminoethanethiol and Cys contain amino groups that can coordinate to the iron center, 3-MPA does not. Thus, by comparing spectroscopic data obtained for ADO incubated with 2-AET, Cys, or 3-MPA, it is possible to infer whether the amino, thiol, and/or carboxylate groups bind to Fe^{II} ion.

Incubation of as-isolated ADO with 3-MPA results in an MCD spectrum that is nearly identical to that of 2-AET-bound ADO (**Figure 2.2B**). Specifically, the onset to a positive feature displayed by ADO incubated with 2-AET in the near UV-region (>32,000 cm⁻¹) is retained, as is the feature in the near-IR region. In addition, the two features in the visible region (at ~14,000 and 18,000 cm⁻¹) display the same saturation behavior as their counterparts in the 2-AET bound asisolated ADO spectrum, indicating that 3-MPA binds in a very similar manner as the native substrate. Thus, our results may indicate that 2-AET coordinates to the Fe^{III}ADO active site in a monodentate fashion, via coordination of only its terminal thiol. Notably, a similar monodentate, thiol-only binding mode has previously been proposed by Pierce *et al.* for 3-MPA coordination to MDO on the basis of EPR experiments.²⁵

Incubation of as-isolated ADO with a 10-fold excess of Cys leads to an MCD spectrum that is drastically different from those observed for ADO treated with 2-AET or 3-MPA (**Figure 2.2C**). While the onset to a positive feature in the near-UV region (>34,000 cm⁻¹) is retained, numerous positively and negatively signed features appear in the visible region that have no counterparts in the other MCD spectra. Notably, these features display a distinctly different saturation behavior than those associated with 2-AET bound Fe^{III}ADO, implying that the Cys adduct of ADO possesses a different spin ground state. Indeed, the variable-temperature

variable-field (VTVH) MCD data collected for the intense feature at 20,964 cm⁻¹ can be fit with an S = 1/2 Brillouin function, consistent with the formation of a low-spin Fe^{III} complex (**Figure 2.4**).

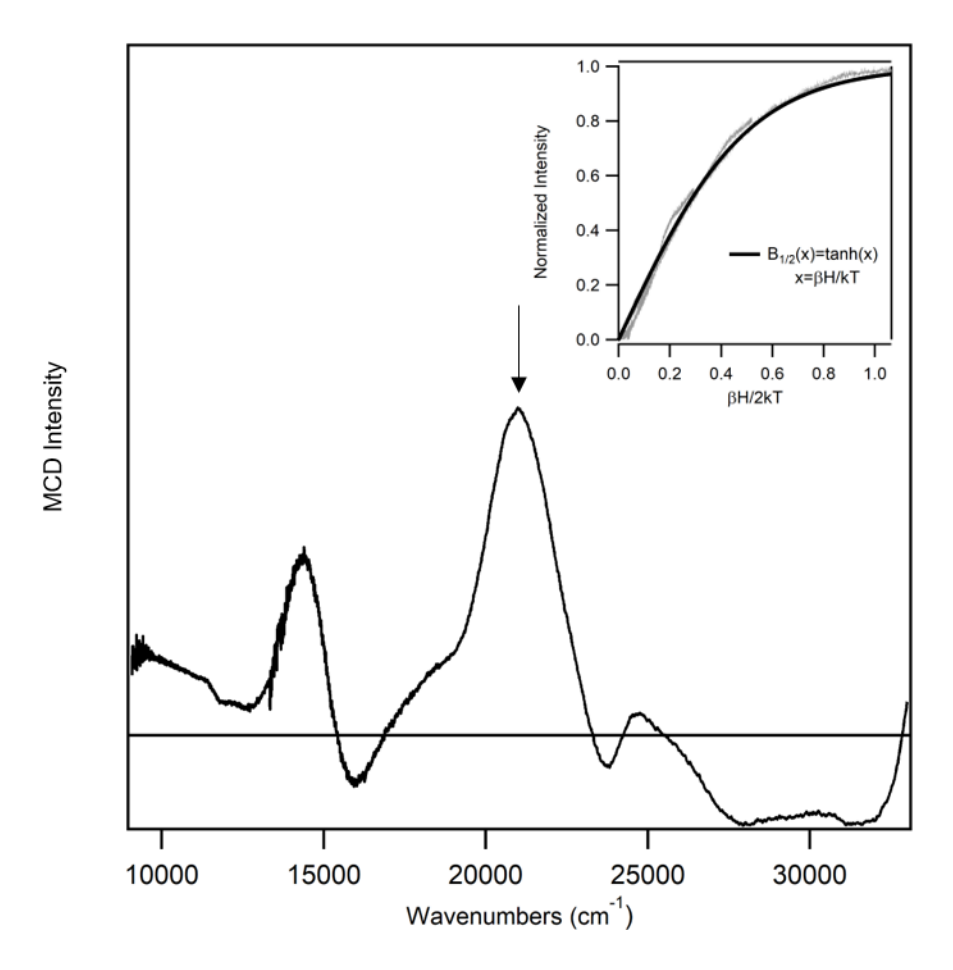


Figure 2.4. MCD spectrum at 4 K of as-isolated ADO incubated with a ~15-fold excess of Cys. Inset: VTVH MCD data (gray) collected for ADO + Cys at 20.964 cm-1 (indicated by vertical arrow) at 2.2, 4.5, 8, 15, and 25 K superimposed by a Brillouin function for S=1/2 (black).

EPR spectroscopy was employed as a complementary tool to probe the electronic structure of the Fe^{III}ADO active site and to monitor changes in response to substrate (analogue) binding. As-isolated ADO exhibits a nearly rhombic, high-spin (S = 5/2) signal centered at $g_{eff} \approx 4.3$ (**Figure 2.5A**), similar to that displayed by as-isolated CDO.³² The addition of 2-AET yields a new, more axial EPR signal attributable to an S=5/2 Fe^{III} species (**Figure 2.5B**). Consistent with our MCD data, the appearance of this distinct high-spin EPR signal demonstrates the formation

of an inner-sphere 2-AET-Fe^{III}ADO complex (see **Appendix 2** for EPR fitting parameters and g-values). Incubation of as-isolated ADO with 3-MPA also results in a more axial high-spin (S = 5/2) EPR spectrum (**Figure 2.5C**). The nearly identical EPR spectra displayed by 3-MPA- and 2-AET-bound Fe^{III}-ADO indicate that 3-MPA binds in a similar manner to the native substrate, supporting our hypothesis that 2-AET coordinates to the Fe^{III}ADO active site solely via its terminal thiol.

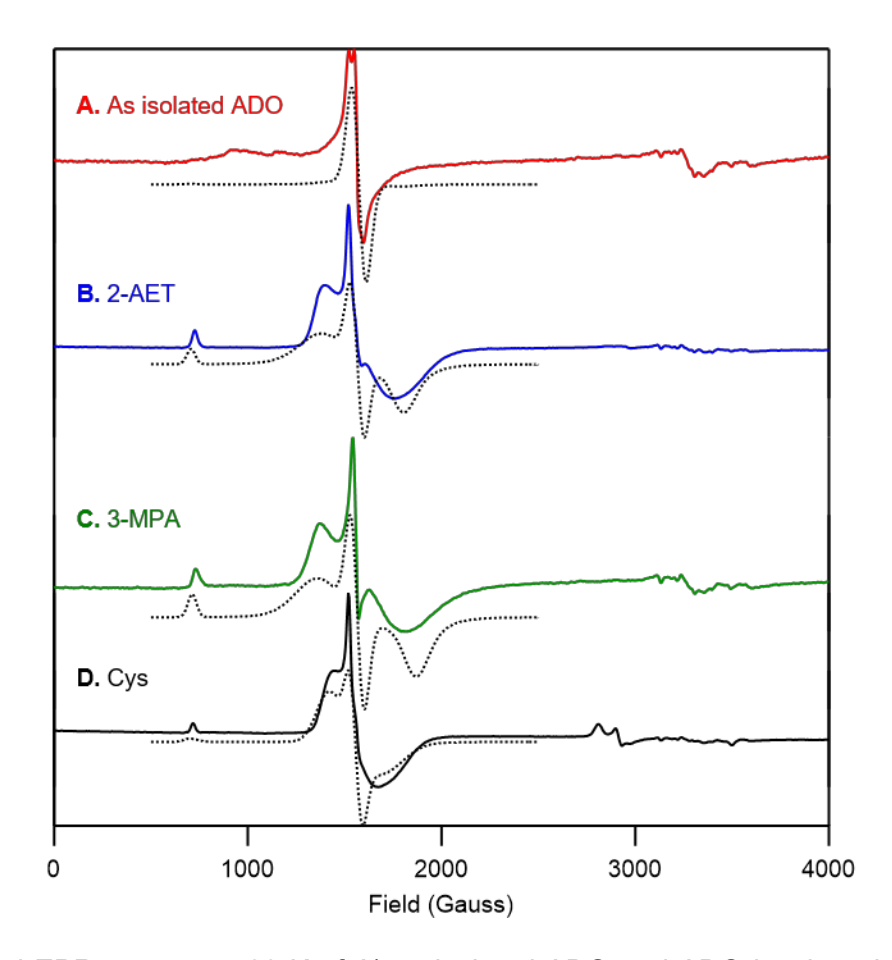


Figure 2.5. X-band EPR spectra at 20 K of A) as-isolated ADO and ADO incubated with B) 2-AET, C) 3-MPA, and D) Cys. Fit parameters are provided in the Supporting Information.

Incubation of as-isolated ADO with Cys results in the formation of a high-spin (S=5/2) species that exhibits a similar, albeit slightly more rhombic EPR signal than 2-AET-bound Fe^{III}-ADO (**Figure 2.5D**), which seemingly conflicts with our MCD spectra of the Cys adduct. However, the high-field region of the EPR spectrum obtained for ADO incubated with the substrate analogue Cys also shows a new signal at $g \approx 2.4$ (**Figure 2.5D**), consistent with the formation of a low-spin

(S=1/2) Fe^{III} species as suggested by our VTVH MCD data (**Figure 2.4**). The fact that both highand low-spin Cys-bound Fe^{III}ADO species contribute to the EPR spectrum may seem puzzling, as the MCD spectrum of Cys-bound ADO is dominated by a low-spin species.

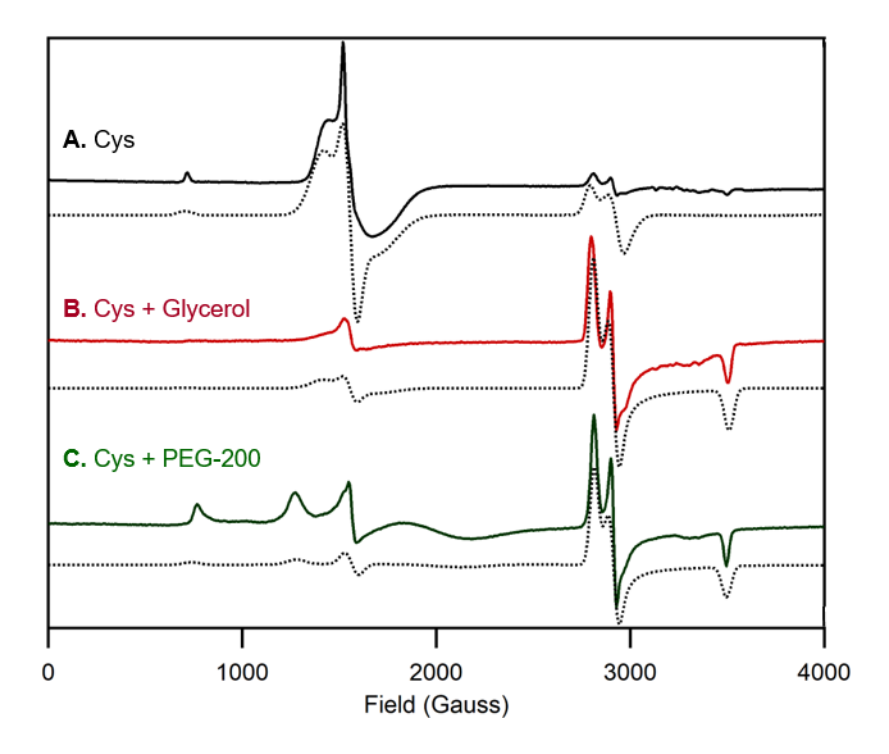


Figure 2.6. X-band EPR spectra at 20 K of as-isolated ADO incubated with A) a 10-fold excess of Cys, B) a 10-fold excess of Cys and 55% (v/v) glycerol, and C) a 10-fold excess of Cys and 55% (v/v) PEG-200. Fit parameters are provided in the Supporting Information.

The apparent discrepancy between the ratio of high-spin and low-spin species contributing to the MCD and EPR spectra of Cys-bound Fe^{III}ADO prompted us to prepare EPR samples with glycerol, the glassing agent used for MCD studies. Upon incubation of ADO with Cys and glycerol, a drastic increase in the relative intensity of the S=1/2 signal is observed (**Figure 2.6B**). Notably, such a change in the relative intensities of the S = 5/2 and S = 1/2 signal was not seen in the presence of 2-AET (data not shown). To assess whether this shift in high-spin to low-spin ratio could be due to glycerol binding to the active site, polyethylene glycol 200 (PEG-200) was used as an alternative glassing agent. Cys was still able to coordinate to Fe^{III}ADO and the low-spin species was found to be the major product (**Figure 2.6C**), though the formation of a distinct high-

spin Fe^{III} species is evident from the appearance of new signals in the 800-1700 Gauss range. Thus, coordination of glycerol to the Cys-bound Fe^{III}ADO active site can be ruled out as being responsible for the formation of a low-spin (S = 1/2) Fe^{III} complex.

Finally, to further validate the 3-His triad implicated in ADO and demonstrate that our spectra are dominated by contributions from Fe residing in the ADO active site, the putative Fe ligand His100 was replaced by Ala and as-isolated H100A ADO was characterized by EPR spectroscopy. Importantly, the high-spin (S=5/2) EPR signals displayed by WT ADO incubated with 2-AET are noticeably absent in the spectrum of H100A ADO in the presence of substrate (**Figure 2.7B**). Thus, we conclude that Fe bound to WT ADO is present in the active site and, thus, that non-specifically bound Fe ions contribute minimally to our MCD and EPR spectra of the WT enzyme.

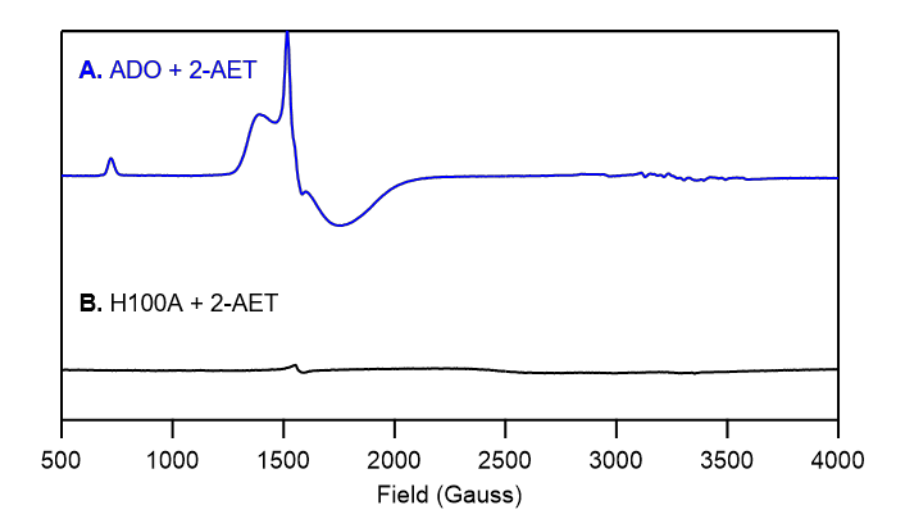


Figure 2.7. X-band EPR spectra at 20 K of A) as-isolated wild-type ADO and B) the H100A ADO variant incubated with a 5-fold excess of 2-AET.

2.4 Discussion

Although ADO was discovered more than ten years ago, relatively little is known about this important sulfur-metabolism enzyme. Apart from one recent study demonstrating the existence of a Cys-Tyr crosslink in ADO that is formed in a very different region of the primary sequence than in CDO,²⁶ little else has been published on ADO's structure and function. To start filling this

knowledge gap, we have used MCD and EPR spectroscopies to ascertain the coordination environment of the ADO active site.

The MCD spectrum of as-isolated ADO incubated with 2-AET is dominated by a pair of positively signed features at 14,400 and 17,800 cm⁻¹ (**Figure 2.2A**) reminiscent of those arising from S→Fe^{III} CT transitions in the MCD spectrum of Cys-bound CDO at 15,250 and 18,570 cm⁻¹. As replacement of a neutral His ligand with an anionic carboxylate would likely result in significant blue-shifts of the S→Fe^{III} CT features, our MCD data of 2-AET-bound ADO provide evidence that ADO also possesses a 3-His active site. In addition, the EPR spectrum of H100A incubated with 2-AET lacks the high-spin ferric signal observed in the EPR spectrum of 2-AET-bound ADO, further corroborating our hypothesis that ADO contains a neutral 3-His active site.

The striking similarities between the MCD spectra of ADO incubated with 2-AET and 3-MPA (Figure 2.3A and 2.3B), along with the fact that the S→Fe^{III} CT transitions of 2-AET-bound ADO are slightly red-shifted from those of Cys-bound CDO (consistent with a lower coordination number in ADO), suggest that 2-AET and 3-MPA bind to ADO in the same manner, potentially in a monodentate fashion through the terminal thiol. Thus, ADO appears to be the second TDO displaying monodentate substrate binding, as a both an EPR study of NO and 3-MPA-bound MDO²⁵ and a Mössbauer study of Cys-bound MDO¹³ afforded evidence for monodentate binding to Fe^{III}MDO via its thiol moiety. The EPR spectra of 2-AET- and 3-MPA-bound Fe^{III}ADO (Figure 2.5A and 2.5B) reveal that these high-spin ferric species exhibit a more axial zero-field splitting (E/D = 0.248 and 0.233, respectively) relative to that reported for Cys-bound Fe^{III}CDO (E/D = 0.171).³² This finding is consistent with a more dominant Fe—S bonding interaction in ADO, further corroborating our hypothesis that 2-AET and 3-MPA bind to Fe^{III}ADO solely through the terminal thiol.

Our MCD and EPR data indicate that Cys can bind directly to the ADO iron center, consistent with the notion that this substrate analogue is a weak competitive inhibitor.²⁴ Interestingly, the VTVH MCD data of Cys-bound ADO (**Figure 2.4**) provide evidence for the

formation of a low-spin (S=1/2) Fe^{III} complex, previously only observed for substrate (analogue)-bound Fe^{III}CDO incubated with the strong-field ligand cyanide.^{39,40} Our EPR data (**Figure 2.6**) reveal that the ratio of a low-spin to high-spin ferric species can be modulated by the addition of glycerol, with the high-spin Cys-Fe^{III}ADO complex being the predominant form in the absence of a glassing agent (**Figure 2.5**). The addition of PEG-200, instead of glycerol, to Cys-bound ADO also yields a low-spin species, arguing against the possibility that a change in spin state is due to direct glycerol coordination to the active site. Rather, our data support the hypothesis that the glassing (i.e., molecular crowding) agents induce a global protein conformational change, which further suggests that the ADO active site environment differs from that of CDO. Such differences in active site architecture are likely responsible for the distinct substrate specificities displayed by the various TDOs.

Comparison of ADO to other TDOs. Recently, the distinct substrate specificities displayed by CDO and MDO were attributed to key structural differences in the respective active site pockets; namely, the presence of an Arg or Gln at position 60 (Figure 2.1) and the presence of a *cis*-peptide bond between residues Ser158 and Pro159 in CDO (all *Rattus norvegicus* CDO numbering) that is absent in MDO.^{19,41,42} Cys binding to CDO occurs via bidentate coordination to the iron through the thiolate and amine groups, with the substrate carboxylate forming a salt bridge to Arg60. Because MDO features a Gln at the position corresponding to Arg60 of *Rn*CDO, it is unable to form a salt bridge with the carboxylate of its native substrate. Nevertheless, 3-MPA binding to MDO appears to occur via monodentate, thiolate-only coordination.²⁵ In contrast to Cys and 3-MPA, 2-AET does not contain a carboxylate. It is thus not surprising that based on sequence alignment, the residue in ADO corresponding to Arg60 of CDO is a Val, which is unable to hydrogen bond with a carboxylate. Although 2-AET features an amine group that could potentially coordinate to the iron of ADO, our EPR and MCD data favor monodentate, thiolate-only coordination of 2-AET, similar to 3-MPA binding to MDO.

Mammalian CDO features a thioether crosslink between Cys93 and Tyr157 (**Figure 2.1**) that has been implicated in properly orienting the substrates and suppressing the binding of a water molecule to Cys-bound Fe^{II}CDO so as to preserve an open coordination site for O₂. ^{19,20} Interestingly, the crosslinked and non-crosslinked forms of CDO can be distinguished via SDS-PAGE. *Bacillus subtilis* CDO does not form a thioether crosslink as it possesses a Gly at the position corresponding to Cys93, but does contain a *cis*-peptide bond that positions Tyr157 similarly as in *Rn*CDO.^{19,43} Despite the lack of both the thioether crosslink and *cis*-peptide bond in MDO, X-ray crystal structures revealed that in this enzyme Tyr159 adopts essentially the same orientation relative to the iron center as Tyr157 does in CDO.¹⁹ Similar to MDO, ADO also appears to lack a thioether crosslink involving the Tyr residue corresponding to Tyr157 in CDO as well as the *cis*-peptide bond. However, ADO has been shown to form a different thioether crosslink between Cys220 and Tyr222 (ADO numbering).²⁶ Although the exact role of this distal thioether crosslink in ADO remains to be elucidated, it is possible that it serves to impose an active site architecture similar to that of MDO, which also does not contain a *cis*-peptide bond.

The spectroscopic data obtained in the present study yield new insight into the active site geometry of ADO. The MCD spectra of the well-characterized Cys-bound Fe^{II} and Fe^{III}CDO species are similar to those of 2-AET-bound ADO,³⁶ strongly suggesting that these enzymes share the same 3-His active site coordination environment. As such, ADO is the fourth thiol dioxygenase that coordinates its metallocofactor via a 3-His triad instead of the more common 2-His-1carboxylate facial triad. Importantly, differences in substrate specificity between ADO and the other thiol dioxygenases likely stem from variations in key second-sphere residues present in CDO and MDO. ADO binds 2-AET and 3-MPA in a similar manner and does not appear to promote coordination of the amine functional group of 2-AET, supporting monodentate binding via the thiol moiety. Finally, a change in spin state of the Cys-bound Fe^{III}-ADO adduct in the presence of osmolytes may suggest that the active site of ADO is more sensitive to solution conditions than CDO.

ACCESSION CODES. ADO: Q6PDY2 CDO: P21816 MDO: Q9I0N5

ACKNOWLEDGMENTS.

The authors are grateful for financial support from the National Institute of General Medical Sciences of the National Institutes of Health (Grant GM117120 to T.C.B.). This research was conducted in part while R.L.F. and S.L.D. were supported by the National Institute of General Medical Sciences of the National Institutes of Health (Grant T32GM008505).

2.5 References

- (1) Huxtable, R. J. (1992) Physiological Actions of Taurine. *Physiol. Rev.* 72 (1).
- (2) Schaffer, S. W.; Ju Jong, C.; KC, R.; Azuma, J. (2010) Physiological roles of taurine in heart and muscle. *J. Biomed. Sci.* 17 (Suppl 1), S2.
- (3) Xu, Y.-J.; Arneja, A. S.; Tappia, P. S.; Dhalla, N. S. (2008) The potential health benefits of taurine in cardiovascular disease. *Exp. Clin. Cardiol.* 13 (2), 57–65.
- (4) Stipanuk, M. H. (1986) Metabolism of sulfur-containing amino acids. *Annu. Rev. Nutr.* 6(1), 179–209.
- (5) Stipanuk, M. H.; Dominy, J. E.; Lee, J.-I.; Coloso, R. M. (2006) Mammalian cysteine metabolism: New insights into regulation of cysteine metabolism. *J. Nutr.* 136 (6 Suppl), 1652S-1659S.
- (6) Cavallini, D.; Scandurra, R.; De Marco, C.(1963) The enzymatic oxidation of cysteamine to hypotaurine in the presence of sulfide. *J. Biol. Chem.* 238.
- (7) Rotilio, G.; Federici, G.; Calabrese, L.; Costa, M.; Cavallini, D. (1970) An electron paramagnetic resonance study of the nonheme iron of cysteamine oxygenase. *J. Biol. Chem.* 245 (22), 6235–6236.
- (8) Jacobsen, R. G.; Smith, L. H. (1968) Biochemistry and Physiology of Taurine and Taurine Derivatives. *Physio. Rev. 48*.
- (9) Dominy, J. E.; Simmons, C. R.; Karplus, P. A.; Gehring, A. M.; Stipanuk, M. H. (2006) Identification and characterization of bacterial cysteine dioxygenases: A new route of

- cysteine degradation for eubacteria. J. Bacteriol. 188 (15), 5561–5569.
- (10) Masson, N.; Keeley, T. P.; Giuntoli, B.; White, M. D.; Lavilla Puerta, M.; Perata, P.; Hopkinson, R. J.; Flashman, E.; Licausi, F.; Ratcliffe, P. J. (2019) Conserved N-terminal cysteine dioxygenases transduce responses to hypoxia in animals and plants. *Science*. 364 (6448), 65–69.
- (11) Stipanuk, M. H.; Simmons, C. R.; Karplus, P. A.; Dominy, J. E. (2011) Thiol dioxygenases: Unique families of cupin proteins. *Amino Acids*. *41*, 91–102.
- (12) McCoy, J. G.; Bailey, L. J.; Bitto, E.; Bingman, C. A.; Aceti, D. J.; Fox, B. G.; Phillips, G.
 N. (2006) Structure and mechanism of cysteine dioxygenase. *Proc. Natl. Acad. Sci.* 103 (9), 3084–3089.
- (13) Tchesnokov, E. P.; Fellner, M.; Siakkou, E.; Kleffmann, T.; Martin, L. W.; Aloi, S.; Lamont, I. L.; Wilbanks, S. M.; Jameson, G. N. L. (2015) The cysteine dioxygenase homologue from *Pseudomonas aeruginosa* is a 3-mercaptopropionate dioxygenase. *J. Biol. Chem.*290 (40), 24424–24437.
- (14) Straganz, G. D.; Nidetzky, B. (2006) Variations of the 2-His-1-carboxylate theme in mononuclear non-heme Fe(II) oxygenases. *ChemBioChem.* 7 (10), 1536–1548.
- (15) Koehntop, K. D.; Emerson, J. P.; Que, L. (2005) The 2-His-1-carboxylate facial triad: a versatile platform for dioxygen activation by mononuclear non-heme iron(III) enzymes. *Journal of Biological Inorganic Chemistry*. 87–93.
- (16) Diebold, A. R.; Neidig, M. L.; Moran, G. R.; Straganz, G. D.; Solomon, E. I. (2010) The three-his triad in Dke1: Comparisons to the classical facial triad. *Biochemistry.* 49 (32), 6945–6952.
- (17) Chen, J.; Li, W.; Wang, M.; Zhu, G.; Liu, D.; Sun, F.; Hao, N.; Li, X.; Rao, Z.; Zhang, X. C. (2008) Crystal structure and mutageinc analysis of GDOsp, a gentisate 1,2-dioxygenase from *Silicibacter Pomeroyi*. *Protein Sci.* 17 (8), 1362–1373.
- (18) Ng, T. L.; Rohac, R.; Mitchell, A. J.; Boal, A. K.; Balskus, E. P. (2019) An N-nitrosating

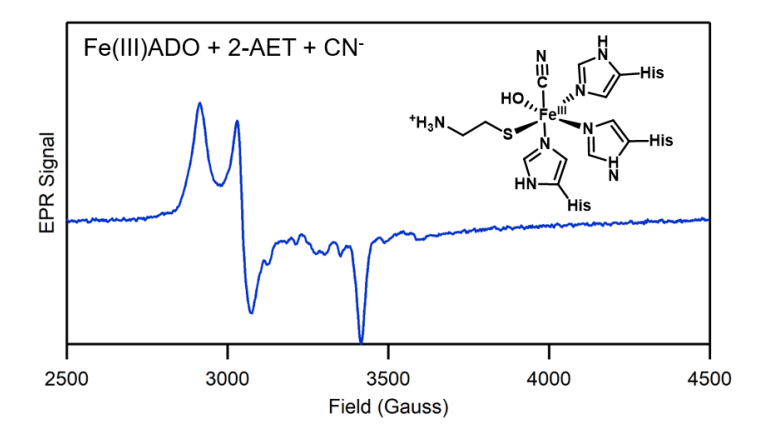
- metalloenzyme constructs the pharmacore of streptozotocin. Nature. 566 (7742) 94–99.
- (19) Aloi, S.; Davies, C. G.; Karplus, P. A.; Wilbanks, S. M.; Jameson, G. N. L. (2019) Substrate specificity in thiol dioxygenases. *Biochemistry*. *58* (19) 2398-2407.
- (20) Driggers, C. M.; Kean, K. M.; Hirschberger, L. L.; Cooley, R. B.; Stipanuk, M. H.; Karplus, P. A. (2016) Structure-based insights into the role of the Cys-Tyr crosslink and inhibitor recognition by mammalian cysteine dioxygenase. *J. Mol. Biol.* 428 (20), 3999–4012.
- Whittaker, M. M.; Ekberg, C. A.; Peterson, J.; Sendova, M. S.; Day, E. P.; Whittaker, J. W. (2000) Spectroscopic and magnetochemical studies on the active site copper complex in galactose oxidase. *J. Mol. Catal. B Enzym. 8* (1–3), 3–15.
- (22) Schnell, R.; Sandalova, T.; Hellman, U.; Lindqvist, Y.; Schneider, G. (2005) Sirohemeand [Fe4-S4]-dependent NirA from *Mycobacterium tuberculosis* is a sulfitre reductase with a covalent Cys-Tyr bond in the active site. *J. Biol. Chem.* 280 (29), 27319–27328.
- (23) Driggers, C. M.; Cooley, R. B.; Sankaran, B.; Hirschberger, L. L.; Stipanuk, M. H.; Karplus, P. A. (2013) Cysteine dioxygenase from pH4 to 9: Consistent Cys-persulfenate formation at intermediate pH and a Cys-bound enzyme at higher pH. *J.Mol.Biol.* 2013. 425, 3121–3136.
- (24) Dominy, J. E.; Simmons, C. R.; Hirschberger, L. L.; Hwang, J.; Coloso, R. M.; Stipanuk, M. H. (2007) Discovery and characterization of a second mammalian thiol dioxygenase, cysteamine dioxygenase. *J. Biol. Chem.* 282 (35), 25189–25198.
- (25) Pierce, B. S.; Subedi, B. P.; Sardar, S.; Crowell, J. K. (2015) The "Glin-type" thiol dioxygenase from *Azotobacter vinelandii* is a 3-mercaptopropionic dioxygenase. *Biochemistry*. *54* (51), 7477–7490.
- (26) Wang, Y.; Griffith, W. P.; Li, J.; Koto, T.; Wherritt, D. J.; Fritz, E.; Liu, A. (2018) Cofactor biogenesis in Cysteamine dioxygenase: C-F bond cleavage with genetically incorporated unnatural tyrosine. *Angew. Chemie Int. Ed. 57* (27), 8149–8153.
- (27) Driggers, C. M.; Hartman, S. J.; Karplus, P. A. (2015) Structures of Arg- and Gln-type

- bacterial cysteine dioxygenase homologs. Protein Sci. 24 (1), 154–161.
- (28) Gibson, D. G.; Young, L.; Chuang, R. Y.; Venter, J. C.; Hutchison, C. A.; Smith, H. O. (2009) Enzymatic assembly of DNA molecules up to several hundred kilobases. *Nat. Methods*. 6 (5), 343–345.
- (29) Gasteiger, E.; Hoogland, C.; Gattiker, A.; Duvaud, S.; Wilkins, M. R.; Appel, R. D.; Bairoch, A. Protein identification and analysis tools on the ExPASy server. In *The Proteomics Protocols Handbook*; Humana Press: Totowa, NJ, 2005; 571–607.
- (30) Fischer, D. S.; Price, D. C. (1964) A simple serum iron method using the new sensitive chromogen tripyridal-S-triazine. *Clin. Chem.* 10, 21–31.
- (31) Blaesi, E. J.; Fox, B. G.; Brunold, T. C. (2015) Spectroscopic and computational investigation of the H155A variant of cysteine dioxygenase: Geometric and electronic consequences of a third-sphere amino acid substitution. *Biochemistry*. *54* (18), 2874–2884.
- (32) Blaesi, E. J.; Fox, B. G.; Brunold, T. C. (2014) Spectroscopic and computational investigation of iron(III) cysteine dioxygenase: Implications for the nature of the putative superoxo-Fe(III) intermediate. *Biochemistry*. 53 (36), 5759–5770.
- (33) Arrott, A. S. (2008) Approximations to Brillouin functions for analytic decriptions of ferromagnetism. *J. Appl. Phys.* 1031 (10), 7–715.
- (34) Stoll, S.; Schweiger, A. (2006) EasySpin, a comprehensive software package for spectral simulation and analysis in EPR. *J. Magn. Reson.* 178 (1), 42–55.
- (35) Pierce, B. S.; Gardner, J. D.; Bailey, L. J.; Brunold, T. C.; Fox, B. G. (2007) Characterization of the nitrosyl adduct of substrate-bound mouse cysteine dioxygenase by electron paramagnetic resonance: Electronic structure of the active site and mechanistic implications. *Biochemistry.* 46 (29), 8569–8578.
- (36) Gardner, J. D.; Pierce, B. S.; Fox, B. G.; Brunold, T. C. (2010) Spectroscopic and computational characterization of substrate-bund mouse cysteine dioxygenase: Nature of

- the ferrous and ferric cysteine adducts and mechanistic implications. *Biochemistry. 49* (29), 6033–6041.
- (37) Solomon, E. I.; Pavel, E. G.; Loeb, K. E.; Campochiaro, C. (1995) Magnetic circular dichroism spectroscopy as a probe of the geometric and electronic structure of non-heme ferrous enzymes. *Coord. Chem. Rev.* 144 (C), 369–460.
- (38) Li, W.; Pierce, B. S. (2015) Steady-state substrate specificity and O₂-coupling efficiency of mouse cysteine dioxygenase. *Arch. Biochem. Biophys.* 565, 49–56.
- (39) Li, W.; Blaesi, E. J.; Pecore, M. D.; Crowell, J. K.; Pierce, B. S. (2013) Second-sphere interactions between the C93-Y157 cross-link and the substrate-bound Fe site influence the O₂ coupling efficiency in mouse cysteine dioxygenase. *Biochemistry*. *52* (51), 9104–9119.
- (40) Fischer, A. A.; Miller, J. R.; Jodts, R. J.; Ekanayake, D. M.; Lindeman, S. V; Brunold, T. C.; Fiedler, A. T. (2019) Spectroscopic and computational comparisons of thiolate-ligated ferric nonheme complexes to cysteine dioxygenase: Second-sphere effects on substrate (analogue) positioning *Inorg. Chem.* 58 (24), 16487–16499.
- (41) Brandt, U.; Schürmann, M.; Steinbüchel, A. (2014) Mercaptosuccinate dioxygenase, a cysteine dioxygenase, from *Variovorax paradoxus* strain B4 is the key enzyme of mercaptosuccinate degradation. *J. Biol. Chem.* 289 (44), 30800–30809.
- (42) Brandt, U.; Galant, G.; Meinert-Berning, C.; Steinbüchel, A. (2019) Functional analysis of active amino acid residues of the mercaptosuccinate dioxygenase of *Variovorax* paradoxus B4. Enzyme Microb. Technol. 120, 61–68.
- (43) Dominy, J. E.; Simmons, C. R.; Karplus, P. A.; Gehring, A. M.; Stipanuk, M. H. (2006) Identification and characterization of bacterial cysteine dioxygenases: A new route of cysteine degradation for eubacteria. *J. Bacteriol.* 188 (15), 5561–5569.

Chapter 3

Spectroscopic Investigation of Iron(III) Cysteamine Dioxygenase in the Presence of Substrate (Analogues): Implications for the Nature of Substrate-Bound Reaction Intermediates



This chapter has been submitted under the following: Fernandez RL, Juntunen ND, Fox BG, Brunold TC. Spectroscopic Investigation of Iron (III) Cysteamine Dioxygenase in the Presence of Substrate (Analogues): Implications for the Nature of Substrate-Bound Reaction Intermediates. *J Bioinorg Chem*

Chapter 3: Spectroscopic Investigation of Iron(III) Cysteamine Dioxygenase in the Presence of Substrate (Analogues): Implications for the Nature of Substrate-Bound Reaction Intermediates

3.1 Introduction

Thiol dioxygenases (TDOs) are a family of non-heme Fe-dependent enzymes that oxidize thiol substrates to their corresponding sulfinic acids via the incorporation of both oxygen atoms from dioxygen. Currently, five classes of TDOs are known: cysteine dioxygenase (CDO); 3-mercaptopropionate dioxygenase (MDO); mercaptosuccinate dioxygenase (MSDO); plant cysteine oxidase (PCO); and cysteamine dioxygenase (ADO). Each TDO class has a unique substrate specificity.

CDO provided the founding structure for the TDO family,¹ which is part of the cupin superfamily. The structure revealed that CDO binds its Fe(II) cofactor via a 3 histidine (3-His) facial triad as opposed to the 2-His-1-carboxylate metal binding triad found in most Fe(II)-dependent oxygenases.²,³ Indeed, this 3-His binding motif is apparently rare, as only a small number of other cupin-fold enzymes feature this Fe binding motif, including CDO,¹ MDO,⁴ and PCO.⁵ Furthermore, CDO contains an unusual thioether linkage between Cys93 and a Tyr157 (*Mus musculus* CDO [*Mm*CDO] numbering) in the secondary sphere of the active site that increases activity by properly positioning the substrate and suppressing water coordination to the substrate-bound Fe(II) site.⁶-৪

CDO oxidizes L-cysteine (Cys) to cysteine sulfinic acid (CSA).⁹ In subsequent steps, CSA is further metabolized into hypotaurine and taurine.^{10–13} Though Cys is essential for life, an elevated level off Cys has potentially devastating neurological effects and has been linked to Alzheimer's and Parkinson's diseases.^{14–16} Hence, tight regulation of intracellular Cys levels is vital. Hypotaurine can also be biosynthesized from the oxidation of cysteamine (2-aminoethanethiol, 2-AET), a reaction catalyzed by ADO.¹⁷ The gene encoding ADO drew attention when researchers noticed a discrepancy between the high levels of taurine and low

levels of *cdo* gene expression in certain tissues. Thus, ADO was postulated to be responsible for taurine production in certain tissues, most notably the brain.

However, recent studies revealed that ADO might also carry out an essential posttranslational modification similar to that reported for PCO,¹⁸ which initiates an N-degron pathway in plants.^{19,20} Under oxic conditions, PCO is able to oxidize the N-terminal Cys of a peptide substrate. The N-terminal CSA then serves as a substrate for arginyl tRNA transferase ATE1, thus marking the arginylated peptide for ubiquitination and proteosomal degradation. Under anoxia, PCO is unable to carry out the N-terminal oxidation and the peptide persists, allowing initiation of a hypoxic response to submergence or waterlogging in plants. Similar to this regulatory role for PCO, it has recently been observed that natriuretic polypeptides such as RGS4 and RGS5 are putative ADO substrates.²¹ These peptides serve as negative regulators of G protein signaling that controls cardiovascular function.²²

Similar to CDO, the ADO active site features a 3-His facial triad that coordinates the Fe(II) ion, as judged on the basis of sequence alignment, ¹⁷ site-directed mutagenesis, ^{17,23} and spectroscopic studies. ^{23,24} In addition, also similar to CDO, the existence of a Cys-Tyr crosslink has been established in *Homo sapiens (Hs)* ADO via incorporation of an unnatural amino acid, 3,5,-difluoro-tyrosine, in conjunction with mass spectrometry and NMR experiments. ²⁵ Interestingly, the positions of the residues contributing to the Cys-Tyr crosslink within the amino acid primary sequence are strikingly different between ADO and CDO (Cys206-Tyr208 in *Mm*ADO vs Cys93-Tyr157 in *Mm*CDO). Beyond these conserved features, ADO and CDO have low sequence identity (~15%) and use different binding modes for their thiol substrate (monodentate thiol in ADO versus bidentate thiol and amino in CDO), ^{23,24,26} raising the question of whether there are also differences in the binding of O₂ to the Fe(II) center and the nature of reaction intermediates, such as the putative Fe(III)-superoxide species.

Direct trapping of O_2 -derived intermediates in the catalytic cycles of TDOs has not yet been achieved. To address this issue, O_2 and superoxide surrogates that do not support turnover

have been productively used to probe the nature of the active site and make deductions about possible reaction intermediates. $^{27-31}$ As azide has similar frontier orbitals and the same charge as superoxide ($O_2^{\bullet \bullet}$), this anion has frequently been used to prepare models of putative Fe(III)-superoxide intermediates that are amenable to a wide range of spectroscopic techniques. 27,28,30 In the case of CDO, azide does not coordinate directly to the Fe(III) center of Cys-bound enzyme but instead occupies a pre-binding site in the enzyme. 27 Alternatively, treatment of Cys-bound Fe(III)CDO with excess cyanide, another widely used $O_2^{\bullet \bullet}$ surrogate, causes the high-spin (S=5/2) electron paramagnetic resonance (EPR) signal to convert to a low-spin (S=1/2) EPR signal, demonstrating the direct coordination of cyanide to the Fe(III) ion to presumably form a six-coordinate adduct where the thiol and amino groups of Cys, cyanide, and the 3-His motif make up the iron coordination sphere. Interestingly, the cyano/Cys-Fe(III)CDO complex not only provides a model of a putative reaction intermediate, but also displays EPR parameters that are sensitive to changes in the secondary coordination sphere of CDO, such as the formation of the Cys-Tyr crosslink. 32

In the present study, we have used electronic absorption (Abs) and EPR spectroscopies to characterize the complexes that are formed upon incubation of Fe(III)ADO with 2-AET or thiol-containing derivatives and azide or cyanide. As ADO appears to feature a similar 3-His metal-binding site as CDO, it is reasonable to assume that oxidation of 2-AET by this enzyme also proceeds via transient formation of an Fe(III)-superoxo species. As such, our results obtained for Fe(III)ADO incubated with 2-AET (analogues) and O_2^{\bullet} surrogates permit a detailed assessment of the geometric and electronic properties of potential ADO reaction intermediates. Similarities and differences between the azide and cyanide complexes of substrate-bound CDO and ADO are discussed, and inferences are made as to the influence of the unique secondary sphere of ADO on substrate specificity. Additionally, the effect of the putative crosslink between residues

Cys206 and Tyr208 on the positioning of substrate (analogues) is assessed via EPR studies of WT and Y208F ADO incubated with cyanide and 2-AET.

3.2 Materials and methods

Recombinant gene expression and protein purification. Gene expression and protein purification of wild-type (WT) *Mus musculus* (*Mm*) ADO were conducted in the same manner as described elsewhere.²³ In brief, the *ado* gene was expressed in *Escherichia coli* Rosetta 2(DE3) cells through induction with isopropyl-β-D-thiogalactopyranoside (IPTG). ADO was purified using an immobilized metal affinity chromatography column and a gel filtration column. After each column, fractions were pooled on the basis of purity visualized via stain-free sodium dodecyl sulfate-polyacrylamide gel electrophoresis (SDS-PAGE). Once enzyme was eluted from the final column, activity was verified via qualitative thin-layer chromatography as described elsewhere.²³

The Tyr208Phe mutation was introduced in *Mm*ADO using primers 5'-GACTGCCACTTCTACCGCGTTG-3' and 5'-CAACGCGGTAGAAGTGGCAGTC-3' purchased from Integrated DNA Technology. The cloned gene sequence was confirmed at the University of Wisconsin-Madison Biotechnology Center. Variant ADO was prepared as described elsewhere with minor adjustments.²³ *E. coli* Rosetta 2(DE3) cells were transformed with the mutant DNA and grown at 37 °C in 4 L of LB medium (containing 10 g of tryptone, 10 g of NaCl, and 5 g of yeast extract per liter). Gene overexpression was induced by adding IPTG to a final concentration of 140 μM along with ferrous ammonium sulfate to a final concentration of 80 μM.

Tyr208Phe ADO was purified using immobilized metal affinity chromatography with a TALON Co-resin column. Protein-containing fractions were pooled according to purity by stain-free SDS-PAGE. Activity was confirmed qualitatively with thin layer chromatography, as described elsewhere.²³

Sample preparation. The Fe(II) and Fe(III) contents of ADO were determined through a colorimetric assay using the iron chelator tripyridyl triazine and an ϵ_{595} of 22.1 mM⁻¹ cm⁻¹.33 The assay was performed in the absence and presence of a reductant to determine the proportion of

Fe(II) versus Fe(III) initially present. Purified ADO was typically 70-80% Fe-loaded, with the majority (~85%) of metalated sites containing Fe(II). As iron-loading of the ADO active sites was incomplete, all concentrations cited herein refer to the Fe-bound fraction, not that of total protein.

All samples were prepared aerobically in 20 mM Tris, pH 8.0 with 250 mM NaCl buffer. Oxidation to Fe(III)ADO was accomplished via a 30-minute reaction of as-isolated ADO (~0.4 mM) with a 3-fold molar excess of potassium hexachloroiridate(IV), followed by buffer exchange via centrifugation to remove any remaining oxidant.³⁴ The desired protein complexes were obtained by incubating 0.4 mM Fe(III)ADO with substrate 2-AET, 3-MPA, or Cys for 2 min and then with a 200-fold molar excess (80 mM) or 10-fold molar excess (4 mM) of azide or cyanide, respectively. A recent study by Wang et al. revealed that upon incubation with substrate, Fe(III)ADO is reduced to Fe(II)ADO within 20 min.²⁴ Thus, to avoid reduction, all samples were frozen within 5 min.

Spectroscopy. Abs spectra were recorded at room temperature with a double-beam Varian Cary 4 Bio spectrophotometer set to a spectral bandwidth of 0.5 nm. X-band EPR data were collected using a Bruker ELEXSYS E500 spectrometer. The sample temperature was maintained at 20 K by an Oxford ESR 900 continuous flow liquid He cryostat regulated by an Oxford ITC-503S temperature controller. All EPR spectra were obtained using the following experimental parameters: frequency = 9.386 GHz; microwave power = 12.62 mW; modulation amplitude = 3 G; modulation frequency = 100 kHz. These parameters were kept constant to allow for a direct comparison of the relative contributions from different (i.e., low-spin versus high-spin) species to the different samples investigated.

3.3 Results

Fe(III)ADO. ADO was isolated with iron occupying ~80% of the active sites. Of the Fe-loaded sites, the majority (~85%) contained catalytically active Fe(II) with the remaining sites containing Fe(III). The Fe(II) sites were oxidized to Fe(III) by the addition of K₂IrCl₆.³⁴

The electronic Abs spectrum of Fe(III)ADO presented in **Figure 3.1A**, **solid line** lacks any discernible features in the UV/Vis spectral region. When incubated with 2-AET or Cys, Fe(III)ADO turns light blue in color due to the appearance of a broad band centered at ~690 nm (λ_{max} of 693 and 692 nm for 2-AET-bound and Cys-bound Fe(III)ADO, respectively, **Figure 3.1B and 3.1D**, **solid line**). Analogous features in the Abs spectra of Fe(III)CDO³⁵ and oxidized superoxide reductase,³⁰ a non-heme iron enzyme with a comparable active site structure, have been assigned as $S_{Cys} \rightarrow Fe(III)$ charge transfer (CT) transitions on the basis of spectroscopic and computational studies. Addition of 3-MPA to Fe(III)ADO causes the appearance of a dominant Abs feature with a λ_{max} of 647 nm, also suggestive of $S \rightarrow Fe(III)$ charge transfer (**Figure 3.1C**, **solid line**). However, the unique peak position of this feature provides the evidence that the electronic structure of the 3-MPA-bound ADO complex is distinct from that of the 2-AET-bound ADO complex.

Azide-Fe(III)ADO adduct. Upon incubation with azide, the color of Fe(III)ADO changes from pale yellow to an orange-pink. This change in color is accompanied by the appearance of a new Abs feature with a λ_{max} of 472 nm (Figure 3.1A, dashed line). A similar feature in the absorption spectrum of Fe(III) superoxide dismutase incubated with azide was previously assigned as an N₃ \rightarrow Fe(III) CT transition on the basis of resonance Raman spectroscopic studies. Likewise, CDO has been reported to form an inner-sphere azide-Fe(III)CDO complex on the basis of Abs, EPR, and MCD spectroscopic studies. Thus, like these other metalloenzymes, azide coordinates directly to the Fe(III) center of ADO in the absence of substrate. The Fe(III)ADO incubated with azide also displays a rhombic, high-spin (S = 5/2) EPR signal that closely resembles that of asisolated ADO (Figure 3.2B and 3.2A, respectively), suggesting that azide binds to the Fe(III)ADO active site by replacing a ligand with comparable donor strength, likely a solvent-derived hydroxide.

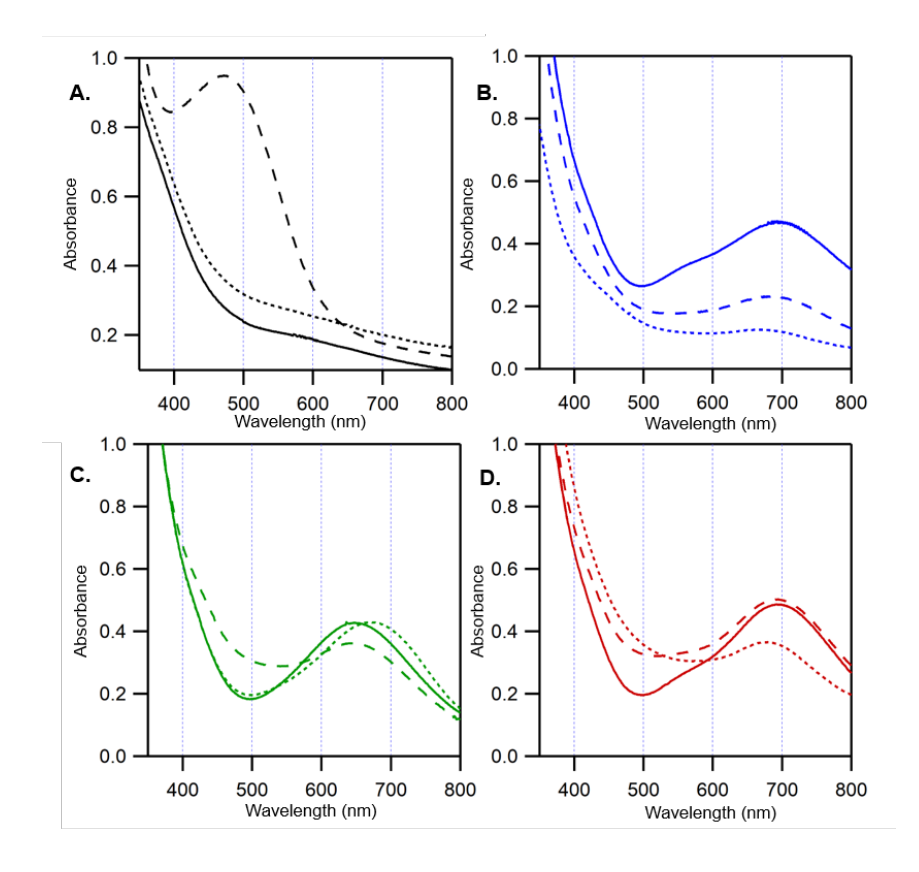


Figure 3.1. Room-temperature UV/Vis spectra of 0.4 mM Fe(III)ADO in the absence and presence of substrate (analogues) and O₂*- surrogates. A) Fe(III)ADO, B) Fe(III)ADO incubated with a 5-fold excess (2 mM) of 2-AET, C) Fe(III)ADO incubated with a 5-fold excess (2 mM) of 3-MPA, and D) Fe(III)ADO incubated with a 10-fold excess (4 mM) of Cys. Spectra were collected either in the absence of an O₂*- surrogate (solid lines), the presence of a 200-fold excess (80 mM) of azide (long dashes), or a 10-fold excess (4 mM) of cyanide (short dashes).

Addition of azide to Fe(III)ADO incubated with substrate 2-AET causes a minor (~9 nm) blue shift of the λ_{max} of the visible Abs feature from 693 nm to 684 nm (Figure 3.1B, dashed line) and a slight increase in the rhombicity of the EPR signal (Figure 3.2D) compared to that displayed by 2-AET-bound Fe(III)ADO in the absence of azide (Figure 3.2C).²³ The relatively small magnitude of the spectral perturbations caused by the addition of azide to 2-AET-bound Fe(III)ADO indicates that this $O_2^{\bullet -}$ surrogate does not bind directly to the Fe(III) center in the majority of active sites. However, the EPR spectrum of Fe(III)ADO incubated with 2-AET and

azide additionally contains a minor low-spin (S = 1/2) signal in the high field region. A similar, weak low-spin EPR signal was previously reported for Fe(III)CDO treated with Cys and azide. In the case of Fe(III)CDO, this S = 1/2 EPR signal was attributed to a minor fraction of Fe(III) centers that form an inner-sphere complex with azide, while the appearance of a slightly perturbed Abs spectrum and retention of the dominant S = 5/2 EPR signal was interpreted to indicate that azide binds in the vicinity of, rather than to, the majority of Fe(III) centers.²⁷ The low affinity of Cysbound Fe(III)CDO for azide was suggested to be due to the presence of a sixth ligand, most likely a hydroxide ion, that saturates the Fe(III) coordination sphere. By analogy, we propose that the Fe(III) center in 2-AET-bound Fe(III)CDO is also six-coordinate, precluding the direct coordination of azide to the vast majority of active sites.

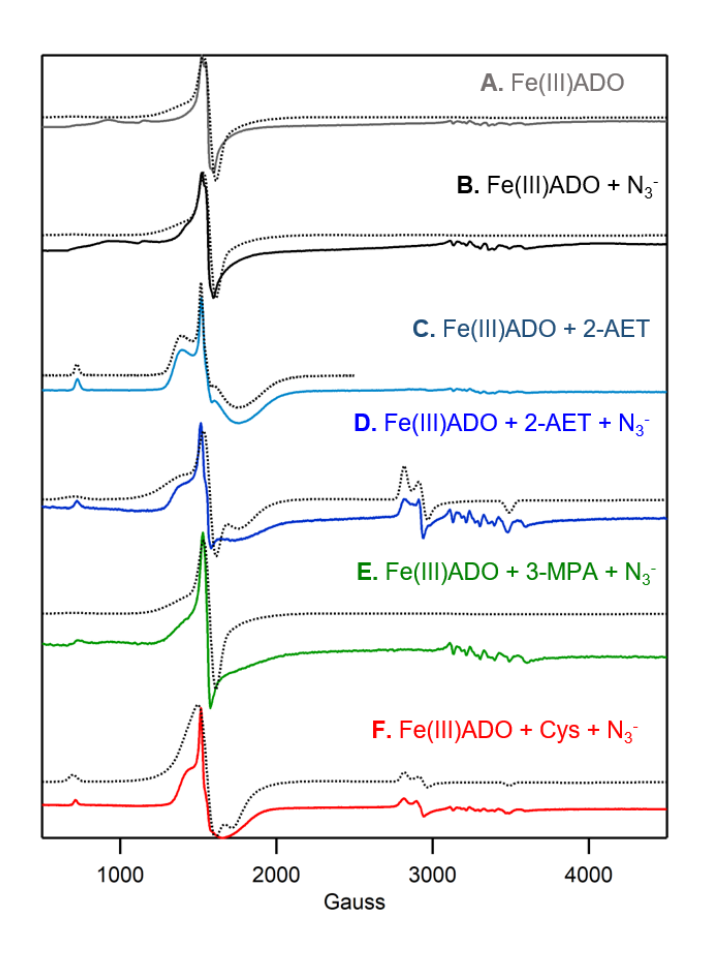


Figure 3.2. X-band EPR spectra at 20 K of 0.4 mM Fe(III)ADO in the absence and presence of various substrate analogues and/or O₂ surrogates. A) Fe(III)ADO, B) Fe(III)ADO incubated with

a 200-fold excess (80 mM) of azide, C) Fe(III)ADO incubated with a 5-fold excess (2 mM) of 2-AET, D) Fe(III)ADO incubated with a 5-fold excess (2 mM) of 2-AET and a 200-fold excess (80 mM) of azide, E) Fe(III)ADO incubated with a 10-fold excess (4 mM) of 3-MPA and a 200-fold excess (80 mM) of azide, and F) Fe(III)ADO incubated with a 5-fold excess (2 mM) of Cys and a 200-fold excess (80 mM) of azide. The signals in the 3000–3700 cm⁻¹ Gauss region are due to a minor Mn(II) impurity. Fit parameters are provided in Appendix 3.

As evidenced by the appearance of a prominent Abs band at 647 nm, the thiol group of 3-MPA can coordinate to Fe(III) in ADO (**Figure 3.1C**, solid line). Addition of azide to 3-MPA-bound Fe(III)ADO causes only a slight blue-shift of the λ_{max} of the prominent Abs band in the visible spectral region to 645 nm (**Figure 3.1C**, **dashed line**), along with a small increase in rhombicity of the S = 5/2 EPR signal (**Figure 3.2E**). Importantly, no low-spin EPR signal characteristic of the azide and thiol-bound enzyme is present. The similarity of λ_{max} and the EPR spectra of 3-MPA-bound ADO in the absence and presence of azide and lack of a signal in the high field region of the EPR spectrum indicate that azide does not directly bind to the Fe(III) ion when 3-MPA is present (note: the small changes in the Abs spectrum observed upon incubation of 3-MPA-bound Fe(III)ADO with azide could be due to a change in ionic strength or binding of azide near the active site without coordinating the iron).

As with 3-MPA, the Abs spectra collected for Cys-bound Fe(III)ADO in the absence and presence of azide (**Figure 3.1D**, **dashed line**) are nearly identical, suggesting that this O_2^{\bullet} surrogate does not directly coordinate to the Fe(III) center in the majority of active sites. While the EPR spectrum of Fe(III)ADO incubated with Cys and azide contains a minor low-spin (S = 1/2) signal (**Figure 3.2F**, **dashed line**), seemingly suggesting that azide directly coordinates to a small subset of Cys-bound Fe(III)ADO active sites, the same low-spin signal is also observed for Cys-bound ADO in the absence of azide.²³ In fact, these spectra overlay perfectly, leading us to conclude that azide minimally perturbs the active site of Cys-bound Fe(III)ADO.

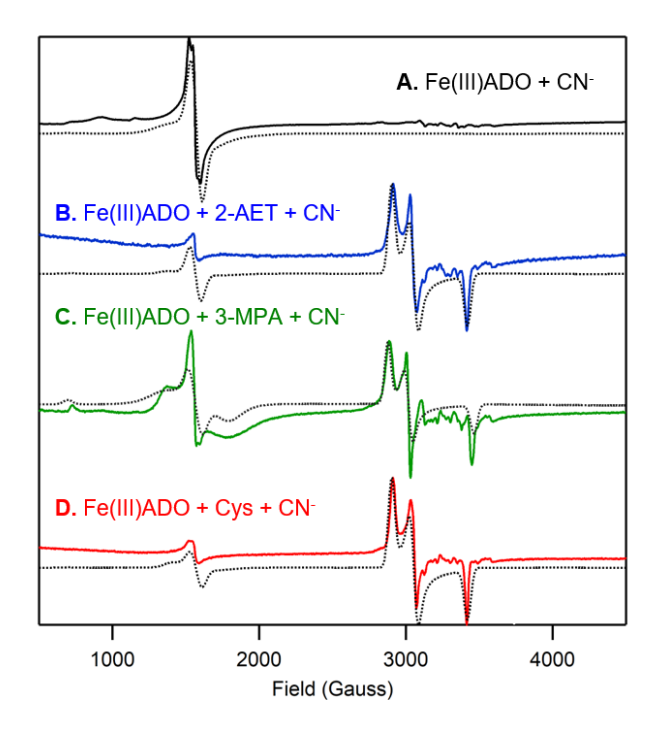


Figure 3.3. X-band EPR spectra at 20 K of 0.4 mM Fe(III)ADO incubated with a 10-fold excess (4 mM) of cyanide in the absence of substrate (A) and in the presence of a 15-fold excess (6 mM) of 2-AET (B), a 5-fold (2 mM) excess of 3-MPA (C), or a 10-fold excess (4 mM) of Cys (D). Fit parameters are provided in Appendix 3.

Cyanide-Fe(III)ADO adduct. The Abs and EPR spectra of Fe(III)ADO collected in the absence and presence of cyanide are nearly identical (**Figure 3.1**, **dotted line**, and 3.**3A**), indicating that this $O_2^{\bullet -}$ surrogate does not coordinate to substrate-free Fe(III)ADO. In contrast, addition of cyanide to 2-AET-bound Fe(III)ADO causes the appearance of a dominant low-spin (S = 1/2) EPR signal (g = 2.30, 2.20, 1.96; **Figure 3.3B**) and a small but noticeable change to the Abs spectrum, signifying direct coordination of the cyanide ion to the Fe(III) center in this species. A similar requirement for the presence of substrate to enable binding of cyanide to the Fe(III) ion has been reported for Fe(III)CDO.³²

Incubation of 3-MPA-bound Fe(III)ADO with cyanide leads to a 25 nm red-shift of the prominent Abs feature at ~650 nm (**Figure 3.1C**, **dotted line**) and the appearance of an identical low-spin EPR signal as observed for 2-AET-bound Fe(III)ADO in the presence of cyanide (**Figure**

3.3C vs **3.3B**), again signaling formation of an Fe(III)-cyano-substrate complex. However, the relative intensity of the residual high-spin (S = 5/2) EPR signal (**Figure 3.3C**) is much higher in the EPR spectrum of cyanide-treated 3-MPA-bound Fe(III)ADO, indicating that cyanide coordinates to a smaller fraction of Fe(III)ADO in the presence of the substrate analogue 3-MPA.

The Abs and EPR spectra of Cys-bound Fe(III)ADO in the presence of cyanide (Fig 3.1D, dotted line and Figure 3.3D) are nearly identical to those obtained for 2-AET-bound Fe(III)ADO incubated with cyanide (Fig 3.1D, dotted line and Figure 3.3D). These data reveal that the active sites of 2-AET- and Cys-bound Fe(III)ADO have comparable affinities for and form similar innersphere complexes with cyanide. Even with this similarity, ADO turnover of Cys is very slow, ¹⁷ suggesting that a step in the catalytic cycle after Cys and O₂ binding to Fe(II)ADO is perturbed. *Impact of crosslink on spectral properties*. Recently, Liu and coworkers demonstrated that a Cys-Tyr crosslink can be formed in human ADO (involving Cys206 and Tyr208 using *Mm*ADO numbering scheme), by genetically incorporating an unnatural amino acid, 3,5-difluoro-tyrosine, specifically into Tyr208 and using mass spectrometry and ¹⁹F NMR spectroscopy. ²⁵ Although in the absence of a crystal structure the position of the crosslink relative to the active site remains unknown, the authors noted that crosslink formation required the presence of cysteamine and O₂, suggesting that it resides in close proximity to the Fe center. In support of this hypothesis, the catalytic activity (determined via O₂ uptake studies) was found to be reduced by a factor of ~4 in the Tyr208Ala ADO variant.

To assess whether a crosslink has any noticeable effect on the interaction between substrate 2-AET and the Fe(III)ADO active site, we prepared the Tyr208Phe ADO variant, which prevents the formation of the thioether crosslink. Notably, the EPR spectra obtained for cyanide/2-AET adducts of WT and Y208F Fe(III)ADO (**Figure 3.4**) are superimposable, suggesting that formation of the Cys206–Tyr208 crosslink has negligible effects on the geometric and electronic properties of the ADO active site. Given the differences in primary sequence positions of residues involved, it is perhaps not surprising that Cys-Tyr thioether bond formation would affect the

substrate/active site interactions differently in ADO and CDO. However, because only a small fraction of as-isolated WT ADO appears to be crosslinked based on mass spectrometry analysis, it is possible that the sample of cyanide/2-AET-bound WT Fe(III)ADO used to collect the EPR data in **Figure 3.4** contained an insignificant fraction of crosslinked enzyme. Also, the modest decrease in catalytic activity displayed by ADO in response to the non-conservative Tyr208Ala substitution variant could be due to more global structural changes rather than the presence of a substantial fraction of crosslinked WT enzyme under physiologically relevant conditions.

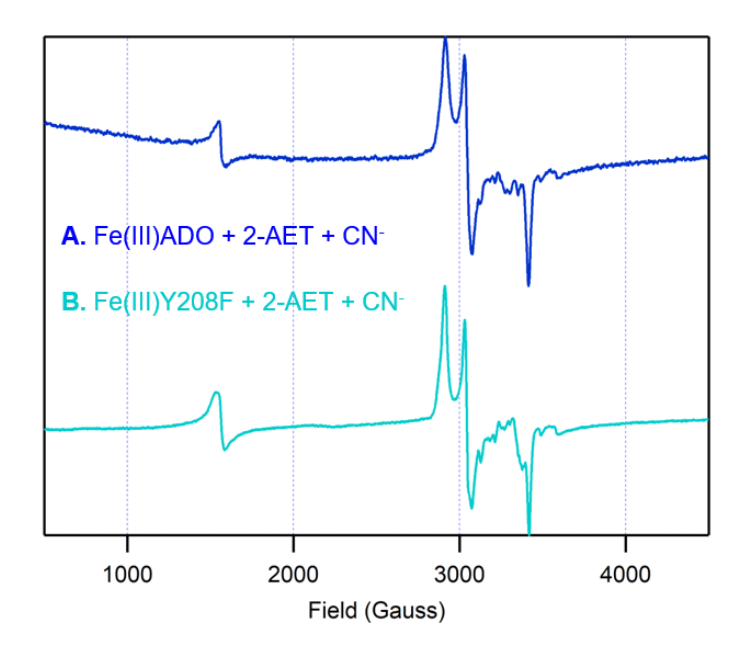


Figure 3.4. X-band EPR spectra at 20 K of (A) 0.4 mM Fe(III)ADO incubated with a 10-fold excess (4 mM) of cyanide in the presence of a 15-fold excess (6 mM) of 2-AET (B) 0.4 mM Y208F Fe(III)ADO incubated with a 10-fold excess (4 mM) of cyanide in the presence of a 15-fold excess (6 mM) of 2-AET.

3.4 Discussion

Despite the significant role that ADO plays in mammalian sulfur metabolism, little is known about its active site structure. Although sequence homology modeling could, in principle, be used to predict the three-dimensional structure of ADO and guide site-directed mutagenesis studies, this approach is hampered by the fact that ADO and other crystallographically characterized

TDOs display low sequence identity (e.g., mouse ADO and CDO share only 14% sequence identity). In particular, it is difficult to assess the influence of secondary sphere residues on the nature of the substrate/active site interactions from homology models. Thus, in this study, we have used Abs and EPR spectroscopy to investigate the binding of superoxide surrogates to Fe(III)ADO in the absence and presence of substrate and substrate analogues.

Azide coordinates to the iron center of Fe(III)ADO in the absence of substrate. When Fe(III)ADO is incubated with azide, an intense Abs feature appears at 472 nm, providing evidence for direct coordination of this $O_2^{\bullet \bullet}$ surrogate to the active site of Fe(III)ADO in the absence of substrate (analogue). The distinct rhombic, high-spin (S = 5/2) signal in the corresponding EPR spectrum indicates that azide likely coordinates to the active site by replacing a ligand with similar donor strength, presumably a solvent-derived hydroxide. Similar spectral changes were noted when substrate-free Fe(III)CDO was incubated with azide.²⁷ A combined spectroscopic and computational analysis of the resulting azide adduct of Fe(III)CDO were consistent with a single azide bound to the Fe(III) center to yield a five-coordinate complex or an azide and a water bound to give six-coordinate complex. Our results indicate that azide-bound Fe(III)ADO also contains a five-coordinate or six-coordinate Fe(III) center possessing hydroxide and azide ligands.

Azide binding to Fe(III)ADO is suppressed in the presence of substrate (analogues). The EPR data of azide/2-AET-bound Fe(III)ADO demonstrate that azide binds directly to only a minor fraction of Fe(III)ADO active sites complexed with 2-AET, suggesting that the Fe(III) center of 2-AET-bound Fe(III)ADO is either coordinatively saturated or otherwise inaccessible in the presence of substrate. The presence of a six-coordinate Fe(III) center has also been proposed for Cys-bound Fe(III)CDO, with a hydroxide ion completing a distorted octahedral coordination environment of the active site Fe(III) ion, and azide occupying an outer-sphere pocket without binding to iron. Unlike Fe(III)CDO, however, Fe(III)ADO appears to bind its 2-AET substrate in a monodentate fashion via coordination of only the thiolate moiety. Thus, we hypothesize that the Fe(III) ion of substrate-bound Fe(III)ADO resides in a distorted octahedral coordination

environment composed of the 3-His facial triad, the 2-AET terminal thiolate, and two hydroxide ions.

While a small fraction of 2-AET-bound Fe(III)ADO active sites form inner-sphere complexes with azide as judged by the presence of a low-spin EPR signal, azide is unable to bind to the 3-MPA-bound or Cys-bound Fe(III)ADO active site. This difference likely stems from the fact that the ADO active site has evolved to promote monodentate binding of the 2-AET substrate (and potentially N-terminal Cys peptides), which causes the non-coordinating, negatively-charged carboxylate groups in 3-MPA- and Cys-bound Fe(III)ADO to repel anionic O₂ surrogates away from the active site. In CDO, an analogous electrostatic repulsion between the substrate carboxylate group and azide is alleviated by the formation of a salt bridge between the Cys carboxylate and the Arg60 outer-sphere residue. The prediction that ADO cannot form a salt bridge that stabilizes substrate binding is consistent with the observation that this enzyme is unable produce cysteine sulfinic acid from Cys. 17

Effect of outer-sphere residues on the cyanide/2-AET-Fe(III)ADO adduct. The EPR g-values of cyanide/Cys-bound Fe(III)CDO have been found to be sensitive to changes in the outer coordination sphere, specifically the absence and presence of the Cys93-Tyr157 crosslink.^{29,31} A spectroscopically validated computational analysis of this adduct revealed that in the absence of the crosslink, the Fe-C-N unit is nearly linear. Upon crosslink formation, the Fe-C-N unit adopts a more bent configuration and the repositioning of Tyr157 perturbs the network of hydrogen bonds between the side chain of Arg60, the phenol of Tyr157, and the substrate Cys carboxylate, causing a lengthening of the Fe-S bond by 0.02 Å. Although seemingly minor, these structural changes have a measurable effect on the electronic and spectroscopic properties of the enzyme active site.

To correlate changes in EPR *g*-values with specific geometric perturbations, Fiedler and coworkers performed CASSCF/NEVPT2 ab initio calculations on active site models of non-crosslinked and crosslinked cyanide/Cys-bound Fe(III)CDO as well as synthetic mimics.²⁹ These

computations indicated that a lengthening of the Fe–S bond causes an overall increase in the spread of *g*-values and a decrease in the intermediate *g*-value. Hence, the significantly smaller *g* spread displayed by cyanide/2-AET-bound Fe(III)ADO (2.30, 2.20, 1.96) relative to those reported for non-crosslinked and crosslinked cyanide/Cys-bound Fe(III)CDO (2.34, 2.21, 1.95 versus 2.38, 2.23, 1.94, respectively) implies that the cyanide/2-AET-bound Fe(III)ADO complex possesses the shortest Fe-S bond of these species. An even smaller *g* spread was found for a synthetic cyanide/Cys-bound Fe(III)CDO mimic (2.20, 2.16, 1.99), which lacks any outer-sphere interactions involving the carboxylate group of the substrate Cys analogue and thus possesses a particularly short Fe-S bond. Collectively, these results suggest that the amine group of 2-AET in substrate-bound Fe(III)ADO engages in some, but considerably weaker interactions with secondary sphere residues than does the carboxylate group of Cys with Arg60 in substrate-bound Fe(III)CDO. This finding is consistent with the much narrower substrate scope displayed by CDO compared to ADO (i.e., while CDO is only capable of turning over L-Cys efficiently, ¹⁴ ADO has been shown to oxidize 2-AET¹⁷ as well as the amino-terminal Cys residue of a much larger polypeptide from RGS5).¹⁸

3.5 Conclusion

The spectroscopic data obtained in this study provide new insights into the nature of the species that are formed upon incubation of Fe(III)ADO with substrate/substrate analogues and O₂*- surrogate, which serve as models of putative reaction intermediates. Azide is only able to coordinate to the Fe(III) center of substrate-free ADO, likely indicating that cysteamine-bound Fe(III)ADO lacks an open coordination site. An analogous inhibitory effect of substrate on azide binding was previously reported for Fe(III)CDO, where the presence of a six-coordinate Fe(III) center with azide occupying an outer-sphere pocket was established on the basis of spectroscopic, computational, and X-ray crystallographic studies. Conversely, the O₂*- surrogate cyanide requires coordination of substrate cysteamine (analogues) before it can bind to the

Fe(III)ADO active site, again paralleling the behavior of Fe(III)CDO. A comparison of the EPR *g*-values obtained for cyanide/cysteamine-bound Fe(III)ADO and those reported for cyanide/Cysbound Fe(III)CDO reveals that the interaction of the thiol substrate with outer-sphere residues is considerably weaker in ADO than in CDO. Lastly, elimination of the putative Cys206–Tyr208 crosslink via Tyr208Phe substitution has negligible effects on the EPR signal of the cyanide/cysteamine adduct, indicating that either an insignificant fraction of as-isolated wild-type enzyme contains the crosslink or that formation of the thioether bond has minimal effects on the electronic structure of the substrate-bound active site.

Appendix

EPR spectral simulation for Y208F Fe(III)ADO incubated with cyanide and 2-AET and complete list of EPR fit parameters

Accession Codes

ADO, UniProt Q6PDY2; CDO, UniProt P21816; MDO, UniProt Q9I0N5; PCO, UniProt Q9SJI9

Funding

The authors are grateful for financial support from the National Institute of General Medical Sciences of the National Institutes of Health (Grant GM117120 to T.C.B.) and the Department of Biochemistry and the Office of the Vice Chancellor for Research and Graduate Education (to B.G.F.). This research was conducted in part while R.L.F. was supported by the National Institute of General Medical Sciences of the National Institutes of Health (Grant T32GM008505).

Acknowledgement

The authors would like to thank Prof. Martha H. Stipanuk for sharing the original mouse ADO plasmid used to begin this work.

3.6 References

(1) McCoy, J. G., Bailey, L. J., Bitto, E., Bingman, C. A., Aceti, D. J., Fox, B. G., and Phillips, G. N. (2006) Structure and mechanism of mouse cysteine dioxygenase. *Proc. Natl. Acad. Sci. 103*, 3084–3089.

- (2) Straganz, G. D., and Nidetzky, B. (2006) Variations of the 2-His-1-carboxylate theme in mononuclear non-heme Fe II oxygenases. *ChemBioChem* 7, 1536–1548.
- (3) Koehntop, K. D., Emerson, J. P., and Que, L. (2005) The 2-His-1-carboxylate facial triad: A versatile platform for dioxygen activation by mononuclear non-heme iron(II) enzymes. *J. Biol. Inorg. Chem.* 10, 87–93.
- (4) Tchesnokov, E. P., Fellner, M., Siakkou, E., Kleffmann, T., Martin, L. W., Aloi, S., Lamont, I. L., Wilbanks, S. M., and Jameson, G. N. L. (2015) The cysteine dioxygenase homologue from Pseudomonas aeruginosa is a 3-mercaptopropionate dioxygenase. *J. Biol. Chem.* 290, 24424–24437.
- (5) White, M. D., Carbonare, L. D., Puerta, M. L., Iacopino, S., Edwards, M., Dunne, K., Pires, E., Levy, C., McDonough, M. A., Licausi, F., and Flashman, E. (2020) Structures of Arabidopsis thaliana oxygen-sensing plant cysteine oxidases 4 and 5 enable targeted manipulation of their activity. *Proc. Natl. Acad. Sci. U. S. A. 117*, 23140–23147.
- (6) Davies, C. G., Fellner, M., Tchesnokov, E. P., Wilbanks, S. M., and Jameson, G. N. L. (2014) The Cys-Tyr cross-link of cysteine dioxygenase changes the optimal ph of the reaction without a structural change. *Biochemistry 53*, 7961–7968.
- (7) Aloi, S., Davies, C. G., Karplus, P. A., Wilbanks, S. M., and Jameson, G. N. L. (2019) Substrate Specificity in Thiol Dioxygenases. *Biochemistry* 2398–2407.
- (8) Driggers, C. M., Kean, K. M., Hirschberger, L. L., Cooley, R. B., Stipanuk, M. H., and Karplus, P. A. (2016) Structure-Based Insights into the Role of the Cys–Tyr Crosslink and Inhibitor Recognition by Mammalian Cysteine Dioxygenase. *J. Mol. Biol.* 428, 3999–4012.
- (9) Yamaguchi, K., and Hosokawa, Y. (1987) Cysteine Dioxygenase. *Methods Enzymol.* 143, 395–403.
- (10) Huxtable, R. J. (1992) Physiological Actions of Taurine. *Physiol. Rev.* 72, 101–163.
- (11) Schaffer, S. W., Ju Jong, C., KC, R., and Azuma, J. (2010) Physiological roles of taurine in heart and muscle. *J. Biomed. Sci.* 17, 101–163.

- (12) Xu, Y.-J., Arneja, A. S., Tappia, P. S., and Dhalla, N. S. (2008) The potential health benefits of taurine in cardiovascular disease. *Exp. Clin. Cardiol.* 13, 57–65.
- (13) Stipanuk, M. H. (1986) Metabolism of sulfur-containing amino acids. *Annu. Rev. Nutr.* 6, 179–209.
- (14) Simmons, C. R., Hirschberger, L. L., Machi, M. S., and Stipanuk, M. H. (2006) Expression, purification, and kinetic characterization of recombinant rat cysteine dioxygenase, a non-heme metalloenzyme necessary for regulation of cellular cysteine levels. *Protein Expr. Purif.* 47, 74–81.
- (15) Heafield, M. T., Fearn, S., Steventon, G. B., Waring, R. H., Williams, A. C., and Sturman, S. G. (1990) Plasma cysteine and sulphate levels in patients with motor neurone, Parkinson's and Alzheimer's disease. *Neurosci. Lett.* 110, 216–220.
- (16) Slivka, A., and Cohen, G. (1993) Brain ischemia markedly elevates levels of the neurotoxic amino acid, cysteine. *Brain Res. 608*, 33–37.
- (17) Dominy, J. E., Simmons, C. R., Hirschberger, L. L., Hwang, J., Coloso, R. M., and Stipanuk, M. H. (2007) Discovery and characterization of a second mammalian thiol dioxygenase, cysteamine dioxygenase. *J. Biol. Chem.* 282, 25189–25198.
- (18) Masson, N., Keeley, T. P., Giuntoli, B., White, M. D., Lavilla Puerta, M., Perata, P., Hopkinson, R. J., Flashman, E., Licausi, F., and Ratcliffe, P. J. (2019) Conserved N-terminal cysteine dioxygenases transduce responses to hypoxia in animals and plants. *Science (80-.)*. *364*, 65–69.
- (19) White, M. D., Klecker, M., Hopkinson, R. J., Weits, D. A., Mueller, C., Naumann, C., O'Neill, R., Wickens, J., Yang, J., Brooks-Bartlett, J. C., Garman, E. F., Grossmann, T. N., Dissmeyer, N., and Flashman, E. (2017) Plant cysteine oxidases are dioxygenases that directly enable arginyl transferase-catalysed arginylation of N-end rule targets. *Nat. Commun.* 8.
- (20) Van, V., and Smith, A. T. (2020) ATE1-Mediated Post-Translational Arginylation Is an Essential Regulator of Eukaryotic Cellular Homeostasis. *ACS Chem. Biol.*

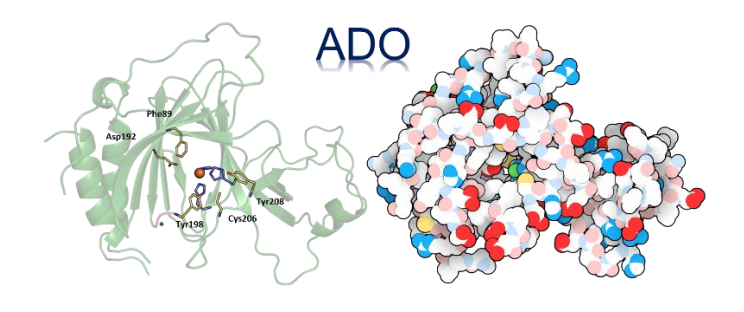
- (21) Lee, M. J., Tasaki, T., Moroi, K., An, J. Y., Kimura, S., Davydov, I. V., and Kwon, Y. T. (2005) RGS4 and RGS5 are in vivo of the N-end rule pathway. *Proc. Natl. Acad. Sci. U. S. A.* 102, 15030–15035.
- (22) Tamirisa, P., Blumer, K. J., and Muslin, A. J. (1999) RGS4 inhibits G-protein signaling in cardiomyocytes. *Circulation* 99, 441–447.
- (23) Fernandez, R. L., Dillon, S. L., Stipanuk, M. H., Fox, B. G., and Brunold, T. C. (2020) Spectroscopic Investigation of Cysteamine Dioxygenase. *Biochemistry 59*, 2450–2458.
- (24) Wang, Y., Davis, I., Chan, Y., Naik, S. G., Griffith, W. P., and Liu, A. (2020)

 Characterization of the nonheme iron center of cysteamine dioxygenase and its interaction with substrates. *J. Biol. Chem.* 295, 11789–11802.
- (25) Wang, Y., Griffith, W. P., Li, J., Koto, T., Wherritt, D. J., Fritz, E., and Liu, A. (2018) Cofactor Biogenesis in Cysteamine Dioxygenase: C–F Bond Cleavage with Genetically Incorporated Unnatural Tyrosine. *Angew. Chemie Int. Ed. 57*, 8149–8153.
- (26) Ye, S., Wu, X., Wei, L., Tang, D., Sun, P., Bartlam, M., and Rao, Z. (2007) An insight into the mechanism of human cysteine dioxygenase: Key roles of the thioether-bonded tyrosine-cysteine cofactor. *J. Biol. Chem.* 282, 3391–3402.
- (27) Blaesi, E. J., Fox, B. G., and Brunold, T. C. (2014) Spectroscopic and Computational Investigation of Iron(III) Cysteine Dioxygenase: Implications for the Nature of the Putative Superoxo-Fe(III) Intermediate. *Biochemistry 53*, 5759–5770.
- (28) Blaesi, E. J., Fox, B. G., and Brunold, T. C. (2015) Spectroscopic and computational investigation of the H155A variant of cysteine dioxygenase: Geometric and electronic consequences of a third-sphere amino acid substitution. *Biochemistry 54*, 2874–2884.
- (29) Fischer, A. A., Miller, J. R., Jodts, R. J., Ekanayake, D. M., Lindeman, S. V, Brunold, T. C., and Fiedler, A. T. (2019) Spectroscopic and Computational Comparisons of Thiolate-Ligated Ferric Nonheme Complexes to Cysteine Dioxygenase: Second-Sphere Effects on Substrate (Analogue) Positioning. *Inorg. Chem.* 58, 16487–16499.

- (30) Clay, M. D., Jenney, F. E., Hagedoorn, P. L., George, G. N., Adams, M. W. W., and Johnson, M. K. (2002) Spectroscopic studies of Pyrococcus furiosus superoxide reductase: Implications for active-site structures and the catalytic mechanism. *J. Am. Chem. Soc. 124*, 788–805.
- (31) Pierce, B. S., Gardner, J. D., Bailey, L. J., Brunold, T. C., and Fox, B. G. (2007) Characterization of the nitrosyl adduct of substrate-bound mouse cysteine dioxygenase by electron paramagnetic resonance: Electronic structure of the active site and mechanistic implications. *Biochemistry* 46, 8569–8578.
- (32) Li, W., Blaesi, E. J., Pecore, M. D., Crowell, J. K., and Pierce, B. S. (2013) Second-sphere interactions between the C93-Y157 cross-link and the substrate-bound Fe site influence the O2 coupling efficiency in mouse cysteine dioxygenase. *Biochemistry* 52, 9104–9119.
- (33) Fischer, D. S., and Price, D. C. (1964) a Simple Serum Iron Method Using the New Sensitive Chromogen Tripyridyl-S-Triazine. *Clin. Chem.* 10, 21–31.
- (34) Crawford, J. A., Li, W., and Pierce, B. S. (2011) Single turnover of substrate-bound ferric cysteine dioxygenase with superoxide anion: Enzymatic reactivation, product formation, and a transient intermediate. *Biochemistry 50*, 10241–10253.
- (35) Gardner, J. D., Pierce, B. S., Fox, B. G., and Brunold, T. C. (2010) Spectroscopic and computational characterization of substrate-bound mouse cysteine dioxygenase: Nature of the ferrous and ferric cysteine adducts and mechanistic implications. *Biochemistry* 49, 6033–6041. (36) Xie, J., Yikilmaz, E., Miller, A. F., and Brunold, T. C. (2002) Second-sphere contributions to substrate-analogue binding in iron(III) superoxide dismutase. *J. Am. Chem. Soc.* 124, 3769–3774.

Chapter 4

Crystal Structure of Cysteamine Dioxygenase Reveals the Origin of the Large Substrate Scope of this Vital Mammalian Enzyme



This chapter has been submitted under the following: Fernandez RL, Elmendorf LD, Smith RW, et al (2021) Crystal Structure of Cysteamine Dioxygenase Reveals the Origin of the Large Substrate Scope of this Vital Mammalian Enzyme. *The Journal of the American Society*.

Chapter 4: Crystal Structure of Cysteamine Dioxygenase Reveals the Origin of the Large Substrate Scope of this Vital Mammalian Enzyme

4.1 Introduction

The metabolism of thiol-containing compounds is vital to mammalian homeostasis. Regulation of hypotaurine, taurine, and cysteine levels preserves cardiac and vascular functions and protects neural cells from excitotoxicity. Additionally, elevated cysteine levels have been associated with Alzheimer's and Parkinson's diseases. To regulate intracellular levels of these thiolate-containing metabolites, mammals use two distinct thiol dioxygenases (TDOs); i.e., cysteine dioxygenase (CDO) and cysteamine dioxygenase (ADO). The definitively established function of CDO is to catalyze the oxidation of cysteine (Cys) to cysteine sulfinic acid (CSA) via the incorporation of both oxygen atoms from molecular oxygen. CSA can then be catabolized into pyruvate, sulfate, and hypotaurine. Under normal conditions, rats or mice convert about 70-90% of CSA to hypotaurine and taurine. Hypotaurine has been identified as a contributor to the growth and progression of aggressive high-grade gliomas in the brain. Additionally, much like excess levels of Cys, the build-up of taurine can damage tissues and cells.

ADO was once believed to exclusively convert cysteamine (2-aminoethanethiol, 2-AET) to hypotaurine (**Scheme 1A**). However, Ratcliffe et al. proposed that the native function of ADO may instead be to catalyze the O₂-dependent conversion of peptides featuring an amino-terminal cysteine (Nt-Cys, **Scheme 1B**) to their CSA derivatives.⁸ They found that mammalian ADO could replace one of the five plant thiol dioxygenases in *Arabidopsis thaliana* (*At*), termed plant cysteine oxidase 4 (PCO4), by oxidizing the plant Nt-Cys peptides both *in vitro* and *in vivo*. Oxidation of the Nt-Cys peptide substrates by PCO promotes arginylation and degradation in the N-degron pathway,⁹ while under anoxic conditions, the peptide persists and enhances Gα catalyzed GTP hydrolysis, leading to an attenuation of G-protein coupled signaling. Newly identified ADO substrates, regulators of G protein signaling RGS4 and RGS5, are part of the mammalian N-

degron pathway and serve as negative regulators of cardiovascular function controlled by G-protein signaling.^{10,11}

A.

$$H_2N$$

SH

 O_2
 O_3
 O_4
 O_4

Scheme 1. (A) ADO was originally believed to solely catalyze the conversion of cysteamine (2-AET) to hypotaurine. (B) In 2019, ADO was shown to also oxidize Nt-Cys residues in various regulatory peptides to their cysteine sulfinic acid derivatives as part of the N-degron pathway.

Five classes of TDOs have been identified to date with differing native functions: namely, CDO, ADO, PCO, 3-mercaptopropionate dioxygenase (MDO), and mercaptosuccinate dioxygenase (MSDO), with CDO and ADO being the only mammalian TDOs. All TDOs belong to the cupin superfamily, which is typified by a common architecture. While cupin proteins tend to have low overall sequence identity, all feature a β-barrel fold and two conserved sequence motifs: $G(X)_5HXH(X)_6G$ and $G(X)_5PXG(X)_2H(X)_3N$. In addition to its classification as a cupin protein, ADO belongs to the PFam family PF07847 (PCO_ADO), which is distinct from the PF05995 (CDO_I) family that includes CDO and MDO. As is typical for members of the cupin superfamily, *Mus musculus* ADO (*Mm*ADO) shares little overall sequence identity with either *Rattus norvegicus* CDO (~14%, *Rn*CDO) or PCO4 (~21%). Nevertheless, all TDOs that have previously been characterized by X-ray crystallography (CDO, MDO, and PCO) feature the same non-heme iron coordination environment, consisting of a relatively rare 3-histidine (3-His) facial triad. The impact on enzyme activity of removal of one of the coordinating His via site-directed mutagenesis and spectroscopic studies provided compelling evidence that ADO also contains the 3-His binding

motif but differs with respect to secondary sphere residues that determine its substrate specificity.^{3,12}

An alignment of the amino acid sequences of *Mm*ADO and *Rn*CDO highlights crucial differences in the active site pocket.³ Perhaps most noticeable, the Cys93 involved in forming the Cys-Tyr cross-link of mammalian CDOs is not conserved in ADO. In *Rn*CDO, this unusual thioether linkage increases activity by properly positioning the Cys and O₂ substrates while also suppressing the coordination of a water molecule that competes with O₂ binding.^{13,14} A Cys-Tyr cross-link motif was identified in human ADO via genetic incorporation of an unnatural amino acid, 3,5,-difluoro-tyrosine, in conjunction with mass spectrometry and NMR experiments.¹⁵ While the cross-link in *Rn*CDO forms between Cys93 and Tyr157, in human ADO the residues involved, Cys206 and Tyr208 (*Mm*ADO numbering), are separated by only one amino acid. Based on sequence alignment, the ADO cross-link motif is plausible in PCOs; however, neither X-ray crystallography nor tandem MS/MS analyses provided evidence for the formation of a Cys-Tyr thioether bond in PCO4.¹⁶ Consequently, the extent of cross-link formation in *Mm*ADO and its physiological role remain uncertain.

The lack of an X-ray crystal structure of mammalian ADO and the low overall sequence identity between ADO and other TDOs have rendered comparisons with other TDOs uncertain. While the presence of a 3-His facial triad coordinating the Fe cofactor was confirmed on the basis of spectroscopic and site-directed mutagenesis experiments, little has previously been established about ADO beyond its first coordination sphere. Thus, a structural characterization of ADO was pivotal to identifying key residues involved in substrate binding and other salient features of the protein. Here, we describe the 1.9 Å X-ray crystal structure of *Mm*ADO. As proposed on the basis of previous studies, ADO features a 3-His facial triad that coordinates the iron center. Both the X-ray crystal structure of ADO and a sequence alignment of various TDOs reveal that the structure of ADO is more similar to that of PCO than CDO. As reported for PCO, cross-link formation between Cys206 and Tyr208 was not observed in the structure of *Mm*ADO.

Interestingly, a pair of Cys residues is identified that could form a disulfide bond, thus blocking a secondary access tunnel and controlling catalytic activity via regulating delivery of the cosubstrate O₂. Finally, molecular dynamics in combination with quantum mechanics/molecular mechanics calculations, validated on the basis of the X-ray crystal structure of resting ADO, were used to generate models of 2-AET and Nt-Cys bound ADO.

4.2 Results

Crystallization and structure determination. The protein was produced as an ADO/SUMO fusion and crystallized under anaerobic conditions upon removal of the His₆SUMO solubility tag. The structure of ADO was solved to a nominal 1.89 Å resolution (crystallographic statistics, *Appendix*, Table A4.1). The crystallographic asymmetric unit comprises four independent copies of the protein. In every case, a loop from a symmetry-related protein, centered at His130 protrudes into the active site, with His130HE2 hydrogen bonding to an iron-bound active site water (*Appendix*, Fig. A4.1). In all four independent monomers, a short loop of 4-8 residues between Phe21 and Pro31 was too disordered to model. In two subunits, a second 4-6 residue loop between Pro217 and Ala224 was also disordered. Coordinates and structure factors have been deposited in the Protein Data Bank (PDB) with PDB ID code 7LVZ.

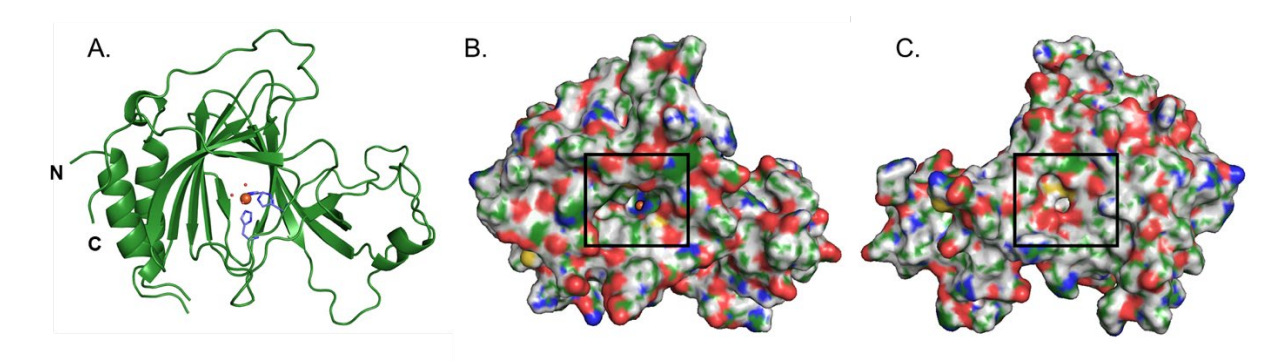


Figure 4.1. (A) Cartoon representation of the overall structure of ADO. The active site consists of an Fe ion (orange sphere) that is coordinated by a 3-His triad (purple) and 3 water molecules (red spheres). (B) Surface representation of the protein with a black box highlighting the peptide substrate access tunnel to the active site. The RBG coloring is as follows: Fe, orange; carbon,

green; hydrogen white, oxygen, red; nitrogen, blue; and sulfur, yellow. (C) Same as in B but rotated 180° to reveal the entrance to the putative co-substrate (O₂) tunnel, which is highlighted by a black box.

Protein architecture. The ADO protein adopts a β-barrel structure typical of the cupin superfamily. The 3-His facial triad coordinating the catalytically relevant Fe ion lies at the center of the protein flanked by β-sheets (**Figure 4.1A**). Interestingly, the His130 side chain of a different ADO monomer is present in the active site (*Appendix*, Fig. A4.1) but does not bind to the Fe cofactor. In PCO, a His residue from the N-terminal His $_6$ tag also protrudes into the active site; however, in contrast to what is observed for ADO, the His residue in the PCO structure binds directly to the Fe cofactor.

The surface representation of ADO highlights a prominent tunnel into the active site through which substrate is likely to bind (**Figure 4.1B**). Although such a tunnel also exists in CDO, the amino acids that define the CDO substrate tunnel are not conserved in ADO, and the large cavity in ADO is in a structurally distinct location as compared to CDO. Interestingly, the surface representation of the "backside" of ADO features a secondary tunnel from the protein surface to the active site (**Figure 4.1C**). It is tempting to speculate that once cysteamine or a bulky Nt-Cys substrate is bound, this much smaller tunnel could provide access for co-substrate O₂ to the Fe cofactor. The entrance to this tunnel is guarded by two Cys residues pointed directly at each other with an S··S distance of ~4 Å (further discussed in *Key conserved residues*).

Active site. The Fe cofactor resides in an octahedral coordination environment composed of His100, His102, and His179 (**Figure 4.2**). In three out of the four crystallographically independent copies in the unit cell, three well-resolved water molecules occupy the remaining coordination sites. In the fourth copy, only two coordinating water molecules are clearly resolved while additional electron density is present in two different regions, 2.18 and 3.65 Å from the Fe center. Although this electron density may seem consistent with a diatomic (e.g., O₂-derived; apparent

O–O distance of 1.89 Å) ligand, it is presumably associated with a third water molecule that is disordered over two positions given that ADO was crystallized under anaerobic conditions.

The active site is surrounded by a hydrophobic pocket with few residues, primarily Leu and IIe, closer than 5 Å to the Fe center. Asp192 of *Mm*ADO corresponds to the PCO4 residue Asp176, which has been shown to be critical for PCO function. Specifically, in the as-isolated Asp176Asn PCO4 variant, only 10% of the active sites contained Fe and the enzymatic activity was decreased ~10-fold even after iron supplementation. ¹⁶ The next set of residues near the ADO active site are Phe89, Cys206, and Tyr208, all located ~7 Å from the cofactor. Although these residues are not close to the Fe cofactor, their locations bordering the substrate access tunnel suggest that they could aid in positioning substrate.

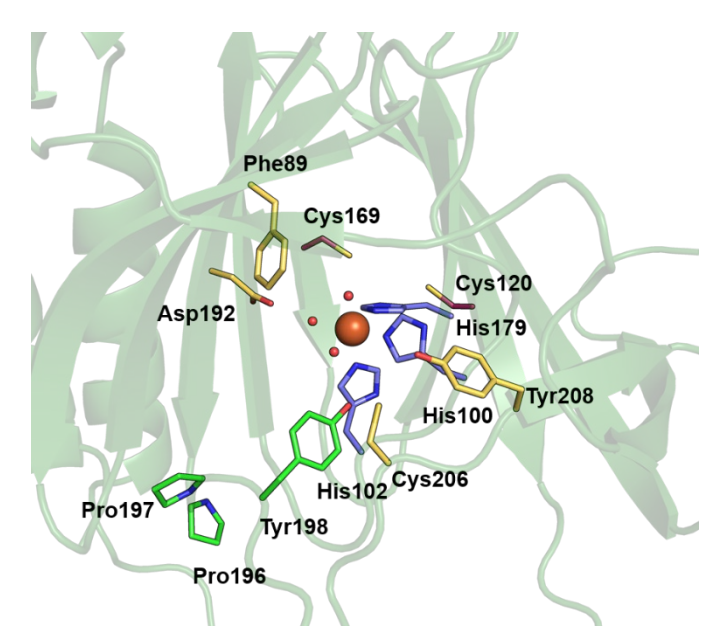


Figure 4.2. Active site region of *Mm*ADO viewed through the substrate tunnel. The Fe ion (orange sphere) is bound by His100, His102, His179 (purple), and three water molecules (red spheres). Other amino acids in the active site are highlighted in yellow (Phe89, Asp192, Cys206, and Tyr208) or green (Pro196, Pro197, and Tyr198).

In human ADO, Cys220 and Tyr222 (corresponding to Cys206 and Tyr208 of *Mm*ADO) have been shown to be capable of forming a thioether cross-link.¹⁵ In the absence of a crystal

structure, these two residues were presumed to be located near the Fe cofactor, as cross-link formation required the presence of 2-AET and O₂. In the *Mm*ADO structure, there is no electron density supporting the existence of a cross-link between Cys206 and Tyr208. Although the absence of a cross-link could be attributed to the fact that the protein used to obtain single crystals of ADO was purified semi-anaerobically and crystallized anaerobically in the presence of 2-AET (see Methods section), the fraction of cross-linked ADO purified aerobically appears to be very small based on published high-resolution mass spectra.¹⁵ Moreover, in the case of PCO4, no cross-link was observed in the X-ray crystal structure or via incubation of protein with substrate and tandem MS/MS analysis.¹⁶ Thus, the physiological relevance of the Cys-Tyr cross-link in ADO remains in question.

Distinguishing ADO motifs. X-ray crystallographic studies revealed that the first coordination spheres of TDOs are identical, with the PCO, CDO, MDO, and, as shown here, ADO active sites all featuring an Fe center coordinated by a 3-His triad. It is the secondary sphere of the active site that boasts unique residues and sequence motifs to tailor the specific reactivity of each enzyme (e.g., the Ser153-His155-Tyr157 catalytic triad in CDO and Gln62 in MDO). The distinguishing MDO and CDO secondary sphere features are neither conserved in the ADO amino acid sequence nor replicated in the X-ray crystal structure. Contrastingly, the ADO and PCO4 active site architectures are remarkably similar, perhaps indicative of closely analogous, or even identical, functions. An alignment of *Mm*ADO, *At*PCO4, *Pa*MDO, *Mm*CDO, and *Bs*CDO was constructed (**Figure 4.3**) to guide the identification of key residues and their location in the ADO crystal structure (**Figure 4.2**).

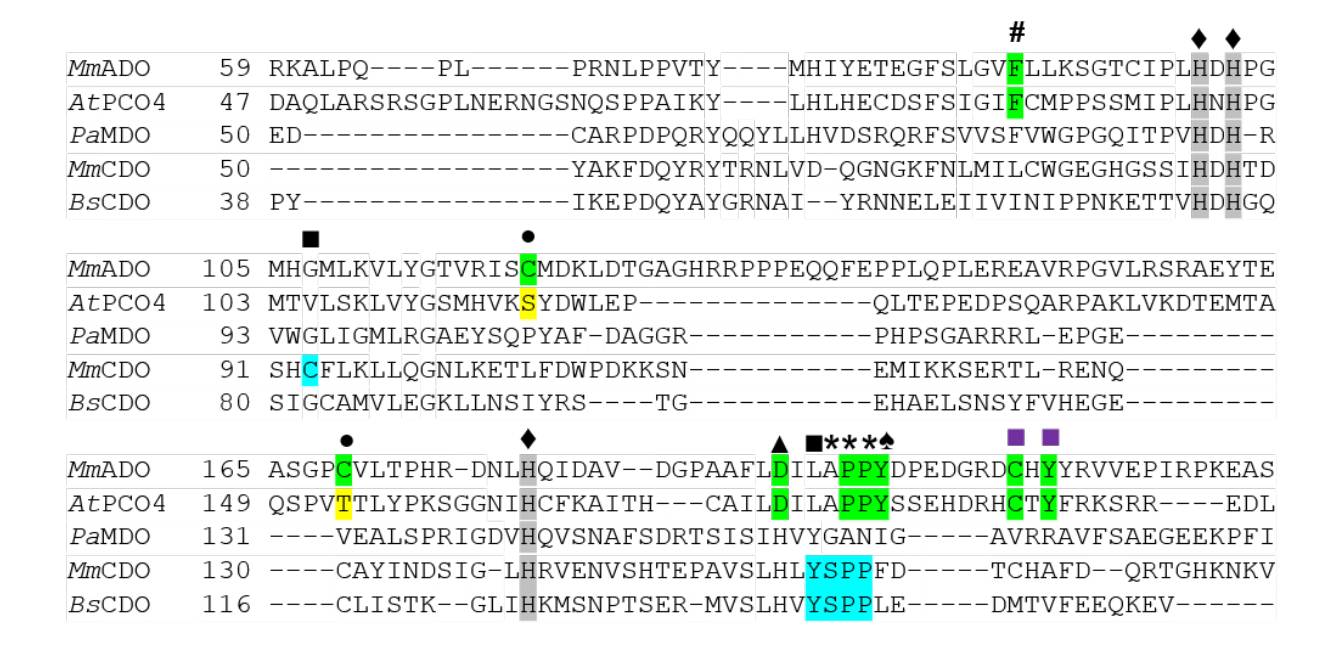


Figure 4.3. Sequence alignment showing conserved residues within TDOs. The sequences of the PCO4 from *Arabidopsis thaliana* (*At*PCO4), the MDO from *Pseudomonas aeruginosa* (*Pa*MDO), and the CDOs from *Mus musculus* (*Mm*CDO) and *Bacillus subtilis* (*Bs*CDO) are compared to the *Mus musculus* ADO (*Mm*ADO) sequence. Important ADO and PCO residues are highlighted in green, for CDO in blue, and key differences in yellow. All proteins possess a 3-His metal-binding motif marked by a ◆ and highlighted in gray. Additional motifs discussed in the text are denoted as follows: # Phe89 (*Mm*ADO numbering), ■ Cys-Tyr cross-link in *Mm*CDO, ■ putative ADO and PCO cross-link motifs, • Cys120 and Cys169 in *Mm*ADO are replaced by Ser118 and Thr153 in PCO4, ▲ Asp192, * denotes a *cis*-peptide bond, and ♠ Tyr198 in *Mm*ADO and Tyr182 in *At*PCO4 adjacent to the *cis*-peptide bond.

TDOs are relatively small proteins with sequences containing 200 to 300 amino acids. *Mm*ADO, composed of 256 amino acids, boasts a remarkable 33 Pro residues, compared to 23 and 7 found in *At*PCO4 and *Rn*CDO, respectively. Interestingly, the ADO structure shows a *cis*-peptide bond between Pro196 and Pro197. Jameson et al. established that the presence or absence of a *cis*-peptide bond between Ser158 and Pro159 results in a different positioning of the key Tyr157 residue (*Rn*CDO numbering) involved in the thioether cross-link of CDO.^{17,18}

Although in CDO the Tyr157 residue precedes this *cis*-peptide motif, in ADO a Tyr residue (Tyr198) is present directly after Pro196 and Pro197; thus, the orientation of Tyr198 is also controlled by a *cis*-peptide motif. Intriguingly, Tyr198 and Tyr208 reside equidistant and in a similar position from Cys206 (**Figure 4.2**, yellow). This Tyr198-Cys206-Tyr208 sandwich borders the substrate tunnel near the protein-solvent barrier. An analogous loop is conserved in PCO4, where it was postulated to play a role in peptide substrate recognition and binding. ¹⁶ On the basis of these observations, it is tempting to speculate that the Tyr198 residue in ADO plays a larger role in substrate binding and enzyme function than does Tyr208.

The backside tunnel to the active site (**Figure 4.1C**) is lined by two surface-exposed Cys residues, Cys120 and Cys169 (**Figure 4.2**, yellow). While not bonded in this crystal structure, the residues are 4.8 Å apart and gate a potential secondary access tunnel to the active site. We hypothesize that under proper oxidizing conditions, these residues could form a disulfide bond so as to control O₂ access to the active site, and thus enzyme activity. Computational studies aimed at assessing the feasibility of this hypothesis, as well as the generation of faithful models of substrate-bound ADO are presented next.

Computational analysis of resting and substrate-bound ADO. Repeated attempts were made to crystallize ADO with substrate 2-AET bound. As these attempts were unsuccessful, computational methods were used to generate whole-protein models of ADO complexed with 2-AET and the CKGL tetramer, representative of RGS5. Initially, a computational model of ADO in the absence of substrate was constructed starting from the crystal structure reported in this study to assess the feasibility of the computational approach chosen. The conformational landscape was sampled by first performing an unrestrained molecular dynamics (MD) simulation in GROMACS,¹⁹ after which a clustering algorithm was used to select five representative ADO structures that encompassed the majority of conformations accessed during the simulation. The geometries of these structures were optimized using a quantum mechanics/molecular mechanics (QM/MM) approach. The optimized model with the lowest energy was used for further analysis

and as the foundation for subsequent calculations of substrate-bound ADO. Importantly, the QM/MM optimized lowest-energy ADO model shows minor deviations from the crystal structure, with the root mean square deviation (RMSD) of the backbone atomic positions being 2.57 Å even though a single ADO monomer was used in our calculations. Additionally, both the prominent substrate channel and smaller secondary channel are preserved in the computational model, as are the bond lengths and angles of the active site (*Appendix*, Fig. A4.2).

In the QM/MM optimized ADO model, the Cys120 and Cys169 residues remain in close proximity, with an S··S distance of 3.5 Å (compared to ~4.8 Å in the crystal structure), hinting at the possibility of disulfide bond formation under oxic conditions. To further evaluate this possibility, a model of ADO containing a disulfide bond between these two residues was generated by altering the crystal structure *in silico* to install an S–S bond and using the computational workflow described above. Interestingly, the optimized ADO models with and without Cys120···Cys169 disulfide display only minor structural differences, both overall and in the active site region (*Appendix*, Figs. A4.3-6). However, a significant narrowing of the backside substrate channel occurs in response to disulfide bond formation, which lends credence to the possibility of a gating mechanism that modulates O₂ access based on cellular oxidative conditions.

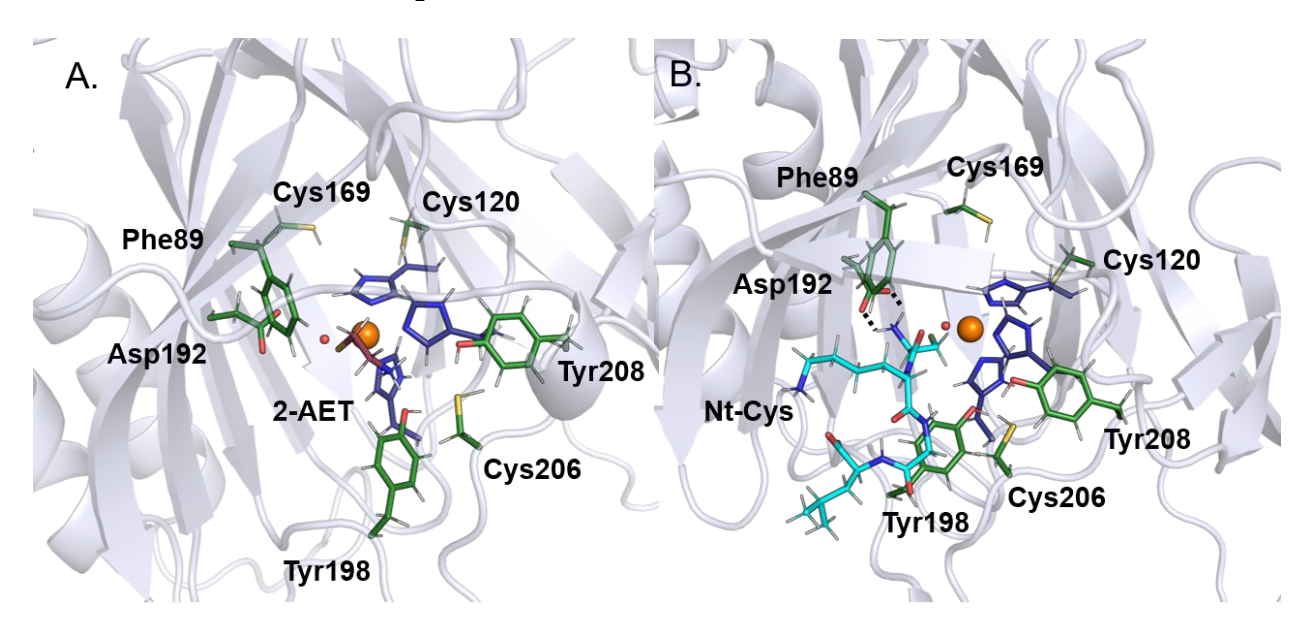


Figure 4.4. Active site regions of the QM/MM-optimized structures of ADO complexed with (*A*) 2-AET (burgundy sticks) and (*B*) the CKGL peptide (cyan sticks), representative of RGS5. The hydrogen-bonding interaction between the amine group of the peptide and Asp192 is indicated by broken lines.

Initial coordinates for substrate-bound ADO models were generated using the docking software AutoDock Vina²⁰ to place substrate into the active site of the QM/MM-optimized ADO model lacking the Cys120···Cys169 disulfide bond. Both 2-AET and the CKGL peptide were bound to Fe in a monodentate fashion with thiol-only coordination, as stipulated by previous spectroscopic studies of substrate-bound ADO. ^{12,21} Despite monodentate substrate binding, two water ligands were removed from the Fe center, as an open coordination site would be required for O₂ binding and enzymatic turnover. These substrate-bound models were then subjected to MD simulations and QM/MM optimizations, as described above for resting ADO. In the case of 2-AET-bound ADO, the large size of the substrate cavity allowed for substantial conformational changes of this small substrate during the MD simulation, with the amine group pointing toward Asp192, Cys206, or nearby water molecules at different time points. In the lowest-energy QM/MM optimized model (Figure 4.4A), the amine group of 2-AET is positioned roughly equidistant from Tyr198 and Cys206. Notably, upon 2-AET binding to ADO, the putative secondary substrate access channel becomes more defined, now extending from the surface to the active site so that it connects to the larger substrate channel.

Visualization of the MD trajectory for the ADO model complexed with the relevant portion of the RGS5 peptide (CKGL) makes it apparent that important differences exist in how 2-AET and peptide substrates interact with the secondary sphere of ADO. Compared to 2-AET, the peptide interacts with a much larger number of residues lining the active site cavity. After an initial equilibration period during the MD simulation, the orientation of the terminal cysteine remained largely unchanged, with the amine group always pointing toward Asp192. In the lowest energy QM/MM optimized structure (**Figure 4.4B**), the distance between these groups is 1.98 Å,

suggesting that Asp192 engages in a hydrogen bonding interaction to properly situate the peptide substrate for catalysis. Another notable residue in the model of peptide-bound ADO is Tyr198, the residue situated next to the Pro196 and Pro197 *cis*-peptide motif. This residue likely participates in stabilizing interactions with substrate, as it is positioned closer than 4 Å from several side chains of the peptide. Finally, while the small backside channel lined by Cys120 and Cys169 appears more restricted than in the 2-AET-bound model, with a small occlusion to the protein's surface, it does not disappear entirely.

4.3 Discussion

Oxidation of 2-AET and Nt-Cys peptides are important biological transformations; yet, little is known about the enzyme, ADO, that catalyzes these reactions. The geometric and electronic structures of substrate-bound ADO have been spectroscopically investigated and both 2-AET and Nt-Cys have been found to coordinate to the Fe via the terminal thiolate moiety. 12,21 While kinetic studies demonstrated that ADO is capable of turning over both 2-AET and Nt-Cys peptides, 3,8 the substrate scope and specificity remain to be established. This work confirms that ADO adopts both the canonical cupin architecture and 3-His facial triad typical of TDOs. However, unique structural motifs and secondary sphere elements are observed in the X-ray crystal structure of ADO that are not present in CDO or MDO. In addition, this structure provides the necessary foundation for future investigations of the mechanisms of dioxygen activation and peptide substrate oxidation employed by this vital mammalian TDO.

As ADO could not be crystallized with substrate bound, MD and QM/MM computations were employed to investigate the interactions between secondary sphere residues and Fe-bound substrate. Upon binding of CKGL (representative of the RGS5 peptide) to Fe(II)ADO, the amine group of the peptide adopts a position close enough to hydrogen bond with Asp192. Interestingly, the CKGL peptide is positioned closer to Tyr198 than Tyr208, the latter of which has been proposed to form a cross-link with Cys206. The small size of 2-AET allows for greater conformational flexibility within the active site, such that the amine does not interact with the same

residues as the representative RGS5 peptide model. In particular, Tyr208 is too far away from 2-AET to affect the Fe–S bonding interaction in 2-AET-bound Fe(III)ADO. In support of this computational prediction, electron paramagnetic resonance spectra obtained for the cyanide/2-AET adducts of WT Fe(III)ADO and its Tyr208Phe variant are superimposable.²²

Computational modeling of peptide-bound ADO shows that substrate RGS5 would likely fill the larger active site tunnel and force co-substrate O₂ delivery through a separate channel. To explore this possibility, MOLE2.5 was used to identify potential tunnels, cavities, and pores.^{23–25} Upon lowering the tunnel radius from the default value of 1.25 to 0.49 Å, a tunnel was identified that starts at residues Cys120 and Cys169 and ends at the Fe atom (Appendix, Fig. A4.7). Thus, our MOLE2.5 analysis corroborates the proposal that this tunnel could selectively allow O2 to access the substrate-bound active site. Furthermore, QM/MM optimized models of ADO with Cys120 and Cys169 in their dithiol and disulfide forms display minor global structural differences, implying that these residues could form a disulfide bond under oxidizing conditions. As such, Cys120 and Cys169 could serve as a redox sensor to regulate O2 access to the active site in response to changes in the intracellular redox potential. As ADO is capable of turning over a variety of Cys-containing substrates, it lacks the high substrate specificity characteristic of other TDOs, like CDO. The oxidation of Nt-Cys by ADO marks RGS5 for arginylation by ATE1, a poorly understood post-translational modification.²⁶ RGS5 is up-regulated in ADO and ATE1 deficient cells, establishing that ADO acts upstream of ATE1.8 The presence of easily oxidizable residues such as Cys120/Cys169 and the use of O₂ as a co-substrate could connect the redox potential of the cell to enzyme activity, coupling arginylation to oxidative signaling and precluding ADO from depleting cells of Nt-Cys substrates, as well as Cys and 2-AET, in the presence of high O₂ levels.

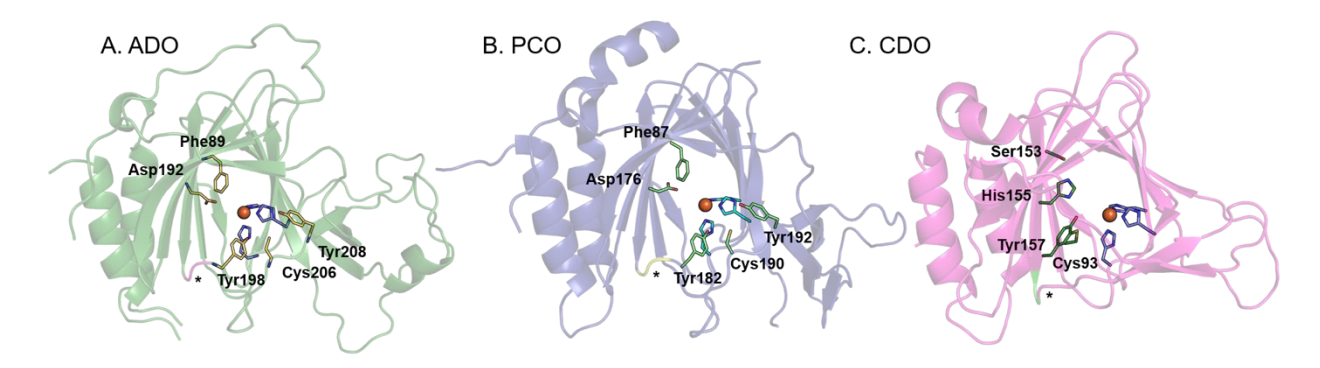


Figure 4.5. Comparison of the protein folds and active site regions of *(A) Mm*ADO (PDB: 7LVZ), *(B) At*PCO4 (PDB:6S7E), and *(C) Rn*CDO (PDB: 4JTO). The unusual *cis*-peptide bond that is preserved in all three enzymes is denoted by an asterisk (*).

Comparison to other thiol dioxygenases. A sequence alignment of relevant TDOs (Figure 4.3) demonstrates that ADO is most closely related to *At*PCO4 (21% sequence identity). Comparison of the *Mm*ADO and the *At*PCO4 X-ray crystal structures demonstrates that these enzymes share similar secondary structures, as well as identical active site residues (Figure 4.5A and B). Intriguingly, ADO has been shown to complement the function of *At*PCO4 both in vivo and in vitro, although sequence similarity analyses have established that a greater than 70% sequence identity is typically needed to extrapolate conservation of function.^{27,28}

Closer inspection of the *Mm*ADO and *At*PCO4 structures discloses distinct substrate and co-substrate access tunnels. While ADO contains one larger and one smaller access tunnel, PCO4 features a single large tunnel. Additionally, residues Cys120 and Cys169, which line the smaller access channel in ADO, are replaced by Ser118 and Thr153 in PCO4. Thus, the coupling of enzymatic activity to the intracellular redox potential that we propose to be important for the mammalian enzyme ADO is unlikely to occur in the plant enzyme PCO4. Considering that intracellular O₂ levels in mammalian cells are highly variable among different tissues, an extra layer of regulation of enzyme activity may be necessary.

The ADO metallocofactor resides in a hydrophobic pocket with one polar residue, Asp192, positioned within hydrogen bonding distance of an Fe-bound water (**Figure 4.5A**). To assess the

functional role of the corresponding residue in PCO4, Asp176 (**Figure 4.5B**), the D176N variant was produced and kinetically characterized. The variant had 10% Fe incorporation and showed minimal activity even upon the addition of exogenous iron in the activity assay. CDO also features a polar residue in the active site, Arg60 (**Figure 4.5C**), which has been shown to promote substrate binding via the formation of a salt bridge to the Cys carboxylate tail. It is likely that the negatively-charged Asp192 in ADO engages in a stabilizing interaction with a positively-charged amine group of Nt-Cys substrate.

Eukaryotic CDO features a cross-link between residues Cys93 and Tyr157 (**Figure 4.5C**). The formation of this cross-link enhances enzymatic activity by repositioning Cys93 and Tyr157 so as to allow for more favorable interactions with the Cys and O₂ substrates, while also preserving an open coordination site for O₂ binding. Although a thioether cross-link has been identified in human ADO by Liu and coworkers, ¹⁵ in the crystal structure of *Mm*ADO these two residues reside ~7 Å from the cofactor and no thioether bond is observed. As such, cross-link formation may not be structurally or functionally relevant in ADO. Intriguingly, as highlighted in **Figure 4.5**, the unusual *cis*-peptide bond that aids in the proper positioning of Tyr157 in CDO (Ser158 and Pro159) is also present in ADO (Pro196 and Pro197). In the QM/MM optimized structure of CKGL-bound ADO, Tyr198 is positioned close to the peptide substrate. The absence of a Cys206...Tyr208 cross-link in the crystal structure of *Mm*ADO, along with the lack of a direct interaction between Tyr208 and Nt-Cys or 2-AET in the computational models of substrate-bound ADO indicate that Tyr198 may be functionally more relevant than Tyr208.

In conclusion, the crystallographic and computational data of ADO presented here have revealed residues that could influence small molecule and peptide positioning within the active site. Although a thioether cross-link is key to increased turnover in mammalian CDO, a comparable contribution remains elusive in the *Mm*ADO as a cross-link is not present in the crystal structure. Of note, computational modeling of Nt-Cys binding to the ADO indicates that Tyr198 may play a key role in positioning a peptide substrate in the active site. Importantly, a backside

tunnel is identified that could serve to deliver O_2 to the peptide-bound ADO active site. This tunnel is lined by Cys120 and Cys169, with a distance and orientation compatible with redox-dependent control of O_2 access through disulfide bond formation. The unique combination of separate peptide substrate and O_2 binding channels, along with the potential for redox-sensitive control of O_2 access to the Fe- and 3-His active site represent a new model for understanding the function of mammalian thiol dioxygenases.

4.4 Materials and Methods

Preparation of Recombinant MmADO. ADO was expressed as previously described ¹² with minor additions to the purification protocol. Briefly, *Escherichia coli* Rosetta 2(DE3) cells were transformed with a pET SUMO expression vector containing a codon-optimized *Mus musculus* ADO gene and protein expression was induced with the addition of isopropyl-β-D-thiogalactopyranoside to a final concentration of 0.2 mM along with ferrous ammonium sulfate to a final concentration of 100 μM. Four hours post-induction, cells were harvested and flash frozen.

Soluble protein was purified via immobilized metal affinity (IMAC) and size exclusion (SEC) chromatography as previously described with additional steps. ¹² All buffers included 5 mM TCEP and were degassed and bubbled with argon gas to minimize oxygen presence in buffer. Post elution from the SEC column, the ADO/SUMO fusion protein was dialyzed via centrifugation into 200 mM Tris IMAC 150 mM NaCl 5 mM TCEP 5 mM imidazole pH 8 buffer. The protein was then incubated overnight at room temperature with SUMO protease (ThermoFisher). ADO was separated from the His-6-SUMO tag via reverse IMAC. Protein aliquots to be used for crystallization were flash frozen under a stream of argon gas and stored at -80 °C.

Crystallization and structure determination. Purified *Mm*ADO was screened for crystallization response using commercial screens, MRC SD2 microplates, and a Mosquito crystallization robot. Initial diffraction studies indicated almost no crystalline diffraction, even though the crystals seemed well-formed by light microscopy. Progressive exclusion of oxygen from protein purification and crystallization environment yielded progressively better diffraction. The

exceptional crystal yielding the refined diffraction data was grown by hanging drop vapor diffusion at 293K in a Coy anaerobic chamber. The reservoir solution was allowed to degas overnight in the anaerobic chamber, and consisted of 15% PEG 3350, 300 mM MgCl2, and 0.1 M Tris HCl pH 8.0. The plate was withdrawn from the chamber, and the crystal was quickly cryoprotected against reservoir solution supplemented with 20% ethylene glycol and cooled by direct immersion in liquid nitrogen.

Diffraction data were collected on an Eiger 9M detector at Life Sciences Collaborative Access Team beamline 21ID-D at the Advanced Photon Source, Argonne National Laboratory. A full 360 degree sweep of data was collected at 1.127Å, 155 mm sample to detector distance, 0.2 degrees/frame, and 0.04 second exposure time. Data were reduced using XDS³⁰ and autoPROC.³¹ Crystallographic structure solution and refinement were conducted within the Phenix suite of programs.³² The structure was solved by molecular replacement as implemented in Phaser,³³ using an edited homology model from SWISS-MODEL³⁴ derived from a PDB:6SBP template, covering residues 10-121 and 153-210 of *Mm*ADO. Molecular replacement initially produced the location and orientation of three copies of *Mm*ADO. The location and orientation of the fourth and final copy was uncovered by molecular replacement using a partially refined model based on the first three positions discovered. The structure was iteratively rebuilt in Coot³⁵ and refined using Phenix.refine.³⁶

Molecular Dynamics (MD) Simulations. MD simulations were performed using the GROMACS (versions 5.1.4 and 2019.6) software package¹⁹ with the AMBER ff19SB force field.³⁷ Initial coordinates were taken from chain D of the crystal structure reported here, keeping all crystallographic waters within 6 Å of that chain. Protonation was performed using phenix.reduce and manually adjusted, as necessary. A missing segment spanning Thr26 to Glu29 was constructed manually in PyMOL. MD parameters were generated in AmberTools,³⁸ using the metal center parameter builder (MCPB.py) modelling tool for Fe(II) and its ligands (His100, His102, His179, Fe-bound waters, and later the Fe-bound substrates).³⁹ The system was solvated

with the SPC/E water model,⁴⁰ and its total charge was neutralized by the addition of Na⁺ ions. Then, an energy minimization step was performed, followed by two equilibration steps: a 100 ps run under the NVT (isothermal-isochoric) ensemble and a 100 ps run under the NPT (isothermal-isobaric) ensemble. For each model, structures from the MD trajectory were clustered based on the RMSD of the protein backbone. The average structures of the five most populated clusters were chosen for QM/MM optimization.

Modifications to this workflow were required for some models. In the case of the disulfide model, a bond between Cys120 and Cys169 was added to the crystal structure *in silico*. This system required an additional 10 ns added to its MD simulation, as the RMSD of the protein backbone was found to still be rising substantially at the end of the first 10 ns. For the substrate-bound models, starting coordinates were taken from the QM/MM-optimized ADO model, with the substrate placed into the active site using the docking software AutoDock Vina.⁴¹

Quantum Mechanics/Molecular Mechanics (QM/MM) Calculations. Geometry optimizations were performed using quantum mechanics/molecular mechanics (QM/MM) approach implemented using the ONIOM method in Gaussian 16.⁴² The QM region was defined as the Fe ion, the side chains of its three histidine ligands (His100, His102, His179), Fe-bound water molecules, 2-AET, and the terminal cysteine of the peptide substrate. The density functional theory (DFT) portion of the calculations was performed with the unrestricted Becke, 3-parameter, Lee-Yang-Parr (UB3LYP) functional, ^{43,44} using the triple-ζ valence plus polarization (TZVP) basis set ⁴⁵ for Fe and its coordinating atoms, and the 6-31G basis set for all other atoms. ⁴⁶ For all atoms outside of the QM region, the MM calculation was performed using the AMBER force field. ⁴⁷ **Acknowledgments.** The authors are grateful for financial support from the National Institute of General Medical Sciences of the National Institutes of Health (Grant GM117120 to T.C.B.). This research was conducted in part while RLF was supported by the National Institute of General Medical Sciences of the National Institutes of Health (Grant T32GM008505). We thank Dr.

Desiree Bates and Jon Ellis for their helpful suggestions regarding the computations.

Crystallization, data collection, and structure solution and refinement were conducted by the Department of Biochemistry Collaborative Crystallography Core at the University of Wisconsin, which is supported by user fees and the department. This research used resources of the Advanced Photon Source, a U.S. Department of Energy (DOE) Office of Science User Facility operated for the DOE Office of Science by Argonne National Laboratory under Contract No. DE-AC02-06CH11357. Use of the LS-CAT Sector 21 was supported by the Michigan Economic Development Corporation and the Michigan Technology Tri-Corridor (Grant 085P1000817).

Accession Codes. ADO, Q6PDY2; CDO, P21816; PCO, Q9SJI9; MDO, Q9I0N5

4.5 References

- (1) Heafield, M. T.; Fearn, S.; Steventon, G. B.; Waring, R. H.; Williams, A. C.; Sturman, S. G. Plasma Cysteine and Sulphate Levels in Patients with Motor Neurone, Parkinson's and Alzheimer's Disease. *Neurosci. Lett.* 1990, 110 (1–2), 216–220. https://doi.org/10.1016/0304-3940(90)90814-P.
- (2) Simmons, C. R.; Hirschberger, L. L.; Machi, M. S.; Stipanuk, M. H. Expression, Purification, and Kinetic Characterization of Recombinant Rat Cysteine Dioxygenase, a Non-Heme Metalloenzyme Necessary for Regulation of Cellular Cysteine Levels. *Protein Expr. Purif.* 2006, 47 (1), 74–81. https://doi.org/10.1016/j.pep.2005.10.025.
- (3) Dominy, J. E.; Simmons, C. R.; Hirschberger, L. L.; Hwang, J.; Coloso, R. M.; Stipanuk, M. H. Discovery and Characterization of a Second Mammalian Thiol Dioxygenase, Cysteamine Dioxygenase. *J. Biol. Chem.* 2007, 282 (35), 25189–25198. https://doi.org/10.1074/jbc.M703089200.
- (4) Stipanuk, M. H.; Dominy, J. E.; Ueki, I.; Hirschberger, L. L. Measurement of Cysteine Dioxygenase Activity and Protein Abundance. *Current Protocols in Toxicology*. 2008. https://doi.org/10.1002/0471140856.tx0615s38.
- (5) Stipanuk, M. H.; Dominy, J. E.; Lee, J.-I.; Coloso, R. M. Mammalian Cysteine Metabolism: New Insights into Regulation of Cysteine Metabolism. *J. Nutr.* **2006**, *136* (6 Suppl), 1652S-

- 1659S.
- (6) Stipanuk, M. H. Metabolism of Sulfur-Containing Amino Acids. *Annu. Rev. Nutr.* 1986, 6(1), 179–209. https://doi.org/10.1146/annurev.nu.06.070186.001143.
- Shen, D.; Tian, L.; Yang, F.; Li, J.; Li, X.; Yao, Y.; Lam, E. W. F.; Gao, P.; Jin, B.; Wang, R. ADO/Hypotaurine: A Novel Metabolic Pathway Contributing to Glioblastoma Development. *Cell Death Discov.* 2021, 7 (1). https://doi.org/10.1038/s41420-020-00398-5.
- (8) Masson, N.; Keeley, T. P.; Giuntoli, B.; White, M. D.; Lavilla Puerta, M.; Perata, P.; Hopkinson, R. J.; Flashman, E.; Licausi, F.; Ratcliffe, P. J. Conserved N-Terminal Cysteine Dioxygenases Transduce Responses to Hypoxia in Animals and Plants. *Science (80-.)*. 2019, 365 (6448), 65–69. https://doi.org/10.1126/science.aaw0112.
- (9) White, M. D.; Klecker, M.; Hopkinson, R. J.; Weits, D. A.; Mueller, C.; Naumann, C.; O'Neill, R.; Wickens, J.; Yang, J.; Brooks-Bartlett, J. C.; Garman, E. F.; Grossmann, T. N.; Dissmeyer, N.; Flashman, E. Plant Cysteine Oxidases Are Dioxygenases That Directly Enable Arginyl Transferase-Catalysed Arginylation of N-End Rule Targets. *Nat. Commun.* 2017, 8. https://doi.org/10.1038/ncomms14690.
- (10) Lee, M. J.; Tasaki, T.; Moroi, K.; An, J. Y.; Kimura, S.; Davydov, I. V.; Kwon, Y. T. RGS4 and RGS5 Are in Vivo of the N-End Rule Pathway. *Proc. Natl. Acad. Sci. U. S. A.* 2005, 102 (42), 15030–15035. https://doi.org/10.1073/pnas.0507533102.
- (11) Tamirisa, P.; Blumer, K. J.; Muslin, A. J. RGS4 Inhibits G-Protein Signaling in Cardiomyocytes. *Circulation* 1999, 99 (3), 441–447. https://doi.org/10.1161/01.CIR.99.3.441.
- (12) Fernandez, R. L.; Dillon, S. L.; Stipanuk, M. H.; Fox, B. G.; Brunold, T. C. Spectroscopic Investigation of Cysteamine Dioxygenase. *Biochemistry* 2020, 59 (26), 2450–2458. https://doi.org/10.1021/acs.biochem.0c00267.
- (13) Driggers, C. M.; Kean, K. M.; Hirschberger, L. L.; Cooley, R. B.; Stipanuk, M. H.; Karplus,

- P. A. Structure-Based Insights into the Role of the Cys-Tyr Crosslink and Inhibitor Recognition by Mammalian Cysteine Dioxygenase. *J. Mol. Biol.* **2016**, *428* (20), 3999–4012. https://doi.org/10.1016/j.jmb.2016.07.012.
- (14) Davies, C. G.; Fellner, M.; Tchesnokov, E. P.; Wilbanks, S. M.; Jameson, G. N. L. The Cys-Tyr Cross-Link of Cysteine Dioxygenase Changes the Optimal Ph of the Reaction without a Structural Change. *Biochemistry* 2014, 53 (50), 7961–7968. https://doi.org/10.1021/bi501277a.
- (15) Wang, Y.; Griffith, W. P.; Li, J.; Koto, T.; Wherritt, D. J.; Fritz, E.; Liu, A. Cofactor Biogenesis in Cysteamine Dioxygenase: C–F Bond Cleavage with Genetically Incorporated Unnatural Tyrosine. *Angew. Chemie Int. Ed.* 2018, 57 (27), 8149–8153. https://doi.org/10.1002/anie.201803907.
- (16) White, M. D.; Carbonare, L. D.; Puerta, M. L.; Iacopino, S.; Edwards, M.; Dunne, K.; Pires, E.; Levy, C.; McDonough, M. A.; Licausi, F.; Flashman, E. Structures of Arabidopsis Thaliana Oxygen-Sensing Plant Cysteine Oxidases 4 and 5 Enable Targeted Manipulation of Their Activity. *Proc. Natl. Acad. Sci. U. S. A.* 2020, 117 (37), 23140–23147. https://doi.org/10.1073/pnas.2000206117.
- (17) Tchesnokov, E. P.; Fellner, M.; Siakkou, E.; Kleffmann, T.; Martin, L. W.; Aloi, S.; Lamont, I. L.; Wilbanks, S. M.; Jameson, G. N. L. The Cysteine Dioxygenase Homologue from Pseudomonas Aeruginosa Is a 3-Mercaptopropionate Dioxygenase. *J. Biol. Chem.* 2015, 290 (40), 24424–24437. https://doi.org/10.1074/jbc.M114.635672.
- (18) Aloi, S.; Davies, C. G.; Karplus, P. A.; Wilbanks, S. M.; Jameson, G. N. L. Substrate Specificity in Thiol Dioxygenases. *Biochemistry* 2019, 2398–2407. https://doi.org/10.1021/acs.biochem.9b00079.
- (19) Abraham, M. J.; Murtola, T.; Schulz, R.; Páll, S.; Smith, J. C.; Hess, B.; Lindah, E. Gromacs:
 High Performance Molecular Simulations through Multi-Level Parallelism from Laptops to
 Supercomputers.
 SoftwareX
 2015,
 1–2,
 19–25.

- https://doi.org/10.1016/j.softx.2015.06.001.
- (20) Trott, O.; Olson, A. J. AutoDock Vina: Improving the Speed and Accuracy of Docking with a New Scoring Function, Efficient Optimization, and Multithreading. *J. Comput. Chem.* 2009, 31 (2), NA-NA. https://doi.org/10.1002/jcc.21334.
- (21) Wang, Y.; Davis, I.; Chan, Y.; Naik, S. G.; Griffith, W. P.; Liu, A. Characterization of the Nonheme Iron Center of Cysteamine Dioxygenase and Its Interaction with Substrates. *J. Biol. Chem.* 2020, 295 (33), 11789–11802. https://doi.org/10.1074/jbc.ra120.013915.
- (22) Fernandez, R. L.; Juntunen, N. D.; Fox, B. G.; Brunold, T. C. Spectroscopic Investigation of Iron (III) Cysteamine Dioxygenase in the Presence of Substrate (Analogues): Implications for the Nature of Substrate-Bound Reaction Intermediates. Submitted 2021.
- (23) Sehnal, D.; Vařeková, R. S.; Berka, K.; Pravda, L.; Navrátilová, V.; Banáš, P.; Ionescu, C. M.; Otyepka, M.; Koča, J. MOLE 2.0: Advanced Approach for Analysis of Biomacromolecular Channels. *J. Cheminform.* 2013, 5 (8), 1–13. https://doi.org/10.1186/1758-2946-5-39.
- (24) Jones, J. C.; Banerjee, R.; Shi, K.; Aihara, H.; Lipscomb, J. D. Structural Studies of the Methylosinus Trichosporium OB3b Soluble Methane Monooxygenase Hydroxylase and Regulatory Component Complex Reveal a Transient Substrate Tunnel. *Biochemistry* 2020, 59 (32), 2946–2961. https://doi.org/10.1021/acs.biochem.0c00459.
- (25) Banerjee, R.; Lipscomb, J. D. Small-Molecule Tunnels in Metalloenzymes Viewed as Extensions of the Active Site. *Acc. Chem. Res.* **2021**, *54* (9), 2185–2195. https://doi.org/10.1021/acs.accounts.1c00058.
- (26) Van, V.; Smith, A. T. ATE1-Mediated Post-Translational Arginylation Is an Essential Regulator of Eukaryotic Cellular Homeostasis. *ACS Chem. Biol.* **2020**. https://doi.org/10.1021/acschembio.0c00677.
- (27) Tian, W.; Skolnick, J. How Well Is Enzyme Function Conserved as a Function of Pairwise Sequence Identity? *J. Mol. Biol.* **2003**, 333 (4), 863–882.

- https://doi.org/10.1016/j.jmb.2003.08.057.
- (28) Gerlt, J. A.; Bouvier, J. T.; Davidson, D. B.; Imker, H. J.; Sadkhin, B.; Slater, D. R.; Whalen, K. L. Enzyme Function Initiative-Enzyme Similarity Tool (EFI-EST): A Web Tool for Generating Protein Sequence Similarity Networks. *Biochim. Biophys. Acta Proteins Proteomics* 2015, 1854 (8), 1019–1037. https://doi.org/10.1016/j.bbapap.2015.04.015.
- (29) Dominy, J. E.; Hwang, J.; Guo, S.; Hirschberger, L. L.; Zhang, S.; Stipanuk, M. H. Synthesis of Amino Acid Cofactor in Cysteine Dioxygenase Is Regulated by Substrate and Represents a Novel Post-Translational Regulation of Activity. *J. Biol. Chem.* **2008**, *283* (18), 12188–12201. https://doi.org/10.1074/jbc.M800044200.
- (30) Kabsch, W. XDS. Acta Crystallogr. Sect. D Biol. Crystallogr. 2010, D66, 125–132. https://doi.org/10.1107/S0907444909047337.
- (31) Vonrhein, C.; Flensburg, C.; Keller, P.; Sharff, A.; Smart, O.; Paciorek, W.; Womack, T.; Bricogne, G. Data Processing and Analysis with the AutoPROC Toolbox. *Acta Crystallogr. Sect. D Biol. Crystallogr.* 2011, 67 (4), 293–302. https://doi.org/10.1107/S0907444911007773.
- (32) Adams, P. D.; Afonine, P. V.; Bunkóczi, G.; Chen, V. B.; Davis, I. W.; Echols, N.; Headd, J. J.; Hung, L. W.; Kapral, G. J.; Grosse-Kunstleve, R. W.; McCoy, A. J.; Moriarty, N. W.; Oeffner, R.; Read, R. J.; Richardson, D. C.; Richardson, J. S.; Terwilliger, T. C.; Zwart, P. H. PHENIX: A Comprehensive Python-Based System for Macromolecular Structure Solution. *Acta Crystallogr. Sect. D Biol. Crystallogr.* 2010, 66 (2), 213–221. https://doi.org/10.1107/S0907444909052925.
- (33) McCoy, A. J.; Grosse-Kunstleve, R. W.; Adams, P. D.; Winn, M. D.; Storoni, L. C.; Read, R. J. Phaser Crystallographic Software. J. Appl. Crystallogr. 2007, 40 (4), 658–674. https://doi.org/10.1107/S0021889807021206.
- (34) Waterhouse, A.; Bertoni, M.; Bienert, S.; Studer, G.; Tauriello, G.; Gumienny, R.; Heer, F. T.; De Beer, T. A. P.; Rempfer, C.; Bordoli, L.; Lepore, R.; Schwede, T. SWISS-MODEL:

- Homology Modelling of Protein Structures and Complexes. *Nucleic Acids Res.* **2018**, *46* (W1), W296–W303. https://doi.org/10.1093/nar/gky427.
- (35) Emsley, P.; Lohkamp, B.; Scott, W. G.; Cowtan, K. Features and Development of Coot. Acta Crystallogr. Sect. D Biol. Crystallogr. 2010, 66 (4), 486–501. https://doi.org/10.1107/S0907444910007493.
- (36) Afonine, P. V.; Grosse-Kunstleve, R. W.; Echols, N.; Headd, J. J.; Moriarty, N. W.; Mustyakimov, M.; Terwilliger, T. C.; Urzhumtsev, A.; Zwart, P. H.; Adams, P. D. Towards Automated Crystallographic Structure Refinement with Phenix.Refine. *Acta Crystallogr. Sect. D Biol. Crystallogr.* 2012, 68 (4), 352–367. https://doi.org/10.1107/S0907444912001308.
- (37) Tian, C.; Kasavajhala, K.; Belfon, K. A. A.; Raguette, L.; Huang, H.; Migues, A. N.; Bickel, J.; Wang, Y.; Pincay, J.; Wu, Q.; Simmerling, C. Ff19SB: Amino-Acid-Specific Protein Backbone Parameters Trained against Quantum Mechanics Energy Surfaces in Solution. J. Chem. Theory Comput. 2020, 16 (1), 528–552. https://doi.org/10.1021/acs.jctc.9b00591.
- (38) D.A. Case; Belfon, K.; Ben-Shalom, I. Y.; Brozell, S. R.; Cerutti, D. S.; T.E. Cheatham, I.; Cruzeiro, V. W. D.; Darden, T. A.; Duke, R. E.; Giambasu, G.; Gilson, M. K.; Gohlke, H.; Goetz, A. W.; Harris, R.; Izadi, S.; Jhala, K. K.-; Kovalenko, A.; Krasny, R.; Kurtzman, T.; Lee, T. S.; LeGrand, S.; Li, P.; Lin, C.; Liu, J.; Luchko, T.; Luo, R.; Man, V.; Merz, K. M.; Miao, Y.; Mikhailovskii, O.; Monard, G.; Nguyen, H.; Onufriev, A.; Pan, F.; Pantano, S.; Qi, R.; Roe, D. R.; Roitberg, A.; Sagui, C.; Schott-Verdugo, S.; Shen, J.; Simmerling, C. L.; Skrynnikov, N.; Smith, J.; Swails, J.; Walker, R. C.; Wang, J.; Wilson, L.; Wolf, R. M.; Wu, X.; York, D. M.; Kollman, P. A. Amber 2020. University of California, San Francisco 2020.
- (39) Li, P.; Merz, K. M. MCPB.Py: A Python Based Metal Center Parameter Builder. *J. Chem. Inf. Model.* **2016**, *56*, 599–604.
- (40) Berendsen, H. J. C.; Grigera, J. R.; Straatsma, T. P. The Missing Term in Effective Pair Potentials. *J. Phys. Chem.* **1987**, 91 (24), 6269–6271.

- https://doi.org/10.1021/j100308a038.
- (41) Trott, O.; Olson, A. J. AutoDock Vina: Improving the Speed and Accuracy of Docking with a New Scoring Function, Efficient Optimization, and Multithreading. *J. Comput. Chem.* 2009, 31 (2), NA-NA. https://doi.org/10.1002/jcc.21334.
- Frisch, M. J.; Trucks, G. W.; Schlegel, H. E.; Scuseria, G. E.; Robb, M. A.; Cheeseman, J. R.; Scalmani, G.; Barone, V.; Petersson, G. A.; Nakatsuji, H.; Li, X.; Caricato, M.; Marenich, A. V.; Bloino, J.; Janesko, B. G.; Gomberts, R.; Mennucci, B.; Hratchian, H. P.; Ortiz, J. V.; Izmaylov, A. F.; Sonnenberg, J. L.; Williams-Young, D.; Ding, F.; Lipparini, F.; Egidi, F.; Goings, J.; Peng, B.; Petrone, A.; Henderson, T.; Ranasinghe, D.; Zakrzewski, V. G.; Gao, J.; Rega, N.; Zheng, G.; Liang, W.; Hada, M.; Ehara, M.; Toyota, K.; Fukuda, R.; Hasegawa, J.; Ishida, M.; Nakajima, T.; Honda, Y.; Kitao, O.; Nakai, H.; Vreven, T.; Throssell, K.; Montgomery, J. A., J.; Peralta, J. E.; Ogliaro, F.; Bearpark, M. J.; Heyd, J. J.; Brothers, E. N.; Kudin, K. N.; Staroverov, V. N.; Keith, T. A.; Kobayashi, R.; Normand, J.; Raghavachari, K.; Rendell, A. P.; Burant, J. C.; Iyengar, S. S.; Tomasi, J.; Cossi, M.; Millam, J. M.; Klene, M.; Adamo, C.; Cammi, R.; Ochterski, J. W.; Martin, R. L.; Morokuma, K.; Farkas, O.; Foresman, J. B.; Fox, J. D. Gaussian 16, Revision C.01. Gaussian, Inc., Wallingford CT., 2016.
- (43) Becke, A. D. Density-Functional Thermochemistry. III. The Role of Exact Exchange. *J. Chem. Phys.* **1993**, *98*, 5648.
- (44) Lee, C.; Yang, W.; Parr, R. G. Development of the Colle-Salvetti Correlation-Energy Formula into a Functional of the Electron Density. *Phys. Rev. B* **1988**, *37* (2), 785–789. https://doi.org/10.1103/PhysRevB.37.785.
- (45) Schäfer, A.; Huber, C.; Ahlrichs, R. Fully Optimized Contracted Gaussian Basis Sets of Triple Zeta Valence Quality for Atoms Li to Kr. J. Chem. Phys. 1994, 100 (8), 5829–5835. https://doi.org/10.1063/1.467146.
- (46) Hehre, W. J.; Ditchfield, K.; Pople, J. A. Self-Consistent Molecular Orbital Methods. XII.

- Further Extensions of Gaussian-Type Basis Sets for Use in Molecular Orbital Studies of Organic Molecules. *J. Chem. Phys.* **1972**, *56* (5), 2257–2261. https://doi.org/10.1063/1.1677527.
- (47) Bayly, C. I.; Merz, K. M.; Ferguson, D. M.; Cornell, W. D.; Fox, T.; Caldwell, J. W.; Kollman, P. A.; Cieplak, P.; Gould, I. R.; Spellmeyer, D. C. A Second Generation Force Field for the Simulation of Proteins, Nucleic Acids, and Organic Molecules. *J. Am. Chem. Soc.* 1995, 117 (19), 5179–5197. https://doi.org/10.1021/ja00124a002.

Chapter 5

Production, purification, and kinetic characterization of recombinant mouse ADO

Chapter 5. Production, purification, and kinetic characterization of recombinant mouse ADO

5.1 Introduction

Thiol dioxygenases (TDOs) are a family of mononuclear non-heme Fe-dependent enzymes that oxidize thiol substrates to their corresponding sulfinic acids via the incorporation of both oxygen atoms from molecular oxygen. Currently, five classes of TDOs are known that are distinguished by their native substrate specificity: cysteine dioxygenase (CDO),¹ 3-mercaptopropionate dioxygenase (MDO),^{2,3} mercaptosuccinate dioxygenase (MSDO),⁴ plant cysteine oxidase (PCO),⁵ and cysteamine dioxygenase (ADO).⁶

CDO, the first characterized TDO, catalyzes the oxidation of cysteine (Cys) to cysteine sulfinic acid (CSA), as shown in **Scheme 5.1**. ⁷ CDO has been extensively studied via structural, ^{1,8–10} spectroscopic, ^{11–15} kinetic, ^{16–20} and computational ^{21,22} techniques. The crystal structure, published in 2006, ⁸ revealed that CDO belongs to the cupin superfamily and binds an Fe(II) cofactor via a novel 3-histidine (3-His) facial triad. The 3-His binding triad has remained exceedingly rare, as apart from TDOs, few other enzymes have been crystallographically confirmed to feature this motif, among them EgtB, ²³ SznF, ²⁴ diketone-cleaving dioxygenase, ²⁵ and gentisate 1,2-dioxygenase. ²⁶ CDO also contains unique secondary sphere residues that contribute to the high substrate specificity and enzymatic activity.

$$\begin{array}{c|c} O & CDO & O & O \\ H_2N & & & & \\ \hline \\ Cysteine (Cys) & & & \\ \hline \\ Cysteine sulfinic acid (CSA) \\ \end{array}$$

Scheme 5.1. Oxidation of Cys to CSA as catalyzed by CDO.

CDO function is key to the necessary regulation of intracellular Cys levels. Elevated Cys levels have been associated with Parkinson's and Alzheimer's diseases.²⁷ After oxidation by CDO, CSA is further metabolized into hypotaurine, and finally taurine. Hypotaurine, which has been identified to negatively affect the growth and progression of aggressive high-grade gliomas

in the brain,²⁸ can also be biosynthesized directly by ADO via oxidation of cysteamine (2-aminoethanethiol, 2-AET, **Scheme 5.2A**).⁶

Scheme 5.2. Reactions catalyzed by ADO. A. Oxidation of 2-AET to hypotaurine. B. Oxidation of Nt-Cys peptides to their corresponding sulfinic acids.

Recent studies by Masson et al.²⁹ have furthered the understanding of the substrate scope of ADO, as it was discovered that ADO also catalyzes the oxidation of N-terminal Cys (Nt-Cys) peptides (**Scheme 5.2B**). The oxidation of Nt-Cys peptides had previously been shown to be catalyzed by *Arabidopsis thaliana* PCOs,^{30,31} which are classified as oxygen sensors as their rate is dependent on O₂ availability under physiologically relevant conditions. Under conditions of low oxygen, PCO is unable to carry out N-terminal oxidation and peptides persist, initiating a submergence response in plants. Under normoxic conditions, the oxidized product, with an N-terminal CSA moiety, then serves as a substrate for the arginyl tRNA transferase ATE1, marking the arginylated peptide as a candidate for ubiquitination. Similar to PCO, ADO is now also believed to oxidize substrates that function as regulators of the N-degron pathway.³² RGS4 and RGS5 peptides serve as negative regulators of cardiovascularly-relevant G protein activity, as RGS fragments can inhibit G protein signaling.³³

The present study was designed to establish the basis for future investigations into the native substrate specificity of ADO via a steady-state kinetic investigation. The Stipanuk,¹⁹ Maroney,²⁰ Jameson,³⁴ and Pierce¹⁶ labs have previously reported CDO kinetic parameters and appropriate assay conditions. However, as ADO shares substrate activity with PCO, optimized assay conditions presented in this chapter were heavily influenced by studies conducted in the

Flashman lab.^{29,31} The protocol involves the use of an ultra-high pressure liquid chromatography mass spectrometer (UPLC-MS) allowing both substrate consumption and product formation to be monitored. To validate the newly developed protocol, CDO kinetic parameters were measured and found to agree with published results. The same methodology was then used to determine the kinetic parameters for the oxidation of 2-AET by ADO.

5.2 Methods

General experimental procedures. Chemicals, reagents, and protein columns were purchased from commercial suppliers (MilliporeSigma, VWR, Alfa Aesar, Cytiva) and used without further purification. UPLC/LC-MS data were collected on an Acquity UHPLC with and Acquity QDA MS detector (Waters) using an Intrada Amino Acid column (Imtakt). Using PRISM 8 Graphpad software³⁵ kinetic data was fit to the Johnson³⁶ Michaelis-Menten equation:

$$\nu = \frac{k_{SP} [S]}{1 + k_{SP} [S] / k_{cat}}$$

where:
$$k_{SP} = V_{max} / K_M$$

Recombinant gene expression and protein purification. Expression of the recombinant Mus musculus cdo gene was performed using Rosetta 2(DE3) E. coli cells under control of the Lac operator in a pVP16 plasmid. The cdo gene was expressed as a fusion protein with an N-terminal 8×His and maltose binding protein (MBP) tags as previously described. Cells were grown in lysogeny broth (LB) containing chloroamphenicol, ampicillin, and ferrous ammonium sulfate (34 μg/mL, 100 μg/mL, and 110 μM, respectively). Gene overexpression was induced by addition of isopropyl β-D-1-thiogalactopyranoside (IPTG), D-lactose, and casamino acids (80.5 μM, 8 mM, and 0.20% w/v, respectively). Cell pellets were resuspended in 25 mM HEPES, 200 mM NaCl, 5 mM imidazole, pH 8 buffer with rLysozyme and sonicated on ice for 30 min. The lysed solution was then centrifuged at 48,400 x g and 4 °C for 75 min. The fusion protein was purified via immobilized metal affinity chromatography (IMAC) with a Ni(II) nitrilotriacetic acid (NTA) agarose resin and eluted along a linear imidazole gradient from 5 mM to 150 mM imidazole. The majority

of the CDO fusion protein eluted at 35% of IMAC B verified via stain-free sodium dodecyl sulfate-polyacrylamide gel electrophoresis (SDS-PAGE). Following elution, the protein was dialyzed overnight in the presence of tobacco etch virus (TEV) protease to cleave the N-terminal 8×His and MBP tags. Tag-free CDO was isolated using subtractive IMAC. The total protein yield was determined using the absorbance at 280 nm and corresponding extinction coefficient (ϵ_{280}) of 28.3 mM⁻¹ cm⁻¹.

Expression of the recombinant *Mus musculus ado* gene was performed using Rosetta 2(DE3) *E. coli* cells under control of the Lac operator in a pET SUMO plasmid as described elsewhere.³⁷ In summary, the fusion protein was isolated via IMAC on a HisTrap column and size exclusion chromatography (SEC) on a HiLoad 16/600 Superdex 200pg gel filtration column. Total protein yield was estimated using an ε_{280} of 41.4 mM⁻¹ cm⁻¹, calculated via ExPASy³⁸ from the SUMO-tag and ADO protein sequences. Protein aliquots to be used for characterization were flash frozen and stored at -80 °C.

The Fe(II) and total Fe contents of the protein were determined through a colorimetric assay using the iron chelator 2,4,6-tris(2-pyridyl)-s-triazine (TPTZ) and an ε_{595} of 22.1 mM⁻¹ cm⁻¹.^{21,39} The assay was performed in the presence and absence of a reductant (hydroxylamine) to determine the proportion of Fe(II) versus Fe(III) initially present. As the fraction of Fe-bound CDO active sites was ~25%, protein was reconstituted anaerobically with ferrous ammonium sulfate.⁴⁰ The fraction of Fe-bound CDO active sites was ~60-70% after Fe reconstitution, and that of asisolated Fe-bound ADO active sites ~70-80%.

Michaelis-Menten kinetic experiments. WT CDO was thawed over ice and then buffer exchanged into 200 mM MES, 150 mM NaCl, 0.1 mM bathocuprionedisulfonate (BCS), pH 6.1 buffer via centrifugation. The protein was concentrated to 100 μM as measured by a Thermo Scientific NanoDrop 2000. Reactions were carried out in 100 μL batches with 1 – 150 mM Cys and a final CDO protein concentration of 50 μM. The enzyme and substrate solutions were equilibrated to

37 °C prior to mixing. After addition of WT CDO, 20 μ L time aliquots were removed every 3 min for 12 min. The reaction was quenched via injection into 180 μ L of quench solution (equal volumes of acetonitrile and 1 M HCl with 1 mM asparagine included as an internal standard). Quenched reactions were centrifuged at 15,000 x g for 3 min and transferred to a 96-well plate prior to UPLC-MS injection of the supernatant. Enzyme activity was quantified by comparing the ratio of the analyte mass peak and the internal standard mass peak to previously generated calibration curves for each analyte.

WT ADO was thawed in hand and then buffer exchanged into 200 mM Tris, 150 mM NaCl, 0.1 mM BCS, pH 8 buffer via centrifugation. During the optimization of assay conditions, 1 mM tris(2-carboxyethyl)phosphine (TCEP) and 1 mM sodium ascorbate (Asc) were included in the activity assay matrix. The protein was concentrated to 400 µM and diluted to 100 µM during the activity assay. The 2-AET concentration was varied from 1 – 150 mM. Reactions were initiated by addition of substrate to protein warmed to 37 °C. Initial rates were measured by periodically quenching 20 µL aliquots removed every 5 min, for a total reaction time of 20 min. Quenched reaction mixtures were manipulated as described above for CDO.

5.3 Results

The quantitative activity assay replicates CDO Michaelis-Menten parameters. The activity of purified CDO and ADO has previously been measured via qualitative thin layer chromatography (TLC) activity assays.^{13,37} In a typical assay, protein is incubated aerobically with substrate in buffer and allowed to react at 37 °C for 30 min. Samples are heat denatured, centrifuged, and spotted onto a silica TLC plate. The plate is placed in a beaker containing 10:10:30 (v/v) H₂O/acetic acid/1-butanol and developed by heat activation of a ninhydrin stain. Substrate and product bands are identified via comparison to the appropriate standard. This method only allows for a qualitative identification of product formation rather than a more quantitative assessment of enzyme activity.

To validate the newly developed quantitative, UPLC-MS based activity assay, CDO was produced, purified, and kinetically characterized. Incubating CDO with various concentrations of Cys at pH 6.1 and analyzing the reaction as described in the Methods section revealed that the formation of product CSA displayed Michaelis-Menten-like kinetics with a fitted K_M of 12 mM and a k_{cat} of 0.72 s⁻¹ (**Figure 5.1**). These experimental parameters were found to be in agreement with those previously reported by Davies et al. for the activity of CDO (**Table 5.1**). ¹⁸

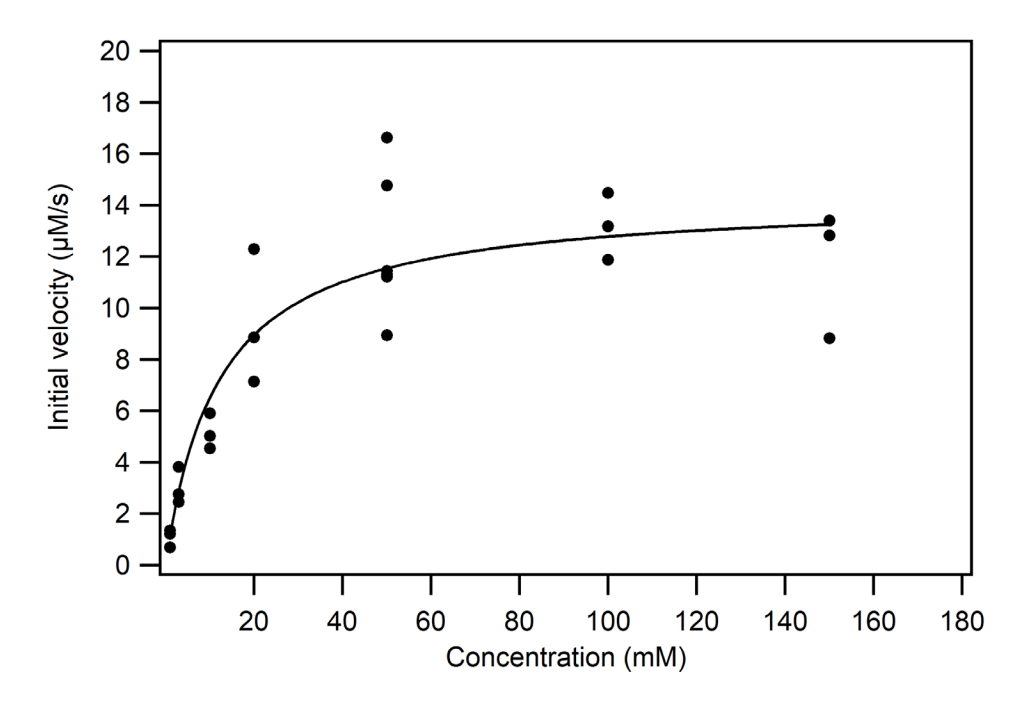


Figure 5.1. Dependence of CDO activity on Cys concentration. CDO activity displayed Michaelis-Menten kinetics with a K_M of 12 mM, a k_{cat} of 0.72 s⁻¹, and a V_{max} of 14 μ M/s. Standard errors are reported in **Table 5.1** and were typically less than 20%. Assays were conducted under aerobic conditions at 37 °C using 200 mM MES, 150 mM NaCl, 0.1 mM BCS, pH 6.1.

Table 5.1. Kinetic parameters for TDOs, obtained from previous publications and fits of the experimental data to the Michaelis-Menten equation using GraphPad PRISM 8.³⁵ Standard errors are reported.

TDO	Substrate	рН	K _M (mM)	k _{cat} (s ⁻¹)	k _{cat} /K _M
RnCDO ¹⁸	Cys	6.1	12	0.3	0.03
BsCDO ⁴⁹	Cys	6.2	3.0	0.39	0.10
PaMDO ²	3MPA	7.5	1	0.11	0.11
	Cys	7.5	8	0.021	0.003
AvMDO ³	3MPA	8.0	0.013	1	76.9
	Cys	8.0	11.4	1.2	0.11
	2-AET	8.0	26	0.29	0.01
AtPCO4 ³¹	Nt-Cys (AtRAP2:	8.0	0.69	31	44.9
AtPCO5 ³¹	CGGAIISDFIPPPR)	8.0	0.16	7.9	49.4
MmADO ⁶	2-AET	8.0	3.8	1.6	0.42
HsADO ²⁹	RGS4	7.5	0.12	20.1	163
	RGS5	7.5	0.072	16.9	236
RnCDO	Cys	6.1	12 ± 0.3	0.72 ± 0.05	0.060 ± 0.004
<i>Mm</i> ADO	2-AET	8.0	36 ± 0.2	0.037 ± 0.004	0.001 ± 0.0001

Recombinant production of ADO. The recombinant production of Mus musculus ADO (MmADO) has previously been reported. 6,37,41 In the current study, the purification of ADO was paired with kinetic characterization of the protein after first using IMAC and then SEC. In a typical experiment, the fusion protein is isolated post cell lysis via IMAC on a HisTrap column. Protein is eluted using a stepwise gradient of 20 mM Tris, 250 mM NaCl, 5 mM imidazole at pH 8.0 (IMAC buffer A) and 20 mM Tris, 250 mM NaCl, 500 mM imidazole at pH 8.0 (IMAC buffer B). Two primary peaks elute at 15% and 50% of IMAC buffer B. SDS-PAGE analysis of the two bands identifies that the first peak constitutes contaminants and untagged protein, while the second peak is comprised mainly of fusion protein (Figure 5.2A). Moreover, the initial turnover rates of the protein in Peak 1 and Peak 2 vary (Figure 5.2B and C); i.e., ADO associated with the second peak has ~3-fold higher activity than ADO isolated from the first peak. Thus, in this study the second fraction was collected

and further purified via SEC to conduct kinetic studies. Previous spectroscopic studies of substrate- and substrate analogue-bound ADO also used protein purified from the second fraction of IMAC eluent (collected on the basis of purity). Notably, in a paper published before we initiated studies of ADO, Dominy et al.⁶ also reported that ADO purified via IMAC elutes in two peaks. As initial tests showed similar ADO activity for the two peaks,⁶ fractions from the first peak were pooled and further purified via SEC.

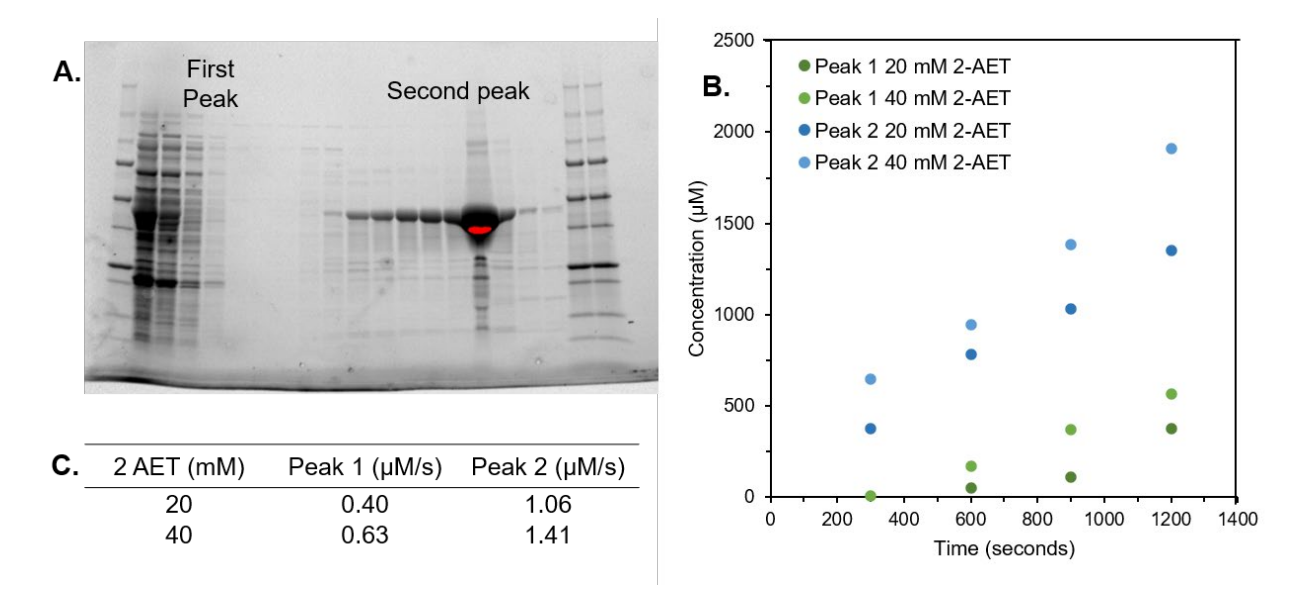


Figure 5.2. Comparison of the activity of ADO associated with IMAC Peak 1 and Peak 2. A. SDS-PAGE gel of ~42 kDa ADO post IMAC purification. ADO elutes in two peaks: the first contains primarily contaminants and untagged protein, while the second contains the ADO fusion protein. B. Initial rates were measured at various 2-AET concentrations to compare the activity of ADO in the two peaks. C. Data presented in this table indicate that the protein in Peak 2 is ~3x more active than Peak 1. Assays were conducted under aerobic conditions at 37 °C using 200 mM Tris, 150 mM NaCl, 0.1 mM BCS, 1 mM TCEP, 1 mM ascorbate, pH 8.0 buffer.

ADO oxidizes 2-AET most efficiently in the presence of reductants. Incubation of WT ADO with various 2-AET concentrations at pH 8.0 and analysis of the reaction progress as described in the Methods section showed that the formation of product displayed Michaelis-Menten kinetics with an estimated K_M of 36 mM and a k_{cat} of 0.037 s⁻¹ (**Figure 5.3A**, black trace). Notably, this K_M is

10-fold larger than that reported by Dominy et al.,⁶ while the k_{cat} is two orders of magnitude smaller (**Table 5.1**). However, if we only consider data points obtained with substrate concentrations of less than 30 mM, the range investigated by Dominy et al., then we obtain the same K_M parameter as they did.

CDO has been demonstrated to be isolated with only a modest fraction of active sites containing Fe(II). The low Fe-loading of WT CDO necessitates either prior reconstitution of the protein with an Fe(II) source, or direct supplementation during kinetic trials. Alternatively, in a typical purification, as-isolated WT ADO is ~80% Fe-loaded and ~75% of the total iron content is Fe(II). As such, the potential increase in activity upon iron reconstitution was not pursued. Instead, the effect of reductants on ADO activity was explored, as has previously been done for other TDOs. 31,42 Addition of 1 mM ascorbate (Asc) and 1 mM TCEP was found to significantly increase the activity of ADO (Figure 5.3A, blue and black trace, respectively). Thus, to achieve maximum ADO activity, both reductants should be retained in future reactions.

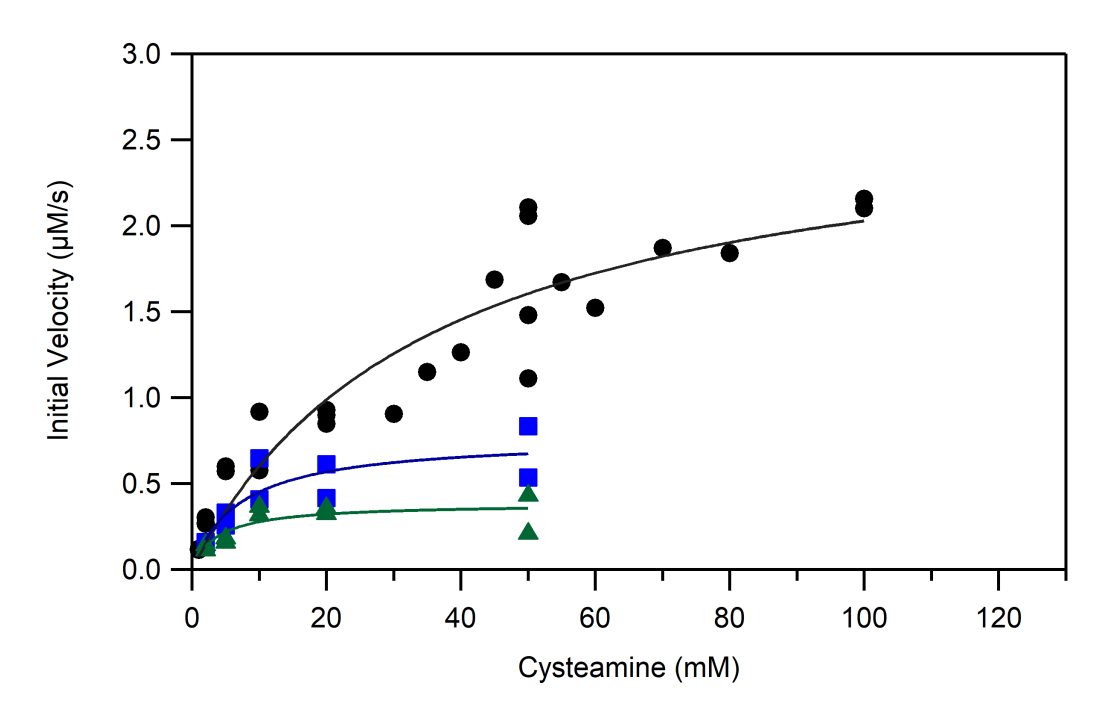


Figure 5.3. Dependence of ADO activity on 2-AET concentration. Assays were conducted under aerobic conditions at 37 °C using 200 mM Tris, 150 mM NaCl, 0.1 mM BCS, pH 8.0 buffer. Green

data points were obtained in the absence of reductant, blue in the presence of 1 mM TCEP, and black in the presence of both 1 mM TCEP and 1 mM ascorbate. In each case, ADO activity displayed Michaelis-Menten kinetics. Highest activity was achieved in the presence of both reductants, yielding a K_M of 36 mM, a k_{cat} of 0.037 s⁻¹, and a V_{max} of 2.8 μ M/s (black data). Standard errors are reported in **Table 5.1** and were typically less than 20%.

5.4 Discussion & Future Directions

Purification of ADO from hepatic tissue and characterization via electron paramagnetic resonance was first accomplished in the 1970s by Rotilio et al.⁴³ In 2007, a study that identified 2-AET as the native substrate of ADO was published, along with a method section detailing the first recombinant production of ADO.⁶ Subsequent studies of ADO have primarily used spectroscopic techniques to elucidate the geometric and electronic structure of substrate-and substrate analogue-bound Fe(II) and Fe(III)ADO.^{37,44} The publication of the X-ray crystal structure of ADO presented within this thesis will guide future studies that seek to characterize the specific secondary sphere interactions that facilitate substrate binding and turnover.

To lay the foundation for future studies aimed at developing a more complete understanding of the role played by specific secondary sphere residues and motifs within the structure of ADO, a kinetic method that monitors both substrate consumption and product formation was developed. This initial kinetic characterization demonstrates that the method used to produce and purify SUMO-tagged ADO fusion protein generates active enzyme that can oxidize 2-AET, albeit very slowly. While the K_M reported in this study for cysteamine turnover is within the same range as previously reported, the k_{cat} is two orders of magnitude smaller. It remains to be seen whether removal of the SUMO-tag affects the activity of the protein. ADO also oxidizes Nt-Cys peptides, although the specific activity of one substrate, in competition with another, has yet to be measured. Intriguingly, the Michaelis Menten parameters obtained in this study are two to three orders of magnitude larger than those published for the oxidation of RGS4 and RGS5 by ADO (**Table 5.1**). Thus, it is of utmost importance to determine the effect of binding of multiple

substrates and putative inhibitors (e.g., Cys, RGS5, and 2-AET) on ADO kinetic parameters. When assayed in competitive conditions, this enzyme will likely display a catalytic activity and a substrate preference that is more representative of an intracellular environment that consists of multiple sulfur-containing compounds.

The TDOs identified in *Arabidopsis*, PCO1-5, oxidize Nt-Cys peptides at rates that depend on the concentration of oxygen within physiologically relevant limits. In contrast, the measured apparent K_M for O₂ (K_MO₂^{app}) of ADO²⁹ is not only higher than typical O₂ tissue concentrations,^{45,46} but also ~3-fold larger than that of PCO4.³¹ As such, the activity of ADO is likely entirely dependent on the availability of intracellular O₂. Additionally, the substrate specificity of ADO may change and favor one substrate over another at different O₂ concentrations. To this end, ADO activity should be measured under varying oxygen concentrations (e.g., air-saturated buffer versus O₂-saturated buffer). Other mammalian enzymes, such as JmjC histone lysine demethylase⁴⁷ and prolyl 4-hydroxylases,⁴⁸ have also been found to be rate-limited by the concentration of their cosubstrate oxygen.

5.5 Conclusions

The newly developed quantitative, UPLC-MS based activity assay for ADO will allow for further exploration of the specific interactions that govern substrate specificity in this unique mammalian TDO. Coupled with spectroscopic and computational characterization, the robust kinetic assay will provide insight into the role that specific amino acids play with respect to enzyme activity and specificity. Further work to characterize the competition kinetics of ADO incubated with 2-AET, Cys, and RGS5 is underway.

5.6 References

- (1) McCoy, J. G., Bailey, L. J., Bitto, E., Bingman, C. A., Aceti, D. J., Fox, B. G., and Phillips, G. N. (2006) Structure and mechanism of mouse cysteine dioxygenase. *Proc. Natl. Acad. Sci. 103*, 3084–3089.
- (2) Tchesnokov, E. P., Fellner, M., Siakkou, E., Kleffmann, T., Martin, L. W., Aloi, S., Lamont, I.

- L., Wilbanks, S. M., and Jameson, G. N. L. (2015) The cysteine dioxygenase homologue from Pseudomonas aeruginosa is a 3-mercaptopropionate dioxygenase. *J. Biol. Chem.* 290, 24424–24437.
- (3) Pierce, B. S., Subedi, B. P., Sardar, S., and Crowell, J. K. (2015) The "Gln-Type" Thiol Dioxygenase from Azotobacter vinelandii Is a 3-Mercaptopropionic Acid Dioxygenase. *Biochemistry 54*, 7477–7490.
- (4) Brandt, U., Galant, G., Meinert-Berning, C., and Steinbüchel, A. (2019) Functional analysis of active amino acid residues of the mercaptosuccinate dioxygenase of Variovorax paradoxus B4. *Enzyme Microb. Technol.* 120, 61–68.
- (5) White, M. D., Carbonare, L. D., Puerta, M. L., Iacopino, S., Edwards, M., Dunne, K., Pires, E., Levy, C., McDonough, M. A., Licausi, F., and Flashman, E. (2020) Structures of Arabidopsis thaliana oxygen-sensing plant cysteine oxidases 4 and 5 enable targeted manipulation of their activity. *Proc. Natl. Acad. Sci. U. S. A. 117*, 23140–23147.
- (6) Dominy, J. E., Simmons, C. R., Hirschberger, L. L., Hwang, J., Coloso, R. M., and Stipanuk, M. H. (2007) Discovery and characterization of a second mammalian thiol dioxygenase, cysteamine dioxygenase. *J. Biol. Chem.* 282, 25189–25198.
- (7) Lombardini, J. B., Singer, T. P., and Boyer, P. D. (1969) Cysteine oxygenase. II. Studies on the mechanism of the reaction with 18oxygen. *J. Biol. Chem.* 244, 1172–1175.
- (8) Simmons, C. R., Liu, Q., Huang, Q., Hao, Q., Begley, T. P., Karplus, P. A., and Stipanuk, M. H. (2006) Crystal structure of mammalian cysteine dioxygenase: A novel mononuclear iron center for cysteine thiol oxidation. *J. Biol. Chem.* 281, 18723–18733.
- (9) Driggers, C. M., Kean, K. M., Hirschberger, L. L., Cooley, R. B., Stipanuk, M. H., and Karplus, P. A. (2016) Structure-Based Insights into the Role of the Cys–Tyr Crosslink and Inhibitor Recognition by Mammalian Cysteine Dioxygenase. *J. Mol. Biol.* 428, 3999–4012. (10) Driggers, C. M., Cooley, R. B., Sankaran, B., Hirschberger, L. L., Stipanuk, M. H., and Karplus, P. A. (2013) Cysteine dioxygenase structures from pH 4 to 9: Consistent Cys-

- persulfenate formation at intermediate pH and a Cys-bound enzyme at higher pH. *J. Mol. Biol.* 425, 3121–3136.
- (11) Li, W., Blaesi, E. J., Pecore, M. D., Crowell, J. K., and Pierce, B. S. (2013) Second-sphere interactions between the C93-Y157 cross-link and the substrate-bound Fe site influence the O2 coupling efficiency in mouse cysteine dioxygenase. *Biochemistry 52*, 9104–9119.
- (12) Gordon, J. B., McGale, J. P., Prendergast, J. R., Shirani-Sarmazeh, Z., Siegler, M. A., Jameson, G. N. L., and Goldberg, D. P. (2018) Structures, Spectroscopic Properties, and Dioxygen Reactivity of 5- and 6-Coordinate Nonheme Iron(II) Complexes: A Combined Enzyme/Model Study of Thiol Dioxygenases. *J. Am. Chem. Soc. 140*, 14807–14822.
- (13) Gardner, J. D., Pierce, B. S., Fox, B. G., and Brunold, T. C. (2010) Spectroscopic and computational characterization of substrate-bound mouse cysteine dioxygenase: Nature of the ferrous and ferric cysteine adducts and mechanistic implications. *Biochemistry* 49, 6033–6041.
- (14) Pierce, B. S., Gardner, J. D., Bailey, L. J., Brunold, T. C., and Fox, B. G. (2007) Characterization of the nitrosyl adduct of substrate-bound mouse cysteine dioxygenase by electron paramagnetic resonance: Electronic structure of the active site and mechanistic implications. *Biochemistry* 46, 8569–8578.
- (15) Blaesi, E. J., Fox, B. G., and Brunold, T. C. (2014) Spectroscopic and Computational Investigation of Iron(III) Cysteine Dioxygenase: Implications for the Nature of the Putative Superoxo-Fe(III) Intermediate. *Biochemistry 53*, 5759–5770.
- (16) Li, W., and Pierce, B. S. (2015) Steady-state substrate specificity and O2-coupling efficiency of mouse cysteine dioxygenase. *Arch. Biochem. Biophys. 565*, 49–56.
- (17) Li, J., Koto, T., Davis, I., and Liu, A. (2019) Probing the Cys-Tyr Cofactor Biogenesis in Cysteine Dioxygenase by the Genetic Incorporation of Fluorotyrosine. *Biochemistry* 58, 2218–2227.
- (18) Davies, C. G., Fellner, M., Tchesnokov, E. P., Wilbanks, S. M., and Jameson, G. N. L. (2014) The Cys-Tyr cross-link of cysteine dioxygenase changes the optimal ph of the reaction

- without a structural change. *Biochemistry* 53, 7961–7968.
- (19) Stipanuk, M. H., Dominy, J. E., Ueki, I., and Hirschberger, L. L. (2008) Measurement of cysteine dioxygenase activity and protein abundance. *Curr. Protoc. Toxicol.*
- (20) Chai, S. C., Jerkins, A. A., Banik, J. J., Shalev, I., Pinkham, J. L., Uden, P. C., and Maroney, M. J. (2005) Heterologous expression, purification, and characterization of recombinant rat cysteine dioxygenase. *J. Biol. Chem.* 280, 9865–9869.
- (21) Blaesi, E. J., Fox, B. G., and Brunold, T. C. (2015) Spectroscopic and computational investigation of the H155A variant of cysteine dioxygenase: Geometric and electronic consequences of a third-sphere amino acid substitution. *Biochemistry 54*, 2874–2884.
- (22) Kumar, D., Thiel, W., and De Visser, S. P. (2011) Theoretical study on the mechanism of the oxygen activation process in cysteine dioxygenase enzymes. *J. Am. Chem. Soc.* 133, 3869–3882.
- (23) Goncharenko, K. V., Vit, A., Blankenfeldt, W., and Seebeck, F. P. (2015) Structure of the sulfoxide synthase EgtB from the ergothioneine biosynthetic pathway. *Angew. Chemie Int. Ed. 54*, 2821–2824.
- (24) Ng, T. L., Rohac, R., Mitchell, A. J., Boal, A. K., and Balskus, E. P. (2019) An N-nitrosating metalloenzyme constructs the pharmacophore of streptozotocin. *Nature 566*, 94–99.
- (25) Straganz, G. D., and Nidetzky, B. (2006) Variations of the 2-His-1-carboxylate theme in mononuclear non-heme Fe II oxygenases. *ChemBioChem* 7, 1536–1548.
- (26) Chen, J., Li, W., Wang, M., Zhu, G., Liu, D., Sun, F., Hao, N., Li, X., Rao, Z., and Zhang, X. C. (2008) Crystal structure and mutagenic analysis of GDOsp, a gentisate 1,2-dioxygenase from Silicibacter Pomeroyi. *Protein Sci.* 17, 1362–1373.
- (27) Heafield, M. T., Fearn, S., Steventon, G. B., Waring, R. H., Williams, A. C., and Sturman, S. G. (1990) Plasma cysteine and sulphate levels in patients with motor neurone, Parkinson's and Alzheimer's disease. *Neurosci. Lett.* 110, 216–220.
- (28) Shen, D., Tian, L., Yang, F., Li, J., Li, X., Yao, Y., Lam, E. W. F., Gao, P., Jin, B., and

- Wang, R. (2021) ADO/hypotaurine: a novel metabolic pathway contributing to glioblastoma development. *Cell Death Discov.* 7.
- (29) Masson, N., Keeley, T. P., Giuntoli, B., White, M. D., Lavilla Puerta, M., Perata, P., Hopkinson, R. J., Flashman, E., Licausi, F., and Ratcliffe, P. J. (2019) Conserved N-terminal cysteine dioxygenases transduce responses to hypoxia in animals and plants. *Science (80-.)*. *364*, 65–69.
- (30) Licausi, F., Kosmacz, M., Weits, D. A., Giuntoli, B., Giorgi, F. M., Voesenek, L. A. C. J., Perata, P., and Van Dongen, J. T. (2011) Oxygen sensing in plants is mediated by an N-end rule pathway for protein destabilization. *Nature 479*, 419–422.
- (31) White, M. D., Kamps, J. J. A. G., East, S., Taylor Kearney, L. J., and Flashman, E. (2018) The plant cysteine oxidases from Arabidopsis thaliana are kinetically tailored to act as oxygen sensors. *J. Biol. Chem.* 293, 11786–11795.
- (32) Lee, M. J., Tasaki, T., Moroi, K., An, J. Y., Kimura, S., Davydov, I. V., and Kwon, Y. T. (2005) RGS4 and RGS5 are in vivo of the N-end rule pathway. *Proc. Natl. Acad. Sci. U. S. A.* 102, 15030–15035.
- (33) Tamirisa, P., Blumer, K. J., and Muslin, A. J. (1999) RGS4 inhibits G-protein signaling in cardiomyocytes. *Circulation* 99, 441–447.
- (34) Fellner, M., Doughty, L. M., Jameson, G. N. L., and Wilbanks, S. M. (2014) A chromogenic assay of substrate depletion by thiol dioxygenases. *Anal. Biochem.* 459, 56–60.
- (35) Swift, M. L. (1997) GraphPad prism, data analysis, and scientific graphing. *J. Chem. Inf. Comput. Sci.* 37, 411–412.
- (36) Johnson, K. A. (2019) New standards for collecting and fitting steady state kinetic data. *Beilstein J. Org. Chem.* 15, 16–29.
- (37) Fernandez, R. L., Dillon, S. L., Stipanuk, M. H., Fox, B. G., and Brunold, T. C. (2020) Spectroscopic Investigation of Cysteamine Dioxygenase. *Biochemistry* 59, 2450–2458.
- (38) Gasteiger, E., Hoogland, C., Gattiker, A., Duvaud, S., Wilkins, M. R., Appel, R. D., and

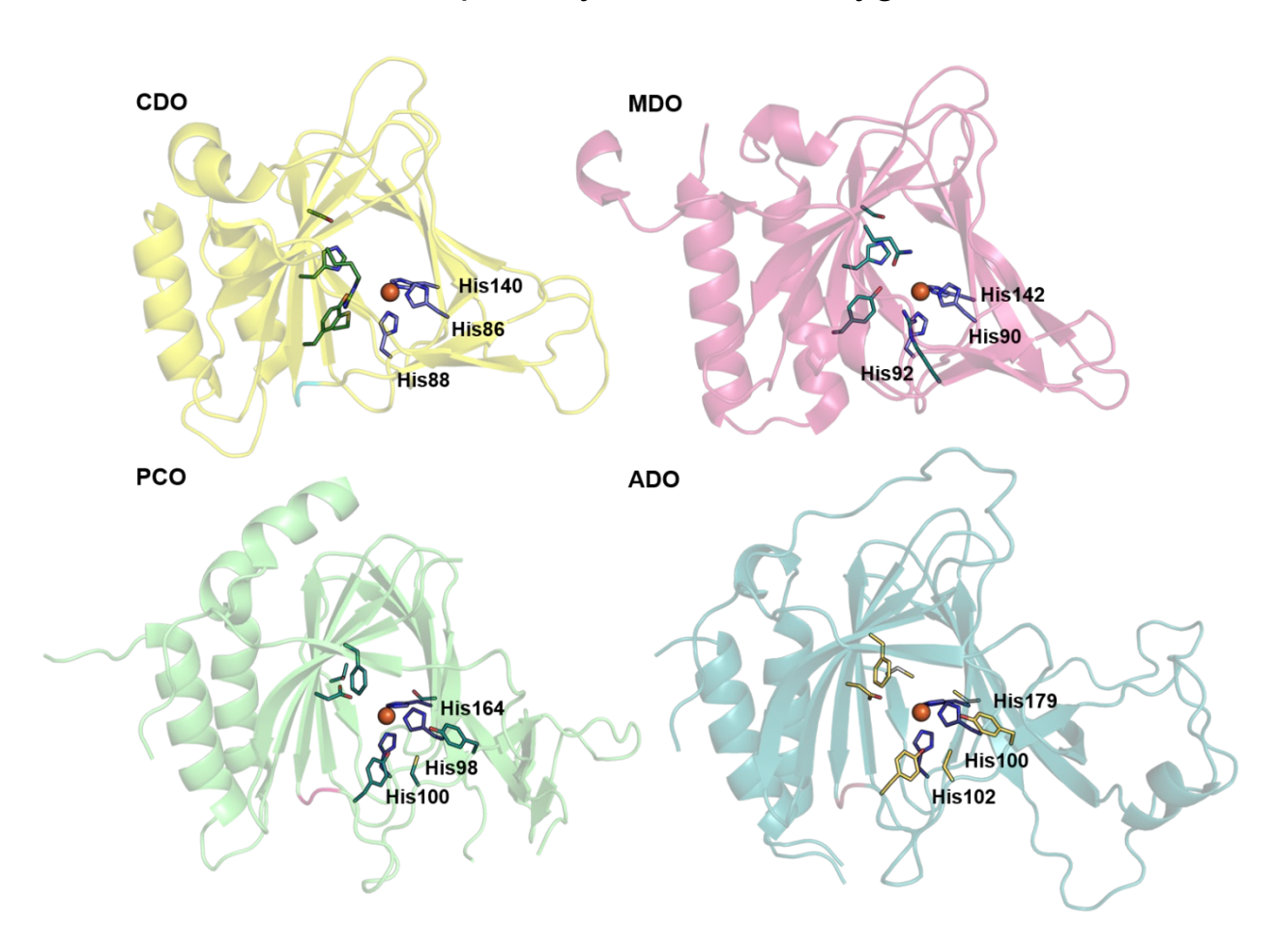
- Bairoch, A. (2005) Protein Identification and Analysis Tools on the ExPASy Server, in *The Proteomics Protocols Handbook*, pp 571–607. Humana Press, Totowa, NJ.
- (39) Fischer, D. S., and Price, D. C. (1964) a Simple Serum Iron Method Using the New Sensitive Chromogen Tripyridyl-S-Triazine. *Clin. Chem.* 10, 21–31.
- (40) Fischer, A. A., Miller, J. R., Jodts, R. J., Ekanayake, D. M., Lindeman, S. V, Brunold, T. C., and Fiedler, A. T. (2019) Spectroscopic and Computational Comparisons of Thiolate-Ligated Ferric Nonheme Complexes to Cysteine Dioxygenase: Second-Sphere Effects on Substrate (Analogue) Positioning. *Inorg. Chem. 58*, 16487–16499.
- (41) Wang, Y., Griffith, W. P., Li, J., Koto, T., Wherritt, D. J., Fritz, E., and Liu, A. (2018) Cofactor Biogenesis in Cysteamine Dioxygenase: C–F Bond Cleavage with Genetically Incorporated Unnatural Tyrosine. *Angew. Chemie Int. Ed. 57*, 8149–8153.
- (42) Imsand, E. M., Njeri, C. W., and Ellis, H. R. (2012) Addition of an external electron donor to in vitro assays of cysteine dioxygenase precludes the need for exogenous iron.
- (43) Rotilio, G., Federici, G., Calabrese, L., Costa, M., and Cavallini, D. (1970) An electron paramagnetic resonance study of the nonheme iron of cysteamine oxygenase. *J. Biol. Chem.* 245, 6235–6236.
- (44) Wang, Y., Davis, I., Chan, Y., Naik, S. G., Griffith, W. P., and Liu, A. (2020)

 Characterization of the nonheme iron center of cysteamine dioxygenase and its interaction with substrates. *J. Biol. Chem.* 295, 11789–11802.
- (45) Erecińska, M., and Silver, I. A. (2001) Tissue oxygen tension and brain sensitivity to hypoxia. *Respir. Physiol.* 128, 263–276.
- (46) Meyron-Holtz, E. G., Ghosh, M. C., and Rouault, T. A. (2004) Mammalian tissue oxygen levels modulate iron-regulatory protein activities in vivo. *Science (80-.).* 306, 2087–2090.
- (47) Hancock, R. L., Masson, N., Dunne, K., Flashman, E., and Kawamura, A. (2017) The Activity of JmjC Histone Lysine Demethylase KDM4A is Highly Sensitive to Oxygen Concentrations. *ACS Chem. Biol.* 12, 1011–1019.

- (48) Hirsilä, M., Koivunen, P., Günzler, V., Kivirikko, K. I., and Myllyharju, J. (2003) Characterization of the human prolyl 4-hydroxylases that modify the hypoxia-inducible factor. *J. Biol. Chem.* 278, 30772–30780.
- (49) Dominy, J. E., Simmons, C. R., Karplus, P. A., Gehring, A. M., and Stipanuk, M. H. (2006) Identification and characterization of bacterial cysteine dioxygenases: A new route of cysteine degradation for eubacteria. *J. Bacteriol.* 188, 5561–5569.

Chapter 6

Bioinformatic analysis reveals the atypical structure/function relationships in cysteamine dioxygenase



Chapter 6: Bioinformatic analysis reveals the atypical structure/function relationships in cysteamine dioxygenase

6.1 Conspectus

The cupin superfamily of proteins is highly represented among all domains with members spanning archaea, bacteria, and eukarya. 1,2 These proteins display remarkable functional diversity, catalyzing reactions ranging from hydroxylation to oxygenation to isomerization.^{3,4} Cupin proteins comprise primarily metalloenzymes that share a low overall degree of sequence identity while maintaining two short, highly conserved sequence motifs (cupin motif 1 and 2) that feature metal-binding residues. One large subcategory within this superfamily is comprised of mononuclear non-heme Fe(II)-dependent enzymes that use molecular oxygen as a co-substrate to catalyze a plethora of oxidation reactions. These enzymes can be separated into two groups based on the identity of the amino acid sidechains that serve as metal-binding ligands. The first group includes enzymes that bind the Fe cofactor by two histidines and one carboxylate side chain (2-His-1-carboxylate), rendering a monoanionic binding motif.⁵⁻⁷ In the resting Fe(II) state, one to three labile solvent molecules typically occupy the remaining coordination sites. Enzymes such as TauD,8 iso penicillin N synthase,9 and prolyl hydroxylase10 exemplify this 2-His-1carboxylate binding motif and have been well-characterized. The second group of cupin-type mononuclear non-heme Fe(II)-dependent metalloenzymes coordinate their metallocofactor via a neutral three histidine (3-His) binding motif. These enzymes have been significantly less wellstudied.

The largest grouping of 3-His binding proteins comprises thiol dioxygenases (TDOs), whose primary functions are to convert a substrate with a sulfhydryl group to its sulfinic acid derivative via the addition of both oxygen atoms from molecular oxygen (**Scheme 6.1**). The first TDOs to be discovered, cysteine dioxygenase (CDO)¹¹ and cysteamine dioxygenase (ADO),¹² were originally purified from liver tissue in the 1960s and later biochemically characterized in 2006¹³ and 2007,¹⁴ respectively. In the past 15 years, three more TDOs have been discovered

with distinct substrate specificities: 3-mercaptopropionate dioxygenase (MDO),^{15,16} plant cysteine dioxygenase (PCO),¹⁷ and mercaptosuccinate dioxygenase (MSDO).¹⁸ Only a few other enzymes have been established via X-ray crystallography to feature a 3-His triad, including EgtB,¹⁹ SznF,²⁰ diketone-cleaving dioxygenase,²¹ and gentisate 1,2-dioxygenase.²²

Scheme 6.1. Oxidation of thiol-containing substrates catalyzed by TDOs

In recent years, considerable progress has been made toward understanding the geometric and electronic structures of TDOs and the contributions of key residues to their function. While X-ray structures have definitively established that an Fe cofactor bound by a 3-His triad is present in all TDOs,²³ these cupin proteins differ in their key secondary sphere residues. Interestingly, the active site of ADO most closely resembles that of PCO, while the active sites of CDO is most similar to that of MDO. To facilitate a discussion of the relationship between ADO and its closest TDO homologs, a multiple sequence alignment (MSA) is presented in **Figure 6.1**. Key structural, spectroscopic, and biochemical properties of the different TDOs are summarized in the following sections.

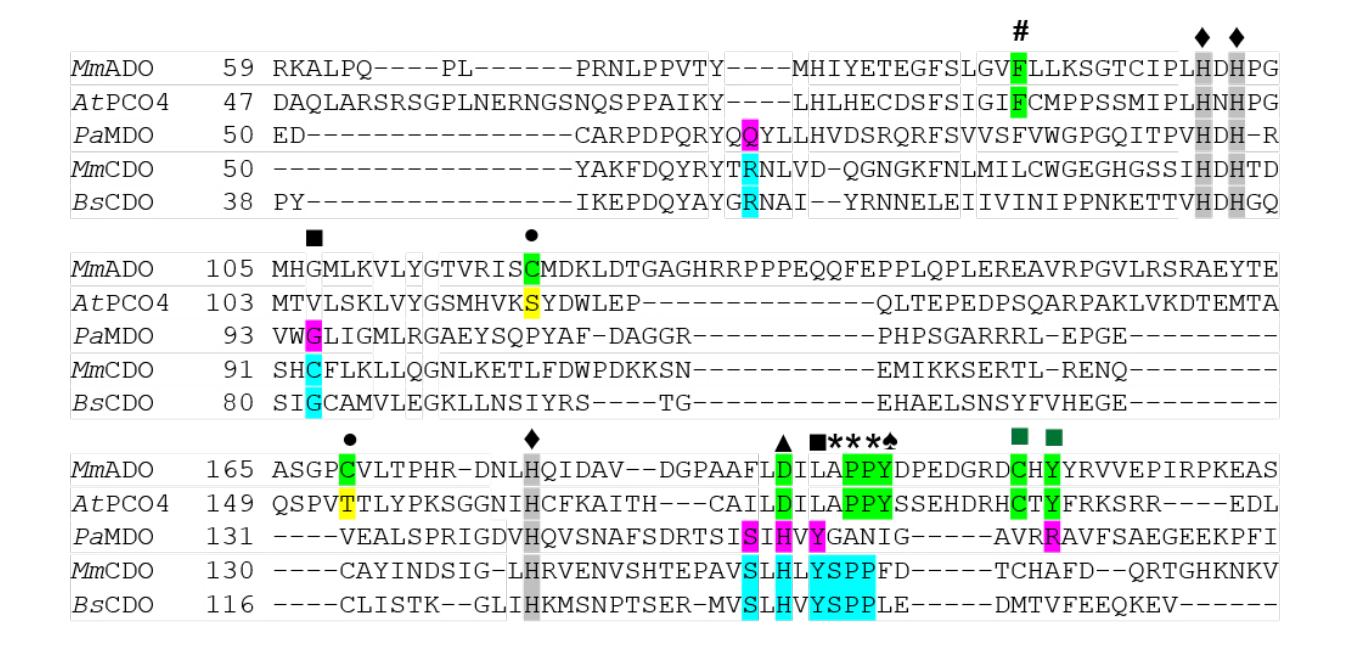


Figure 6.1. Sequence alignment showing conserved residues within TDOs. The sequences of the PCO4 from *Arabidopsis thaliana* (*At*PCO4), the MDO from *Pseudomonas aeruginosa* (*Pa*MDO), and the CDOs from *Mus musculus* (*Mm*CDO) and *Bacillus subtilis* (*Bs*CDO) are compared to the *Mus musculus* ADO (*Mm*ADO) sequence. Important ADO and PCO residues are highlighted in green, MDO in purple, CDO in blue, and key differences in yellow. All proteins possess a 3-His metal-binding motif marked by a ◆ and highlighted in gray. Additional motifs discussed in the text are denoted as follows: # Phe89 (*Mm*ADO numbering), ■ Cys-Tyr cross-link in *Mm*CDO, ■ putative ADO and PCO cross-link motifs, ◆ Cys120 and Cys169 in *Mm*ADO are replaced by Ser118 and Thr153 in PCO4, ▲ Asp192, * denotes a *cis*-peptide bond, and ♠ Tyr198 in *Mm*ADO and Tyr182 in *At*PCO4 adjacent to the *cis*-peptide bond.

6.2 Bioinformatic Analysis of ADOs and PCOs

In 2006, a position specific iterative basic local alignment search tool (PSI-BLAST)²⁴ analysis using the rat CDO sequence yielded only 82 similar sequences.²⁵ Today, the PCO_ADO protein family (Pfam) alone, which includes the two most recently crystallized TDOs, consists of 2101 sequences. The exponential growth of sequence and protein information is a well-documented phenomenon. To deal with this large amount of information, techniques such as

sequence similarity network (SSN) analyses have been developed to draw conclusions from the clustering of protein families. To visualize relationships between ADO and PCO, an SSN was generated with the Pfam defined PCO_ADO family (PF07847) via the resources provided by the Enzyme Function Initiative-Enzyme Similarity Tool (Figure 6.2).²⁶ Included in the SSN were 3402 protein sequences, represented by 1941 nodes. As Swiss-Prot proteins have been manually added and annotated from the literature or reviewed computational studies, these form the basis of our similarity comparisons instead of the more predictive TrEMBL (translation from EMBL) database proteins, which are obtained via translation of coding sequences found in the DDBJ, EMBL, and GenBank nucleotide sequence databases. The ADO/PCO SSN is comprised of only 8 Swiss-Prot reviewed proteins: 2 ADOs, 1 probable ADO, and 5 PCOs.

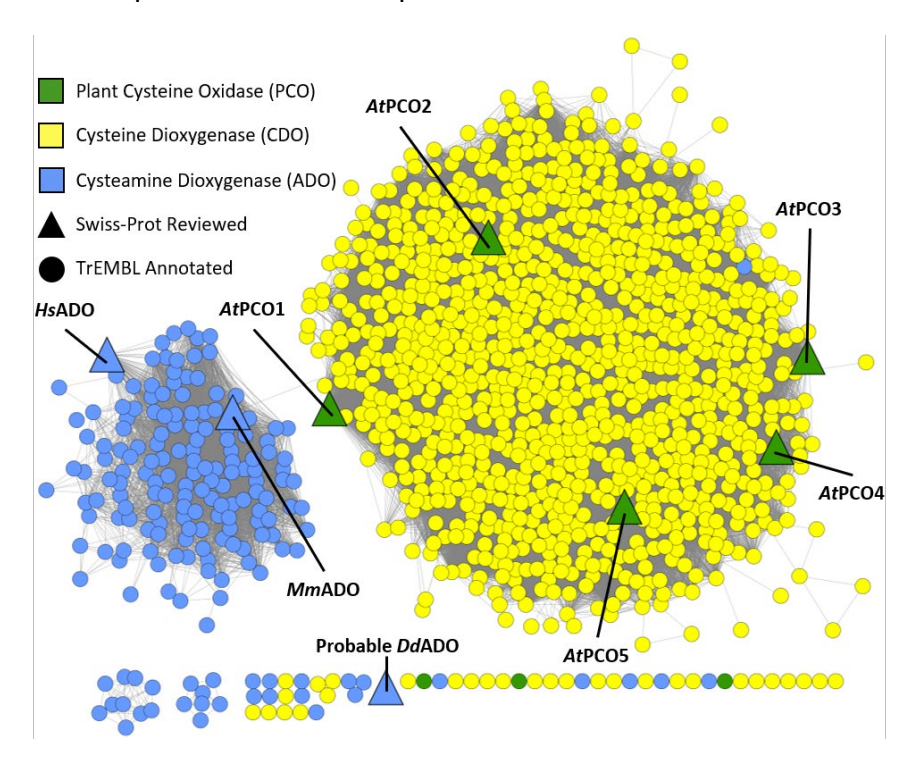


Figure 6.2. Sequence similarity network of proteins in the PCO/ADO family at an E-value threshold of 1 x 10^{-33} . Nodes indicate between 1 and 103 sequences with $\geq 55\%$ identity. Nodes without sequence functionality described as thiol dioxygenases were removed for clarity. The network was visualized in Cytoscape²⁷ and the TDOs are colored as follows: PCO, green; ADO,

blue; and CDO, yellow. Annotation status is represented by node shape: ▲ Swiss-Prot reviewed and • TrEMBL.

At the initial minimum stringency cutoff, a single cluster was present, consisting of ADOs and PCOs. Increasing the stringency to an E-value of 1 x 10⁻³³ resulted in the cluster separating into 2 large independent clusters of ADOs and PCOs (**Figure 6.2**). As explained above, the majority of sequences in this SSN were predicted by TrEMBL. Importantly, by this method all PCOs are assigned as CDOs. While PCOs do oxidize a cysteinyl residue, they have only been shown to oxidize N-terminal Cys residues of peptides. As such, all CDOs that have been experimentally validated to display PCO function, or have similar sequences, have been manually labelled as PCOs in **Figure 6.2**. A re-classification of TDOs is not unprecedented. As discussed in the MDO section, MDOs were originally believed to be CDOs, but were reclassified due to a distinguishing Gln residue and unique substrate specificity. The following sections summarize key structural and functional characteristics of CDO, MDO, PCO, and ADO that are evidenced by bioinformatic analysis.

6.3 Cysteine Dioxygenase (CDO)

The best-characterized TDO, CDO, was shown to oxidize cysteine (Cys) to cysteine sulfinic acid (CSA) by incorporating both oxygen atoms from co-substrate O₂ into Cys (**Scheme 6.2**).^{28–30} The regulation of Cys is vital to mammalian cellular function as a build-up of Cys, or its disulfide form cystine, can cause blockages³¹ and organ failure.^{32,33} CSA can be further broken down into pyruvate and sulfite or decarboxylated into hypotaurine. A buildup of Cys can contribute to neurological malfunction and has been linked to Alzheimer's and Parkinson's diseases.^{34–36} Because a lack of regulation of these sulfur-containing compounds has proven to be cytotoxic and neurotoxic to mammals, developing a fundamental understanding of the broad mechanism of CDO function is of considerable interest.

An X-ray crystal structure of Cys-bound CDO revealed that binding of the native substrate Cys occurs in a bidentate fashion, involving the coordination of the Fe cofactor by the sulfur and

nitrogen atoms. CDO has been demonstrated to be extremely substrate specific, and only two alternative substrates have been identified; namely, D-Cys and cysteamine (2-aminoethanethiol, 2-AET).³⁷ However, neither of these alternative substrates are oxidized at a rate comparable to that for L-Cys, and the corresponding reactions are significantly more oxidatively decoupled than the native reaction.³⁷ Homocysteine³⁸ and selenocysteine (SeCys)³⁹ have both been shown to bind to the Fe(II)CDO center, though neither is oxidized by this enzyme. A spectroscopic study using magnetic circular dichroism (MCD), resonance Raman (rR), electron paramagnetic resonance (EPR) techniques confirmed that the catalytically active species is Fe(II)CDO and revealed that although SeCys binds to the Fe center in a similar fashion as Cys, it does not act as a substrate for CDO.³⁹ A subsequent computational analysis of SeCys-bound Fe(II)CDO indicated that O₂ binding to this species is thermodynamically unfavorable, which may explain why CDO is unable to oxidize SeCys.⁴⁰

$$\begin{array}{c|c}
O & CDO & O & O \\
H_2N & OH & OH \\
\hline
Cysteine (Cys) & Cysteine sulfinic acid (CSA)
\end{array}$$

Scheme 6.2. Oxidation of Cys to CSA as catalyzed by CDO.

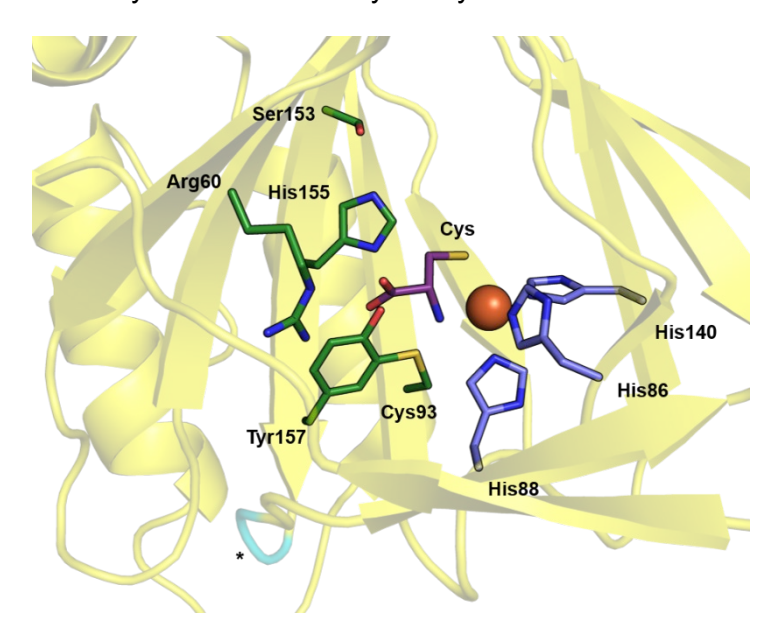


Figure 6.3. Active site region of Cys-bound *Rn*CDO (PDB code 4JTO). The Fe ion (orange sphere) is coordinated by three His residues (lavender) and substrate Cys (purple). Other important amino acids in the active site are highlighted in green. The * marks the *cis*-peptide bonds that help position Tyr 157.

The exceptional substrate specificity of mammalian CDO is determined by the unique secondary coordination sphere that includes Arg60, a Ser153-His155-Tyr157 catalytic triad, *cis*-peptide bonds between residues Ser158-Pro159-Pro160, and a thioether cross-link between Cys93 and Tyr157 (*Mm*CDO numbering, **Figure 6.3**). In substrate-bound CDO, the Cys carboxylate tail forms a salt bridge with the side chain of Arg60. Substitution of Arg60 by Ala reduces the catalytic efficiency ~82-fold, demonstrating that this interaction directly affects protein function ($k_{cat}/K_M = 3200 \text{ M}^{-1}\text{s}^{-1}$ and 39 M⁻¹s⁻¹ for WT and Arg60Ala CDO, respectively).⁴¹

One particularly unusual feature of eukaryotic CDOs is the presence of a cross-link between Cys93 and Tyr157, whose role with regards to CDO function has been the subject of many studies. 37,42–46 This cross-link is generated during turnover of the enzyme, and although not required for catalysis, its presence causes at least a 20-fold increase in protein activity. 47 A kinetic study of cross-linked and non-cross-linked CDO demonstrated that while both isoforms are active, the optimal pH decreases with the presence of the cross-link as the formation of the thioether bond decreases the pKa of Tyr157. 48 Equally important, the cross-link also ties up the Cys side chain to prevent any deleterious interactions involving the thiolate of Cys93. Intriguingly, Cys93-Tyr157 cross-link formation in the Arg60Ala CDO variant can be induced by the addition of both Cys and 2-AET. Although cross-link formation is not a direct observation of turnover, Dominy et al. hypothesized that the Arg60Ala CDO variant could have relaxed substrate specificity. 41 Interestingly, bacterial CDOs lack the Cys-Tyr cross-link, and remain as active as eukaryotic CDOs. 25 In bacterial CDOs the key Cys residue is replaced by a smaller Gly residue.

The presence of a Ser-His-Tyr motif (**Figure 6.3**) has been used successfully in screens of protein sequences to identify members of the cupin superfamily with CDO activity, which also

led to the discovery of several bacterial homologs.²⁵ According to a Cys-bound CDO crystal structure,⁴⁹ Ser153 hydrogen bonds to His155,⁴² which in turn hydrogen bonds to Tyr157. The His155Ala CDO variant³⁷ displays a ~100-fold decrease in activity relative to WT enzyme. The absence of the His-Tyr hydrogen bond in the His155Ala CDO variant increases the conformational freedom of the Cys93-Tyr157 cross-link, allowing a water molecule to bind to the Cys-Fe(II)CDO adduct in the position typically occupied by oxygen.⁵⁰ The Ser153-His155-Tyr157 triad is also important for supporting the role of Tyr157 as a catalytic acid/base.⁴² Intriguingly, the positioning of Tyr157 is additionally controlled by the presence of *cis*-peptide bonds between Ser158-Pro159-Pro160. These *cis*-peptide bonds, together with the Cys93-Tyr157 cross-link, lock the Tyr hydroxyl group into a favorable position for hydrogen bonding to substrate Cys and the superoxide moiety that is formed during O₂ activation of Cys.^{16,51}

Treatment of Cys-bound Fe(III)CDO with excess cyanide, a superoxide surrogate, causes the high-spin (S = 5/2) EPR signal to be replaced by a low-spin (S = 1/2) signal, demonstrating the direct coordination of cyanide to the Fe(III) center to form a six-coordinate adduct. Interestingly, the cyano/Cys-Fe(III)CDO complex not only provides a model of a putative reaction intermediate, but also displays EPR parameters that are sensitive to the absence or presence of the Cys-Tyr cross-link.³⁷ QM/MM optimized structures of non-cross-linked and cross-linked cyano/Cys-bound Fe(III)CDO adducts revealed that the orientation of the cyanide ligand and carboxylic acid group of substrate Cys is sensitive to the presence of the cross-link; in the absence of the cross-link, the Fe-C-N unit is significantly more linear.³⁷ Fiedler and coworkers⁵² were able to establish the structural basis for subtle differences in EPR *g* values between active site models of non-cross-linked and cross-linked cyanide/Cys-bound Fe(III)CDO, as well as synthetic mimics. The presence of the Cys-Tyr cross-link lengthens the Fe-S bond and induces a decrease in the Fe-C-N angle, causing an increased spread of *g* values. These cross-link induced perturbations exemplify the role that secondary sphere residues play to enhance substrate binding and turnover.

6.4 3-mercaptopropionate dioxygenase (MDO)

Sequence alignment of known CDOs revealed a seemingly new category of bacterial CDOs in which the Arg60 residue was substituted by a Gln (*Mm*CDO numbering). However, these "Gln-type" CDOs were subsequently found to display much higher rates for the conversion of 3-mercaptopropionate (3-MPA) to 3-sulfinopropanoate than for Cys oxidation (**Scheme 6.3**), and they were thus reclassified as MDOs.^{15,16} Unlike other TDOs, different orthologs of MDO are able to oxidize thiol-containing compounds in addition to 3-MPA; e.g., *Av*MDO additionally turns over L-Cys and 2-AET,¹⁵ and *Pa*MDO also turns over L-Cys.¹⁶

Scheme 6.3. Oxidation of 3-MPA to 3-sulfinopropionic acid as catalyzed by MDO.

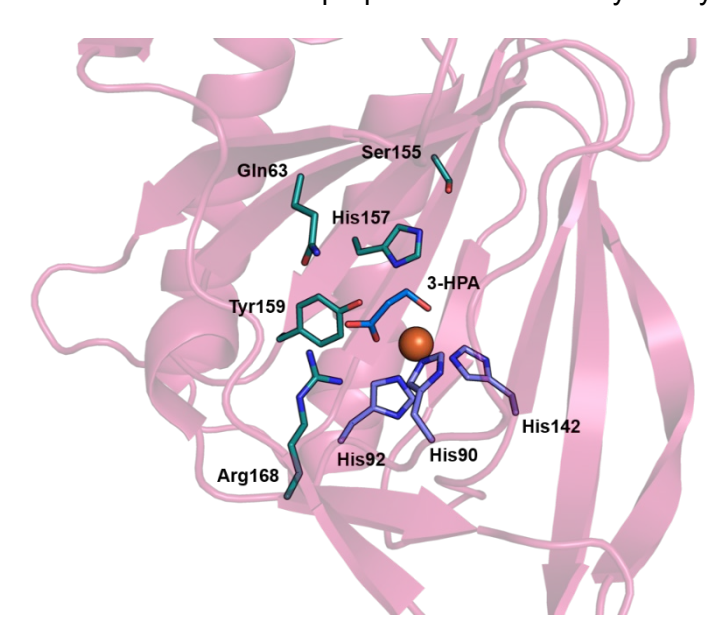


Figure 6.4. Active site region of 3-HPA-bound *Pa*MDO (PDB code 6XB9). The Fe ion (orange sphere) is bound by three His residues (lavender) and the substrate analogue 3-HPA (blue). Other significant amino acids in the active site are highlighted in teal.

The crystal structure of MDO revealed a number of similarities between the active sites of this enzyme and CDO. Most notable is the conservation of the 3-His binding motif typical of TDOs, as well as the Ser-His-Tyr catalytic triad first identified in CDO (**Figure 6.4**). Importantly, this enzyme lacks the *cis*-peptide bonds featured in CDO. Similar to bacterial CDO, MDO is also unable to form the Cys-Tyr cross-link found in eukaryotic CDOs, as a Gly is present at the position occupied by Cys93 in eukaryotic CDOs. Aloi et al.⁵¹ predicted that the lack of a *cis*-peptide bond, in addition to the absence of the Cys-Tyr cross-link would allow for the formation of a stabilizing salt bridge between Arg168 and the carboxylate tail of enzyme-bound 3-MPA.

The mode by which the native substrate 3-MPA binds to *Av*MDO and *Pa*MDO remains an active field of research. A Mössbauer study led to the proposal that both 3-MPA and Cys bind to *Pa*MDO in a monodentate fashion via their thiolate moieties. ¹⁶ Recently, however, an X-ray crystal structure was published of *Av*MDO complexed with the substrate analogue and competitive inhibitor 3-hydroxypropionic acid (3-HPA). ⁵³ In this structure, 3-HPA displays bidentate binding to the Fe cofactor. Complementary computational and spectroscopic studies indicated that 3-MPA also likely coordinates in a bidentate fashion. To stabilize the substrate analogue, and by extension the native substrate, the side chain of Arg168 participates in a hydrogen bonding interaction with the carboxylate tail.

6.5 Plant Cysteine Dioxygenase (PCO)

The importance of regulating intracellular levels of sulfur-containing compounds via oxidation is sufficiently high that TDOs have evolved across all forms of life. In plants, the molecular adaptation to high oxygen concentrations (hypoxia) is mediated by proteins that belong to the group VII ethylene response factors (ERF-VIIs). Five members of the ERF-VII family have been identified in *Arabidopsis thaliana* that feature the conserved N-terminal motif CGGA(I/V)ISD(F/Y). The concentrations of these five N-terminal cysteine (Nt-Cys) peptides, RAP2.2, RAP2.3, RAP2.12, HRE1, and HRE2,^{54,55} are controlled by five distinct plant cysteine dioxygenase (PCOs).⁵⁶ These five PCOs oxidize Nt-Cys to their corresponding CSA (**Scheme**

6.4), although their specificity and efficiency varies by ERF-VII substrate. Oxidation of its Nt-Cys marks the ERF-VII peptide for arginylation by arginyltransferases and subsequent ubiquitination and degradation.

Scheme 6.4. Oxidation of Nt-Cys peptides to the corresponding sulfinic acids as catalyzed by PCO.

In *Arabidopsis*, overproduction of an ERF-VII protein improved tolerance to submergence and up-regulation of genes associated with the hypoxic response.⁵⁵ As such, the studies of PCOs have largely been motivated by a desire to optimize flood tolerance of plants. By controlling the plant hypoxic response mechanism within the N-degron pathway, which PCOs affect, researchers hope to engineer more flood resistant plants. Importantly, the X-ray crystal structures of PCO4 and PCO5 were recently published by White et al.¹⁷ These structures provide the structural basis for site-specific substitutions of key residues that could provide an effective route to improving stress tolerance in plants.

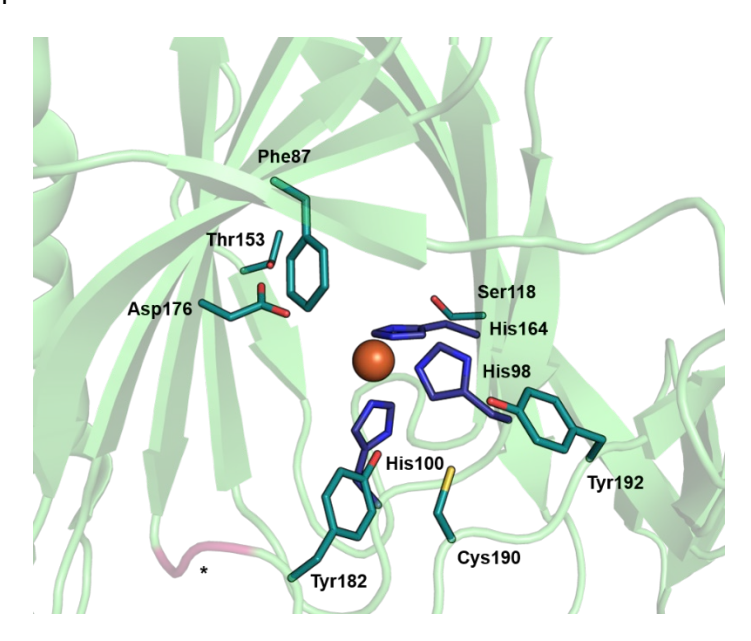


Figure 6.5. Active site region of *At*PCO4 (PDB code 6S7E). The Fe ion (orange sphere) is bound by three His residues (purple). Other important amino acids in the active site are highlighted in teal. The * marks the *cis*-peptide bond adjacent to Tyr182.

Comparison of the first X-ray crystal structures of PCOs to those of CDO and MDO highlight many differences. Although PCOs also feature a 3-His triad that bind the Fe cofactor (Figure 6.5), few other active site residues are conserved between PCOs and CDOs. For example, the Ser-His-Tyr catalytic triad is absent in PCO. Instead, sequence alignment in conjunction with structural comparisons disclose that the CDO catalytic triad (Figure 6.3) is replaced by residues Asp176, Ile177, and Leu178 (Figure 6.5). Substitution of Asp176 by an Asn proved to almost abolish the specific activity of the enzyme. Additionally, the levels of Fe incorporation into this variant were extremely low. Inclusion of a reductant and iron supplementation during the activity assay restored some activity, although the specific activity of the Asp176Asn PCO variant remained ~7-fold lower than that of the WT enzyme.

As discussed above, the catalytic activity of mammalian CDOs is enhanced by the formation of a thioether cross-link between Cys93 and Tyr157. A distinct thioether cross-link motif has been proposed by Wang et al. to exist in human ADO, between Cys220 and Tyr222 (see below).⁵⁷ For this reason, and because PCO and ADO share sequence homology in this region (**Figure 6.1**), the possibility was evaluated that a cross-link could also be formed in PCOs involving the corresponding Cys residue (Cys190, *At*PCO4 numbering), which is sandwiched between Tyr182 and Tyr192. However, no electron density for a cross-link was observed in the X-ray crystal structures of PCO4 and PCO5. In addition, tandem MS/MS analysis of PCO4 did not identify a cross-link, even after incubation of the enzyme with substrate. Finally, substitution of Cys190 by an Ala did not affect enzymatic activity. Alternatively, replacement of Tyr182 by a Phe was found to cause a ~7-fold decrease in specific activity, indicating that Tyr182 may play a role in substrate positioning.

As the only published crystal structures of PCO do not show bound substrate, much is left to speculation as to which specific interactions within the outer coordination sphere facilitate substrate recognition and binding. Inspection of the PCO4 protein surface reveals a prominent tunnel to the active site through which Nt-Cys substrates are likely to coordinate to the Fe. This tunnel is marked by a hairpin loop (residues Tyr182 to Cys190) consisting almost exclusively of charged, polar residues. White et al. speculated that this hairpin loop, close to the active site, may play a role in substrate binding and recognition.¹⁷ The specific position of this loop is defined by a *cis*-peptide bond between residues Pro180 and Pro181. As described above, in CDO the analogous *cis*-peptide bond motif has been observed to play a pivotal role in positioning Tyr157, the residue forming a cross-link with Cys 93 (*Mm*CDO numbering, **Figure 6.3**), within the active site.

6.6 Cysteamine dioxygenase (ADO)

The gene responsible for ADO production was identified when Dominy et al. noticed a discrepancy between the levels of taurine and CDO in various tissues. ¹⁴ This discovery suggested that the conversion of cysteamine (2-aminoethanethiol, 2-AET) to hypotaurine by ADO could be responsible for the majority of taurine production in some tissues, particularly the brain. Thus, ADO was believed to play a significant role in taurine biosynthesis. Ten years later, Masson et al. reported a new ADO substrate, regulators of G protein signaling 4 and 5 (RGS4 and RGS5), and demonstrated that ADO, like PCO,⁵⁸ oxidizes Nt-Cys peptides.⁵⁹ Similar to the PCO substrates, RGS4 and RGS5 function as substrates of the mammalian N-degron pathway.⁶⁰ Additionally, RGS4 and RGS5 have been shown in cardiomyocytes to inhibit G-protein-mediated signaling.⁶¹

ADO converts substrate 2-AET to hypotaurine with a K_M of 3.8 mM and k_{cat} of 1.6 s⁻¹ at pH 8.0 (**Scheme 6.5A**). Although this enzyme features the same 3-His active site as CDO, ADO was shown to be unable to turn over Cys. Additionally, Cys did not serve as an effective inhibitor; i.e., even when a 6-fold molar excess of Cys over 2-AET was used, only a 35% decrease in activity was observed. Intriguingly, Masson et al. subsequently discovered that ADO oxidizes

RGS5 much more effectively than 2-AET, with a K_M of 71.5 μ M and a k_{cat} of 16.9 s⁻¹ (**Scheme 6.5B**).⁵⁹

Scheme 6.5. Reactions catalyzed by ADO. A. Oxidation of 2-AET to hypotaurine. B. Oxidation of Nt-Cys peptides to their corresponding sulfinic acids.

Dominy et al. performed a sequence alignment of ADO and CDO that highlighted many dissimilarities between these two enzymes. Although the 3-His triad was maintained, no other secondary sphere residues identified in CDO were conserved in the *Mm*ADO sequence. Notably, the ADO sequence lacks the residues necessary for the Cys-Tyr cross-link observed in mammalian CDOs. However, in 2019 Wang et al. posited the existence of a new cross-link motif in human ADO (*Hs*ADO). Genetic incorporation of an unnatural amino acid, 3, 5,-difluoro-tyrosine, in conjunction with mass spectrometry and NMR experiments, identified a thioether bond between Cys220 and Tyr222 (*Hs*ADO numbering). Substitution of Tyr222 by an Ala was found to cause a modest (~3-fold) decrease in activity, seemingly supporting the existence of cross-link in the WT enzyme. However, in CDO, cross-link formation has a much larger effect on enzyme turnover, leading to an ~20-fold increases in activity. Thus, although the Tyr222 residue appears to moderately affect protein function, the physiological relevance and exact catalytic role of the putative cross-link it forms have yet to be determined.

Magnetic circular dichroism (MCD) and electron paramagnetic resonance (EPR) spectroscopic results obtained for ADO incubated with substrate and substrate analogues were distinct from those obtained for other TDOs, despite their identical first coordination spheres. By

comparing spectroscopic data obtained with substrate and substrate analogues, 2-AET was deemed to bind in a monodentate, thiolate-only fashion to the Fe(II) cofactor.²³ Intriguingly, the MCD and EPR spectra of Fe(III)ADO incubated with the substrate analogue Cys in the presence of glycerol revealed the formation of a unique low-spin complex, while the other TDOs only form low-spin species in the presence of a strong-field ligand such as cyanide. This finding provided the first spectroscopic evidence that the secondary coordination environment of ADO differs from that of other TDOs, underscoring the significant role that secondary-sphere residues play in dictating substrate specificity.

TDO reaction intermediates are short-lived and have yet to be trapped and spectroscopically or structurally characterized. To address this issue, a spectroscopic study was carried out on putative reaction intermediates that are formed upon incubation of Fe(III)ADO with substrate/substrate analogues and the superoxide surrogates azide and cyanide. 62 This study revealed that despite monodentate binding of 2-AET, the Fe center of substrate-bound Fe(III)ADO is likely coordinatively saturated, additionally featuring solvent-derived hydroxide ligands. Azide was found to coordinate directly to the Fe(III) center of substrate-free ADO, forming a complex with spectroscopic signatures nearly identical to those of azide-bound Fe(III)CDO. In contrast, azide was unable to coordinate to 2-AET-bound Fe(III)ADO, implying that the Fe(III) center lacks an open coordination site or azide competes with cysteamine for the same binding site. The superoxide surrogate cyanide did bind to either 2-AET- or Cys-bound Fe(III)ADO to yield a lowspin (S = 1/2) species displaying an EPR signal that is distinct from the low-spin EPR signal observed for cyanide/Cys-bound Fe(III)CDO, which provided further evidence that the active site pockets of ADO and CDO are different. Finally, EPR spectra obtained for cyanide/cysteamine adducts of wild-type Fe(III)ADO and its Tyr208Phe variant were superimposable, implying that either an insignificant fraction of as-isolated wild-type enzyme is crosslinked or that formation of the thioether bond has minimal effects on the positioning of substrate and substrate analogues.

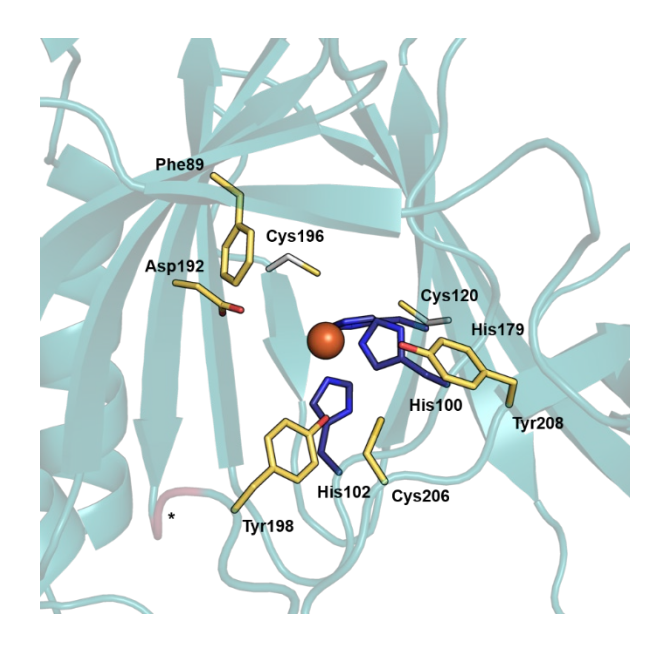


Figure 6.6. Active site region of *Mm*ADO (PDB code 7LVZ). The Fe ion (orange sphere) is bound by three His residues (purple). Other key amino acids in the active site are highlighted in yellow. The * marks the *cis*-peptide bond that aids in the positioning of Tyr198.

The recently published X-ray crystal structure of ADO provides the structural basis for assessing the importance of residues proposed via MSA to be critical to ADO function. In the ADO active site (**Figure 6.6**) few residues are within 5 Å of the cofactor; the closest residues are Asp192 and Phe89 at a distance of 4 and 7 Å, respectively. Located 8 Å from the Fe is the purported cross-linking residue Tyr208. The X-ray crystal structure revealed a lack of electron density between Cys206 and Tyr208, indicating that *Mm*ADO does not form a thioether cross-link under the experimental conditions used to obtain the single crystals for X-ray crystallography. Intriguingly, equidistant from Cys206 is Tyr198, which sandwiches Cys206 between aromatic residues. In ADO, the positioning of Tyr198 is influenced by a *cis*-peptide bond between Pro196 and Pro197 (**Figure 6.6**, pink highlight). In CDO, a similar *cis*-peptide bond motif has been shown to be critical for the proper positioning of the cross-linking Tyr157 for maximum catalytic activity (see above). The Pro196-Pro197-Tyr198 motif identified in ADO is also maintained in the PCO4 sequence (Pro180-Pro181-Tyr182). As described above, replacement of Tyr182 with a Phe in PCO4 (equivalent to Tyr198 in *Mm*ADO) significantly decreased enzyme activity. Tyr182 in PCO4

and Tyr198 in *Mm*ADO are both similarly positioned near the end of the putative substrate access tunnel to the active site, and after a *cis*-Pro peptide bond. Thus, it is likely that in ADO, replacement of Tyr198 will influence enzymatic activity more than substitution of Tyr208.

The specificity of TDOs is governed by the secondary sphere residues and sequence motifs that promote substrate binding and recognition. Critical to the function of CDO and MDO are residues Ser153, His155, and Tyr157 (*Mm*CDO numbering), as they engage in an extended hydrogen-bonding network that promotes substrate and co-substrate coordination.⁴¹ These residues are not conserved in the sequence of *Mm*ADO but rather are replaced by residues Asp192, Ile193, and Leu194, suggesting that the positioning of substrates 2-AET and Nt-Cys occurs via distinct binding interactions. Intriguingly, in PCO4 the sequence and structural location of this Asp-Ile-Leu motif is preserved, underscoring the likely importance of these residues. Although an X-ray crystal structure of substrate-bound ADO is not yet available, spectroscopic studies provided evidence for monodentate coordination of the terminal thiolate residues for both 2-AET and Nt-Cys.^{23,63} A computational study of 2-AET and Nt-Cys-bound ADO, using molecular dynamics in conjunction with quantum mechanics/molecular mechanics methods, revealed that the large substrate cavity lends 2-AET significant conformational freedom. In contrast, the large size of the Nt-Cys peptide allows for interactions with more residues lining the active site cavity, including Asp 192 and Tyr198.

The necessity of ordered binding of the Cys substrate prior to co-substrate oxygen coordination was demonstrated spectroscopically for CDO. By extension, it is likely that ordered binding of Nt-Cys, followed by O₂, also occurs in ADO. On the basis of structural and computational data, Nt-Cys peptide substrates are predicted to enter the active site and coordinate to the Fe(II) ion through a large substrate access tunnel. Inspection of the ADO surface uncovers an additional, smaller tunnel that leads from the protein surface to the active site, lined by residues Cys120 and Cys169. Although an intra-disulfide bond between these two residues was not observed in the ADO X-ray crystal structure, these two residues are ~4 Å apart and thus

within bonding distance of each other. We hypothesized that upon Nt-Cys binding, the peptide would fill the large tunnel, precluding co-substrate oxygen from binding to the Fe(II) center. Thus, the smaller access tunnel, gated by Cys120 and Cys169, could serve to transport O₂ to the active site. Delivery of oxygen via this pathway would cause a coupling of the turnover rate to the intracellular redox potential, instead of the intracellular substrate concentration.

6.7 Conclusions

Many intracellular thiol oxidation reactions are known to occur via enzymatic catalysis. The TDOs that catalyze these reactions show a high degree of substrate specificity, which allows them to precisely regulate the level of a particular thiol substrate. The importance of the secondary coordination sphere in tailoring substrate specificity and reactivity is apparent from the significant variation in key TDO residues and sequence motifs. Originally, CDO and MDO were both believed to catalyze Cys oxidation and were first distinguished as either "Arg- or Gln-type" enzymes. Further kinetic characterization separated the two enzymes as they differed in their native substrate specificity. Recently, both PCO and ADO have been shown to oxidize Nt-Cys peptides. The X-ray crystal structures of these two TDOs display very similar active site structures and key sequence motifs in the outer coordination sphere. Importantly, in ADO, a hypothesized co-substrate access tunnel is lined by Cys120 and Cys169, which may serve as a gating mechanism to prevent ADO from depleting the cell of all Nt-Cys containing molecules under conditions of high O₂ levels. The newly obtained X-ray crystal structure of ADO provides an excellent framework for future studies aimed at exploring its unique structure/function relationships.

6.8 Methods

The SSN was generated with the Pfam defined PCO_ADO family (PF07847) via the resources provided by the Enzyme Function Initiative-Enzyme Similarity Tool.²⁶ Upon retrieval of the sequences and the primary network generation, the dataset was pared down to further refine the information provided and yield a suitable file size. A 55% representative node cutoff was used to accommodate the large number of sequences with an E-value of 16 as the minimum stringency

cutoff. The ADO cluster consisted of 613 sequences represented by 273 nodes and included the *Mm*ADO and *Hs*ADO characterized sequences. A cluster with 1258 nodes representing 2316 sequences shared one edge with the ADO cluster. This cluster was primarily composed of predicted CDOs but also included 5 characterized PCOs: *At*PCO1-5. The SSN was visualized using Cytoscape.²⁷ MSAs were performed using the Multiple Sequence Comparison by Log-Expectation (MUSCLE)⁶⁴ and visualized using Unipro UGENE.⁶⁵ Alignment positions with ≥ 67% gaps were removed to allow effective comparison of consensus sequences between unique cluster alignments. Highly conserved residues in ADO and PCO were located and visualized using Pymol.

In the cluster consisting of CDOs and PCOs, the only characterized sequences are AtPCOs1-5, and sequence alignment of these enzymes with a representative characterized CDO show much greater sequence identity with PCO than CDO. Moreover, protein descriptions used in this analysis to identify sequences by TDO type are provided by Uniprot. In recent months, a number of descriptions have changed; notably, sequences in the cluster containing characterized PCOs were labelled as PCOs and ADOs instead of CDOs as late as October 2020. Currently, members of the PCO_ADO Interpro family belonging to the viridiplantae supergroup are redescribed as CDOs. This is reasonable in the sense that PCOs are cysteine dioxygenases, but they act on amino-terminal cysteine peptides instead of the free cysteine substrate native to CDO. By these two criteria, the predicted CDOs in this cluster are expected to in fact be PCOs. With this reclassification, largely isofunctional clustering of PCOs and ADOs can be seen.

6.9 References

- (1) Dunwell, J. M., Khuri, S., and Gane, P. J. (2000) Microbial Relatives of the Seed Storage Proteins of Higher Plants: Conservation of Structure and Diversification of Function during Evolution of the Cupin Superfamily. *Microbiol. Mol. Biol. Rev.* 64, 153–179.
- (2) Uberto, R., and Moomaw, E. W. (2013) Protein Similarity Networks Reveal Relationships among Sequence, Structure, and Function within the Cupin Superfamily. *PLoS One 8*.

- (3) Dunwell, J. M., Purvis, A., and Khuri, S. (2004) Cupins: The most functionally diverse protein superfamily? *Phytochemistry* 65, 7–17.
- (4) Stipanuk, M. H., Simmons, C. R., Karplus, P. A., and Dominy, J. E. (2011) Thiol dioxygenases: Unique families of cupin proteins. *Amino Acids 41*, 91–102.
- (5) Straganz, G. D., and Nidetzky, B. (2006) Variations of the 2-His-1-carboxylate theme in mononuclear non-heme Fe II oxygenases. *ChemBioChem* 7, 1536–1548.
- (6) Leitgeb, S., and Nidetzky, B. (2008) Structural and functional comparison of 2-His-1-carboxylate and 3-His metallocentres in non-haem iron(II)-dependent enzymes. *Biochem. Soc. Trans. 36*, 1180–1186.
- (7) Koehntop, K. D., Emerson, J. P., and Que, L. (2005) The 2-His-1-carboxylate facial triad: A versatile platform for dioxygen activation by mononuclear non-heme iron(II) enzymes. *J. Biol. Inorg. Chem.* 10, 87–93.
- (8) Price, J. C., Barr, E. W., Tirupati, B., Bollinger, J. M., and Krebs, C. (2003) The First Direct Characterization of a High-Valent Iron Intermediate in the Reaction of an α-Ketoglutarate-Dependent Dioxygenase: A High-Spin Fe(IV) Complex in Taurine/α-Ketoglutarate Dioxygenase (TauD) from Escherichia coli. *Biochemistry 42*, 7497–7508.
- (9) Roach, P. L., Clifton, I. J., Charles, M. H., Shibata, N., Schofield, C. J., Hajdu, J., and Baldwin, J. E. (1997) Structure of isopenicillin N synthase complexed with substrate and the mechanism of penicillin formation. *Nature* 387, 827–830.
- (10) McDonough, M. A., Li, V., Flashman, E., Chowdhury, R., Mohr, C., Liénard, B. M. R., Zondlo, J., Oldham, N. J., Clifton, I. J., Lewis, J., McNeill, L. A., Kurzeja, R. J. M., Hewitson, K. S., Yang, E., Jordan, S., Syed, R. S., and Schofield, C. J. (2006) Cellular oxygen sensing: Crystal structure of hypoxia-inducible factor prolyl hydroxylase (PHD2). *Proc. Natl. Acad. Sci. U. S. A. 103*, 9814–9819.
- (11) Yamaguchi, K., and Hosokawa, Y. (1987) Cysteine Dioxygenase. *Methods Enzymol.* 143, 395–403.

- (12) Cavallini, D., Scandurra, R., and De Marco, C. (1963) The Enzymatic Oxidation of Cysteamine to Hypotaurine in the Presence of Sulfide. *J. Biol. Chem.* 238, 2999–3005.
- (13) McCoy, J. G., Bailey, L. J., Bitto, E., Bingman, C. A., Aceti, D. J., Fox, B. G., and Phillips, G. N. (2006) Structure and mechanism of mouse cysteine dioxygenase. *Proc. Natl. Acad. Sci.* 103, 3084–3089.
- (14) Dominy, J. E., Simmons, C. R., Hirschberger, L. L., Hwang, J., Coloso, R. M., and Stipanuk, M. H. (2007) Discovery and characterization of a second mammalian thiol dioxygenase, cysteamine dioxygenase. *J. Biol. Chem.* 282, 25189–25198.
- (15) Pierce, B. S., Subedi, B. P., Sardar, S., and Crowell, J. K. (2015) The "Gln-Type" Thiol Dioxygenase from Azotobacter vinelandii Is a 3-Mercaptopropionic Acid Dioxygenase. *Biochemistry* 54, 7477–7490.
- (16) Tchesnokov, E. P., Fellner, M., Siakkou, E., Kleffmann, T., Martin, L. W., Aloi, S., Lamont, I. L., Wilbanks, S. M., and Jameson, G. N. L. (2015) The cysteine dioxygenase homologue from Pseudomonas aeruginosa is a 3-mercaptopropionate dioxygenase. *J. Biol. Chem.* 290, 24424–24437.
- (17) White, M. D., Carbonare, L. D., Puerta, M. L., Iacopino, S., Edwards, M., Dunne, K., Pires, E., Levy, C., McDonough, M. A., Licausi, F., and Flashman, E. (2020) Structures of Arabidopsis thaliana oxygen-sensing plant cysteine oxidases 4 and 5 enable targeted manipulation of their activity. *Proc. Natl. Acad. Sci. U. S. A. 117*, 23140–23147.
- (18) Brandt, U., Schürmann, M., and Steinbüchel, A. (2014) Mercaptosuccinate dioxygenase, a cysteine dioxygenase homologue, from Variovorax paradoxus strain B4 is the key enzyme of mercaptosuccinate degradation. *J. Biol. Chem.* 289, 30800–30809.
- (19) Goncharenko, K. V., Vit, A., Blankenfeldt, W., and Seebeck, F. P. (2015) Structure of the sulfoxide synthase EgtB from the ergothioneine biosynthetic pathway. *Angew. Chemie Int. Ed. 54*, 2821–2824.
- (20) Ng, T. L., Rohac, R., Mitchell, A. J., Boal, A. K., and Balskus, E. P. (2019) An N-nitrosating

- metalloenzyme constructs the pharmacophore of streptozotocin. Nature 566, 94–99.
- (21) Diebold, A. R., Neidig, M. L., Moran, G. R., Straganz, G. D., and Solomon, E. I. (2010) The three-his triad in dke1: Comparisons to the classical facial triad. *Biochemistry* 49, 6945–6952.
- (22) Chen, J., Li, W., Wang, M., Zhu, G., Liu, D., Sun, F., Hao, N., Li, X., Rao, Z., and Zhang, X.
- C. (2008) Crystal structure and mutagenic analysis of GDOsp, a gentisate 1,2-dioxygenase from Silicibacter Pomeroyi. *Protein Sci. 17*, 1362–1373.
- (23) Fernandez, R. L., Dillon, S. L., Stipanuk, M. H., Fox, B. G., and Brunold, T. C. (2020) Spectroscopic Investigation of Cysteamine Dioxygenase. *Biochemistry 59*, 2450–2458.
- (24) Altschul, S. (1997) Gapped BLAST and PSI-BLAST: a new generation of protein database search programs. *Nucleic Acids Res. 25*, 3389–3402.
- (25) Dominy, J. E., Simmons, C. R., Karplus, P. A., Gehring, A. M., and Stipanuk, M. H. (2006) Identification and characterization of bacterial cysteine dioxygenases: A new route of cysteine degradation for eubacteria. *J. Bacteriol.* 188, 5561–5569.
- (26) Gerlt, J. A., Bouvier, J. T., Davidson, D. B., Imker, H. J., Sadkhin, B., Slater, D. R., and Whalen, K. L. (2015) Enzyme function initiative-enzyme similarity tool (EFI-EST): A web tool for generating protein sequence similarity networks. *Biochim. Biophys. Acta Proteins Proteomics* 1854, 1019–1037.
- (27) Smoot, M. E., Ono, K., Ruscheinski, J., Wang, P. L., and Ideker, T. (2011) Cytoscape 2.8: New features for data integration and network visualization. *Bioinformatics* 27, 431–432.
- (28) Stipanuk, M. H., Dominy, J. E., Lee, J.-I., and Coloso, R. M. (2006) Mammalian cysteine metabolism: new insights into regulation of cysteine metabolism. *J. Nutr.* 136, 1652S-1659S.
- (29) Lombardini, J. B., Singer, T. P., and Boyer, P. D. (1969) Cysteine oxygenase. II. Studies on the mechanism of the reaction with 18oxygen. *J. Biol. Chem.* 244, 1172–1175.
- (30) Chai, S. C., Jerkins, A. A., Banik, J. J., Shalev, I., Pinkham, J. L., Uden, P. C., and Maroney, M. J. (2005) Heterologous expression, purification, and characterization of recombinant rat cysteine dioxygenase. *J. Biol. Chem.* 280, 9865–9869.

- (31) Schulz, J. B., Lindenau, J., Seyfriend, J., and Dichgans, J. (2000) Glutathione, oxidative stress and neurodegeneration. *Eur. J. Biochem.* 267, 4904–4911.
- (32) Wilmer, M. J., Emma, F., and Levtchenko, E. N. (2010) The pathogenesis of cystinosis: Mechanisms beyond cystine accumulation. *Am. J. Physiol. Ren. Physiol.* 299.
- (33) Elmonem, M. A., Veys, K. R., Soliman, N. A., Van Dyck, M., Van Den Heuvel, L. P., and Levtchenko, E. (2016) Cystinosis: A review. *Orphanet J. Rare Dis.* 11, 1–17.
- (34) Simmons, C. R., Hirschberger, L. L., Machi, M. S., and Stipanuk, M. H. (2006) Expression, purification, and kinetic characterization of recombinant rat cysteine dioxygenase, a non-heme metalloenzyme necessary for regulation of cellular cysteine levels. *Protein Expr. Purif.* 47, 74–81.
- (35) Heafield, M. T., Fearn, S., Steventon, G. B., Waring, R. H., Williams, A. C., and Sturman, S. G. (1990) Plasma cysteine and sulphate levels in patients with motor neurone, Parkinson's and Alzheimer's disease. *Neurosci. Lett.* 110, 216–220.
- (36) Slivka, A., and Cohen, G. (1993) Brain ischemia markedly elevates levels of the neurotoxic amino acid, cysteine. *Brain Res.* 608, 33–37.
- (37) Li, W., Blaesi, E. J., Pecore, M. D., Crowell, J. K., and Pierce, B. S. (2013) Second-sphere interactions between the C93-Y157 cross-link and the substrate-bound Fe site influence the O2 coupling efficiency in mouse cysteine dioxygenase. *Biochemistry* 52, 9104–9119.
- (38) Tchesnokov, E. P., Wilbanks, S. M., and Jameson, G. N. L. (2012) A strongly bound high-spin iron(II) coordinates cysteine and homocysteine in cysteine dioxygenase. *Biochemistry 51*, 257–264.
- (39) Gardner, J. D., Pierce, B. S., Fox, B. G., and Brunold, T. C. (2010) Spectroscopic and computational characterization of substrate-bound mouse cysteine dioxygenase: Nature of the ferrous and ferric cysteine adducts and mechanistic implications. *Biochemistry* 49, 6033–6041.
- (40) Blaesi, E. J., Gardner, J. D., Fox, B. G., and Brunold, T. C. (2013) Spectroscopic and computational characterization of the NO adduct of substrate-bound Fe(II) cysteine

- dioxygenase: Insights into the mechanism of O2 activation. *Biochemistry* 52, 6040–6051.
- (41) Dominy, J. E., Hwang, J., Guo, S., Hirschberger, L. L., Zhang, S., and Stipanuk, M. H.
- (2008) Synthesis of amino acid cofactor in cysteine dioxygenase is regulated by substrate and
- represents a novel post-translational regulation of activity. *J. Biol. Chem.* 283, 12188–12201.
- (42) Simmons, C. R., Liu, Q., Huang, Q., Hao, Q., Begley, T. P., Karplus, P. A., and Stipanuk,
- M. H. (2006) Crystal structure of mammalian cysteine dioxygenase: A novel mononuclear iron
- center for cysteine thiol oxidation. J. Biol. Chem. 281, 18723-18733.
- (43) Li, J., Koto, T., Davis, I., and Liu, A. (2019) Probing the Cys-Tyr Cofactor Biogenesis in
- Cysteine Dioxygenase by the Genetic Incorporation of Fluorotyrosine. Biochemistry 58, 2218-
- 2227.
- (44) Driggers, C. M., Kean, K. M., Hirschberger, L. L., Cooley, R. B., Stipanuk, M. H., and
- Karplus, P. A. (2016) Structure-Based Insights into the Role of the Cys-Tyr Crosslink and
- Inhibitor Recognition by Mammalian Cysteine Dioxygenase. J. Mol. Biol. 428, 3999–4012.
- (45) Siakkou, E., Rutledge, M. T., Wilbanks, S. M., and Jameson, G. N. L. (2011) Correlating
- crosslink formation with enzymatic activity in cysteine dioxygenase. Biochim. Biophys. Acta -
- Proteins Proteomics 1814, 2003–2009.
- (46) Njeri, C. W., and Ellis, H. R. (2014) Shifting redox states of the iron center partitions CDO
- between crosslink formation or cysteine oxidation. Arch. Biochem. Biophys. 558, 61-69.
- (47) Ye, S., Wu, X., Wei, L., Tang, D., Sun, P., Bartlam, M., and Rao, Z. (2007) An insight into
- the mechanism of human cysteine dioxygenase: Key roles of the thioether-bonded tyrosine-
- cysteine cofactor. J. Biol. Chem. 282, 3391-3402.
- (48) Davies, C. G., Fellner, M., Tchesnokov, E. P., Wilbanks, S. M., and Jameson, G. N. L.
- (2014) The Cys-Tyr cross-link of cysteine dioxygenase changes the optimal ph of the reaction
- without a structural change. Biochemistry 53, 7961–7968.
- (49) Driggers, C. M., Cooley, R. B., Sankaran, B., Hirschberger, L. L., Stipanuk, M. H., and
- Karplus, P. A. (2013) Cysteine dioxygenase structures from pH 4 to 9: Consistent Cys-

- persulfenate formation at intermediate pH and a Cys-bound enzyme at higher pH. *J. Mol. Biol.* 425, 3121–3136.
- (50) Blaesi, E. J., Fox, B. G., and Brunold, T. C. (2015) Spectroscopic and computational investigation of the H155A variant of cysteine dioxygenase: Geometric and electronic consequences of a third-sphere amino acid substitution. *Biochemistry 54*, 2874–2884.
- (51) Aloi, S., Davies, C. G., Karplus, P. A., Wilbanks, S. M., and Jameson, G. N. L. (2019) Substrate Specificity in Thiol Dioxygenases. *Biochemistry* 2398–2407.
- (52) Fischer, A. A., Miller, J. R., Jodts, R. J., Ekanayake, D. M., Lindeman, S. V, Brunold, T. C., and Fiedler, A. T. (2019) Spectroscopic and Computational Comparisons of Thiolate-Ligated Ferric Nonheme Complexes to Cysteine Dioxygenase: Second-Sphere Effects on Substrate (Analogue) Positioning. *Inorg. Chem.* 58, 16487–16499.
- (53) York, N. J., Lockart, M. M., Sardar, S., Khadka, N., Shi, W., Stenkamp, R. E., Zhang, J., Kiser, P. D., and Pierce, B. S. (2021) Structure of 3-mercaptopropionic acid dioxygenase with a substrate analog reveals bidentate substrate binding at the iron center. *J. Biol. Chem.* 296, 100492.
- (54) Licausi, F., Van Dongen, J. T., Giuntoli, B., Novi, G., Santaniello, A., Geigenberger, P., and Perata, P. (2010) HRE1 and HRE2, two hypoxia-inducible ethylene response factors, affect anaerobic responses in Arabidopsis thaliana. *Plant J.* 62, 302–315.
- (55) Licausi, F., Kosmacz, M., Weits, D. A., Giuntoli, B., Giorgi, F. M., Voesenek, L. A. C. J., Perata, P., and Van Dongen, J. T. (2011) Oxygen sensing in plants is mediated by an N-end rule pathway for protein destabilization. *Nature* 479, 419–422.
- (56) Weits, D. A., Giuntoli, B., Kosmacz, M., Parlanti, S., Hubberten, H. M., Riegler, H., Hoefgen, R., Perata, P., Van Dongen, J. T., and Licausi, F. (2014) Plant cysteine oxidases control the oxygen-dependent branch of the N-end-rule pathway. *Nat. Commun.* 5.
- (57) Wang, Y., Griffith, W. P., Li, J., Koto, T., Wherritt, D. J., Fritz, E., and Liu, A. (2018) Cofactor Biogenesis in Cysteamine Dioxygenase: C-F Bond Cleavage with Genetically

- Incorporated Unnatural Tyrosine. Angew. Chemie Int. Ed. 57, 8149–8153.
- (58) White, M. D., Kamps, J. J. A. G., East, S., Taylor Kearney, L. J., and Flashman, E. (2018) The plant cysteine oxidases from Arabidopsis thaliana are kinetically tailored to act as oxygen sensors. *J. Biol. Chem.* 293, 11786–11795.
- (59) Masson, N., Keeley, T. P., Giuntoli, B., White, M. D., Lavilla Puerta, M., Perata, P., Hopkinson, R. J., Flashman, E., Licausi, F., and Ratcliffe, P. J. (2019) Conserved N-terminal cysteine dioxygenases transduce responses to hypoxia in animals and plants. *Science (80-.)*. *364*, 65–69.
- (60) Lee, M. J., Tasaki, T., Moroi, K., An, J. Y., Kimura, S., Davydov, I. V., and Kwon, Y. T. (2005) RGS4 and RGS5 are in vivo of the N-end rule pathway. *Proc. Natl. Acad. Sci. U. S. A.* 102, 15030–15035.
- (61) Tamirisa, P., Blumer, K. J., and Muslin, A. J. (1999) RGS4 inhibits G-protein signaling in cardiomyocytes. *Circulation* 99, 441–447.
- (62) Fernandez, R. L., Juntunen, N. D., Fox, B. G., and Brunold, T. C. Spectroscopic Investigation of Iron (III) Cysteamine Dioxygenase in the Presence of Substrate (Analogues): Implications for the Nature of Substrate-Bound Reaction Intermediates. *J. Bioinorg. Chem.*
- (63) Wang, Y., Davis, I., Chan, Y., Naik, S. G., Griffith, W. P., and Liu, A. (2020)

 Characterization of the nonheme iron center of cysteamine dioxygenase and its interaction with substrates. *J. Biol. Chem.* 295, 11789–11802.
- (64) Edgar, R. C. (2004) MUSCLE: Multiple sequence alignment with high accuracy and high throughput. *Nucleic Acids Res.* 32, 1792–1797.
- (65) Okonechnikov, K., Golosova, O., Fursov, M., Varlamov, A., Vaskin, Y., Efremov, I., German Grehov, O. G., Kandrov, D., Rasputin, K., Syabro, M., and Tleukenov, T. (2012) Unipro UGENE: A unified bioinformatics toolkit. *Bioinformatics* 28, 1166–1167.

CHAPTER 7

Conclusions and Future Directions

Chapter 7: Conclusions and Future Directions

7.1 Research Progress on Cysteamine Dioxygenase

This research thesis presents a successful investigation into the previously little studied thiol dioxygenase (TDO), cysteamine dioxygenase (ADO). Prior to my graduate research, it was known that ADO catalyzed the oxidation of cysteamine (2-aminoethanethiol, 2-AET) to hypotaurine. Although a three-histidine (3-His) facial triad had previously been implicated on the basis of sequence alignment and site-directed mutagenesis studies, little was known about the ADO active site environment. To remedy the significant gap in the understanding of this mammalian TDO, I developed a protocol to generate a significant amount of high-purity ADO fusion protein. Enzyme production has enabled spectroscopic, structural, and initial kinetic characterization of substrate- and substrate analogue-bound Fe(II) and Fe(III)ADO. As such, the groundwork has been laid for investigations into the roles that various secondary sphere residues may play in catalysis, as well as for further determination of the catalytic mechanism of ADO.

The X-ray crystal structure of ADO confirms that this TDO possesses a 3-His active site and reveals a wide substrate access tunnel, consistent with the broad substrate scope displayed by ADO. Despite a similar first coordination sphere, spectroscopic results obtained for ADO incubated with substrate and substrate analogues were distinct from those obtained for other Fe(II)-dependent TDOs. In fact, substrate 2-AET has been determined to bind monodentate to the Fe(II) cofactor.² Intriguingly, incubation of Fe(III)ADO with substrate analogue cysteine (Cys) in the presence of glycerol displays a unique low-spin complex, previously observed in TDOs only the presence of a strong-field ligand. This finding suggested, and was later confirmed by the X-ray crystal structure, that the secondary coordination environment of ADO differs from that of other TDOs, underscoring the significant role that secondary-sphere residues play in dictating substrate specificity.

The ADO structure reveals an additional, smaller tunnel that leads from the opposite face of the protein to the active site, through which co-substrate oxygen may be delivered to the Fe

cofactor. This tunnel is gated by two Cys residues that could serve as a redox sensor to regulate O₂ delivery in response to changes in the intracellular redox potential. Notably, the thioether crosslink observed to be critical to the increased function of mammalian CDOs, and proposed to exist in human ADO,³ is not present in this structure. To identify residues important for substrate/active site interactions, three-dimensional models of 2-AET and N-terminal Cys (Nt-Cys) peptide-bound ADO were generated using molecular dynamics in conjunction with quantum mechanics/molecular mechanics calculations. Computational analysis suggests that Tyr198 may play a key role in stabilizing bound N-terminal Cys substrate. A quantitative ultra-high purity liquid chromatography mass spectrometry activity assay has been developed to aid in the characterization of secondary sphere interactions that facilitate the oxidation of substrate and substrate analogues by ADO.

To investigate potential catalytic intermediates, a spectroscopic characterization of Fe(III)ADO with sulfhydryl-containing substrates and the superoxide surrogates, azide and cyanide, was conducted. This study suggested that it is likely that Fe(III)ADO is coordinatively saturated by the presence of solvent-derived hydroxide ligands. Our data revealed that azide is able to coordinate to the Fe(III) center of substrate-free ADO. In contrast, azide does not coordinate to cysteamine-bound Fe(III)ADO, implying that the Fe(III) center lacks an open coordination site and/or azide competes with cysteamine for the same binding site. The surrogate cyanide binds to either 2-AET- or Cys-bound Fe(III)ADO to yield a low-spin (*S* = 1/2) EPR signal that is distinct from the low-spin EPR signal observed for cyanide/Cys-bound Fe(III)CDO suggesting that the amine group of 2-AET engages in weak interactions with a secondary sphere residue. Finally, EPR spectra obtained for cyanide/cysteamine adducts of wild-type Fe(III)ADO and its Tyr208Phe variant are superimposable, implying that either an insignificant fraction of asisolated wild-type enzyme is crosslinked or that formation of the thioether bond has minimal effects on the positioning of substrate and substrate analogues.

7.2 Additional Variant Studies

Initial spectroscopic characterization of a Tyr208Phe variant and the determination of the ADO X-ray crystal structure has indicated that it is unlikely that the purported cross-link in human ADO is functionally relevant in mouse ADO. However, due to the significant impact that this cross-link has on the activity of mammalian CDO the functional relevance of the Cys206-Tyr208 mouse ADO cross-link should be investigated. To accomplish this goal, undergraduate Nick Juntunen has produced a Tyr208Phe variant and begun to spectroscopically characterize substrate-bound Tyr208Phe ADO. Kinetic experiments should be prioritized to compare the activity and Michaelis-Menten parameters of the Tyr variant to WT ADO to definitively determine whether Tyr208 affects the activity of mouse ADO. If performing kinetic experiments with the full RGS5 14-mer substrate is prohibitively expensive, computational analysis has determined that only the first 4-6 residues reside in the ADO substrate tunnel. As such, a shorter sequence, such as a CKGL tetramer, could be used in its place. However, it will be important to test that the tetramer has similar activity and Michaelis-Menten parameters as the 14-mer, as previous experiments with a non-heme iron enzyme, proline hydroxylase-domain containing enzyme, have determined that a change in peptide length affects the binding of both substrate and oxygen co-substrate.

A wide range of substrate analogues and superoxide surrogates have been employed to investigate the ADO active site. Now that an X-ray crystal structure of ADO is available, informed mutagenesis of key secondary sphere residues and sequence motifs can be undertaken. In particular, substitution of Tyr198 would elucidate the importance of this residue to the binding and oxidation of substrates 2-AET and Nt-Cys. A Tyr to Phe PCO4 variant has previously elucidated the importance of this residue in PCOs, as this variant displayed significantly reduced activity. Intriguingly, a computational study of Nt-Cys-bound ADO demonstrated that the peptide substrate may indeed interact with Tyr198. As such I recommend that first the Tyr198Phe ADO variant be spectroscopically and kinetically characterized. If no noticeable changes in substrate binding or turnover between this variant are observed, then the phenolic group of Tyr198 is unlikely to play

a role in substrate positioning. To assess if van der Waals interactions with Tyr198 promote substrate binding, a subsequent characterization of the Tyr198Ala variant could be conducted. Alternatively, the importance of the large substrate tunnel could be investigated by substituting a bulky amino acid into the protein channel. Generation of Tyr198Trp or Tyr198Arg variants may prove to favor smaller substrates, such as 2-AET, over Nt-Cys peptides.

The crystal structure of ADO also revealed a small tunnel through which we propose that co-substrate O₂ will enter the active site. This tunnel is lined by residues Cys120 and Cys169. Intriguingly, a Western blot probing for *ado* gene expression in various mouse tissues showed that ADO travels as multiple bands. CDO was previously observed to travel as two bands both via Western blot and sodium dodecyl sulfate-polyacrylamide gel electrophoresis (SDS-PAGE) due to its cross-linked and non-cross-linked isoforms. The multiple bands identified in ADO may be due to distinct dithiol or disulfide isoforms regulated by Cys120 and Cys169. To investigate the existence of a disulfide, a Cys120Ser ADO variant should be produced. A subsequent mass spectrometry analysis of excised Western blot or SDS-PAGE bands may identify the various isoforms observed when compared to WT ADO. To encourage generation of either the dithiol or disulfide isoform, reducing and oxidizing conditions could be introduced into the buffer matrix. Additionally, the Cys120Ser variant may produce more, "well-behaved" protein that is more amenable to crystallization. If crystallization is pursued, it would be advisable to crystallize ADO in the presence of substrates, like RGS5, or substrate inhibitors.

Finally, the impactful medical application of ADO lies in its predicted ability to affect the stability of signaling molecules which transduce a rapid response to hypoxia. It has been shown that ADO boasts a K_M^{app} of O_2 that is higher than that of the available concentration of oxygen in tissues. In context, while the K_M^{app} for O_2 (55 μ M⁶) is ~3x that of the similar enzyme PCO4,⁷ it lies at the lower end of the range (65-240 μ M⁴ or 240-1700 μ M⁷) of what has previously been measured in proline hydroxylase domain-containing enzymes (PHDs), which also regulate a hypoxic response in cells. To investigate the functional relevance of the purported ADO O_2 tunnel,

variants that affect the opening, like Cys120Met or Cys120Gly, should be generated. If the channel controls O₂ delivery to the active site, these variants will likely diminish the activity of the protein. Alternatively, directed evolution could be used to mutate key residues in the co-substrate tunnel to allow the enzyme to select the most advantageous mutation. Importantly, understanding oxygen delivery to the ADO active site may facilitate the design of inhibitors for this potential mammalian oxygen sensor.⁶ Although it is unlikely that the Brunold lab would ever test the efficacy of enzyme inhibitors in vitro, and especially in vivo, inhibitors of mammalian oxygen sensors have previously been developed by Nobel prize winners, Peter Ratcliffe and Greg Semenza.

7.3 Trapping of Catalytic Intermediates

The oxidation of thiol-containing substrates by ADO to their respective sulfinic acids occurs on a time-scale amenable to the trapping of intermediates through freeze-quench methods. However, on-pathway intermediates, such as superoxo/2-AET-bound Fe(III)ADO, have yet to be trapped using this technique. Collaboration with the Pierce Lab at the University of Alabama would allow for the direct observation of catalytic intermediates through the use of their rapid freeze-quench set-up. Once the superoxo/substrate-bound intermediate is trapped, it will be necessary to characterize the species via spectroscopic techniques such as resonance Raman, magnetic circular dichroism, and parallel mode electron paramagnetic resonance. It will likely prove difficult to generate such intermediates in the high concentrations required for protein resonance Raman studies; thus, extremely pure ADO, without a SUMO tag, will need to be generated to avoid fluorescence during data collection.

7.4 Structural and Computational Investigation of PCO and ADO

The recent publication of the PCO and ADO X-ray crystal structures allows for the computational study of the reaction mechanisms of these two proteins. As these enzymes have been shown to accomplish similar reactions, it would be interesting to assess computationally the viability of putative catalytic intermediates. The 3-His metal coordination environment observed in all TDOs makes it likely that both CDO and ADO oxidize their respective substrates via similar

catalytic mechanisms. Direct observation of a catalytic intermediate, as proposed in the previous section, should be supported by computational analysis of this species. It may prove that investigation into the interactions that facilitate the activation of bound O₂ elucidates critical residues necessary for ADO to deliver oxygen to the Fe cofactor.

Although ADO features a 3-His triad as observed in other TDOs, the MCD data collected for 2-AET-bound ADO lacks the characteristic S→Fe(II) charge transfer (CT) transitions observed in the MCD spectra of Cys-bound CDO and 3-MPA-bound MDO. Instead, this spectrum exhibits a feature in the near IR region that is typically observed in the MCD spectra of five-coordinate non-heme Fe(II) dependent enzymes.⁸ Further investigation via DFT and TD-DFT of an optimized whole protein model of cysteamine-bound ADO would help corroborate the proposed 5-coordinate 2-AET-bound ADO structure previously suggested by MCD data.

7.5 Final Outlook

As described in this thesis, significant process has been made towards characterizing the resting and substrate-bound geometric and electronic structures of *Mm*ADO. The spectroscopic techniques employed are capable of selectively probing the substrate-bound active site. The specific interactions that support substrate and substrate analogue coordination in ADO have been hypothesized. Targeted substitution of unique secondary sphere residues, supported by spectroscopic and kinetic studies, will yield additional insight.

7.6 References

- Dominy, J. E., Simmons, C. R., Hirschberger, L. L., Hwang, J., Coloso, R. M., and Stipanuk,
 M. H. (2007) Discovery and characterization of a second mammalian thiol dioxygenase,
 cysteamine dioxygenase. *J. Biol. Chem.* 282, 25189–25198.
- (2) Fernandez, R. L., Dillon, S. L., Stipanuk, M. H., Fox, B. G., and Brunold, T. C. (2020) Spectroscopic Investigation of Cysteamine Dioxygenase. *Biochemistry 59*, 2450–2458.
- (3) Wang, Y., Griffith, W. P., Li, J., Koto, T., Wherritt, D. J., Fritz, E., and Liu, A. (2018) Cofactor Biogenesis in Cysteamine Dioxygenase: C-F Bond Cleavage with Genetically Incorporated

- Unnatural Tyrosine. Angew. Chemie Int. Ed. 57, 8149-8153.
- (4) Ehrismann, D., Flashman, E., Genn, D. N., Mathioudakis, N., Hewitson, K. S., Ratcliffe, P. J., and Schofield, C. J. (2007) Studies on the activity of the hypoxia-inducible-factor hydroxylases using an oxygen consumption assay. *Biochem. J.* 401, 227–234.
- (5) White, M. D., Carbonare, L. D., Puerta, M. L., Iacopino, S., Edwards, M., Dunne, K., Pires, E., Levy, C., McDonough, M. A., Licausi, F., and Flashman, E. (2020) Structures of Arabidopsis thaliana oxygen-sensing plant cysteine oxidases 4 and 5 enable targeted manipulation of their activity. *Proc. Natl. Acad. Sci. U. S. A. 117*, 23140–23147.
- (6) Masson, N., Keeley, T. P., Giuntoli, B., White, M. D., Lavilla Puerta, M., Perata, P., Hopkinson, R. J., Flashman, E., Licausi, F., and Ratcliffe, P. J. (2019) Conserved N-terminal cysteine dioxygenases transduce responses to hypoxia in animals and plants. *Science (80-.)*. 364, 65–69.
- (7) White, M. D., Kamps, J. J. A. G., East, S., Taylor Kearney, L. J., and Flashman, E. (2018) The plant cysteine oxidases from Arabidopsis thaliana are kinetically tailored to act as oxygen sensors. *J. Biol. Chem.* 293, 11786–11795.
- (8) Solomon, E. I., Pavel, E. G., Loeb, K. E., and Campochiaro, C. (1995) Magnetic circular dichroism spectroscopy as a probe of the geometric and electronic structure of non-heme ferrous enzymes. *Coord. Chem. Rev.* 144, 369–460.

CAPÍTULO 8

Una investigación sobre cisteamina dioxigenasa

The Wisconsin Initiative for Science Literacy (WISL) at UW-Madison sponsors the writing of a thesis chapter that explains a students' research to a lay audience. Agradezco mucho las correcciones y los fondos que WISL me ha dado para escribir este trabajo.

Capítulo 8: Una investigación sobre cisteamina dioxigenasa

Tengo la suerte de conocer muchos científicos cuya meta es la accesibilidad de los resultados científicos especialmente para gente que no estudia química. Para apoyar esta meta, el fideicomiso de la Wisconsin Initiative for Science Literacy at UW-Madison patrocina el desarrollo de un capítulo de me tesis doctoral para que sea accesible al público en general. Agradezco mucho las correcciones y los fondos que WISL me ha dado para escribir este trabajo. Personalmente al ser hispano-hablante, quiero incluir una versión en español. La traducción fue editada por mi papá, el Profesor Salvador Fernández.

¿Que son las proteínas y cómo las como?

Al escuchar la palabra proteína, lo primero que se me viene a la mente es mi mamá al discutir lo que comerá para la cena. A ella le gusta comer algún tipo de proteína para cada comida. Su proteína favorita es filete miñón, pero como yo tengo un gusto vegetariano, como frijoles, soya, o nueces (**Imagen 8.1**).

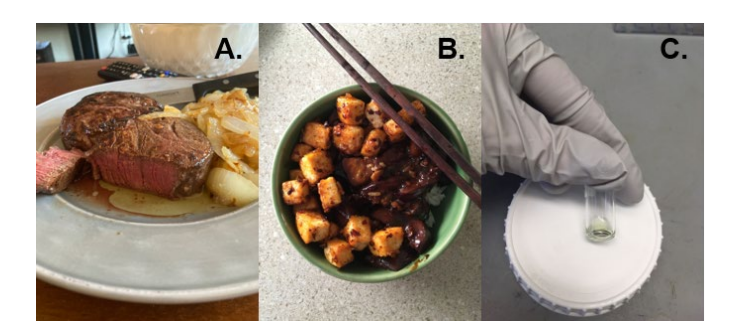


Imagen 8.1 Tres diferentes tipos de proteína. A. La carne es un recurso común de proteína (Fotografía de Liz Laudadio). B. El tofu, las nueces, y los frijoles también proveen proteínas. C. ADO es mi proteína favorita.

¿Cómo es que en estas dos cenas tan diferentes pueden tener proteína? Las proteínas se hacen de aminoácidos. Como un collar que tiene perlas y cuentas de muchos colores, los aminoácidos integran la cadena de cada proteína. En total hay veinte aminoácidos. De esos veinte, podemos obtener nueve de ellos al comer ciertas comidas. Por lo tanto, los tipos de aminoácidos determinan los diferentes tipos de proteína. Es por eso que tenemos que comer

una variedad de proteínas para alimentarnos con los nueve aminoácidos que vienen de nuestra comida.

También tenemos proteínas en nuestro cuerpo. La proteína más abundante que tenemos se llama colágeno y se puede encontrar en tejidos que conectan partes del cuerpo como el cartílago, los huesos, y los ligamentos. ¡El colágeno te mantiene el cuerpo sano y flexible! Mientras que algunas proteínas conectan tejidos, otras pueden crear cosas. Las proteínas que hacen productos se llaman enzimas. De hecho, la función de las enzimas se asemeja al cocinar. Para cocinar un pozole rico se mezclan los ingredientes necesarios, los pones a fuego lento (o energía) por unas horas y después de un tiempo tienes un almuerzo riquísimo. Son las especies como el comino, el orégano y los chiles que hacen el pozole tan rico. En cuanto a las enzimas, éstas tienen una función similar a las especies. Casi un tercio de las enzimas usan un metal para hacer que las reacciones ocurran más rápido y con una mayor frecuencia. Los metales como hierro, cobalto, níquel, y zinc son unos de los más comunes que se encuentran en el cuerpo.

Es aquí donde encajan mis investigaciones: yo estudio una enzima, llamada cisteamina dioxigenasa (ADO), que contiene un hierro (Fe) en su centro (**Imagen 8.2A**). Se llama así porque cuando los científicos descubrieron esta proteína, descubrieren que ADO incorpora dos oxígenos en la molécula cisteamina (**Imagen 8.2B**). O sea, cambia un azufre a un azufre con dos oxígenos.

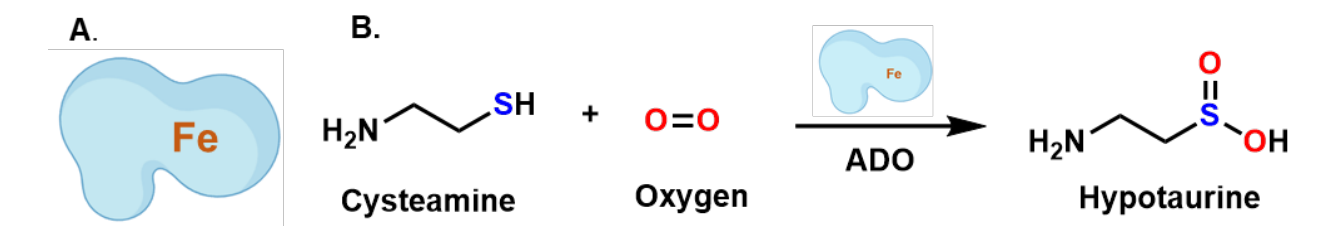


Imagen 8.2. ADO es una proteína con un hierro. A. Esta es imagen de una mancha genérica con un hierro. Cuando empecé mi programa de investigación doctoral no sabíamos cómo se miraba ADO. Solo entendíamos que la enzima incorporaba un átomo de hierro. B. También sabíamos que ADO combinaba la cisteamina y el oxígeno para construir la hipotaurina.

¿Por qué nos importa el azufre?

Es importante tener el propio equilibrio de moléculas que contienen azufre en tu cuerpo. La cisteína es un aminoácido y una de las moléculas que tienen un azufre. El desequilibrio de la cisteína puede afectar la función cerebral y contribuir a enfermedades como el Alzheimer y Parkinson. ADO regula otras moléculas que tiene azufre, como la cisteamina, que en torno afecta el nivel de cisteína en tu cuerpo. ¡De verdad no sabemos nada sobre cómo funciona ADO! Pero es por eso que estas investigaciones son tan conmovedoras. ¡Y complicadas! ADO controla el equilibrio de tantos sistemas en tu cuerpo, aunque solamente sabemos las cosas más básicas de esta proteína.

Hay muchas abreviaciones en mis investigaciones, pero quiero que recuerden esta:

ADO: Cisteamina dioxigenasa, es la enzima con la cual trabajo y Mami, Papi, esta es la proteína que me apasiona.

¿Cómo hago estas "investigaciones"?

A mí me encanta trabajar en el mundo académico haciendo investigaciones. Significa que en una semana puedo leer artículos, platicar con y preguntarle cosas a mis compañeros, realizar experimentos, pasar tiempo en la bici y hasta enseñarles a mis compañeros como desarrollar una nueva habilidad. ¿Pero, qué hacemos en el laboratorio? Nosotros somos "espectropistas bioinorgánicos." Esto significa que usamos la luz (espectropía) para mirar moléculas grandes con metales de importancia para el funcionamiento biológico (bioinorgánico). En mi caso yo investigo la ADO, una proteína que contiene hierro.

Mi proyecto es especial porque hago mi propia proteína. ¡Este proceso es difícil, pero me encanta! Cultivo mi ADO en *E. coli* y lo purifico. El proceso de crecer proteína se parece a cocinar la capa superior de barras de limón, donde lo cocinas añadiendo ingredientes (huevos, limón, mantequilla, azúcar) y luego colas la mezcla para hacer que todo sea una textura. Para crecer ADO, añades tus células (que llevan la proteína) a un consomé lleno de sustancias nutritivas. Calientas y mezclas tu sustancia añadiendo más consomé y células por tres días. Cuando

termina de crecer, tienes que purificar la proteína con coladores bien finos para separar el puro ADO.

Ya entendemos cómo crecer ADO, pero ¿por qué necesitamos tanta proteína? Antes mencioné que no sabemos mucho sobre ADO. Cuando empecé este proyecto, lo único que teníamos era una receta para crecer ADO. Por lo tanto, en esta etapa mi trabajo era mejorar su sabor. No es una broma, yo tenía que descubrir que hacía y cómo funcionaba. Hay un concepto esencial en la bioquímica definido por las relaciones entre estructura y función. Esta idea explica que cómo algo funciona se puede controlar por su estructura. En el caso de ADO, no sabíamos ni cómo se miraba. Entonces, para empezar a entender como funcionaba, tenía que tomarle una foto.

¿Qué uso para ver a ADO?

Mis colegas y yo normalmente usamos la luz para investigar a las proteínas. Una de las técnicas espectroscópicas que use se llama dicroísmo circular magnético, o DCM (**Imagen 8.3**). Para que sepan, el DCM es una técnica increíblemente especializada. No más hay aproximadamente 4 de estos instrumentos en el EE.UU. Déjenme explicarles que significa DCM.

- Dicroísmo circular. La luz pasa como una ola en el océano o en un lago con mucho viento.
 La luz también puede ser polarizada en dos direcciones, a la izquierda y a la derecha. En este caso, viaja como un remolino o en una dirección de sacacorchos.
- Magnético. La parte más cara del DCM (\$208K) es el criostato magnético que tiene un imán hecho de metales superconductores. La superconducción es una propiedad de un metal que hace que cuando el metal se enfría a 4.5 K (o -269 °C) y al darle energía eléctrica se queda a 90.92 amps de corriente para siempre. Para que sepas, algo como 15 amps sale de un enchufe. ¡Dicroísmo circular magnético!



Imagen 8.3. Foto de la nueva DCM instalada en Feb 2021. Una DCM tiene tres partes importantes, la caja que genera la luz polarizada (blanca, a la izquierda), el imán donde queda tu muestra (también blanca, en el medio) y el detector que captura la luz transmitida (adentro de la caja a la derecha). En esta técnica, a lo más básico uno observa el color de la solución, en la presencia de un campo magnético, a temperaturas súper frías (4.5 K = 269 °C = -452 °F).

¿Qué descubrí?

La DCM nos puede dar información sobre como el hierro al centro de la proteína está unido a otros átomos. Para que pueda funcionar la ADO, una molécula reactiva (la cisteamina) tiene que unirse al hierro. Le llamamos esta molécula reactiva un sustrato. Este es el primer paso en un proceso que honestamente no entendemos muy bien. Pasé un año y medio creciendo ADO para verificar que sí establecía una ligadura con el azufre de la cisteamina. ¡Yo descubrí esto! Yo hice una receta extraordinaria para crecer ADO, unas porciones de proteína deliciosas y de una gran calidad. ¡Fui la primera persona en todo el mundo que investigó a fondo la ADO! Lo importante de mi descubrimiento es que ADO se une con el azufre, y únicamente con el azufre. Imagen 8.4 es una foto de cómo se ve el centro de la proteína. El frasco de vidrio es una mezcla de la cisteamina y la ADO. ¡ y su color es un azul celeste!

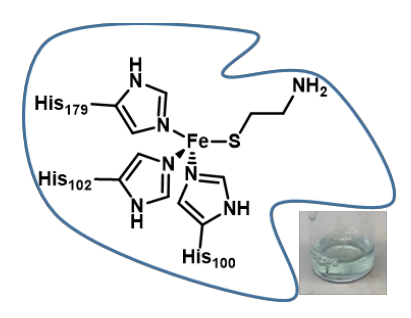


Imagen 8.4. ADO unida a la cisteamina. El azufre de la cisteamina se une al hierro al centro de ADO.

Déjame explicar los experimentos que produjeron la evidencia necesaria para demostrar la existencia de este vínculo. Básicamente, mezclé unos elementos y encontré las semejanzas y diferencias entre los datos que coleccioné. Este experimento se asemeja a cocinar pozole, pero con distintas salsas. Mezcle ADO (el consomé) con dos reactantes (las salsas): la cisteamina (salsa de chiles anchos) y el ácido 3-mercaptopropiónico (3-MPA, salsa de tomatillos). Estas dos son moléculas que se parecen a la cisteamina, pero tienen unas diferencias importantes que nos ayudan identificar qué sustancia se une a otra. La cisteamina tiene un nitrógeno y un azufre mientras que el 3-MPA tiene un oxígeno y un azufre (Imagen 8.5).



Imagen 8.5. Las estructuras de cisteamina y 3-MPA. Un sustrato es el ingrediente (o reactante) que se une a ADO. Algunas veces rápidamente se convierte en un producto (¡como el pozole!). Otras veces lentamente hace el producto o solamente se une al hierro.

En estos dos casos la molécula se unió al ADO (¡yay!). Sabemos que pasó esto porque los datos del DCM se ven diferentes cuando los comparas a los datos de ADO sin otras moléculas presentes. Pero aún más importante, los gráficos (o espectra) de ADO unidos a cisteamina y 3-MPA se ven igual (**Imagen 8.6**). Como el azufre es la única sustancia que tienen en común la cisteamina y el 3-MPA, descubrimos que ADO se une al sustrato con solo un vínculo, al azufre.

Esta afirmación es de gran importancia. No solo no es común, pero nos indicó por primera vez la pista de cómo se ve ADO.

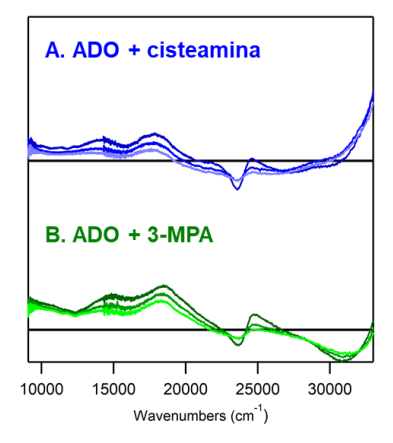


Imagen 8.6. Cisteamina y 3-MPA unidos a ADO. Las semejanzas en los gráficos de cisteamina unida a ADO (A) y 3-MPA unido a ADO (B) nos enseña que estas moléculas se unen al hierro a través del azufre.

¿Por qué importa?

Aunque no sabemos mucho sobre esta sustancia, ni se menciona cuando platicamos, el enzima con que trabajo es importante para la función de los mamíferos. No sabemos exactamente cómo ADO te puede dañar o ayudar, pero sí sabemos su importancia. Lo estudiamos para que un día sea más fácil diseñar una medicina que ayude a ADO funcionar mejor en nuestro cuerpo. Esta idea caracteriza a las investigaciones fundamentales, como las mías. De hecho, pocos van a leer las investigaciones que hice durante mis estudios posgraduados, pero creo que un día el saber cómo se mira ADO y cómo se une a la cisteamina, le ayudará a otra investigadora entender cómo funciona.

Looking at Cysteamine Dioxygenase

I am lucky enough to be surrounded by scientists that seek to make their science accessible to a broad audience. In support of this mission, the Wisconsin Initiative for Science Literacy (WISL) at UW-Madison sponsors the writing of a thesis chapter that explains a students' research to a lay audience. I appreciate the edits and financial support that WISL provided during

the writing of this chapter. As a native Spanish speaker looking to make her work more accessible, I included a Spanish version of the following work, translated by my father Professor Salvador Fernández.

What are proteins and how do I eat them?

When I hear the word protein what comes to mind is my mom talking about what she will eat for dinner. She likes to have some kind of protein with every meal. While her favorite protein source is a filet mignon, I lean towards being a vegetarian and eat beans, soy, and nuts (**Figure 8.1**).



Figure 8.1. Three different types of proteins. A. Meat is a common protein source (Photo credit to Liz Laudadio). B. Tofu, nuts, and beans can provide protein as well. C. This is my favorite kind of protein, ADO.

How can these very different meals both contain this thing called protein? Proteins are made up of amino acids. Like a necklace that has different colorful beads that make a pretty chain, proteins form chains with amino acids. There are 20 total amino acids; nine of the 20 we can only replenish through the food that we eat. Protein sources vary in what amino acids they provide, so we have to eat a variety of protein to get all nine of the food-based amino acids.

We also have proteins in our body. The most abundant protein is collagen, and it is found in connective tissues such as cartilage, bones, and ligaments. It keeps you young and stretchy. While some proteins just connect things, others actually make things! The proteins that make things (products) are called enzymes. Think of making pozole (a.k.a. Mexican hominy soup): you take raw ingredients, give it time and a little heat (or energy), and you've made your delicious

breakfast. Approximately 1/3 of enzymes use a metal to make reactions happen more quickly and more often. They are the spices like cumin, oregano, and chiles that stand out. Metals like iron, cobalt, nickel, and zinc are some of the most commonly found in the body.

This is where my research fits in: I study an enzyme, called Cysteamine dioxygenase (ADO), with an iron (Fe) at its center (**Figure 8.2A**). It's named this way because when scientists discovered this protein, they saw that ADO incorporated two oxygens into the molecule cysteamine (**Figure 8.2B**). More simply, it turns a sulfur into a sulfur with two oxygens attached to it.

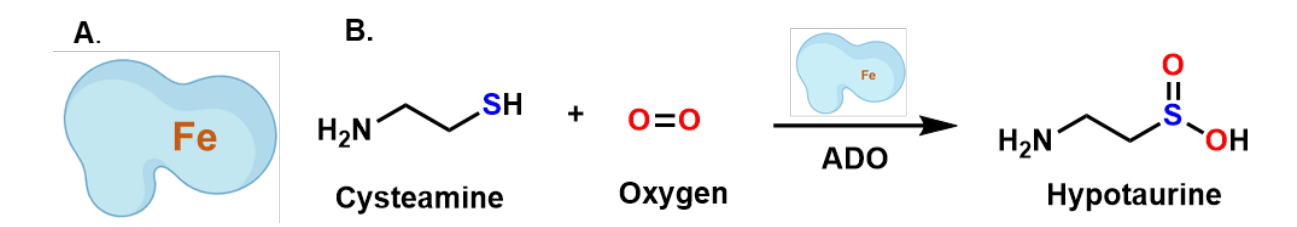


Figure 8.2. ADO is an Fe protein. A. When I started graduate school, we did not know what ADO looked like, only that the enzyme bound one Fe atom. This is a picture of a generic protein blob with one Fe atom. B. We also knew that ADO combined cysteamine and oxygen to make hypotaurine.

Why do we care about sulfur?

It is important to have the right balance of sulfur containing compounds in your body. Cysteine is an amino acid and one of many sulfur-containing molecules. A lack of cysteine regulation has been shown to affect brain function and can contribute to brain diseases such as Alzheimer's and Parkinson's. ADO regulates other sulfur-containing molecules, like cysteamine, which affects the amount of cysteine in your cells. We actually don't know very much about ADO or how it works! That's why this research is so exciting. And complicated! ADO can affect the levels of so many different systems in your body and we are just starting to learn the most basic things about it.

There are too many abbreviations in my research, but let's keep this one straight:

ADO: Cysteamine dioxygenase, the one that I work with (Mami, Papi, this is the exciting one)

How do I "do research"?

I love doing research in academia. It means that my week can consist of reading scientific papers, asking people questions, performing experiments, leaving work early to bike, and working with my labmates to teach them a new skill. But what do my labmates and I do? We are "bioinorganic spectroscopists." This means that we look at big molecules that are relevant to biological function (bioinorganic) with light (spectroscopy). In my case, I look at the Fe-containing protein ADO.

My project is special because I make my own protein. This is difficult, but fun! I grow my ADO protein in *E. coli* and purify it. The process of growing protein can be compared to making the top of lemon bars, where you heat and stir the ingredients (eggs, lemon, butter, sugar), then strain the mixture to make it all one texture. In growing ADO, you add your cells (that hold your protein) to a broth full of nutrients. You heat and stir your batch in increasing quantities for three days, adding nutrients at certain points. Once it's done growing, you have to purify out your protein with finer and finer strainers to get the pure ADO.

The real question is, why do I need to grow gobs of protein? I mentioned earlier that we don't know very much about ADO. When I started this project, all we had was a recipe for making ADO. My job was to find out what it tasted like. Just kidding, my job was to figure out what it did and how it worked. There's a fundamental concept in biochemistry called structure/function relationship. It means that how something works is defined by what it looks like. For ADO, we had no idea what it looked like so to even start to figure out how it worked, I needed to get a picture.

What do I use to see ADO?

Our research group tends to investigate proteins with light. One of the spectroscopic techniques that I used is called magnetic circular dichroism, or MCD (**Figure 8.3**). For context, MCD is an incredibly specialized technique. There are only ~4 other MCD instruments in the entire US! Let's dig a little deeper into the name.

- Magnetic. The most expensive part of the MCD is a magnetocryostat (\$208K to be exact) that
 has a magnet made out of superconducting metals. Superconducting means that when these
 metals are cooled to 4.5 K (or -452 °F !!!!!) and powered, it will remain at this 90.92 amps of
 current indefinitely. For context, about 15 amps come out of a wall socket.
- Circular dichroism. Light typically travels in a wave, like on the ocean or a windy lake. Light
 can also be circularly polarized in two directions left and right, in which case it travels like a
 whirlpool in a corkscrew direction. Magnetic circular dichroism!



Figure 8.3. Picture of the new MCD installed Feb 2021. An MCD has three main parts, the box that makes circularly polarized light (white, far left), the magnet where your sample sits (also white, middle), and the detector that captures the transmitted light (inside the box, right). In this technique you are essentially measuring the color of a solution in the presence of a magnetic field, at very low temperatures (4.5 K = -269 °C = -452 °F).

What did I discover?

MCD can give us information about how the iron center forms bonds with other atoms. For ADO to function, one reactant molecule (cysteamine) has to form a bond to the Fe. We call this reactant a substrate. This is the first step in a complex process that we actually do not understand well. I spent a year and a half trying to grow ADO and then proving that it did in fact bind the sulfur of cysteamine. I discovered this!! I made an incredible recipe to grow ADO. High quality, delicious batches of protein. Then I was the first person in the entire world to be able to study ADO in depth! The key finding is that ADO binds the sulfur, and only the sulfur. **Figure 8.4** is a picture of what

the center of the protein looks like. The glass vial is what the mix of cysteamine and ADO look like irl (in real life). It's sky blue!

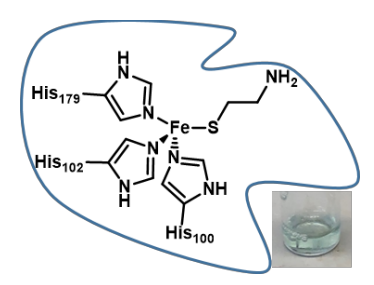


Figure 8.4. Cysteamine-bound ADO. The sulfur of cysteamine forms a bond with the Fe center of ADO.

Let's break down the experiments that provided the evidence for this bond. In the most basic terms, I mixed things together and compared and contrasted the data I collected. This is similar to making pozole, but with a different sauce. I mixed ADO (the "broth") with two different reactants ("sauces"): cysteamine ("red ancho chile") and 3-mercaptopropionic acid (3-MPA, "green tomatillo chile"). These are all molecules that are similar to cysteamine but have key differences that help us identify what is binding to what. Cysteamine has a nitrogen and a sulfur, and 3-MPA has an oxygen and a sulfur (Figure 8.5).



Figure 8.5. Structure of cysteamine and 3-MPA. A substrate is the ingredient (or reactant) that ADO binds to. In some cases, it quickly turns it into a product (like soup!). In other cases, it either very slowly turns it into a product, or simply binds it.

In the two cases, the molecule bound to ADO (yay!). We can tell this because the MCD data looks different when you compare them to ADO without any other molecule present (data not shown). Most importantly, the graphs (a.k.a. spectra) of ADO bound to cysteamine and 3-MPA looked the same (**Figure 8.6**). Since the only thing in common between these cysteamine and 3-MPA was a sulfur, we discovered that ADO binds its substrate with only one bond, to the

sulfur end. This was huge. Not only is this rare, but this was the first time we had a hint to what ADO could look like.

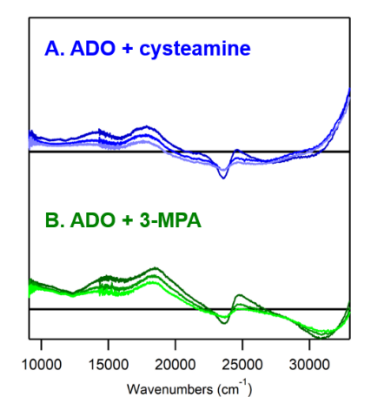


Figure 8.6. Cysteamine and 3-MPA coordinated to ADO. The similarities in the graphs of cysteamine bound to ADO (A) and 3-MPA bound to ADO (B) show us that these molecules bind to the Fe via the sulfur.

Why does it matter?

Although it's not something we know very much about, or even mention in conversation, the enzyme that I work with is important to mammalian function. We don't know exactly in what ways ADO could damage or help you, but we do know it's important. We study it so that hopefully one day it will be that much easier to design medicine that could help ADO function in your body. This is called fundamental research. The research that I did during graduate school will likely be read by few people. However, hopefully understanding what ADO looks like and how it binds cysteamine will help a future chemist understand how it works.

Chapter 9

Student-Led Climate Assessment Promotes a Healthy Graduate School Environment



This chapter has been published under the following: Beasley MS, Lumley MA, Janicki TD, et al (2020) Student-Led Climate Assessment Promotes a Healthier Graduate School Environment. J Chem Educ 97:643–650. https://doi.org/10.1021/acs.jchemed.9b00611

Chapter 9: Student-Led Climate Assessment Promotes a Healthy Graduate School Environment

9.1 Introduction

Recent reports have emerged that highlight a prevalence of mental health disorders among graduate students. 1-10 These studies show that graduate students are disproportionately susceptible to mental health disorders when compared to the general population, due in part to unique challenges associated with the graduate school experience. 5, 11 The majority of incoming students are recent college graduates in their early 20s and their transition to graduate life is typically preceded by a relocation that separates them from their social networks and support systems. Graduate programs that are able to assist students during the transition into their departments will benefit from a happier, healthier and more productive group of young researchers. Although it is not universally recognized among faculty that chemistry graduate programs need to adapt to better support the needs of graduate students, a few departments have initiated major institutional efforts to improve the research and educational climate in graduate school. 1,8,13

Here, we define "climate" to encompass all aspects of the graduate student experience such as research practices, mentorship, social activities, work-life balance, and maintaining a healthy lifestyle. Along with the general challenges associated with graduate school, each individual department has unique elements that influence its culture, such as size and demographics, geographic location, and whether the university is private or public. These differences notwithstanding, many challenges that graduate students experience appear to be universal. Accurate evaluation of graduate program climate and student mental health has been hindered by the transient nature of the graduate student population but, encouragingly, graduate programs across the country have begun developing metrics to examine departmental climate and the graduate student experience. In 2014, the University of California, Berkeley administered a survey to assess the well-being of graduate students in all departments at the university.⁸ In

2018, Mousavi et al. demonstrated the successful implementation of a survey tailored to the Department of Chemistry at the University of Minnesota (UMN).¹ At UMN, the development of a climate survey was initiated by faculty, with student involvement, and the survey results were used to guide institutional changes to improve graduate student culture. These results are further discussed alongside our **Recommendations and Initiatives**.

Based on the practices elucidated by these previous efforts, we report the development and implementation of a student-led climate and mental health survey in the Department of Chemistry at the University of Wisconsin-Madison (UW-Madison). In contrast with previous administratively-driven climate assessments, the survey process described here was initiated, developed, and implemented predominantly by graduate students. This effort was strongly supported by the faculty and staff who, along with mental health professionals and select department alumni, provided significant input throughout every step of an iterative survey development process. Within our department there are approximately 320 graduate students, 40 postdocs, 50 research-active faculty and faculty affiliates, and 100 academic and research staff. In order to effectively represent such a large student body, the department supports an organization—the Graduate Student Faculty Liaison Committee (GSFLC)—which facilitates discussion between graduate students and faculty and serves as a conduit for graduate student concerns. The integral and dynamic role of graduate students in our department was critical for the success of the initiatives discussed below.

The large size and resources of our department were instrumental in developing a climate survey that was specifically tailored to meet the needs of graduate students and postdocs in STEM programs. However, the survey reported here is meant to serve as a tool that is accessible to departments of all sizes and across disciplines. We therefore describe the development of our survey in detail, specifically highlighting the design and implementation process that proved to be successful for our department. Our climate survey was designed as a tool to poll the department, identify both strengths and challenges in our community, and begin a conversation about graduate

student mental health. We present a few representative examples of major findings that may be of interest across STEM fields and discuss how our department (students, faculty, and staff) responded to these results. Finally, we illustrate changes that have been made since the implementation of the survey, including both student- and administration-led initiatives. We hope that providing the details of our process will enable this survey to serve as a framework to assist other graduate students and faculty who are interested in assessing climate in their own departments, thereby lowering the barrier for survey administration and fostering a healthier graduate school climate.

9.2 Survey Process

Survey Development

The UW-Madison climate survey was developed by the Climate Survey Team (CST), a group composed of eight students from different research labs and years in graduate school who provided unique perspectives on the graduate school experience. The chemistry department at UW-Madison represents one of the largest national programs¹⁴ and has non-uniform demographics throughout the department, i.e. among research groups, across subfields, and between years (breakdown of department demographics versus survey respondents is provided in the **Appendix 9**). Given these variations, we sought input from fellow graduate students, faculty, staff, representatives from University Health Services (UHS), and select department alumni, including a human resources expert, throughout each step of the survey design process.

Prior to the development of the 2017 climate survey described here, a chemistry department-wide survey was distributed to graduate students and postdocs in 2015. The previous survey was formulated by two highly motivated graduate students from the GSFLC who worked in collaboration with UHS staff. This first iteration had an exceptionally high response rate of about 62%, attesting to student interest in obtaining a quantitative assessment of the graduate student climate. Hence, the 2015 survey marked a significant turning point in our departmental culture that was characterized by the advent of conversations about mental health and a more explicit

focus on creating an inclusive and supportive department climate. However, this earlier survey considered only negative impacts of graduate research and social practices and did not provide a complete picture of the department climate. Spurred by the desire for a more holistic view of the department and to acquire more detailed information on students' self-reported mental health, the 2017 CST was assembled to revise the initial 2015 survey, which served as the framework for the more comprehensive assessment described here.

Survey Scope

The survey described here was written to obtain a balanced view of the graduate student climate, encompassing positive, negative, and neutral experiences. This grassroots effort was not meant as a rigorous research study but rather to identify strengths and challenges within our department and continue conversations surrounding mental health, work-life balance, and mentorship. The questions were designed to be answered in both a structured and free response manner. Questions designed to probe the same topic proved to yield consistent answers. We also included questions that probed changes in the departmental climate since 2015. However, because the questions asked in the survey described here were heavily edited compared to their first iteration, we are not able to draw direct quantitative comparisons between years. Thus, we are not including any data from the 2015 survey in this report. In the future, we hope to administer the survey every two years to assess the reliability of the study. **Figure 9.1** summarizes the breakdown of question topics and the timeline for our survey development, implementation, and dissemination of results. Note that the full list of survey questions and an overview of methods of data analysis are available in the **Appendix 9**.

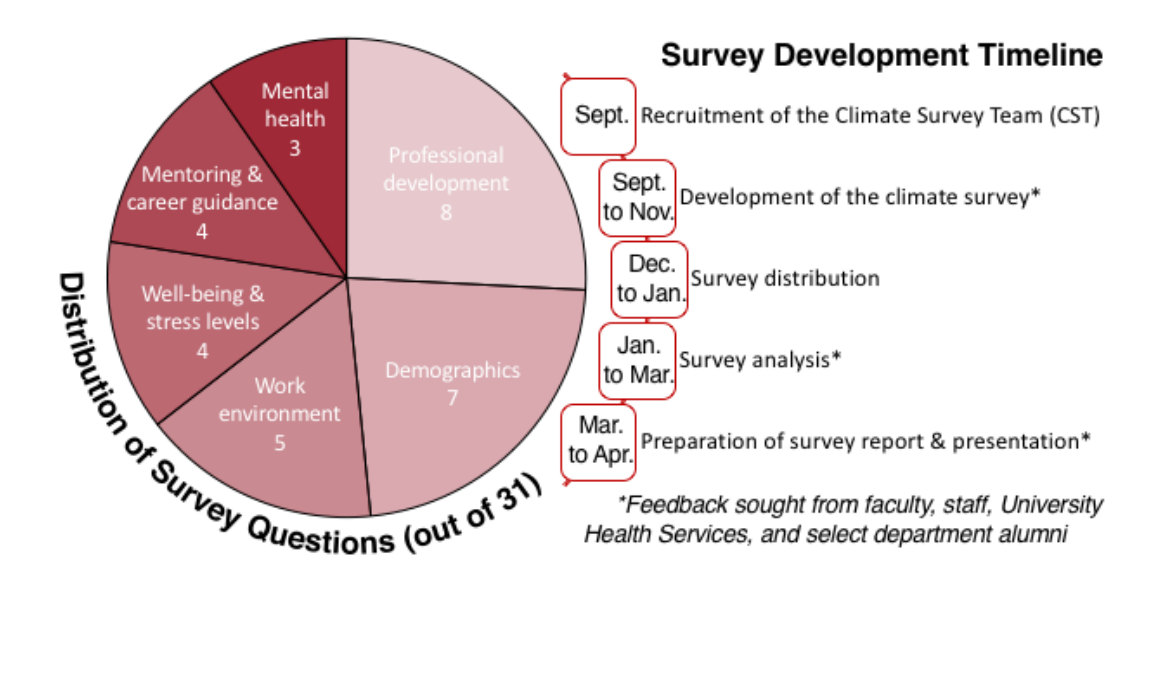


Figure 9.1. The survey was comprised of questions focusing on five main themes to assess the needs of graduate students and postdocs as well as their usage of department and campus resources. Demographic information was collected to identify response correlations among represented groups. The tally presented here does not include open-ended comment sections, which were incorporated throughout the survey (See **Appendix 9** for full survey questionnaire). The complete survey process, from survey design to presentation of results, took place over the course of seven months, from September 2017 through April 2018.

Because the CST is not a professional mental health organization, we worked closely with a trained mental health professional on the writing and analysis of the questions that focused specifically on stress, anxiety, depression, and mental health. Our survey included modified questions from the Patient Health Questionnaire (PHQ-9)¹⁵ and Generalized Anxiety Disorders (GAD-7)^{16,17}, which are tools commonly used to asses symptoms of anxiety and depression. Our survey was not meant to diagnose mental health disorders, but rather to facilitate qualitative comparison of related symptoms in graduate students and postdocs in our department compared with other universities and the general population.

Being a predominantly student-led effort, we did face specific challenges during the survey administration process that are worth highlighting. As with any climate assessment, there is the possibility of a sample bias wherein students who are least satisfied with graduate school may be the most motivated to participate. The results of such a process would paint the department in a non-representative negative light and, as such, faculty may not be receptive to the use of a survey as a tool to accurately assess department climate. To mitigate this perception, we actively sought input from the department chair, individual faculty and staff members, and select department alumni during every step of the survey writing, implementation, and data analysis process. We encourage students in other departments to involve analogous groups in all steps of their climate survey process.

Survey Implementation

The survey was implemented using the online program Qualtrics. Students could work on the survey both on- and off-campus and were able to save their progress so that responses could be edited before submission. The survey was distributed by email and completed by 52% of the graduate student and postdoc population (187 respondents). For comparison, a 24% response rate is typical for surveys administered via email. We also recognized that the timeframe during which surveys are administered may impact the results, as perception of climate is dynamic and context-sensitive. Our survey was open from December 2017 to January 2018. We chose this timeframe for two reasons: 1) This period coincided with winter break, giving students time to thoughtfully answer questions without the burden of classwork or teaching responsibilities, and 2) This period was after first-year students had joined research groups, thus they would be able to provide meaningful responses about the group joining process and their work environments.

Moving forward, we plan to administer a similar survey to graduate students and postdocs in December 2019, with the intention to continue surveying the department every two years. We emphasize that assessment itself is not meant for research purposes, but as a tool to catalyze meaningful changes in graduate education. As we collect an increasing number of survey

responses, we will be able to correlate experiences of different groups (i.e. based on gender and ethnicity), which will enable focused efforts to improve the climate for all members of our community. Further regular assessment will also allow for quantitative evaluation of the effectiveness of the initiatives that are being implemented to improve departmental climate, discussed in detail below.

Survey Analysis

A summary of survey respondent demographics compared to the department demographics and the complete list of survey questions and response options can be found in the associated **Appendix 9**. Major survey findings were determined from both quantitative and qualitative responses and illuminate the factors that most impacted students' and postdocs' experiences with respect to emotional well-being, stress, work-life balance, and mental health. These themes were identified from common multiple-choice answers (see **Representative Survey Findings**) and comments were analyzed by the CST, where frequently used phrases or sentiments were collected. When available, context is provided by comparing quantitative responses to the general population. We acknowledge that the general population may not be an ideal control group; however, providing this comparison puts into context the often extreme nature of stress and mental health disorders experienced by graduate students.⁵ Qualitative (written) responses themselves are not included in this report in order to protect the anonymity of respondents.

Dissemination of Findings

Following a thorough analysis of the survey responses by the CST, both quantitative results and selected comments (with identifying information redacted) were presented to the entire department. We note that this presentation was one of the most well-attended of the year. The seminar was entirely run by the students, which helped to mitigate the effects of the power dynamic often present in faculty-led town halls. The audience, including faculty and staff, had a chance to ask and respond to questions after the presentation. Feedback obtained during and

after this presentation will be used to inform the development of future surveys. We note that there are many possible ways to distribute information and facilitate discussion on a department-wide level. We found that having students themselves give voice to student concerns and bringing the whole community together for a discussion of climate and mental health was an effective method for our department. An alternative example of how to facilitate discussion and receive feedback from all stakeholders in a department was presented recently by Stachl et al.¹³ The dissemination of the survey findings, as well as the survey itself, served as a catalyst for creating an informed dialogue about mental health in the department.

9.3 Representative Survey Findings

By publishing our survey process we aim to provide other graduate students and programs with a framework to explore climate and mental health in their own departments. An important part of this process is analyzing survey data to identify challenges that can be addressed by leveraging existing resources within a department. Faculty, staff, and mental health professionals should be engaged throughout the process to capture perspectives from across the community. Below, we provide a few representative examples of our survey findings and how they were used to inform recommendations to address unique challenges in our department. Our results echo those that have been recently reported, 1, 13 and we emphasize steps that can be taken towards improving the climate responsible for graduate student well-being.

Emotional Well-Being and Work-Life Balance

Graduate students and postdocs were asked what factors influenced their emotional well-being over the course of the previous year. It is clear from these data (**Figure 9.2**) that personal relationships, ranging from PI involvement to peer interactions, have a significant impact on the emotional well-being of students.²⁰ Notably, the advisor/PI was ranked highly as both a positive and negative influence, depending on the respondent, representing the outsized effect of PI-student interactions on the overall graduate school experience. Of the respondents who indicated that their relationship with their advisor/PI had a negative impact on their emotional well-being at

least once per month (22%), 5% identified as male and 17% did not identify as male (details of how demographic responses were grouped can be found in the **Appendix 9**). From this data, it is clear that differences in PI-student relationships may be related to gender, although we could not elucidate more specific causes from this survey. The significance of the PI-student relationship, regardless of gender, is further supported by a global PhD student survey in 2017 that reports "good (PI) mentorship was the main factor driving (graduate student) satisfaction levels."^{21,22}

Respondents were asked specifically to assess how often (percent of time over the course of one year) they felt they met their Pl's expectations. On average, those who identified as male felt they met expectations 67% of the time while those who did not identify as male felt they met expectations only 45% of the time. Encouragingly, there was no significant difference in responses to this question based on ethnicity. Written comments within our survey revealed that a lack of clarity in PI expectations was a prominent source of stress among graduate students. The development of clear expectations documents by faculty may help to lessen the significant stress that many graduate students feel about meeting the milestones required to complete their degrees. In practice, these expectations can be outlined in a written document that describes what are often implicit 'rules' or degree expectations associated with a particular research group. Students can concurrently manage their graduation progress by developing an individual development plan (IDP) to help organize their short- and long-term goals and track their professional progress throughout graduate school. (The ACS has an easily accessible IDP form.)^{23,24}

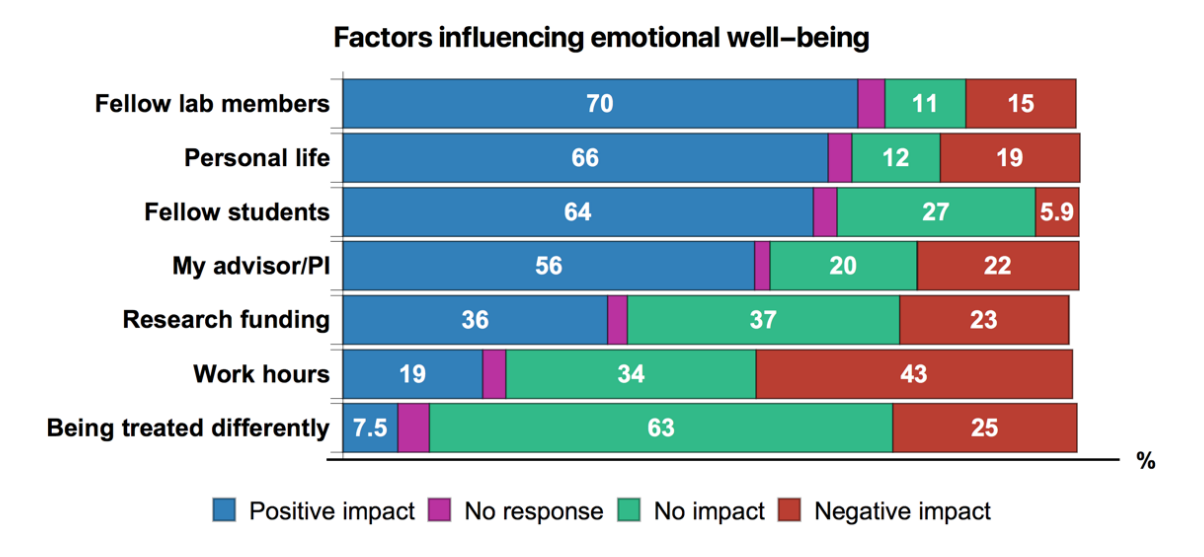


Figure 9.2. Question: "How have the following factors impacted your emotional well-being in the past twelve months?" Selected responses: Top four positive (blue) and negative (red) factors identified. Note that advisor/PI was reported as having both a significant positive and negative impact.

Other studies reporting mental health issues among graduate students cited stress as being one major factor that contributes to overall well-being. 1-5, 25 Stress is endemic to professional life, but the frequency and degree are important in qualifying whether stress becomes detrimental to physical and emotional health. We asked respondents to self-asses how frequently extreme or unhealthy levels of stress hindered their day-to-day lives, specifically interference with productivity at work, ability to take care of oneself, and ability to maintain important relationships. Notably, 58% of graduate students and postdocs indicated that they experience extreme levels of stress at least 1-2 times per month (40% of these respondents identified as male, 60% did not identify as male, and there was no significant difference based on ethnicity.) This is nearly three times the frequency reported in a 2016 survey of the general U.S. population, where 20% of Americans rated their stress levels as extreme. 26 Additionally, 50% of our respondents indicated that their stress levels were influenced primarily by factors related to graduate school.

The disparities in stress levels experienced by graduate students compared to the general population are alarming and attest to the need to assess individual departmental climates and,

when possible, revise policies to alleviate student concerns. Graduate students in our department reported experiencing extreme anxiety surrounding both the group joining process and unclear graduation requirements. Unbeknownst to many students, there was an ongoing process among the faculty and staff to make major changes to the program. An earlier 'divisional' structure of the department led to the implementation of disparate degree requirements. The results of the climate assessment were a powerful voice that spurred faculty to unify graduation requirements across sub-disciplines, which are now standardized for all students. The UW-Madison chemistry department revised its group joining process for first-year graduate students and designed a centralized matching process that is coordinated at the departmental level. To address the uncertainties surrounding research expectations that are often viewed as implicit, a working group was also formed to develop an 'expectations document' template that makes explicit the standards held by each of the individual research groups. We hypothesize that these efforts will increase student productivity through clear understanding of what is expected of them and help to reduce stress stemming from uncertainties in degree progress that are often present in graduate school.

To mitigate extreme stress levels experienced in graduate school, we suggest that students themselves also take the initiative to encourage open communication about stress in graduate school, organize workshops about how to manage stress, and seek help when they need it. In addition, departments should make space for student engagement to enable a healthier climate. The combined efforts of and discussions among the whole department community are essential to creating a climate that values healthy researchers.

Work Environment

To develop a more quantitative picture of the graduate student/postdoc experience, we asked students to assess both the positive and negative factors present in their work environment, including student-student interactions. **Figure 9.3A** demonstrates that many students have experienced supportive work environments, with more than 70% reporting effective mentorship

by senior graduate students/postdocs, their PI, and other group members. However, more than 25% of students indicated that they encountered ineffective mentorship in their research groups, although specific challenges were not investigated in this survey. While mentorship was largely viewed positively in our survey, personal definitions of "effective mentorship" may depend heavily on personal experiences or cultural expectations.

Demographic correlations regarding perceived mentorship efficacy revealed some dependence on ethnicity. For example, 83% of those who identified as Caucasian experienced effective mentorship by senior graduate students/postdocs, compared to only 58% of those who did not identify as Caucasian. Similarly, 90% of respondents who identified as Caucasian reported supportive interactions with their PI in the past 12 months, in contrast with 63% who do not identify as Caucasian. Variations in responses based on ethnicity reflect many factors, such as the diversity (or lack thereof) among the students and faculty members and will vary across departments and over time. In response to trends revealed from demographic correlations and the negative experiences reported in Figure 9.3B, we recommend the installation of regular implicit bias training, mentorship, and conflict resolution workshops. Outside the scope of this survey, we and other departments are making a concerted effort to improve minority representation in chemistry, necessitating shifts in climate that respect and integrate a more diverse student pool. These data serve as an important baseline from which to gauge the effect of new policies through future assessments. The climate survey administered by the Department of Chemistry at the University of California, Berkeley echoes these sentiments and emphasizes the importance of creating a welcoming work environment for women and underrepresented minorities.¹³

Looking beyond interactions within individual research groups, we also wanted to probe peer-to-peer interactions throughout the department. It has been reported that students who lack a strong peer network are less likely to feel accomplished and more likely to be subject to stress and burnout during their graduate career.²⁷ More than 80% of our survey respondents reported

experiencing supportive interactions with their peers in the department, which is in agreement with results from other institutions.^{1,8} In our department, students are actively involved in planning regular social events to encourage positive informal interactions among graduate students, postdocs, faculty, and staff to increase and improve communication among the various members of our department who are spread across the UW-Madison campus. Providing a forum for department members to come together promotes a strong sense of community and is an essential part of creating a positive department climate.

Inspired by the climate survey, our graduate student committee (GSFLC) was reorganized to grow its membership and increase student involvement in the department by providing opportunities to plan regular seminars and workshops on a range of topics. When students are involved, they feel like they truly have a voice in the department, which has been shown to increase levels of satisfaction. While these efforts may divert some activity away from the research lab, we believe that it is empowering for graduate students and postdocs to pursue leadership positions and take on an active role in their communities, learning about how policies are established and beginning new initiatives that continuously improve the culture of the workplace.

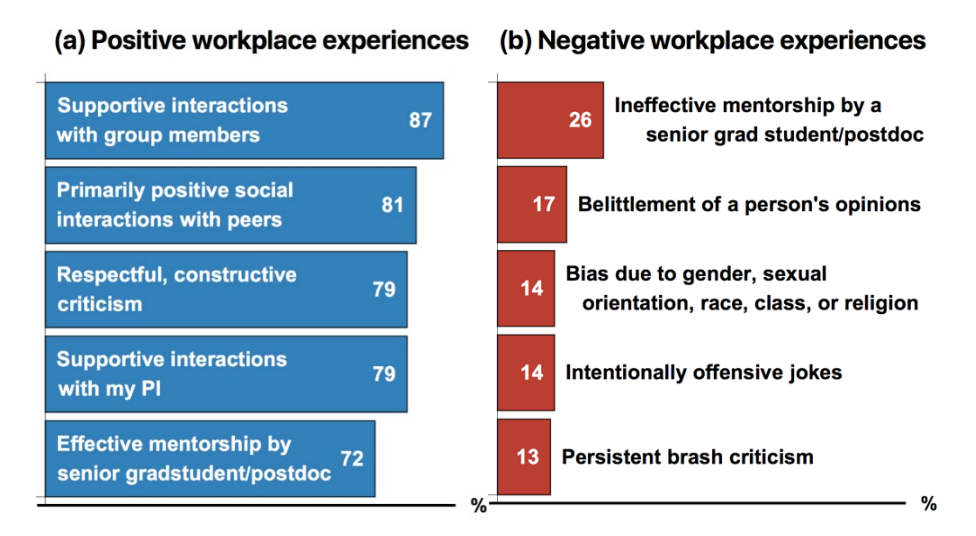


Figure 9.3: Question: "How have the following factors impacted your emotional well-being in the past twelve months?" (a) Positive experiences reported by graduate students and postdocs in the

department. Overall, respondents reported a high frequency of positive interactions in the department. (b) Negative experiences reported by graduate students and postdocs in the department. Although this percent of respondents was lower (each less than 30%) there are still instances of negative experiences.

Mental Health

Another critical element to consider when evaluating the graduate school experience is the prevalence of anxiety and depression among graduate students. **Figure 9.4** summarizes the most striking results from our survey. These measures were not used to diagnose mental health disorders, but rather to identify participants' symptoms of anxiety and depression. We note that our survey questions asked about a timeframe of three months to represent an entire semester. As the timeframe used in the question may impact responses, comparisons to the general public may be only qualitative in nature and details will be provided for each specific example.

A cumulative 59% of graduate students and postdocs reported feeling depressed or sad (a symptom of depression) at least a few times per month compared with 37% of adults surveyed among a broader population (one-month timeframe).²⁸ Additionally, high percentages of graduate students and postdocs reported exhibiting symptoms of anxiety, with 25% of students experiencing a panic or anxiety attack at least once per month. For comparison, a 2012 study reported that 31.2% of adults had some anxiety disorder, where 4.7% had a panic disorder, specifically.²⁹ The most shocking observation from our climate survey was that 9.1% of graduate students and postdocs reported experiencing thoughts that they would be better off dead or hurting themselves at least a few days a month. This alarming number is comparable with that reported for graduate students from other universities using similar methods.^{1,8}

To address and attempt to mitigate the struggles of graduate students and postdocs, we recommend increasing access to and awareness of mental health resources through education and structured conversations. If faculty are educated about the mental health resources available on campus, they are in a better position to direct their students to the appropriate resources if

needed. Most, if not all, graduate schools will have an on-campus mental health organization (at UW-Madison this is the University Health Services (UHS)). Collaboration with professionals is essential to making mental health support for graduate students and postdocs accessible. Our department now hosts bi-weekly "Office Hours" with a UHS professional providing drop-in confidential consultation sessions for graduate students and postdocs inside of the chemistry building, significantly lowering the barrier to seek support. We encourage graduate students at other institutes to connect with their on-campus health professionals and inquire about implementing a similar program.

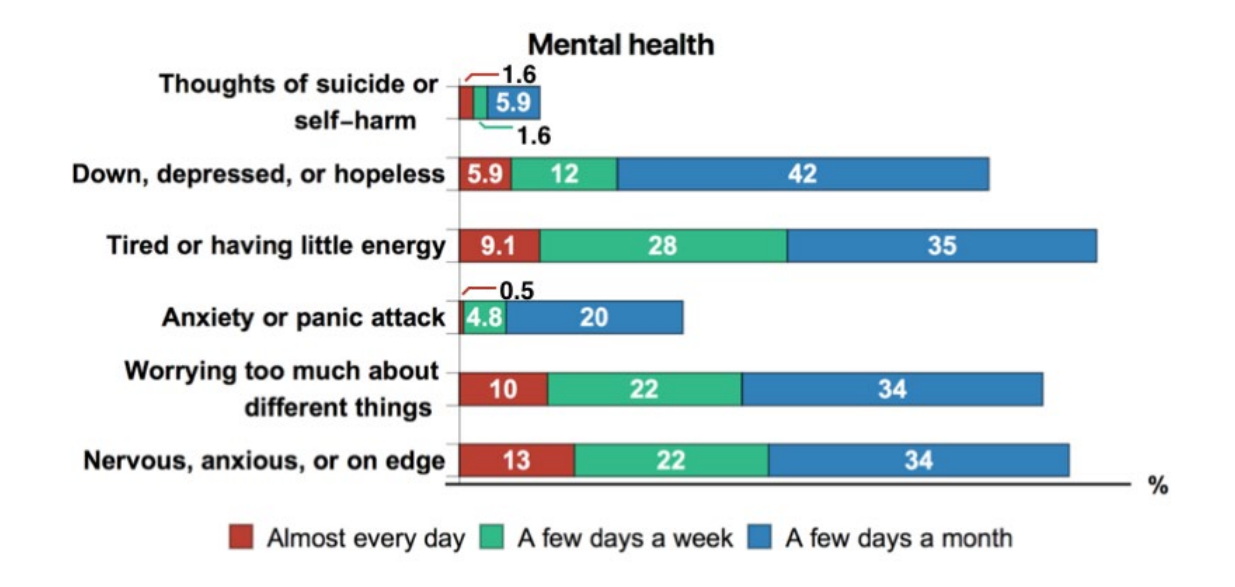


Figure 9.4. Question: "How often have you experienced the following in the past three months?" Selected Responses: 9.1% (cumulative) experienced thoughts of suicide or self-harm, 25% (cumulative) experienced an anxiety or panic attack, and 59% (cumulative) experienced feeling down, depressed or hopeless at least a few days a month.

9.4 Recommendations and Initiatives Implemented Based on Climate Survey Results

To guide department-wide actions moving forward, the CST developed a list of recommendations based on the major survey findings discussed above. This list serves as a framework to guide discussions about the unique challenges that graduate students and postdocs

experience. The recommendations for the department aimed to destignatize discussions about mental health, promote open communication, and improve climate. The recommendations for faculty centered on defining the guidelines they may have for their research groups in order to align faculty and student expectations. The recommendations for graduate students and postdocs encouraged students to take the initiative to develop strategies that alleviate some of the stress associated with graduate school. Additionally, graduate students/postdocs were encouraged to establish regular forums to discuss mental health and provide suggestions to improve departmental policies.

The above guidelines generated from our survey focus on creating a more open dialogue about mental health and improving the graduate school experience, which is mirrored by the recommendations of Mousavi et al.¹ and Stachl et al.¹³ Both reports emphasize the importance of student involvement, and we further stress the beneficial effects of student leadership. Student buy-in for any climate discussions in the department is essential and faculty support is equally crucial to the success of implementing lasting change. Faculty acceptance of student participation in various activities (e.g. being a member of a student council) and engagement in conversations about mental health signals that students' well-being is valued in addition to their research productivity. With the coordinated efforts of students and faculty, department curricula can be updated to provide explicit and detailed program requirements for graduate students. We encourage graduate students in other programs to work with faculty and staff to design and carry out a plan to foster a healthy graduate school climate based on the specific needs of their departments. Utilizing a survey such as ours provides a starting point to gather information that is critical to creating lasting change. A list of the major initiatives, which have been implemented in the UW-Madison chemistry department to address our own unique challenges, can be found below.

- The advent of conversations surrounding graduate student struggles with stress, anxiety, and depression, which have provided a framework for both individuals and research groups to discuss related problems.
- The organization of a regular department-wide town hall to discuss relevant issues.
- An increase in the number of events focused on raising awareness about mental health disorders and resources available on-campus.
- Revision of graduate program policies to reduce stresses associated with the transition into a research group and subsequent graduation requirements.
- An effort to develop an expectations document for independent research labs to mitigate stress surrounding graduation requirements.
- A focus on providing leadership opportunities for graduate students and postdocs to further increase student involvement.

9.5 Conclusions

This report describes a survey implemented in the UW-Madison Department of Chemistry designed to assess and improve the quality of graduate education by identifying and responding to the unique challenges experienced by graduate students and postdocs. We would like to emphasize that the survey disclosed here was a genuine graduate student-led effort, which we believe was crucial to effecting change in the department. Hearing comments directly from students made faculty pay attention to the concerns that were being raised, and we have received an outpouring of faculty support since the dissemination of our survey results. Throughout all steps of the survey process, we received input from all groups in the department—the department chair, faculty, staff, fellow graduate students, and select alumni—which was integral to our success.

Since the results of our climate survey were presented last year, graduate students at UW-Madison outside of the chemistry department have contacted the CST to discuss the

184

implementation of similar surveys in their own departments. We have encouraged these other

groups to use our survey as a starting point and modify the questions as needed. We recognize

that each department will have unique challenges which will need to be addressed. It is also

notable that assessments can identify positive aspects of the department climate and may provide

insight into the programs or initiatives that are making an impact. With that in mind, we have

included our complete survey and additional helpful documents in the associated Appendix 9.

This manuscript provides an accessible framework for survey implementation and we hope that

departments at other universities will join us in our endeavor to better the mental health of

graduate students and postdocs across disciplines.

Appendix 9

The survey administration and results dissemination timeline, recommendations for future

iterations of the survey, a list of GSFLC events, the one-page summary of the survey, the full

survey questionnaire (including Qualtrics .qsf file), and department vs. respondents'

demographics can be found in the Appendix 9.

Author Information

Corresponding Author

*Email: arbuller@wisc.edu

Acknowledgements

We could not have completed this endeavor without the support of many different groups

both on and off campus. We would like to acknowledge the Department of Chemistry and

University Health Services at the University of Wisconsin-Madison for support throughout this

process. Specifically, we would like to thank Professors Judith Burstyn, Mark Ediger, and Tehshik

Yoon, Ryan Stowe, and UHS representatives Bjorn Hanson and Alyssa Levy-Hussen, chemistry

staff members Arrietta Clauss, Matt Sanders, Kayla Driscoll, and Tatum Lyles Flick. Additional

thanks to Jo Eisenhart and the other members of the Chemistry Board of Advisors. We would

also like to thank the UW-Madison Institutional Review Board staff for ensuring that publication

guidelines were followed. Finally, we would like to acknowledge all other graduate students and postdocs for helpful feedback through the survey writing and reporting process. R.L.F. was supported by the National Institute of General Medical Sciences of the National Institutes of Health under award number T32GM008505. T.D.J. acknowledges this is material is based upon work supported by the National Science Foundation Graduate Research Fellowship under Grant No. DGE-1747503.

9.6 References

- (1) Mousavi, M. P. S.; Sohrabpour, Z.; Anderson, E. L.; Stemig-Vindedahl, A.; Golden, D.; Christenson, G.; Lust, K.; Bühlmann, P., Stress and Mental Health in Graduate School: How Student Empowerment Creates Lasting Change. *J. Chem. Educ.* **2018**, *95*, 1939-1946.
- (2) Gould, J., Stressed Students Reach out for Help. *Nature* **2014**, *512*, 223-224.
- (3) Kreger, D. W., Self-Esteem, Stress, and Depression among Graduate Students. *Psychological Reports* **1995**, *76*, 345-346.
- (4) Wang, L., Managing Grad School Stress. *Chemical & Engineering News Archive* **2015**, 93, 59-61.
- (5) Stress and Relief for American Graduate Students: Results from a Nationwide Survey; Graduate Resources: 2011.
- (6) Kuniyoshi, C. S., J.; Kirchhoff, M., 2013 Acs Graduate Student Survey. 2013.
- (7) Kemsley, J., Grappling with Graduate Student Mental Health and Suicide. *Chemical & Engineering News* **2017**, 95, 28-33.
- (8) Graduate Student Happiness & Well-Being Report; The Graduate Assembly, University of California-Berkeley: 2014.
- (9) Evans, T. M.; Bira, L.; Gastelum, J. B.; Weiss, L. T.; Vanderford, N. L., Evidence for a Mental Health Crisis in Graduate Education. *Nat. Biotechnol.* **2018**, *36*, 282.
- (10) Gewin, V., Mental Health: Under a Cloud. Nature 2012, 490.
- (11) Kemsley, J., Supporting Mental Health. *C&EN Global Enterprise* **2017**, *95*, 28-33.

- (12) Curtin, N.; Stewart, A. J.; Ostrove, J. M., Fostering Academic Self-Concept:Advisor Support and Sense of Belonging among International and Domestic Graduate Students. *American Educational Research Journal* **2013**, *50*, 108-137.
- (13) Stachl, C. N.; Hartman, E. C.; Wemmer, D. E.; Francis, M. B., Grassroots Efforts to Quantify and Improve the Academic Climate of an R1 Stem Department: Using Evidence-Based Discussions to Foster Community. *J. Chem. Educ.* **2019**.
- (14) Shulman, J. *Survey of Ph.D. Programs in Chemistry*; Committee on Professional Training: American Chemical Society, 2008.
- (15) Manea, L.; Gilbody, S.; McMillan, D., Optimal Cut-Off Score for Diagnosing Depression with the Patient Health Questionnaire (Phq-9): A Meta-Analysis. *Canadian Medical Association Journal* **2012**, *184*, E191-E196.
- (16) Beard, C.; Björgvinsson, T., Beyond Generalized Anxiety Disorder: Psychometric Properties of the Gad-7 in a Heterogeneous Psychiatric Sample. *Journal of Anxiety Disorders* **2014**, *28*, 547-552.
- (17) Spitzer, R. L.; Kroenke, K.; Williams, J. B. W.; Löwe, B., A Brief Measure for Assessing Generalized Anxiety Disorder: The Gad-7. *JAMA Internal Medicine* **2006**, *166*, 1092-1097.
- (18) Sheehan, K. B., E-Mail Survey Response Rates: A Review. *Journal of Computer-Mediated Communication* **2001**, *6*, 0-0.
- (19) Heerman, W. J.; Jackson, N.; Roumie, C. L.; Harris, P. A.; Rosenbloom, S. T.; Pulley, J.; Wilkins, C. H.; Williams, N. A.; Crenshaw, D.; Leak, C., *et al.*, Recruitment Methods for Survey Research: Findings from the Mid-South Clinical Data Research Network. *Contemporary Clinical Trials* **2017**, 62, 50-55.
- (20) Tenenbaum, H. R.; Crosby, F. J.; Gliner, M. D., Mentoring Relationships in Graduate School. *Journal of Vocational Behavior* **2001**, *59*, 326-341.
- (21) Woolston, C., Graduate Survey: A Love-Hurt Relationship. 2017; Vol. 550, p 549-552.

- (22) Barnes, B. J.; Williams, E. A.; Archer, S. A., Characteristics That Matter Most: Doctoral Students' Perceptions of Positive and Negative Advisor Attributes. *NACADA Journal* **2010**, *30*, 34-46.
- (23) Chemidp. https://chemidp.acs.org/ (accessed 5/31/2019).
- (24) National Institute of Environmental Health Sciences. General Explanation of Idps. https://www.niehs.nih.gov/careers/research/fellows/career/individual/explanation/index.cfm (accessed 8/20/2019).
- (25) Garcia-Williams, A. G.; Moffitt, L.; Kaslow, N. J., Mental Health and Suicidal Behavior among Graduate Students. *Academic Psychiatry* **2014**, *38*, 554-560.
- (26) American Psychological Association (2017). Stress in America: Coping with Change. Stress in America™ Survey.
- (27) Kim, B.; Jee, S.; Lee, J.; An, S.; Lee, S. M., Relationships between Social Support and Student Burnout: A Meta-Analytic Approach. *Stress and Health* **2018**, *34*, 127-134.
- (28) Stress in America: The Impact of Discrimination. https://www.apa.org/news/press/releases/stress/2015/impact-of-discrimination.pdf (accessed 4/18/2019).
- (29) Kessler, R. C.; Petukhova, M.; Sampson, N. A.; Zaslavsky, A. M.; Wittchen, H.-U., Twelve-Month and Lifetime Prevalence and Lifetime Morbid Risk of Anxiety and Mood Disorders in the United States. *International Journal of Methods in Psychiatric Research* **2012**, *21*, 169-184.

APPENDIX

Appendix

Chapter 2

Spectroscopic Investigation of Cysteamine Dioxygenase

Rebeca L. Fernandez, †a Stephanie L. Dillon, †a Martha H. Stipanuk, *Brian G. Fox, \$\sqrt{}\$ and Thomas C. Brunold †*

Figure A2.1. SDS-PAGE gel of SUMO-tagged ADO. Lanes 2-6 were concentrated on the basis of purity considerations.

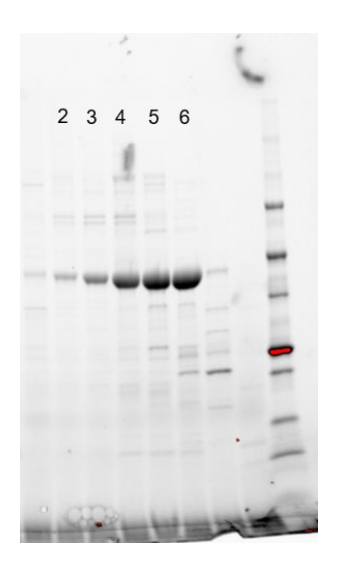


Figure A2.2. Results of TLC activity screen. Lane 1: Hypotaurine control standard; Lane 2: cysteamine control; Lane 3: ADO negative control; Lane 4: ADO incubated with cysteamine

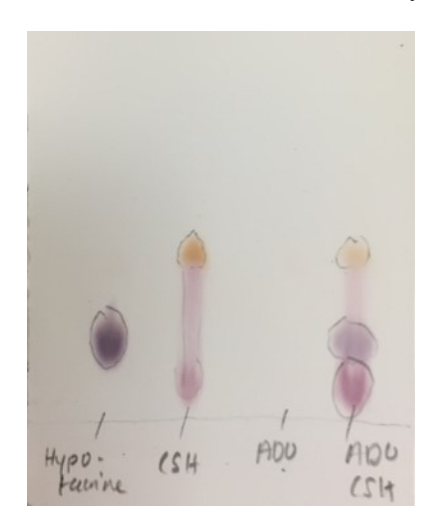


Table A2.1. Table of parameters used to fit experimental EPR spectra via EasySpin (version 5.2.25).

Sample	Species	Percent	g 1	g ₂	gз	D (cm ⁻¹)	E/D
As isolated ADO	Minor high-spin	22	1.99	2.00	1.98	1.47	0.261
	Major high-spin	78	1.99			1.35	0.332
2-AET-bound Fe ^{III} ADO	Major high-spin	92	2.1	2.00	1.998	4.24	0.248
	Minor high-spin	8	2.00			1.52	0.33
3-MPA-bound Fe ^{III} ADO	Major high-spin	94	2.1	2.00	1.998	4.25	0.233
	Minor high-spin	6	2.00			1.63	0.328
Cys-bound Fe ^{III} ADO	Major high-spin	81	2.1	2.01	2.01	3.34	0.260
	Minor high-spin	10	2.01			1.63	0.327
	Minor low-spin	9	2.401	2.28	2.25		
Cys-bound Fe ^{III} ADO with glycerol	Minor high-spin	18	2.10	2.01	2.01	3.34	0.260
	Minor high-spin	2	2.00			1.63	0.327
	Major low-spin	80	2.39	2.30	1.91		
Cys-bound Fe ^{III} ADO with PEG-200	Minor high-spin	18.8	2.19	2.10	1.9	3.40	0.178
	Minor high-spin	1.2	2.00			1.63	0.328
	Major low-spin	80	2.38	2.30	1.92		

Chapter 3

Spectroscopic Investigation of Iron(III) Cysteamine Dioxygenase in the Presence of Substrate (Analogues): Implications for the Nature of Substrate-Bound Reaction Intermediates

Rebeca L. Fernandez,¹ Nicholas D. Juntunen,¹ Brian G. Fox,² and Thomas C. Brunold^{1*}

¹Department of Chemistry, University of Wisconsin-Madison, Madison, Wisconsin 53706, United States

²Department of Biochemistry, University of Wisconsin-Madison, Madison, Wisconsin 53706, United States

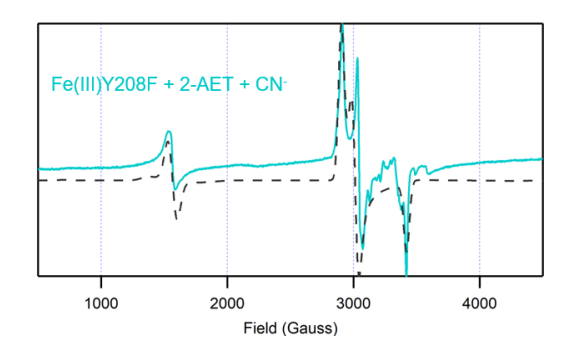


Figure A3.1. X-band EPR spectra at 20 K of Y208F Fe(III)ADO incubated with a 10-fold excess of cyanide in the in the presence of a 15-fold excess of 2-AET. An EPR spectral simulation (dashed line) is overlaid on the experimental spectrum (solid line) for comparison. Fit parameters are provided in Table A3.1.

Table A3.1. Parameters used to fit experimental EPR spectra via EasySpin (Version 5.2.25)¹

Samples	Species	Percent	g ₁	g ₂	g ₃	E/D	D (cm ⁻¹)
Fe ^{III} ADO	Major high-spin	85	2	1.99	1.99	0.28	4.19
	Minor high-spin	15	1.99			0.33	1.44
Fe ^{III} ADO with azide	Major high-spin	85	2	1.99	1.99	0.28	4.19
	Minor high-spin	15	1.99			0.33	1.44
2-AET-bound Fe ^{III} ADO	Major high-spin	92	2.1	2.00	1.99	0.25	4.24
	Minor high-spin	8	2.00			0.33	1.52
2-AET-bound Fe ^{III} ADO with azide	Major high-spin	84	2.01	2.00	1.99	0.28	4.34
	Minor high-spin	6	2.01			0.33	1.63
	Minor low-spin	10	2.38	2.28	1.92		
3-MPA-bound Fe ^{III} ADO with azide	Major high-spin	85	2.01	1.99	1.99	0.28	4.19
	Minor high-spin	15	1.99			0.33	1.44
Cys-bound Fe ^{III} ADO with azide	Major high-spin	88	2.001	2.00	1.99	0.28	4.19
	Minor high-spin	9	2.01			0.33	1.63
	Minor low-spin	3	2.38	2.28	1.92		
Fe ^{III} ADO with cyanide	Major high-spin	75	1.99	1.99	2.00	0.26	1.47
	Minor high-spin	25	1.99			0.33	1.44
2-AET-bound Fe ^{III} ADO with cyanide	Minor high-spin	12	2.10	2.00	2.00	0.24	4.29
	Minor high-spin	8	2.00			0.33	1.52
	Major low-spin	80	2.31	2.19	1.96		
Cys-bound Fe ^{III} ADO with cyanide	Minor high-spin	14	2.10	2.00	2.00	0.26	3.37
	Minor high-spin	6	2.00			0.32	1.63
	Major low-spin	80	2.31	2.19	1.96		
3-MPA-bound Fe ^{III} ADO with cyanide	Major high-spin	64	2.10	2.03	1.99	0.25	4.25
	Minor high-spin	8	2.00			0.33	1.52
	Minor low-spin	28	2.33	2.22	1.93		
2-AET-bound Fe III Y208F with cyanide	Minor high-spin	12	2.1	2.01	2.01	0.24	4.29
	Minor high-spin	8	2			0.33	1.52
	Major low-spin	80	2.31	2.19	1.96		

References

(1) Stoll, S., and Schweiger, A. (2006) EasySpin, a comprehensive software package for spectral simulation and analysis in EPR. *J. Magn. Reson.* 178, 42–55.

Chapter 4

Structure of Cysteamine Dioxygenase

- Rebeca L. Fernandez, Laura Elmendorf, Robert W. Smith, Craig A. Bingman, Brian G. Fox, and
- Thomas C. Brunold

This appendix includes:

- **Table A4.1.** Data collection and refinement statistics
- Figure A4.1. His130 residue of unit A is present in the active site of symmetry-related unit D
- **Figure A4.2**. Comparison of the ADO X-ray crystal structure with a QM/MM optimized structure of ADO
- Figure A4.3. Front and back of the QM/MM optimized structure of ADO
- **Figure A4.4**. Surface representation of the backside of QM/MM optimized structure of ADO highlighting the co-substrate tunnel
- **Figure A4.5**. Front and back of the QM/MM optimized structure of a putative form of oxidized ADO
- **Figure A4.6**. Surface representation of the backside of QM/MM optimized structure of oxidized ADO
- **Figure A4.7.** Tunnels calculated by MOLE2.5 into the active site of ADO

Table A4.1. Data collection and refinement statistics

	<i>Mm</i> ADO
Wavelength	1.127
Resolution range	39.17 - 1.89 (1.958 - 1.89)
Space group	P 21 21 21
Unit cell	54.296 139.525 142.007 90 90 90
Total reflections	1144403 (108025)
Unique reflections	86883 (4059)
Multiplicity	13.2 (12.6)
Completeness (%)	87.21 (47.39)
Mean I/sigma(I)	12.34 (0.99)
Wilson B-factor	34.34
R-merge	0.1844 (1.657)
R-meas	0.1919 (1.726)
R-pim	0.05248 (0.4784)
CC1/2	0.994 (0.474)
CC*	0.998 (0.802)
Reflections used in refinement	76076 (4059)
Reflections used for R-free	2519 (161)
R-work	0.1911 (0.2749)
R-free	0.2275 (0.3125)
CC(work)	0.954 (0.753)
CC(free)	0.945 (0.789)
Number of non-hydrogen atoms	
macromolecules	7597
ligands	10
solvent	561
Protein residues	965
RMS(bonds)	0.01
RMS(angles)	0.88
Ramachandran favored (%)	98.09
Ramachandran allowed (%)	1.49
Ramachandran outliers (%)	0.42
Rotamer outliers (%)	0.36
Clashscore	1.79
Average B-factor	46.47
macromolecules	46.74
ligands	42.78
solvent	42.91
Number of TLS groups	16

Number of TLS groups 16
Statistics for the highest-resolution shell are shown in parentheses.

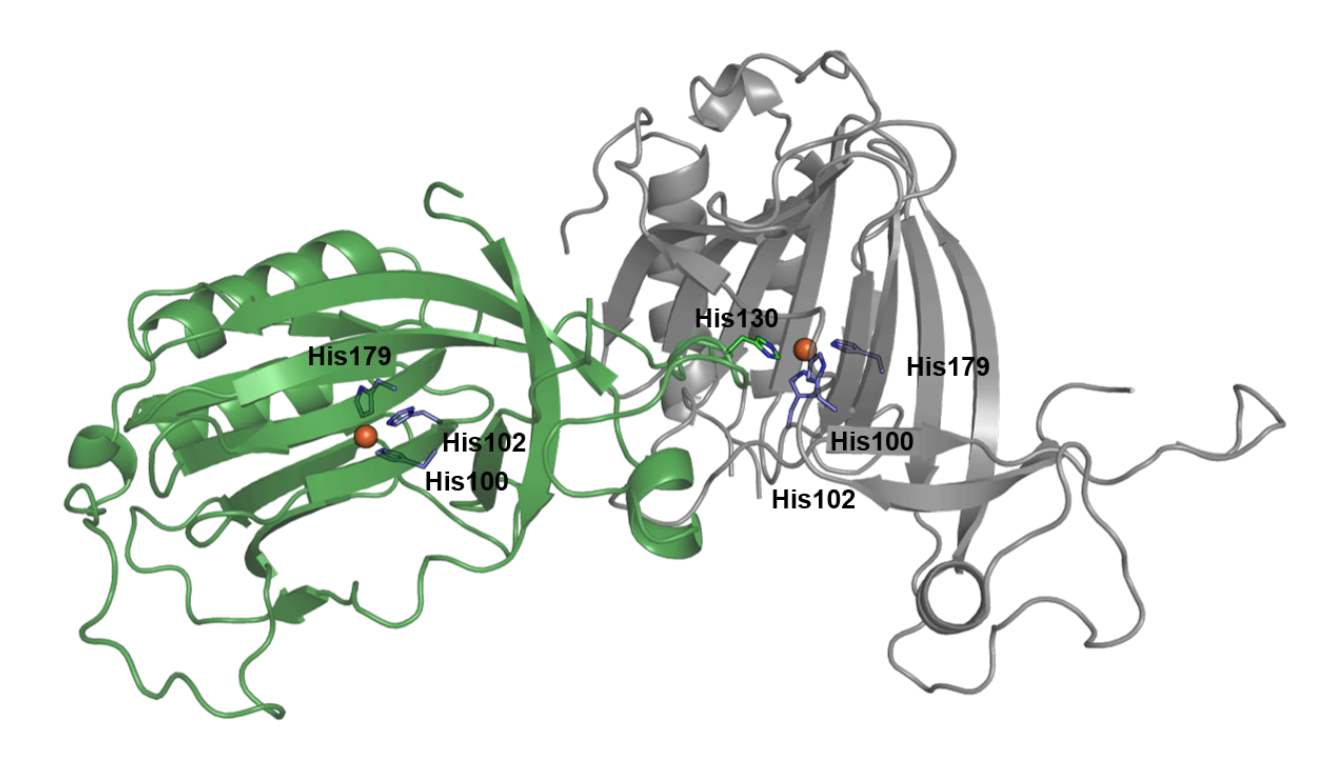


Figure A4.1. His 130 residue of unit A is present in the active site of symmetry-related unit D.

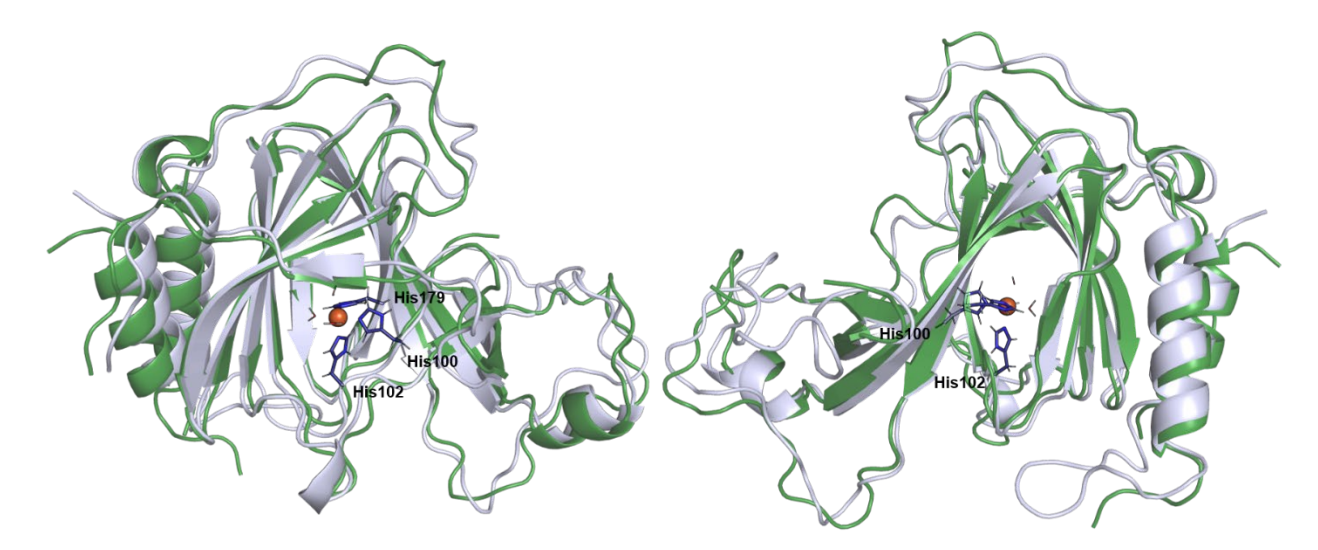


Figure A4.2. Comparison of the ADO X-ray crystal structure with a QM/MM optimized structure of ADO. The X-ray structure is shown in green and the QM/MM optimized model in gray.

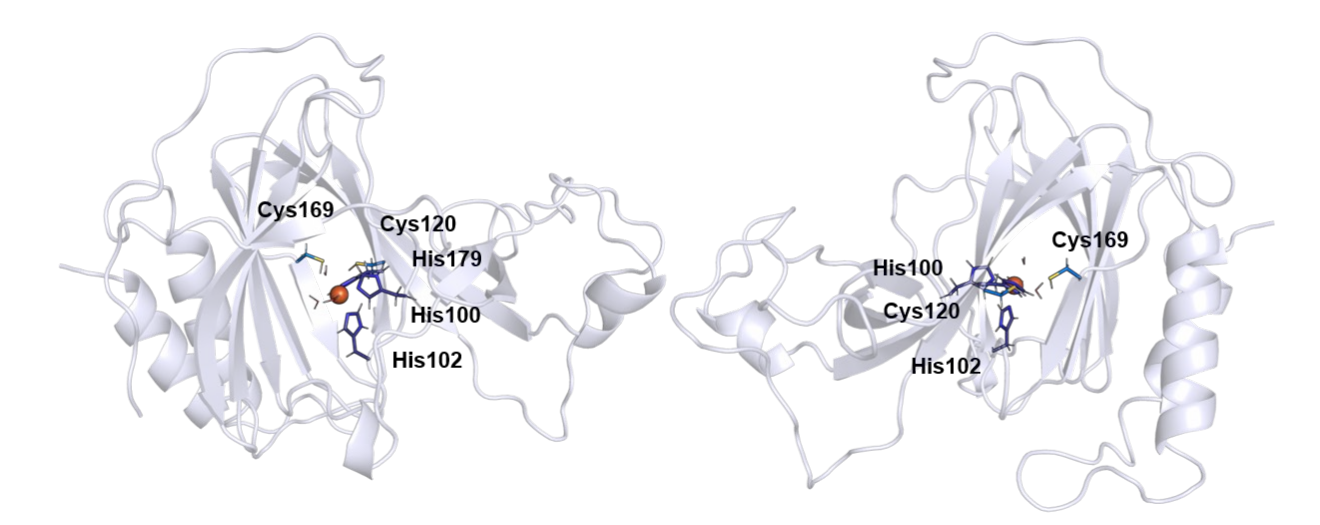


Figure A4.3. Front and back of the QM/MM optimized structure of ADO.

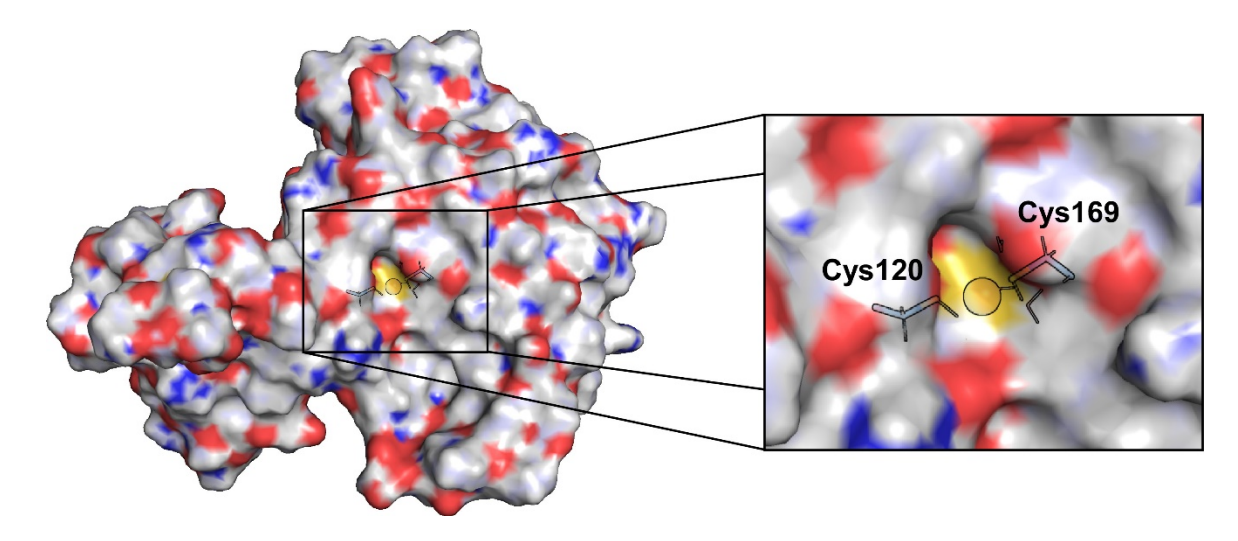


Figure A4.4. Surface representation of the backside of QM/MM optimized structure of ADO highlighting the co-substrate tunnel. The RBG coloring is as follows: Fe, orange; carbon, green; hydrogen white, oxygen, red; nitrogen, blue; and sulfur, yellow.

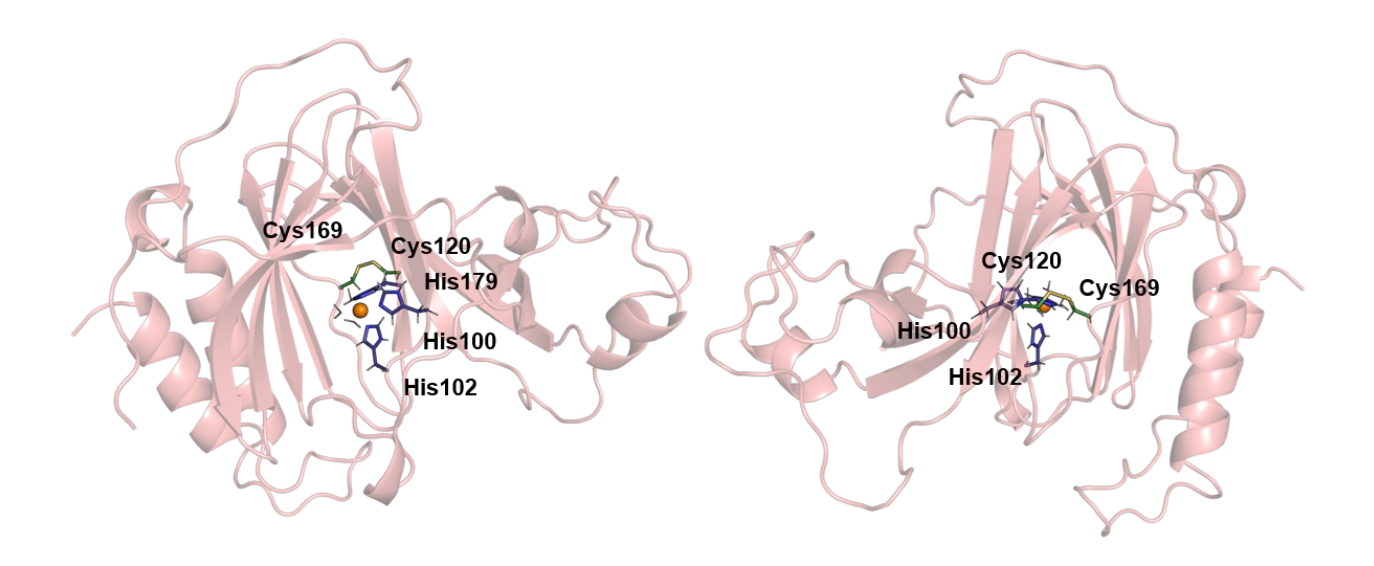


Figure A4.5. Front and back of the QM/MM optimized structure of a putative form of oxidized ADO. This structure has a disulfide bond between Cys120 and Cys169 (disulfide bond in yellow).

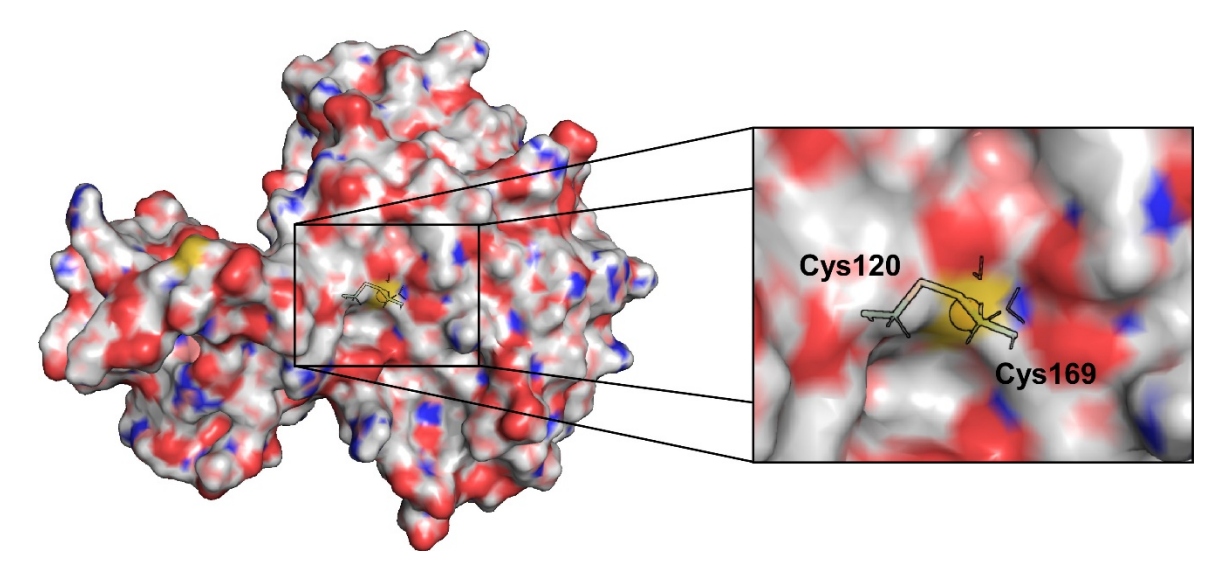


Figure A4.6. Surface representation of the backside of QM/MM optimized structure of oxidized ADO. A disulfide bond between Cys120 and Cys169 closes the back co-substrate tunnel. The RBG coloring is as follows: Fe, orange; carbon, green; hydrogen white, oxygen, red; nitrogen, blue; and sulfur, yellow.

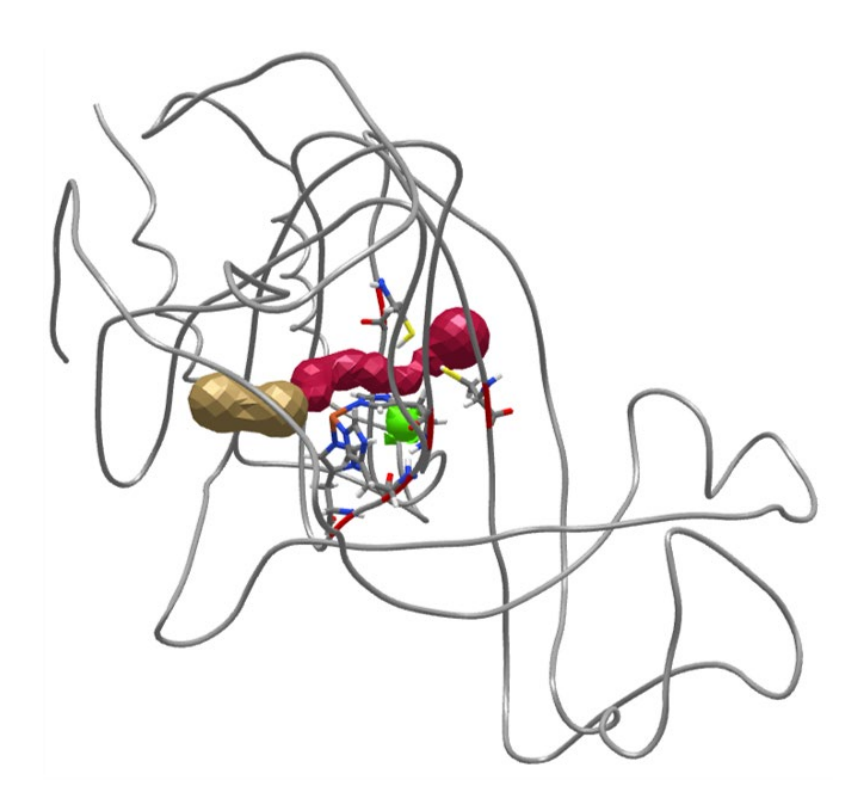


Figure A4.7. Tunnels calculated by MOLE2.5 into the active site of ADO. To generate these tunnels the following parameters were used: internal threshold of 0.9, bottleneck radius of 0.49, and a cutoff ratio of 0.5.

Chapter 9

Student-Led Climate Assessment Promotes A Healthier Graduate School Environment Survey Timeline

Program Timeline: September 2017 – April 2018

September 2017: Recruitment of the climate survey team (CST)

September 2017-November 2017: Development of the climate survey

 Graduate students, faculty, and staff in the department were consulted along with a University Health Services (UHS) representative and select department alumni

International representatives from the GSFLC were asked to review the survey for clarity

December 2017-January 2018

• The climate survey was open to graduate students and postdocs and reminders to complete the survey were sent out weekly

A coffee, cookies, complete survey event was held in January

January 2018-March 2018: Survey analysis

 Shortly after the survey closed, we sent an email to the department announcing the number of survey participants, the date of the climate survey presentation, and a thank you to everyone who participated in the survey

 We had ~3 months between the time the survey closed and the time the results were presented so we wanted to send an email explaining that we were working on survey analysis

During this time, we analyzed all quantitative results and identified themes from the qualitative results

 Upon survey closing all partial responses, including any completed questions, were collected, leaving a data set of 187 usable responses

Numerical analysis was primarily performed using Microsoft Excel with visualization in Wolfram Mathematica

- Qualitative responses were manually processed by the CST and categorized based on correlation with quantitative responses
- In the full survey report and presentation released to the department, written responses
 were incorporated adjacent to relevant statistics
 - These comments were redacted to omit personal information which might identify the respondents

March 2018–April 2018: Preparation of survey report and presentation to chemistry department

- Two weeks before our presentation of the survey results, we sent a draft of the survey report to chemistry department faculty and staff, UHS representatives, and select department alumni
- The full survey report was sent to the department prior to the presentation
 - The report was sent individually to faculty members
- Graduate students and postdocs from diverse backgrounds were asked to attend a
 practice talk prior to the presentation
- Graduate students and postdocs were asked to read quotes from the comments section of the survey report
- The presentation to the department took place on a Friday afternoon
 - The talk was ~45 minutes from start to finish
 - 15 minutes were allowed for Q&A
- After the presentation, the PowerPoint slides were sent out to the whole department
 - Sent to faculty members individually

Recommendations for Future Climate Surveys

General suggestions

Make an effort to have a diverse climate survey team. We were a team of 8 women, which
is not representative of the department demographics. This should include diversity based
on gender, ethnicity, year in grad school, path, etc.

- 2. The percentage of international students who took the survey was low compared to the percentage of international students in the department. Think about strategies to encourage international student participation. We believe that the language barrier was probably a reason why international students did not participate as much.
- 3. Consider surveying students who have left the program with a master's degree or at another point prior to completing their PhD.
- 4. Ask respondents if they are okay with having their response shared after each comment section instead of just at the beginning of the survey.
- 5. In general, think about the best way to group gender and ethnicity categories so that meaningful correlations can be made without singling out a small group of students.

Questions to add or revise in future climate surveys

- Ask a question that asks how grad students/postdocs feel overall about the climate in the department.
- 2. Ask a question about whether PIs are meeting the expectations of their students. (i.e. How effective is your PI as a mentor? Does your PI offer career advice?
- 3. Ask a question about lab safety and department safety culture.
- 4. Ask a question about gossip in the department and how it has affected the overall experience of grad students and postdocs.
- Revise questions so that research group and department are not lumped into the same category.
- 6. Prompt students to give positive feedback, especially about effective mentorship.
- 7. Update the question "Do you have any comments or observations about how any groups are treated based on gender, sexual orientation, race, class, religion, or other?" to include "national origin".
- 8. Add "Jewish" as an ethnicity/race option in the demographics section.

GSFLC Events by Subcommittee

Annual departmental picnic
Outreach:
Food bank drive
Science Saturday volunteering
Outreach scholarship
Professional Development:
Lunch and Learns hosting panels that discuss transitions into careers (e.g. graduate student to
postdoc or postdoc to faculty member)
Individual development plan (IDP) workshop
IUPAC Global Women's Breakfast
Careers Day
Conference travel awards
Mentorship awards
Graduate poster session
ACS Career Kickstarter
Social:
Recurring- Board game nights (monthly), Trivia nights (monthly), Summer social hours (monthly),
Student-Faculty breakfasts (once a semester)
Apple picking
1 st year pizza welcome
Summer Mallards baseball game
Cookie making contest
Hockey night
Ice skating
Wellness:

Nutrition seminar

Yoga for chemists

Indoor and outdoor bike rides

Mental health resources seminar

1st year wellness workshop

Knit night and recurring lunches

Therapy dog visit

LGBTQ+ Ally seminar

Meditation event

How to handle your first summer of research panel

Graduate school degree dash

Diversity chemist slide scroll

Shamrock Shuffle 5K Team

Redacted Climate Survey Report One Page Summary

UW-Madison Department of Chemistry Climate Survey | Summary of Findings | 2017-2018

Top Factors Affecting Emotional Well-Being

Top factors with	Fellow lab members					
Positive Impact	Fellow students Advisor/PI Work hours Unclear expectations Being treated differently from others in research group/department					
Top factors with						
Negative Impact						
8 Major Findings	 Relationship with PI Clarity of PI Expectations Faculty Involvement in Department Issues 					
Related to graduate student and	4. Mentorship5. Group Dynamics					
postdoc experiences, including	6. Work-Life Balance7. Diversity and Bias					
those with positive and negative	8. Gender Disparities					
impacts on mental health and						
emotional well-being.	omity]					
Demographics	<u>Department</u> <u>Survey Respondents</u>					
The response rate was 52%	58.2% male 41.7% male 41.7% female 42.2% female					
lial annuana da ta 107						
Recommendations	 Establish a town hall for open communication. Create research group expectations documents. 					

Full Survey Questions

2017 UW-Madison Chemistry Department Climate Survey of Graduate Students & Postdocs

2017 Department Climate Survey of Graduate Students & Postdocs Conducted by the Graduate Student Faculty Liaison Committee (GSFLC), Department of Chemistry, UW-Madison

Background: It is estimated that 21.7% of U.S. adults 18-25 and 20.9% of U.S. adults 26-49 are diagnosable for one or more mental health disorders (<u>SAMHSA 2015</u>). The numbers are thought to be even higher among graduate students and postdocs, nearing 46% for depression alone (<u>Berkeley 2015</u>).

Purpose: The Graduate Student Faculty Liaison Committee (GSFLC), the Chemistry Department's student council, wants the department to be one in which you can be the best scientists, students, and teachers that you can be. Your feedback is very important to us. This is a chance for you to have a voice and make a difference in the department. We are administering this department climate survey in an effort to evaluate issues related to stress, mental health, and work environment. We will also collect feedback and appraise changes since the last climate survey, implemented in the 2015-2016 academic year. We encourage both positive feedback and constructive criticism. Your responses will help the department evaluate the need for more resources and areas that might require improvement.

Anonymity: Identities of survey respondents will be strictly anonymous. Any question can be skipped, and all metadata will be automatically deleted upon submission -- i.e. your responses cannot be traced back to your IP address. The GSFLC Climate Survey Team will organize the aggregated results into a report that will be presented at an open departmental meeting. The raw data will be analyzed by the subcommittee for important correlations, but these data will never be shared or distributed. Please fill out as much of the survey as you are comfortable with -- any question can be skipped. Your written responses are particularly important in identifying areas needing

- O I permit my written responses to be used in the survey report with all identifying information removed.
- I do not wish for my written responses to be published in the survey report. I acknowledge my responses will be scanned for key words by the survey committee.

Your responses in progress will be automatically saved. After submission, you will not be able to edit your responses. On Friday, January 12, 2018, all partially completed surveys will be collected. Upon collection (whether by submission or automation), all metadata will be erased.

Q1 and Q2 address emotional well-being and stress levels.

Q1. How have the following factors impacted your emotional well-being in the past twelve months?

	Negatively (weekly)	Negatively (monthly)	No impact	Positively (monthly)	Positively (weekly)
Access to equipment and equipment maintenance	0	0	0	0	0
Being treated differently from others within my research group and/or the department	0	0	0	0	0
Research funding	0	\circ	\circ	\circ	\circ
Personal finances	0	\circ	\circ	\circ	\circ
Lab safety	0	\circ	\circ	0	\circ
My advisor/PI	0	\circ	\circ	\circ	\circ
Fellow lab members	0	0	0	0	0
Fellow students	0	0	\circ	0	\circ
Personal life	0	\circ	\circ	\circ	\circ
Teaching	0	\circ	\circ	\circ	0
Ethical research practices	0	\circ	\circ	\circ	\circ
Unethical research practices	0	\circ	\circ	\circ	\circ
Work hours	0	\circ	\circ	\circ	\circ
Other (please clarify)	0	\circ	\circ	\circ	\circ
Other (please clarify)	0	\circ	\circ	\circ	\circ

Q2a. Extreme or unhealthy stress levels while a graduate student/postdoc in this department have interfered with my life (e.g., productivity at work, ability to take care of myself, ability to maintain important relationships)...

 1-2 times per week.
 1-2 times per month.
 1-2 times per year.
○ 3-4 times per year.
o not at all.
Q2b. My stress levels are influenced by
 mostly factors related to graduate school.
 mostly factors related to my personal life and/or support system.
 both of these aspects, equally.
Q2c. Describe how your experiences in the Chemistry Department have affected your health emotional well-being, and/or stress levels. There will also be a comment box at the end for general comments.

Q3-6 address experiences and interactions in your work environment. This includes time spent in lab, office, meetings, and electronic interactions.

Q3a. Have you ever experienced or witnessed any of the following while you have been a member of this department? Select as many as apply.

Work performance and expectations

	Experienced	Witnessed	Heard About	I am not aware of this activity in the department
Willingness and action taken to help labmates succeed				
Information withheld purposefully				
Intentional distribution of incorrect information				
Interference with a person's personal belongings or work equipment				
Recognition of achievements				
Unwarranted or undeserved punishment				
Reasonable lab deadlines				
Impossible deadlines that will set up the individual to fail				
Clearly defined work guidelines				
Constantly changing work guidelines				

Interpersonal interactions with those affiliated with the department

	Experienced	Witnessed	Heard About	I am not aware of this activity in the department
Primarily positive social interactions with peers				
Malicious rumors, gossip, or innuendo				
Exclusion or isolation of someone socially				
Sexual harassment (verbal)				
Sexual assault (physical)				
Bias due to gender, sexual orientation, race, class, or religion				
Intimidation of a person				
Respected privacy (physical & electronic)				
Intrusion on a person's privacy by pestering, spying, or stalking				
Jokes that are intentionally offensive (made in person/spoken or over email)				
Candid, yet respectful, conversation				
Aggressive use of profanity or yelling				

Lab/working environment

	Experienced	Witnessed	Heard About	I am not aware of this activity in the department
Supportive interactions with my PI				
Supportive interactions with group members				
Effective mentorship by senior grad student/postdoc				
Ineffective mentorship by senior grad student/postdoc				
Instances of undermining or deliberately impeding a person's work				
Physically safe working conditions				
Physical abuse or threat of physical abuse				
Emotionally safe working conditions				
Respectful, constructive criticism				
Persistent or constant brash criticism				

	Experienced	Witnessed	Heard About	I am not aware of this activity in the department
Fair/appropriate distribution of group responsibilities				
Assignment of unreasonable duties or workload in a way that creates unnecessary pressure				
Lack of responsibility, creating a feeling of uselessness				
Clearly stated leave or vacation policies				
Blocked applications for training, leave, or promotion				
Opportunities for professional development permitted by your PI				
Removal of responsibility without cause				
Acceptance of new ideas				
Belittlement of a person's opinions				
Q3b. Do you have any comments department based on gender, sexual	orientation, ra	ce, class, religi	ing and up to traduate studer	Please elaborate. hree components
Access to equipment and maintenance	equipment	0	0	
Being treated differently from of my research group and/or the de		0	0	
Personal finances				
		0	0	

Lab safety	0			\circ				
My advisor/PI	0			0				
Fellow lab members	0			0				
Fellow students	0			0				
Personal life	0			0				
Teaching	0			0				
Ethical research practices	0			0				
Unethical research practices	0			0				
Work hours	0			0				
Other (please clarify)	0			0				
Other (please clarify)	0			0				
Q5a. On average, how many hours do you week? Activities include, but are not limited to: nome. Please omit hours devoted to lunch, coffee	time in la	b, classe	es, m	eeti	ngs,	wor		
0	10 20	30 40	50	60	70	80	90	100
Average time in lab (hours/week) ()				_				
Q5b. If you are unable to choose an average, plea	ase explain	1.				— — —		

Q5c. What percent of the time do you feel you meet your advisor/PI's expectations for research (i.e. time, productivity, etc.) over the course of the year?

		0	10	20	30	40	50	60	70	80	90	100
Per	cent of time expectations are met ()											
Q5d - - -	. If you are unable to choose a percent OR	if y	ou ha	ave s	selec	ted ·	<10%	%, ple	ease	exp	lain.	
Q6.	If you wish, please elaborate on your answ	ers	to Q	3-5.								
	address how you are supported in you											
Q۲.	To whom have you gone for career guidan ⊃ My advisor/PI	ce a	and m	nento	oring	? S	elect	as r	nany	as a	apply	/.
(Other faculty (not my PI)											
	☐ My labmates											
(Other peers in the department											
(☐ Path coordinators											
(Research staff (e.g. staff scientists,	faci	lity d	irect	tors))						
(Graduate student coordinator		•		,							
(Other staff (e.g. business office pers	onr	nel)									
	☐ Non-department family or friend											
(☐ On-campus services (e.g. Career Ce	ente	er)									
	Off-campus services											
	Other (please clarify)			_								
(\supset I have not talked with anyone about	car	eer g	guida	ance	and	d/or	men	torir	ng.		

Q8. If you've had a problem with the following department members, with whom did you talk with resolve this problem? Select as many as apply.

	Problem with my advisor/PI	Problem with other faculty	Problem with labmates	Problem with research staff	Problem with other staff
My advisor/PI					
Other faculty					
Labmates					
Other peers in the department					
Path coordinators					
Research staff					
[Graduate student coordinator] or other staff					
Non-department family or friend					
Chemistry active listeners					
On-campus services (e.g. UHS programs, Ombuds)					
Off-campus services					
I did not talk to anyone					
I did not have this problem					
Other					
Q9. Please elaborate on you	ur answers to	Q7 and Q8 i	f you can be	e more specific.	

Q10-13 address resources and events held by departmental and university organizations.

Q10a. Which of the following resources have you used to address mental health and departmental climate concerns?	I use this resource	I have heard of this resource and have considered using it	I have heard of this resource but have not considered using it	I have not heard of this resource
Graduate student support groups (through UHS)	0	0	0	0
Private counseling (through UHS)	0	0	0	0
Office Hours with [UHS representative]	0	0	0	0
Let's Talk	0	0	0	0
Health and financial benefits seminar	0	0	0	0
Climate coordinating team	0	0	0	0
Climate and diversity committee	0	0	0	0
Department suggestion box	0	0	0	0
SCIRep (Students in Chemistry for Inclusive Representation)	0	0	0	0
GSFLC (Graduate Student Faculty Liaison Committee)	0	0	0	0
Catalyst	0	\circ	\circ	\circ

Q10b. Are you aware of any specific steps that have been taken to improve the Chemistry Department climate since the 2015-2016 Climate Survey? Please elaborate on your answer.

Q11a. Chemistry Conversations initiates discussion among all members of the UW-Madison Chemistry Department on topics ranging from department structure and history to inclusion and bias. From the list below, please select all of the Chemistry Conversations events you have attended in the past year (a dated list of events was provided).

Q11b. From the list below, please select all of the ACID (Achieving Career Insight & Development) events you have attended in the past year (a dated list of events was provided).

Q11c. SCIRep (Students in Chemistry for Inclusive Representation) is a student organization which offers a discussion platform for issues of equity and inclusion for graduate students and

postdocs in the UW-Madison Chemistry Department. From the list below, please select all of the SCIRep events you have attended in the past year (a dated list of events was provided). Q11d. The GSFLC (Graduate Student Faculty Liaison Committee) is a group of graduate students, postdocs, and faculty representatives committed to bridging the gap between students and faculty in the UW-Madison Chemistry Department. From the list below, please select all of the GSFLC events you have attended in the past year (a dated list of events was provided). Q12a. The Catalyst program is designed to help first-year graduate students from under-served populations succeed in the UW-Madison Chemistry Department. Are you or have you been a part of Catalyst? (If yes, a dated list of events was provided).	: :
○ Yes	
○ No	
Q13a. What could the department do to maximize positive aspects of your work environment? In your response, please consider both current initiatives you enjoy and other initiatives you would like to see in the future.	
Q13b. What professional development events would you be interested in seeing in the Chemistry Department?	,
O12a. How would you prefer to receive information regarding department events?	
Q13c. How would you prefer to receive information regarding department events? Department newsletter	
☐ Chemistry website calendar	
☐ GSFLC website	
□ Email from listserv	
☐ Email from an individual	
☐ Facebook	
☐ Twitter	
☐ Instagram	
Q14. Please provide any other comments or identify major topics that have not been addressed in this survey.	

The questions on this page are derived from UHS Mental Health Services. M1 and M2 originate from PHQ9 and GAD7. The \underline{PHQ} and \underline{GAD} are standardized measures used to assess depression and anxiety. M1-4 are optional but recommended.

M1. In the past three months, how often have you experienced the following?

	Rarely/never	A few days a month	A few days a week	Almost every day
Little interest or pleasure in doing things	0	0	0	0
Feeling down, depressed, or hopeless	0	0	0	0
Trouble falling or staying asleep, or sleeping too much	0	0	0	0
Feeling tired or having little energy	0	0	\circ	0
Poor appetite or overeating	0	\circ	\circ	0
Feeling bad about yourself that you are a failure or let yourself or your family down	0	0	0	0
Trouble concentrating on things, such as reading the newspaper or watching television	0	0	0	0
Moving or speaking so slowly that other people have noticed	0	0	0	0
Thought that you would be better off dead or hurting yourself	0	0	0	0

M2. In the past three months, how often have you experienced the following?

	Rarely/never	A few days a month	A few days a week	Almost every day
Feeling nervous, anxious, or on edge	0	0	0	0
Being unable to sleep or control worrying	0	0	\circ	0
Worrying too much about different things	0	0	\circ	0
Trouble relaxing	0	0	0	0
Being so restless that it is hard to sit still	0	0	\circ	0
Becoming easily annoyed or very irritable	0	0	\circ	0
Feeling afraid, as if something awful might happen	0	0	0	0
Experiencing an anxiety attack or panic attack	0	0	0	0

M3. In the past three months, how often have you experienced the following?

	Rarely/never	A few days month	a A few days a week	Almost every day
Alcohol, tobacco, or other Irugs helped me cope with the stresses of work/school		0	0	0
was unable to get through vithout using drugs or alcohol	0	0	0	0
was unable to stop using alcohol or drugs when I vanted to	0	0	0	0
Someone close to me complained about my alcohol or drug use		0	0	0
My use of alcohol or drugs caused problems in my personal relationships		0	0	0
My use of alcohol or drugs negatively impacted my performance at work/school		0	0	0
4. Please elaborate on you	r answers to M1-3	3 if you can be m	nore specific.	

Demographic information helps us determine if there are subsets of the department who are not being adequately supported. You may skip this section or any part of it.

D1a. W	ere you present when the 2015 survey was administered?
	Yes
\circ	No
\circ	Prefer not to answer
	you were present when the 2015 survey was administered, please comment on any s that you have noticed in the department since the results of the 2015 survey.
 D2_W/it	h which of the following groups do you identify?
	First year student
	Non-dissertator graduate student
	Graduate student with dissertator status
	Postdoc
	Prefer not to answer
D3. My	activities in the past 12 months included:
	Teaching
	Taking classes
	Path requirement (e.g. second-year report/TBO, RP, departmental seminar)
	Applying for funding
	Research
	Writing thesis
	Preparing manuscripts for publications
	Looking for a job
	Prefer not to answer

D4. The path with which I most closely associate is:
○ Analytical
O Chem Bio
 Inorganic
Materials
○ Organic
○ Physical
Prefer not to answer
D5. I identify my gender as (select as many as apply):
☐ Male
☐ Female
☐ Trans man
☐ Trans woman
☐ Non-binary
☐ Self-identify (specify, if desired)
☐ Prefer not to answer
D6. I identify my ethnicity/race as (select as many as apply):
☐ Caucasian
☐ African-American
☐ Hispanic/Latino
☐ Asian or Pacific Islander
☐ American Indian or Alaska Native
Other (specify, if desired)
☐ Prefer not to answer
D7. Are you a domestic student or international student?
 Domestic
 International
Prefer not to answer

Proceed to submit your survey responses. You will not be able to edit your submission past this page.

Key Demographic Information

The response rate for this survey was 52% of the total graduate student/postdoc population, which corresponds to 187 respondents. Respondents were given the option to report their gender and ethnicity.

The department graduate student/postdoc demographics for gender are 61% male and 39% non-male, and we report a survey response rate of 42% and 42% for these groups, respectively (16% of respondents gave no response for gender or indicated that they preferred not to choose an option). Options for gender included male, female, transgender male, transgender female, non-binary, self-identify, or prefer not to answer. To protect the anonymity of minority groups, we grouped gender into two categories for analysis and reporting: male and non-male.

The department graduate student/postdoc demographics for ethnicity are 60% Caucasian and 40% non-Caucasian, and we report a survey response rate of 66% and 22% for these groups, respectively (13% of respondents gave no response for ethnicity or indicated that they preferred not to choose an option). Options for ethnicity included Caucasian, African-American, Hispanic/Latino, Asian or Pacific Islander, American Indian or Alaska Native, other/self-identify, and prefer not to answer. To protect the anonymity of minority groups, we grouped ethnicity into Caucasian, non-Caucasian, or prefer not to answer/no response.

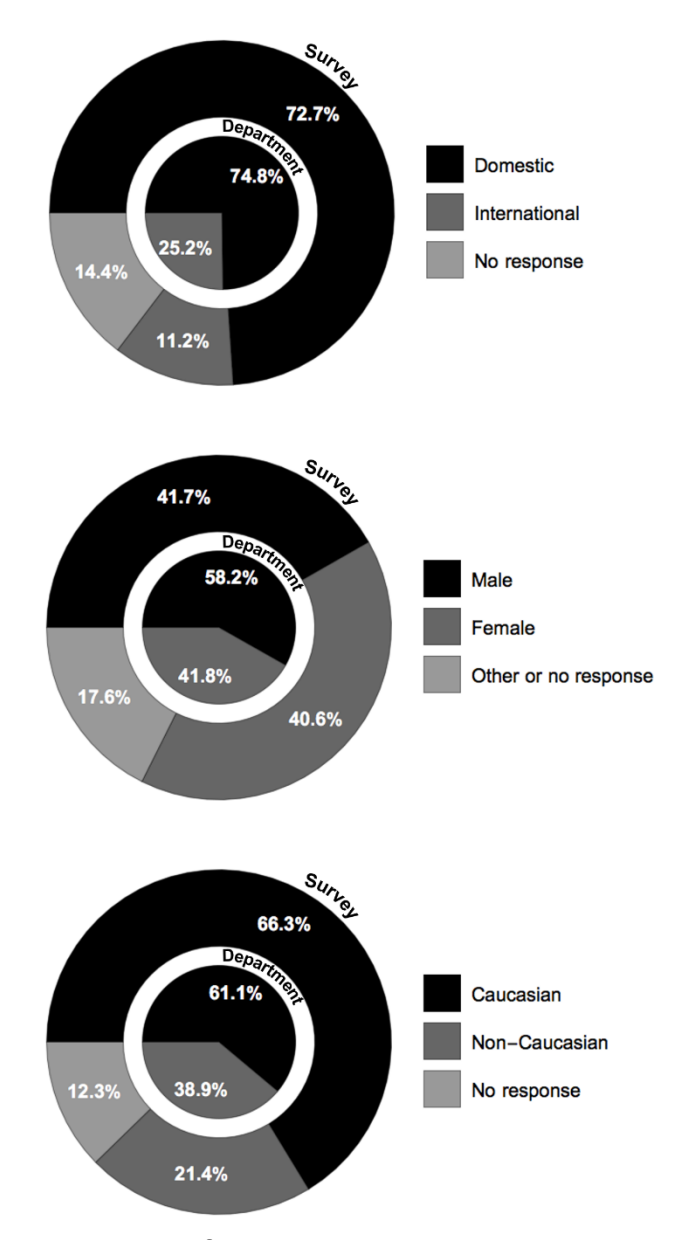


Figure A9.1: Demographic data of the department and the survey respondents